Stratified management of oral cancer – reducing side effects, improving outcomes.

Thesis submitted in accordance with the requirements of the University of Liverpool for the degree of Doctor in Philosophy

Rachel Catherine Brooker

August 2022

Supervisors: Dr J Sacco, Mr A Schache & Dr J Risk

For my bears

Abstract:

Stratified management of oral cancer – reducing side effects, improving outcomes

Rachel Catherine Brooker

This thesis aims to investigate potential avenues of personalising head and neck cancer care in order to offer improved outcomes, and where possible, reduce the impact of treatment related side effects upon quality of life.

The adjuvant management of locally advanced head and neck cancer utilises risk stratified radiotherapy with or without chemotherapy in order to reduce the chance of local recurrence and improve rates of cure. Unfortunately, despite these aggressive and complex management plans, survival outcomes remain poor, with patients living with an often extensive list of long term side effects which are challenging to manage and can severely impact upon patients wellbeing.

One such side effect is osteoradionecrosis of the mandible (ORN). ORN following head and neck radiotherapy can have a profound impact upon quality of life, whereby the mandible becomes exposed and a non-healing ulcer forms; leading to pain, poor function and in some, major corrective surgical procedures. Patients experience varying grades of ORN despite receiving identical treatment courses and it is currently difficult to predict who will experience this severe side effect prior to treatment. The individual radiosensitivity of normal tissues is likely to be influenced by common genetic variants, however in the past, work to identify these predictive biomarkers have focussed upon side effects which are subjective, difficult to quantify and poorly recorded/reported. By attempting to characterise which genetic alterations and radiotherapy doses make an individual more susceptible to ORN, it may be possible to alter radiotherapy dose constraints/treatment techniques thus improving the long term quality of life of patients with head and neck cancer.

Minimising standard of care therapy toxicities (such as ORN) will facilitate the future move to much needed escalated treatments for patients with poor prognosis locally advanced head and neck cancers. The addition of neo-adjuvant or additional

adjuvant anticancer drugs will be paramount in improving survival outcomes for this patient group. The recent NICE approval of checkpoint inhibitors as a first line treatment option for patients diagnosed with recurrent/metastatic head and neck cancer has spurred investigation of these agents in radical management strategies. This work will present initial results from one such phase II study (NICO trial), which has utilised checkpoint inhibition in the window of opportunity prior to cancer resection in a poor prognosis cohort (locally advanced oral cavity cancers) so as to improve outcomes and investigate response biomarkers. These biomarkers may, in the future, be used to allocate individual patients to the most beneficial treatment pathways.

The ultimate aim of this work is to promote personalised head and neck cancer care through discovering predictive biomarkers for developing long-term radiotherapy related toxicity and, (following the modification of the adjuvant management of locally advanced head and neck cancer) make future plans to discover response biomarkers.

Table of Contents:

Tables

Figures

List of Appendices

Acknowledgements

Firstly I would like to thank the Clatterbridge Cancer Charity for funding my research fellowship and the Liverpool Clinical Trials Centre and Aintree Research Forum for their support during my projects.

To the patients who took part in the NICO trial; your willingness to give up your time and take part in our study after receiving your diagnosis is humbling. Thank you for making this work possible.

It seems like a life-time ago turning up at the Cancer Research Centre never having picked up a pipette before! There are so many people I am thankful to, who took me under their wing, provided guidance and pearls of wisdom.

I consider myself extremely lucky for the opportunity to collaborate with John Fenwick and Phil Antczak; our discussions together would blow my mind but were so insightful and valuable.

I thank Neil Farquhar for his pep talks over our weekly cheese panini; Phil Gunning for his block slicing skills; Ben 'Chuck' Kita for sharing my passion for lasso and Laura Taylor for being my science sister in arms.

I will forever be indebted to Mike Davies, Lakis Liloglou and Janet Risk for their inspirational passion for research, unbelievable patience and boundless knowledge. A special thanks also to Richard Shaw and Christian Ottensmeier for your guidance and support. To Frances Greaney-Davies, I only wish we had become friends earlier; I would have been lost without you.

I'm not sure many students could call their supervisors friends but I am one of the lucky few. Thank you Joe Sacco and Andrew Schache; you taught me to find an open window when every door closes and I am so grateful to you both for believing in me.

Finally, but most importantly, the biggest thank you is to my family.

James, this thesis was built on your cups of tea and unconditional love; thank you for your unwavering support. My boys, Ted and Finn, you give me so much joy; I know you'll never read this, but it's all been for you.

Chapter 1
Introduction

1.1 Head and Neck Squamous Cell Carcinoma

Cancers arising from sites within the upper aerodigestive tract are commonly classified by their anatomical position within the head and neck (figure 1). These sites include the oral cavity, oropharynx, hypopharynx, larynx and nasopharynx. Other, rarer sites include salivary gland and paranasal sinuses. Head and neck cancers encompass a variety of histological subtypes, by far the most common are the squamous cell carcinomas, which are the focus of this work and will be explored in succeeding sections.

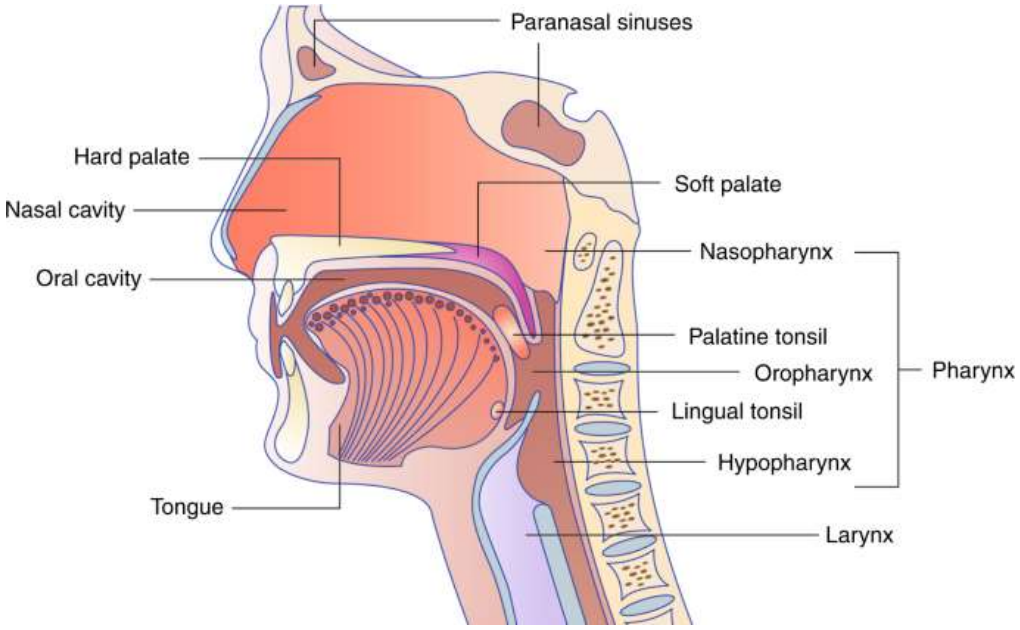

Figure 1: Anatomy of the head and neck. Image extracted from Sabatini ME, Chiocca S. Human Papillomavirus as a driver of head and neck cancers. Br J Cancer, 2020: 122; 306-314. https://doi.org/10.1038/s41416-019-0602-7 [1]

1.1.1 Incidence

The worldwide incidence of Head and neck squamous cell cancer (HNSCC) is estimated to be between 400,000 and 600,000 new cases per year with around 300,000 deaths [2, 3]. Subtypes of HNSCC are more prevalent in certain regions, such as oral cancer accounting for one third of cancer diagnoses within the Indian Subcontinent and nasopharyngeal cancer within Southeast Asia and China [4].

Within the United Kingdom (UK) there were 12,312 new HNSCC registrations in 2017, which represents 3% of all cancer cases, making it the 8th most common cancer [5]. These tumours predominantly affect males and present later in life with a steadily rising incidence from 40 years peaking around 70 years. HNSCC has a propensity for regions with higher levels of socioeconomic deprivation where poorer diet, smoking and excessive alcohol consumption can pose significant health challenges [6,7]. Despite declining numbers of smokers within the UK we are currently witnessing an increase in incidence of HNSCC across both sexes and subsites; across 2002-11 there was a 100% increase in oropharyngeal cancer cases and 50% increase in oral cavity cancer cases, which does not seem wholly attributable to rising rates of Human papillomavirus (HPV) (see section 1.1.2)[8].

1.1.2 Aetiology

There is a subset of patients diagnosed with HNSCC where environmental factors and viral infections are driving carcinogenesis (namely smoking and HPV infection). These exposures are partly responsible for the rising incidence of HNSCC and are discussed below.

1.1.2.1 Environmental exposures

Smoking is a well-recognised cause of HNSCC and a large proportion of cases in the UK are attributed to tobacco product exposure (e.g. 64% in laryngeal primary cancers [9]). Tobacco (with its additives) contains multiple carcinogenic compounds and instigates DNA damage through release of reactive oxygen species (ROS) and resultant oxidative stress. This leads to a chronic inflammatory state, impaired repair and genomic instability [10]. Continued smoking during and after HNSCC treatment not only increases chances of loco-regional relapse and with this inferior survival outcomes, but also leads to a rise in treatment related complications and second malignancies [11].

Similarly chronic alcohol consumption increases the risk of HNSCC development and negatively impacts upon overall and disease specific survival [12]. Again the mechanism by which this occurs is via the accumulation of ROS and the direct carcinogenic effect of acetylaldehyde which is an intermediary in the breakdown of

ethanol to acetate [13]. The International Head and Neck Cancer Epidemiology (INHANCE) consortium quantified the risk of alcohol consumption after examining 21,384 cases across all subsites of SCCHN and 30,651 controls. Both drinking intensity and duration were collectively associated with tumour development with those within the highest consumption brackets having odds ratios (OR) of 8.0 (95% CI: 4.6–13) for oral cavity, 12.9 (95% CI: 7.2–23.7) for oropharynx, 25 (95% CI: 11.6–51.5) for hypopharynx and 6.6 (95% CI: 4.9–9) for laryngeal cancers [14].

Other environmental factors can also significantly impact on the risk of developing HNSCC for example, areca nut/betel leaf chewing endemic in South East Asia accounting for the high rates of oral cancers, and excess salt cured fish consumption in parts of Southern China contributing to the elevated risk of nasopharyngeal cancer [4, 15]. Of note, betel quid related oral cavity cancer is now a concern within certain areas of the UK, especially those with large communities of individuals with south Asian heritage[16].

1.1.2.2HPV

HPV is a sexually transmitted, double stranded DNA virus which codes for the oncoproteins E6 and E7. E6 and E7 indirectly degrade and block the p53 and retinoblastoma (RB) proteins which negate their respective tumour suppressor properties and promote carcinogenesis [1]. Infection with this virus is a well-documented driver for the development of oropharyngeal cancer and the prevalence of this infection in European patients has been reported as 40-60% in one meta-analysis [17]. This link is less established in other HNSCC subsites where much lower HPV infection rates are observed e.g. 5% in oral cavity cancers [18]. Rising HPV infection rates (attributed to change in sexual behaviours and number of sexual partners) have contributed to the increased incidence of oropharyngeal carcinomas globally and patients affected with HPV related HNSCC are often younger, non-smokers with reduced alcohol intake [19]. There are considerable positive prognostic implications of HPV driven oropharyngeal cancers; although subsets of patients exist where coexisting environmental factors give rise to poorer outcomes (i.e. smokers) [20, 21]. Ang et al categorised patients into high, intermediate and low risk groups depending upon tumour stage, smoking habits and HPV status after reporting improved 3 year

overall survival of 82.4% (95% CI 77.2-87.6) for patients with HPV positive oropharyngeal cancer versus 57.1% (95% CI 48.1-66.1) for HPV negative tumours [22]. The development of HPV as a prognostic biomarker has led to its inclusion in staging considerations [23] and aided the design of multiple treatment de-escalation studies; the premise being to maintain improved survival outcomes whilst minimising the toxicities of multimodal therapies.

1.1.2.3Physical factors

6% of cancer cases across the UK are attributable to being overweight or obese (inclusive of HNSCC); while having a healthy diet, rich in vitamin C and folate are thought to be protective against oral cavity/pharyngeal cancer [9, 24].

Poor dental hygiene and resultant chronic periodontitis is a contributor to the development of HNSCC (in particular cancers of the oral cavity). The microbiome profile of the oral cavity has been mapped via the Human Oral Microbiome Database [25]. Over 700 species within the oral cavity create a delicate balance which can be tipped by poor diet, oral hygiene smoking etc., leading to dysbiosis. The result of this imbalance and subsequent chronic inflammation is thought to have an impact upon the development of local malignancies and also those elsewhere (e.g. NSCLC and colorectal cancer) [26, 27].

1.1.3 Genetic/Epigenetic changes

The genomic landscape of HNSCC is heterogeneous, reflecting, the different routes of oncogenesis and at least in part, the influence of HPV, chemical carcinogens and varying anatomical sites. Shared genetic mutations exist across anatomic subsites including TP53, CASP8, NSD1 and CDKN2A [28]. Most CASP8 mutations are evident in oral cavity tumours, whereas TP53, NSD1 and CDKN2A exhibited decreased mutation rates in oropharyngeal tumours [29]. The distinct genetic differences between HPV negative and positive HNSCC are outlined in table 1. HPV negative tumours predominately demonstrate inactivating mutations in CDKN2A, TP53, FAT1 and AJUBA along with greater frequencies of tyrosine kinase receptor amplifications (EGFR, ERBB2 and FGFR1). Whereas HPV positive tumours are characterised by a reduced mutational load, amplification of PIK3CA oncogene

and/or E2F1, the recurrent deletions and truncation of TNF receptor-associated factor 3 (TRAF3), and the mutation/fusion of FGFR2/3 gene [30, 28].

In addition to classifying genetic differences according to HPV status, further molecular classification exists which include basal, classical, mesenchymal and atypical subtypes. HPV negative tumours reside within classical and basal subtypes whereas HPV positive tumours tend to lie within the atypical and mesenchymal subtypes however overlap between sites and HPV status exist (figure 2) [28, 30].

HNSCC is driven not only by accumulating genetic mutations but also epigenetic modifications such as DNA methylation, small and non-coding RNA and histone alterations. The resultant changes in gene expression promoting carcinogenesis.

1.1.4 Tumour Immune Microenvironment

The tumour microenvironment consists of stromal cells (e.g. cancer-associated fibroblasts and endothelial cells), tumour infiltrating lymphocytes (TILs) (T and B cells) and myeloid cells (e.g. dendritic cells and myeloid derived suppressor cells) [29]. The activity, abundance and balance of immune cells, within the tumour microenvironment are pivotal in allowing the immune-evasion of cancers. SCCHN are known to create an immunosuppressive environment that down-regulates human leukocyte antigen (HLA) enough to evade immune detection. Antigen presentation is impaired by producing immunosuppressive cytokines such as interleukin-6 (IL-6) and transforming growth factor beta (TGFβ) whilst recruiting regulatory T cells (Tregs), myeloid derived suppressor cells (MDSC) and tumour associated macrophages (TAMs) [31]. Through expanding immunosuppressive cell populations, evading cytotoxic T cell recognition and immune cell dysfunction, tumour growth can continue.

There have been clear reported differences in the immune landscape between HPV positive and negative tumours. HPV positive having proportionally higher TIL densities, CD8+ T cells, Treg and NK cells with the opposite true of HPV negative disease.

Gene	Mutation	Prevalence	Function
HPV negative HNSCC			
TP53	Chromosomal loss at 3p/17p. Copy number alteration	Very common >80%	Tumour suppressor loss of function
CDKN2A/RBI	Chromosomal loss at 9p	Very common >80%	Tumour suppressor loss of function
HRAS	Activating mutation	5-10%	Activation of RAS pathway
CASP8	Inactivating mutation	Occurrence with HRAS mutation	Suppression of cell death
EGFR, ERBB2 and FGFR1	Amplification	Approx. 30%	Activation of receptor tyrosine kinase pathway
FAT1, AJUBA	Inactivating mutation/deletion	Common	WNT/b catenin signalling
NOTCH1	Mutation/deletion	Common	Differentiation
TP63	Gain of function	Common	Differentiation
HPV positive HNSCC			
E6/E7	Viral oncogene	100%	Cellular transformation/ Functional inhibition of p53/RB protein
CDKN2A/RBI	Low mutation rate, inactivation	Rare 5-10%	HPV driven
PIK3CA	Amplification / mutation	>50%	AKT/mTOR pathway
TRAF3	Truncation / recurrent deletion	10-15%	Uncontrolled NF-kB signalling
FGFR2/3	Alteration/oncogene fusion (FGFR3-TACC3)	>10%	Activation of receptor tyrosine kinase pathway
CD8 / CD56 / ICOS / LAG3 / HLA-DR	Elevated immune gene expression / enhanced immune cell infiltration	IMS subtype	CD8+ /NK cell infiltration

Table 1: Major differences in HPV positive and HPV negative genetic landscape. Adapted from Canning M, Guo G, Yu M, et al. Heterogeneity of the head and neck squamous cell carcinoma immune landscape and its impact on immunotherapy. Front Cell Dev Biol. 2019; 7:1-19. doi:10.3389/fcell.2019.00052

Overall The infiltration of CD8+ T cells is a positive prognostic factor in both HPV positive and negative patients and in addition, high proportions of infiltrating Treg (FoxP3) correlate to improved locoregional control and fewer lymph node metastases

[32,33] which is contrary to reports in other solid tumours. Keck et al and The Cancer Genome Atlas Network (TCGA) have suggested a new classification of SCCHN tumours based on gene expression profiling, within which there is an inflamed mesenchymal subtype belonging to both HPV related and non HPV related tumours and is represented by overexpression immune signatures such as CD8, ICOS, LAG3 and HLA-DAS [28,30].

PD-1 is present within the family of CD28/B7 receptors and expressed and up-regulated on activated immune cells and Tregs in response to chronic inflammation. Its presence is a hallmark of exhausted T cells and its main function is to limit auto-immunity thus preventing damage to normal tissues. Its ligands, PD-L1 and PD-L2, are expressed on antigen presenting cells and up-regulated on tumour cells. The PD1/PD-L1/PD-L2 pathways are exploited within the cancer process and enable the effective evasion of immune detection and destruction. PD-L1 seems to be overexpressed in the majority of oropharyngeal cancers with no preference to HPV positivity (71%) compared to HPV negative tumours (61%) [34]. Conversely within the oral cavity, where the proportion of patients with HPV positive tumours is below 5%[34], a much lower number of cancers expressing PD-L1 were reported; out of 217 patients 18.3% showed tumour PD-L1 expression (expression >5%) [35]. There is considerable heterogeneity in PD-L1 expression between studies and between tumour types [36, 37]. Although a metanalysis of PD-L1 expression in non-Head and Neck epithelial cancers was associated with poorer overall survival [36], an analysis of PD-L1/PD-1 status in 402 surgically treated head and neck cancer patients revealed that PD-L1 expression on tumour cells did not affect recurrence free survival or overall survival [37, 38].

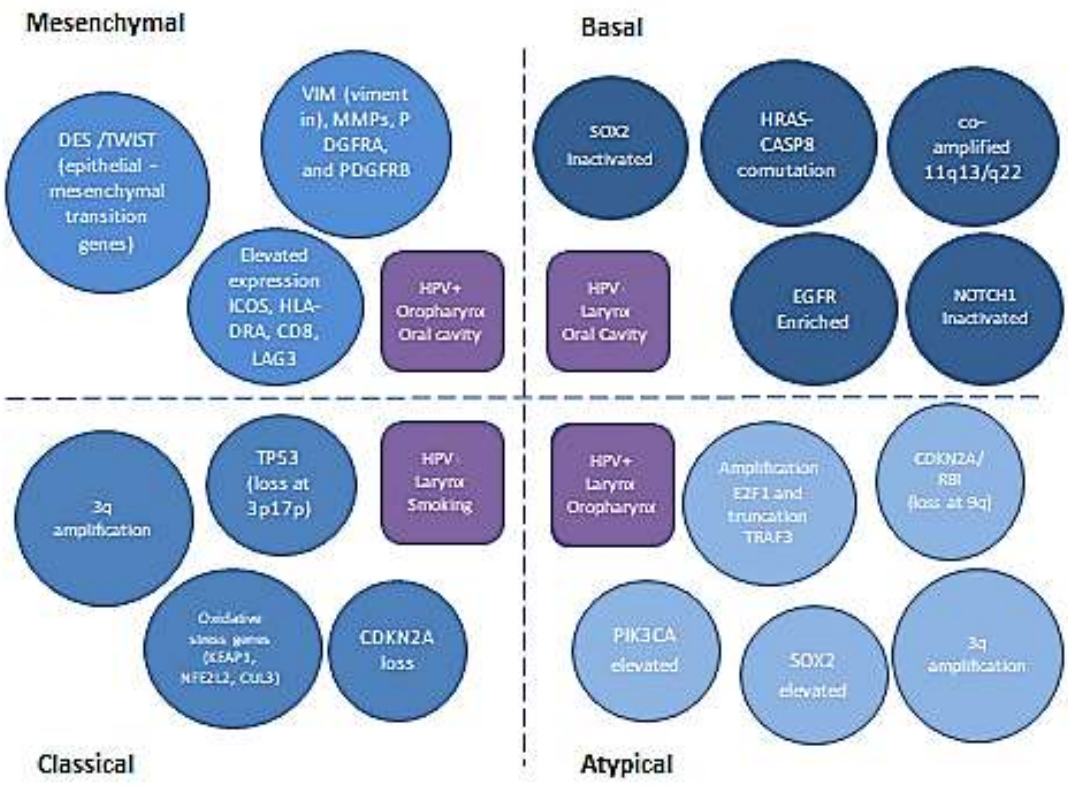

Figure 2: Schematic representation of molecular HNSCC classification and predominate HPV / anatomical subtype residing within each class.

1.2 Oral Cavity Squamous Cell Carcinoma

As discussed in section 1.1 primary malignancies originating within the oral cavity, pharynx (nasopharynx, oropharynx and hypopharynx), and larynx (supraglottis, glottis and subglottis) are encompassed within the HNSCC umbrella. This work will focus mainly upon malignancies arising from the oral cavity which includes buccal mucosa, retromolar, upper/lower alveolus and gingiva, hard palate, anterior two third/inferior tongue and floor of mouth subsites (figure 3).

Oral cavity tumours present multiple challenges; most notably poor outcomes for those with locally advanced disease (see section 1.3.2). Due to tumour location (and its consequent impact on nutritional state) and high incidence of comorbidities, smoking and alcohol misuse within this patient group, individuals often present with poor performance status, impaired nutritional reserve and psychosocial issues. In addition, these tumours require multimodal therapies including complex surgical procedures, radiotherapy and chemotherapy; with consequent high burden side effects, significantly impacting long term quality of life (see section 1.4).

Focussing upon the oral cavity tumours will provide a cohort of patients who will benefit from intensification of therapy and avoid the heterogeneity encountered between the subgroups, with findings (due to the low prevalence of HPV driven tumours [18]) applicable more generally to HPV negative disease.

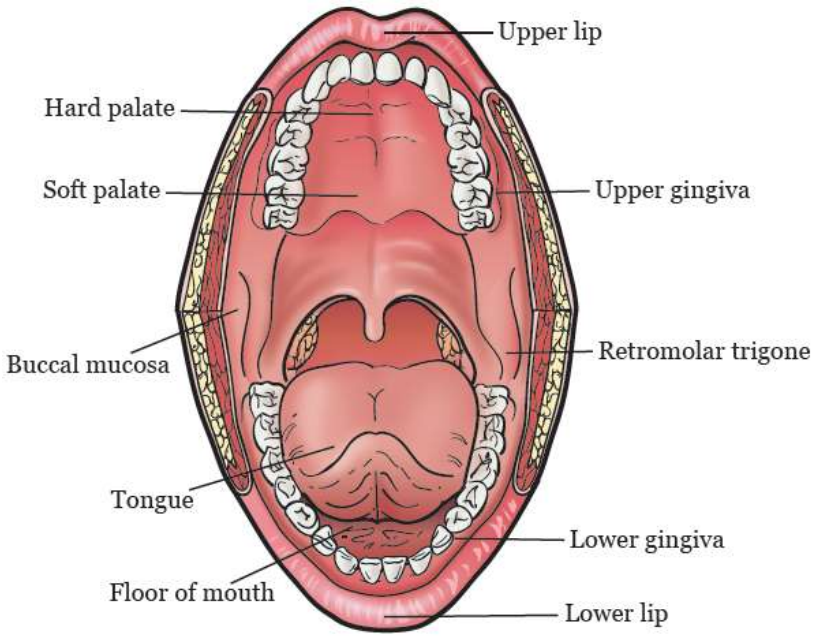

Figure 3: Anatomy of oral cavity. Extracted from Memorial Sloan Kettering Cancer Centre early- stage oral cavity cancer patient & caregiver education. Accessed 14/6/21 https://www.mskcc.org/cancer-care/patient-education/early-stage-oral-cavity [39]

1.2.1 Clinical presentation

Patients with oral cavity squamous cell cancer (OCSCC) can present in the following ways:

- Non-healing painful ulceration
- Lumps, white or red patches within the oral mucosa
- Loose teeth or poorly fitting dentures
- Mouth/jaw or ear pain
- Paraesthesia within oral cavity/face

- Neck lump
- Dysphagia, dysarthria and subsequent weight loss

1.2.3 Diagnosis

The diagnosis of OCSCC is suspected following examination by direct visualisation and palpation. Flexible nasendoscopy is helpful in assessing extent of disease, presence of second primary cancers and laryngeal function. Typically, a biopsy of the lesion will confirm the presence of invasive squamous cell carcinoma (see section 1.2.4). Radiological assessment with Magnetic Resonance Imaging (MRI) or computer tomography (CT) of the neck provides initial staging through describing the extent of the infiltrating lesion and presence/absence of metastatic nodal involvement [40]. Choice of imaging modality of the primary site is influence by accessibility to scanners (CT and/or MRI) and the preference of reporting radiologists. Neck ultrasound scan (USS) may confirm nodal involvement if difficult to appreciate on MRI/CT sequences. CT of the chest will inform if there are any concerning lung lesions suggestive of metastatic cancer spread.

1.2.4 Histopathology

OCSCC originates from mucosal stratified epithelium and can develop de novo or from pre-malignant areas of dysplasia (leukoplakia/erythroplakia). It follows distinct progressive steps from normal mucosa through to hyperplasia, then to dysplasia (mild, moderate, severe) and finally invasive carcinoma; incrementally accumulating genomic instability and driver mutations [41]. Each stage of progression is thought to be a result of tumour suppressor inactivation, e.g. p16 and 9p21 deletion in the transition from normal mucosa to hyperplasia and PTEN inactivation towards the later stages of carcinogenesis [42].

The diagnosis of SCC is classified histologically by the extent of cellular atypia and degree of keratinisation. Well differentiated SCC demonstrates organised tumour cells resembling normal epithelium and frequent keratin pearls, whereas poorly differentiated tumours are lacking in organisation or keratinisation, they have a high mitotic rate and nuclear pleomorphism [41]. The degree of SCC differentiation correlates closely with HPV status and OCSCC are noted to be predominately

well/moderately differentiated tumours (accounting for the low prevalence of HPV driven cases) [43] . Perineural and lymphovascular invasion (PNI/LVI) are examined during pathological assessment and are prognostic indicators conferring an increased risk of lymph node metastases/local recurrence and overall survival [44]. Information on pathological appearances (presence of extracapsular spread, margin status) and stage (see section 1.2.5) provides an overall picture of prognosis and guides adjuvant treatment strategies.

1.2.5 Pathological Staging

The pathological staging of OCSCC is described by the eighth edition of the American Joint Committee on Cancer (AJCC) [45]. This was revised in 2018 to incorporate depth of invasion and extracapsular spread (ECS) as both increase likelihood of locoregional relapse and negatively impact survival outcomes [46]. Tumour (T), nodal (N) and metastases (M) are scored and used to stratify patients into overall stage (see tables 2a and b).

Primary Tumour (T) pathological classification	
Tx	Primary tumour cannot be assessed
Tis	Carcinoma in situ
T1	Tumour ≤2cm with depth of invasion (DOI) ≤5mm
T2	Tumour ≤2cm with DOI >5mm and ≤10mm; or Tumour >2cm and ≤4cm, with DOI ≤10mm
T3	Tumour >2cm and ≤4cm, with DOI >10mm; or Tumour >4cm with DOI ≤10mm
T4a	Tumour invades through cortical bone of mandible, maxillary sinus or skin of face
T4b	Tumour invades masticator space, pterygoid plates, skull base or encases internal carotid artery.
Regional node (N) pathological classification	
Nx	Regional lymph nodes cannot be assessed
N0	No regional lymph node metastasis
N1	Single ipsilateral lymph node, ≤3cm without extracapsular spread (ECS)
N2a	Single ipsilateral lymph node ≤3cm with ECS; or >3cm ≤6cm without ECS
N2b	Multiple ipsilateral lymph nodes, ≤6cm without ECS
N2c	Bilateral or contralateral lymph nodes ≤6cm without ECS
N3a	Involved lymph node >6cm without ECS
N3b	Involved lymph node >3cm with ECS; or Multiple ipsilateral/contralateral/bilateral lymph nodes with ECS
Distant metastasis	
M0	No distant metastasis
M1	Distant metastasis

(a)

Stage	T	N	M
I	T1	N0	M0
II	T2	N0	M0
III	T3	N0	M0
	T1-3	N1	M0
IVA	T4a	N0-1	M0
	T1-4a	N2	M0
IVB	Any T	N3	M0
	T4b	Any N	M0
IVC	Any T	Any N	M1

(b)

Table 2: Oral Cavity AJCC Cancer TNM Classification (a) and TNM Staging (b) (eighth edition) [45]

1.3 Overview of radical treatment and outcomes

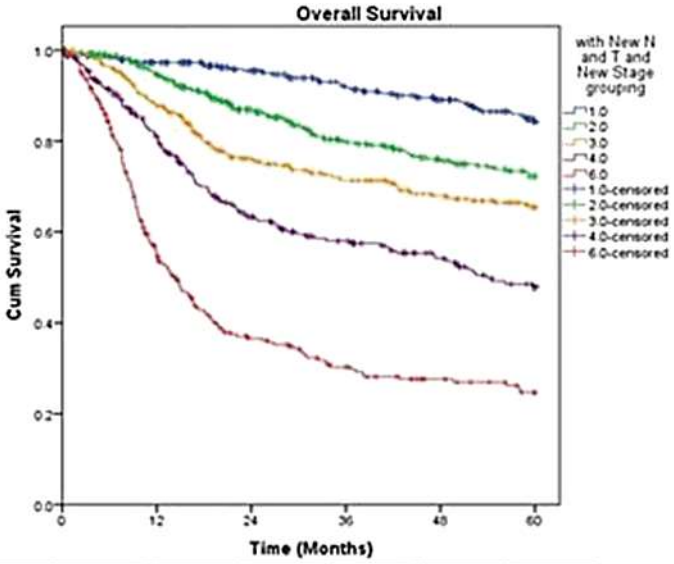

# of pts						
I	337	295	252	215	184	147
II	462	398	309	250	210	182
III	414	339	247	211	179	141
IVA	271	197	138	113	92	71
IVB	303	146	81	59	43	31

Figure 4: Overall Survival in Patients With Oral Cancer After Adjustment of Stage Groups (Memorial Sloan Kettering Cancer Center–Princess Margaret Hospital Data)[47]. Published in: William Lydiatt; Brian O'Sullivan; Snehal Patel; American Society of Clinical Oncology Educational Book 38505-514. DOI: 10.1200/EDBK_199697. [45].

Radical treatment strategies are informed by staging categories, patient comorbidities and fitness. These can be separated into early and locally advanced.

1.3.1 Early

Early OCSCC (i.e. Stage I and II) has favourable prognosis with 5 year survival figures range from 70-90% depending upon subsite [46]. It is treated surgically with excision of primary tumour plus reconstruction where required. This provides patients with optimal functional outcomes and avoids long term toxicities associated with primary radiotherapy however the latter may be employed for certain situations where patients are unable to tolerate surgical resection [48]. Management of the neck in early oral cancer is advocated over a watch and wait policy and whilst elective neck dissection is considered the gold standard for the treatment of possible occult cervical lymph node metastases, sentinel lymph node biopsy (SLNB) has been introduced and its use is consistent with National Institute for Clinical Excellence (NICE) guidance[49, 50].

1.3.2 Locally Advanced

Locally advanced OCSCC tumours require multimodality therapies i.e. surgery, radiotherapy (RT) and chemoradiotherapy (CRT) in order to offer patients optimal survival outcomes, however even with these complex treatment strategies 3 year survival rates approach 50% (figure 4) [51].

Surgical resection, neck dissection and reconstruction is the primary treatment of choice with reported 5 year disease specific survival (DSS) of 68% when compared to 12% for primary CRT in one phase III trial comparing the two modalities in the oral cavity subsite [52]. Retrospective studies have also reported improved outcomes for this strategy, the largest of which was a National Cancer Database Analysis including a propensity matched cohort of 2286 patients and concluded 3 year overall survival (OS) rate of 51.8% for surgery plus adjuvant RT versus 39.3% for primary CRT [53]. Primary radical CRT or palliative RT can be considered in individual cases where surgery is not feasible.

Complete tumour resection with a margin cut off of >5mm has traditionally been suggested in order to reduce the risk of local recurrence [54]. The existence of close

(≤5mm) or involved margins (≤1mm) along with other pathological risk factors (see Table 3) increases local recurrence rates and necessitates risk stratified postoperative adjuvant therapy in the form of RT or CRT [55,56]. Of note, retrospective data in patients with oral tongue cancers has shown that margins of ≤2.2mm increase locoregional relapse rather than the previous arbitrary figure of 5mm. Zanoni et al reported equivalent 2 year locoregional survival for patients with margins 2.3-5mm to those with margins of >5mm (93.5% and 91.8% respectively) however this study mainly included patients with T1 and T2 tumours so cannot be applied to patients with locally advanced disease [57]. In addition, Bajwa et al confirmed the association between margins of <1mm and unfavourable prognosis and emphasised the absent survival difference between those with traditionally classified 'clear' or 'close' margins [58].

High Risk	**Intermediate Risk**	**Low Risk**
ECS	T3/T4 tumour	T1/T2
Involved margin ≤1mm	LVI/PNI	N0 or N1
	Close margin ≤5mm	Margin >5mm
	N+	
	Poorly/moderately differentiated lesions	

Table 3: High risk features to suggest consideration of adjuvant CRT. For those with intermediate features clinicians may consider adjuvant RT.

The improvement in locoregional control (translating to survival benefit) offered by adjuvant RT was acknowledged in the 1970s, following this, publication of phase III randomised trials confirmed the advantage of treating in the postoperative period [59]. Examples being RTOG 73-03 which reported improved loco-regional control in patients with stage II-IV HNSCC (14% OCSCC) receiving 60Gy adjuvant RT when compared to 50Gy neo-adjuvant RT (2 year locoregional relapse rates 30% and 6% respectively) [60]. Along with Mishra et al demonstrating a 30% disease free survival advantage of adjuvant RT compared over observation alone in patients with locally advanced buccal SCC [61].

As reports of the additive benefit of concurrent chemotherapy with RT in patients with unresectable disease emerged, this approach was incorporated into the

adjuvant management of those with resectable disease with encouraging initial results [62]. Adjuvant CRT for patients with resected locally advanced disease and high risk features became standard of care following the results of EORTC 22931 and RTOG 9501 [63,64]. EORTC 22931 recruited 167 patients (28% OCSCC) to receive 54-66Gy in 33 fractions (#) of RT and 167 patients (25% OCSCC) to same RT regimen but with the addition of three cycles of concurrent cisplatin (100mg/m^2). All patients had locally advanced HNSCC (T3-4 N+ or T+ N2/3) and at least one high risk feature (positive surgical margins, PNI, ECS or vascular tumour embolism). Median progression free survival was 23 months (95% CI 33-75) in adjuvant RT group and 55 months (95% CI 33-75) in CRT group with an overall survival benefit for CRT of 13% at 5 years (hazard ratio (HR) for death 0.70 95%CI, p=0.02) [63]. These results were echoed in RTOG 9501 where patients (27% OCSCC) were randomised to the same treatment arms as in EORTC 22931 however alternative inclusion criteria (invasion of two or more lymph nodes, ECS and involved resection margins) and radiotherapy dose of 60-66Gy. Once again a significantly longer disease free survival was reported in CRT group compared to RT group (HR for disease or death 0.78, 95%CI 0.61-0.99, p=0.04) however this did not confer to an overall survival benefit (HR for death 0.84, 95% CI 0.65-1.09, p=0.19). Locoregional relapses were significantly reduced in CRT group (16%) when compared to RT alone (29%) [64]. The Pignon metanalysis confirmed the benefit of concomitant chemotherapy in patients with non-metastatic head and neck cancer in the post-operative (and radical) setting after including 87 trials [51]. There was an absolute benefit of 6.5% at 5 years with concomitant chemotherapy (HR 0.81 p<0.001) however this became less with increasing age, with hazard ratios approaching 1 in 61-70 age group (HR 0.88 95%CI 0.78-1.00) and over 70s (HR0.97 95%CI 0.76-1.23). Although these studies demonstrate the survival benefits of CRT in the adjuvant setting, documented rates of grade 3 toxicity (CTCAE v5.0 [65]) were more pronounced in combined treatment groups (41% vs 21% p=0.001 EORTC 22931 and 77% vs 34% p<0.01 RTOG 9501) and the rates of severe long term toxicities were similarly high in both study arms (EORTC 22931: 38% vs 49% and RTOG 9501: 17% vs 21%) [63,64]. These rates were reported in patients who were seemingly fit, with performance status 0-1 and younger than 70 years highlighting the importance of careful patient selection prior to embarking on such aggressive management regimes.

1.4 Adjuvant treatment considerations

1.4.1 RT dose, fractionation and timing

The principles of post-operative RT dose and fractionation proposed in the early 1970s still form the basis of treatment today. Fletcher championed elective neck irradiation in the radical setting after using 50Gy in 2Gy fractions to reduced regional recurrence rates from occult lymph node metastasis [66]. Prospective randomised trials reported improved local control for patients with locally advanced SCCHN receiving adjuvant radiotherapy with doses to the operative bed in excess of 57.6Gy; areas of high risk (involved margins and ECS) were boosted to 63Gy in 1.8Gy fractions without discernible improvement in control when escalating doses above this [67]. After confidence increased in the tolerability of fraction sizes >1.8Gy and with pressure to reduce RT treatment length, 2Gy fractionation became standard of care [63,64]. Interestingly, clonogenic tumour cell re-population during prolonged RT delivery (and between surgical resection and RT initiation), seemed to be influencing patient responses to a greater degree than other dosimetric factors [68,69]. The prolongation of overall treatment time is now widely recognised as an adverse predictor of outcome [70]; different groups have quoted a variety of time measures for example treatment package time (TPT), however it is generally accepted that a delay to initiation of RT of over 50 days negates the survival benefit offered by adjuvant treatment [71,72].

Investigation into RT hyperfractionation (dose delivered with typically twice daily fractions), RT acceleration (shortening time period over which a given dose is delivered) and a combination of the two began, with the hope of escalating dose intensity and reducing the impact of repopulation. In one metanalysis altered fractionation RT improved 5 year survival rates by approximately 3% with a greater absolute benefit in patients receiving hyperfractionation (8%) rather than acceleration (2%) and under 50s gaining the most benefit (HR 0.78, 95%CI 0.65-0.94) [73]. Although there is a clear, albeit modest, advantage to altered fractionation, it has not been adopted in routine UK clinical practice, due to the increase in short term side effects seen with this technique along with difficulties in service provision of bi-daily RT.

1.4.2 Cisplatin dose and frequency

Cisplatin chemotherapy was a natural choice for inclusion in radical and adjuvant regimes due to its well documented radiosensitising effects along with confirmation of activity in the recurrent/metastatic setting (see section 1.4.4) [74]. The optimum dose and timing of cisplatin concurrent chemotherapy has been an area of much debate and variation in practice exists [75]. Although standard of care of care is 100mg/m^2 on days 1, 22 and 43, a high proportion of patients (40%) who could not complete this notoriously toxic treatment triggered the adoption of alternative dosing regimens; the premise being to reduce toxicities, unscheduled treatment interruptions whist maintaining dose intensity [76]. The majority retrospective reviews have largely shown equivalence in efficacy when comparing high dose cisplatin with lower dose regimes (i.e. 40mg/m^2 weekly) however the side effect profile seems to swing towards a greater proportion of grade 3/4 myelosuppression for those having high dose and high grade mucositis with lower dose [77]. The non-inferiority randomised controlled trial conducted by Noronha et al, examined using 30mg/m^2 weekly versus 100mg/m^2 every three weeks with adjuvant radiotherapy in a population with a high proportion of OCSCC (approximately 90%). 2 year local control was superior in the high dose arm 73.1% compared with 58.5% in the weekly arm (p0.014; HR 1.76 95%CI 1.1- 2.8) with a cost of increased acute high grade toxicity (84.6% vs 71.6% p 0.006) [78]. The comparator arm being below 40mg/m^2 within this trial still led to unanswered questions over whether higher weekly doses would have altered findings. Following the suggestion of a possible cumulative dose-response relationship to cisplatin administration by MACH-NC meta-analysis [51] subsequent prospective data has confirmed survival advantage when patients receive cumulative doses of 200mg/m^2 with models suggesting an increase in absolute OS benefit of 2.2% (95%CI 0.4-4) for every 10 mg increase in cumulative cisplatin dose [75]. Despite the uncertainty over optimal cisplatin dose/timing schedules, the extremely high rates of acute toxicity and unplanned dosing omissions during adjuvant treatment once again highlight the need for an alternative treatment approach in individuals whose poor physical fitness may preclude cisplatin administration.

1.4.3 Evolving radical treatment strategies

Due to the pronounced adverse effects of adjuvant regimes and the high rates of locoregional relapse despite maximal multimodality therapies there is naturally enthusiasm to develop alternative options for radical treatment, particularly for those with pre-existing comorbidities. In the oropharyngeal subsite, focus has turned to de-escalation strategies where the positive outlook awarded by HPV positive tumours lends to prioritising long term side effect reduction. The converse is true in OCSCC, where attention is turned to intensifying therapies with newer agents in order to improve outcomes without increasing severity of current side effect profiles. Evidence supporting the use of systemic anticancer agents in the metastatic setting have strengthened hypothesis that these treatments may offer a survival advantage in the radical setting.

1.4.4 Current active systemic anticancer agents in HNSCC

There are a variety of active agents which can be utilised in the management of HNSCC however traditional chemotherapies are limited in offering survival benefit and bring the burden of significant side effects. Prior to the approval of cisplatin in the 1970's, methotrexate (MTX) and bleomycin were the most frequently utilised cytotoxics. The antitumour activity of cisplatin in HNSCC was confirmed by Jacobs et al in 1980 and subsequent phase III trials systematically investigated differing platinum doublet combinations [79]. Forastiere et al confirmed superior response rates when cisplatin was combined with 5-fluorouracil (32% vs 10% single agent), however an overall survival advantage of cytotoxic agents in recurrent/metastatic HNSCC was only confirmed following the publication of the EXTREME trial in 2008 [80, 81]. This phase III trial reported an overall survival advantage of 10.1 months versus 7.4 months when the epidermal growth factor receptor (EGFR) inhibitor cetuximab was added to platinum and 5-fluorouracil (5-FU) in the first line setting. In the UK, NICE took the decision to approve this regime in the oral cavity site alone where hazard ratios approached 0.4 (CI 0.26-0.63) in an unplanned analysis [82].

There has been a dearth of options for patients who had progressed following first line platinum regimes; both methotrexate and taxanes can be used in the second line but result in modest response rates, lack a proven overall survival benefit and

patients are often too unwell from their advancing disease to withstand the side effects of these agents [83]. In addition to the use of standard cytotoxics, the use of newer, targeted agents such as bevacizumab (antiangiogenic monoclonal antibody) and panitumumab (anti-EGFR monoclonal antibody) have limited efficacy in the metastatic setting with higher rates of grade 3 toxicities than standard of care chemotherapies [84, 85].

The immune checkpoint inhibitors (ICI) have renewed optimism in improving HNSCC outcomes and expanding treatment options. The PD-1 and PD-L1 inhibitors (e.g. pembrolizumab, nivolumab, durvalumab) target and abrogate key immune evasion mechanisms; activating the immune response against malignant cells [86]. The safety and activity of these agents in R/M HNSCC have been confirmed in the Keynote-012 trial with a response rate of 18% to pembrolizumab in patients whose tumours were PD-L1 positive [87]. Similar findings were observed in the phase II Keynote-055 study with a response rate of 16% and 15% adverse events (>/= grade 3) [88]. Durvalumab has also proven to be efficacious and safe with response rates of 12% and minimal grade 3 AEs (8%) in a heavily pre-treated population [89]. The phase III CheckMate 141 study subsequently demonstrated a survival benefit for patients with metastatic HNSCC receiving nivolumab in comparison to single agent methotrexate, docetaxel or cetuximab. Median overall survival was 7.5 months (95% CI 5.5-9.1) in the nivolumab group compared to 5.1 months (95% CI 4.0-6.0) in the standard therapy group with fewer grade 3/4 side effects along with delayed time to deterioration in quality of life [90, 91]. Updated long term follow up data reported a consistent overall survival benefit and estimated 24 month overall survival rate of 16.9% with nivolumab [95% CI 12.4%–22.0%]) compared with 6.0% in the standard therapy population [95% CI 2.7%–11.3%] [92]. A further phase III study (Keynote-040) in the same setting examined the use of pembrolizumab versus investigators choice of chemotherapy. This showed similar results with updated survival analysis from reporting an improvement in median overall survival in the intention to treat population (8.4 months vs. 6.9 months; HR = 0.8; 95% CI, 0.65-0.98); this benefit was more pronounced in those with PD-L1 combined positive score greater than 1 and PD-L1 tumour proportion score ≥50% [93]. Following on from this the Keynote-048

study reported improved outcomes when pembrolizumab as monotherapy and in combination with cisplatin/5FU chemotherapy was compared to EXTREME regimen (HR 0.71 95% CI 0.57, 0.89 and 0.62 95% CI 0.50, 0.78 respectively) [94]. Objective response rates were 19% (49/257) in those with combined positive scores of ≥1 treated with pembrolizumab monotherapy with 51% of patients in this group alive at 12 months. Median response duration was 23.4 months with 55% (164/300) reporting all cause grade 3+ adverse events in those having pembrolizumab monotherapy compared to response duration of 4.5 months and grade 3+ adverse events in 83% (239/287) of those having chemotherapy and cetuximab.

Following this, nivolumab and pembrolizumab have been approved by NICE in the R/M setting, and have become part of standard of care in the UK (figure 5) [95]. A raft of further studies are investigating other anti PD1/PDL1 agents (e.g. durvalumab) in R/M HNSCC, combinations of alternative ICI (e.g. CTLA-4 inhibitors) and also combinations utilising radiotherapy, the results of which are awaited.

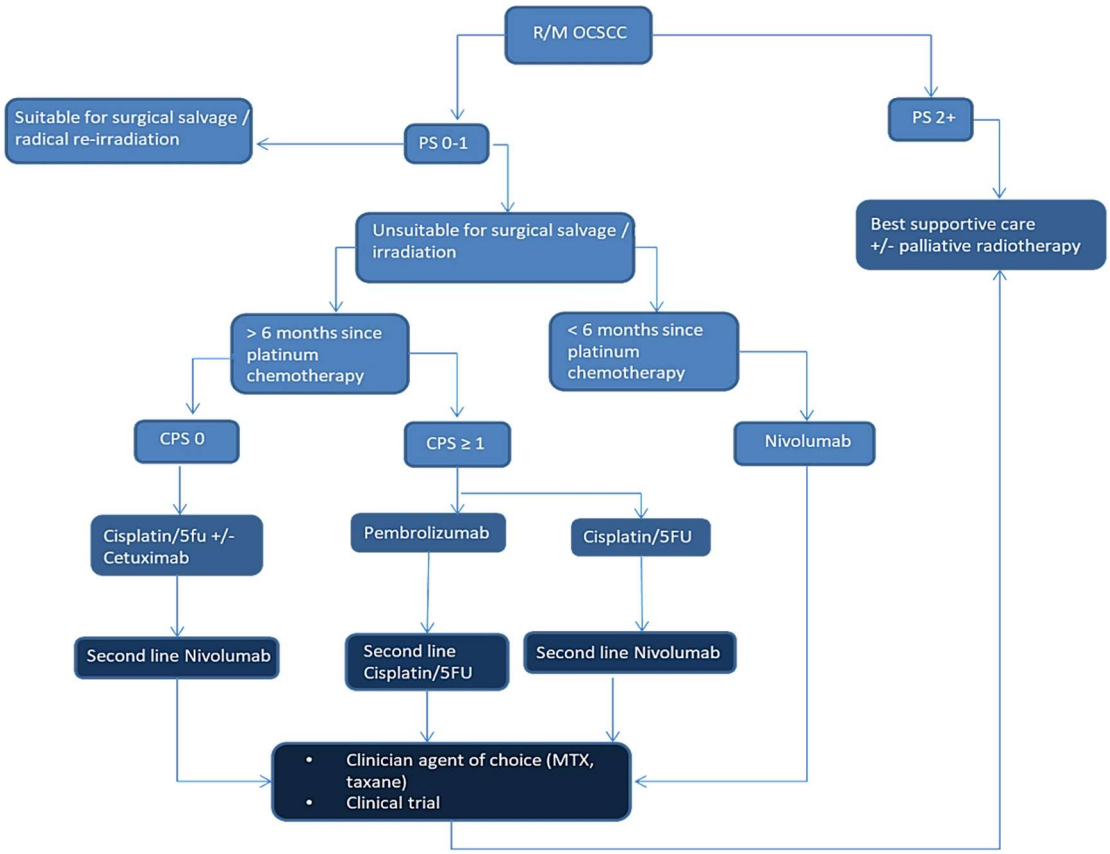

Figure 5: Options for treatment of metastatic OCSCC in the UK.

1.4.5 Intensification of radical treatment

Previous attempts to escalate radical treatments for those with poorer prognosis tumours have included using the traditional chemotherapies and additional concurrent agents. The routine use of neoadjuvant chemotherapies in OCSCC is generally not supported following the absence of demonstrable survival benefit when cisplatin/5FU containing regimens were administered to patients with locally advanced disease prior to radical surgery [96]. Despite this, Bossi et al demonstrated that patients with pathological complete responses at surgery had higher 10 year overall survival figures than those without (76.2% versus 41.3%, P=0.0004) [97] and Zhong et al reported an 80% response rate following neoadjuvant taxane/cisplatin/5FU administration in a cohort of over 250 patients with locally advanced OCSCC [98] .

Similarly intensification with anti - EGFR monoclonal antibodies either concurrently (in addition to RT and concurrent chemotherapies) or neoadjuvantly have failed to offer improved overall survival outcomes but have added significantly to treatment toxicities. One such study was the phase III GORTEC 2007-01 study which recruited over 400 patients with locally advanced HNSCC and failed to improve overall survival after adding cetuximab to RT and concurrent carboplatin/5FU chemotherapy; there was however, an improvement in 3-year PFS rates of 52.3% compared to 40.5% in the cetuximab plus RT arm [99].

The immune checkpoint inhibitors (ICI) may be ideal candidates for intensification in radical therapy for locally advanced OCSCC. As outlined in section 1.5.1, they are a relatively new class of agent that have activity in metastatic SCCHN. Most evidence around their use involves Programmed Death 1 (PD-1) and PD Ligand 1 (PD-L1) inhibitors, which are generally well tolerated and are associated with better quality of life compared to chemotherapy [100]. The longevity of response in some has led naturally into the expectation of priming the immune system prior to CRT/RT and enables treatment with these agents where tumour burden is low and overall fitness is optimal.

1.4.6 Emerging evidence (neo)adjuvant ICI HNSCC

Hypotheses that ICI may improve outcomes when used in the locoregional management of OCSCC have been strengthened by studies in melanoma and non-small cell lung cancer where the use of adjuvant ICI has improved recurrence free survival for patients with high risk locally advanced disease [101, 102] . There is much speculation as to how these drugs will integrate into the multimodality treatment of HNSCC and is the focus of the work outlined later in this thesis. Early data supporting the use of ICI in the (neo)adjuvant setting in HNSCC will be discussed at length in Chapter 3 along with novel study design investigating the feasibility of integrating into the management of OCSCC.

1.5 Treatment Toxicities

The short term complications of adjuvant treatment are numerous and have a profound impact upon treatment tolerability and delivery (table 4). Rates of grade 3+ toxicities during adjuvant RT and CRT are as high as 34 and 77% respectively and lead to high proportions of unscheduled hospital admissions [64,103]. Similarly long term side effects can have devastating consequences on patient quality of life and wellbeing; one such toxicity being osteoradionecrosis of the mandible.

1.5.1 Osteoradionecrosis of the mandible

Osteoradionecrosis (ORN) of the mandible is characterised by the presence of non-healing, necrotic bone for longer than 3 months in an area previously exposed to radiotherapy without evidence of recurrent tumour [104]. ORN usually presents 6 months to 1 year after irradiation however there are reports of it occurring years after treatment and the risk remains high life-long [105]. The severity of ORN can vary from a small non healing area within the alveolar margin to pathological fracture and skin fistulae which is understandably detrimental to patient's function and quality of life [106]. It is most likely to occur in patients who have sustained higher doses of radiation to the mandible during their course of treatment, those who go on to have dentoalveolar surgery, smoke, drink alcohol to excess and have poor oral hygiene [107]. Modern series set within the intensity modulated radiotherapy (IMRT) era quote an incidence between 4-8% in patient cohorts predominantly treated with radical CRT and oropharyngeal site [108, 109] .

Expected	RT Short Term	RT Long Term	Additive Cisplatin toxicity
Expected 50-100%	Mucositis	Skin fibrosis	Mucositis
	Thick, sticky secretions	Skin pigmentation	Nausea/vomiting
	Loss of taste	Dry mouth	Diarrhoea
	Dry mouth	Taste change	Lethargy
	Skin soreness	Lymphoedema	Taste change
	Patchy hair loss		Loss of appetite
	Lethargy		
Common 10-50%	Swallowing difficulty (requiring feeding tube)	Hypothyroidism	Kidney injury
	Hearing change	Trismus	Neutropenic sepsis
			Anaemia
			Thrombocytopenia
			Electrolyte disturbance
Less Common <10%	Laryngeal oedema	Swallowing difficulty (requiring feeding tube)	Tinnitus/hearing loss
	Aspiration pneumonia	Chondronecrosis of larynx	Peripheral neuropathy
	Dehydration	Osteoradionecrosis of mandible	Arrhythmias

Table 4: Expected, common and less common acute and long term side effects of RT with additive cisplatin side effects. Adapted from Royal College of Radiologists National Radiotherapy Consent Form – Head and Neck Cancer (lower sites) [110]

1.5.1.1 Grading

There have been various suggestions regarding severity classification for ORN however the Notani grading (figure 6) is now the most widely adopted and focusses on clinical/radiological appearances of ORN for risk stratification and treatment decision making [106]. Three scoring grades exist; grade 1 where ORN is confined to alveolar bone, grade 2 where ORN remains above the level of inferior alveolar canal (IAC) and finally grade 3 where ORN extends past the level of IAC, causing fistula and/or mandibular fracture. Shaw et al proposed an additional classifier whereby the area of exposed bone is taken into account [111]. This facilitates the appreciation of smaller 'minor bone spicules' in which mucosal healing occurs spontaneously thus preventing over-diagnosis of clinically insignificant lesions.

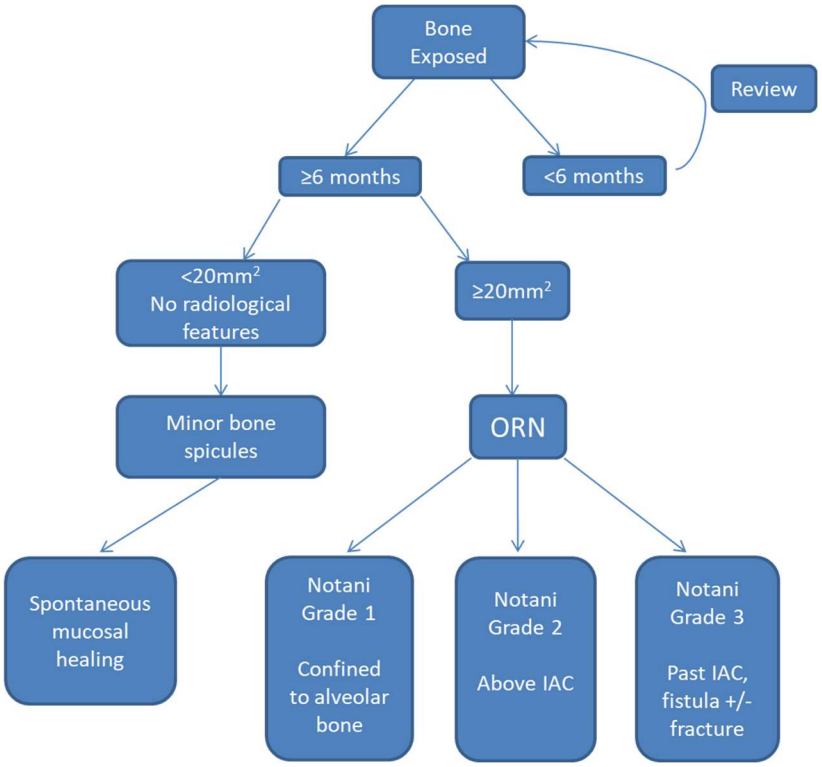

Figure 6:Notani classification of ORN, incorporating additional proposed 'minor bone spicules', adapted from Shaw et al, Oral Oncology 64 (2017) 73–77[111]. IAC: Inferior Alveolar Canal.

1.5.1.2Pathophysiology

The pathophysiology of ORN is still not completely understood and theories have evolved from infection following trauma after RT to RT induced cellular and vascular damage leading to hypoxia and tissue breakdown [112, 113]. More recently, radiation induced fibrosis has been linked to reactive oxygen species created by the acute inflammatory response. This seems to cause abnormal myofibroblasts to form which, in turn, leads to dysregulation of collagen, tissue remodelling, fragility and fibrosis [114]. The promotion of fibrosis and resultant prevention of effective vascularisation has been confirmed through the examination of dento-alveolar bone cores following irradiation; a reduction in microcapillaries correlating to increasing RT doses [115].

1.5.1.3Management

Treatment for patients who have developed this complication remains a great challenge and individuals frequently suffer considerable discomfort, repeated infections with very slow healing times and compromise to functions associated with normal daily living. A variety of treatment modalities have been recommended

including surgical debridement with or without hyperbaric oxygen therapy (HBO) and medical treatments such as combined Pentoxifylline and Tocopherol [116, 117]. The lack of robust randomised control trial evidence, disparities in clinical outcomes and treatment cost implications has, however, resulted in variations in practice that are both broad and inconsistent. The recently reported HOPON trial was set up to clarify whether HBO would prevent ORN in a high risk patient population (surgery/dental extraction in the irradiated mandible). Surprisingly the incidence of ORN in their patient cohort was much less than previously reported at only 6% and so the use of HBO could not be supported in the prevention of ORN [118]. The closed DHANCA 21 (NCT00760682) trial has the potential to shed more light on whether hyperbaric oxygen will have a place in the treatment of established ORN. Despite limited evidence, the use of Vitamin E and Pentoxifylline in combination with Clodronate (PENTOCLO) or Doxycycline has been advocated for those with less severe forms of ORN [119]. The soon to open, NIHR funded, RAPTOR trial will finally determine the efficacy of this medical management in a non-randomised trial of PENTOCLO versus supportive measures [120]. In those with treatment refractory or advanced ORN, surgical intervention, typically involving resection of involved bone and microvascular reconstructive surgery is frequently undertaken [117].

1.5.2 Why do patients get RT toxicity?

As with all tumour sub-sites, head and neck radiotherapy aims to achieve maximal cancer cell kill with minimal impact upon surrounding normal tissues. Unfortunately, due to the anatomy of the head and neck there are a number of vitally important structures in close proximity which can suffer long term damage from radiotherapy to this area e.g. spinal cord. Although three-dimensional conformal radiotherapy brought improved dose distribution when compared with two-dimensional techniques, patients would still develop profound acute and late toxicities due to the unavoidable inclusion of normal tissues in the radiation field. The development of intensity modulated radiotherapy (IMRT) revolutionised the treatment of head and neck cancers; larger beams were split into many smaller 'beamlets' of varying intensity in order to produce unrivalled dose distribution [121]. For the first time we were able to create shaping similar to target structures and rapid dose fall-off in order

to achieve improved target coverage whilst maintaining constraints to nearby normal structures [122]. With this success came challenges; stretching departmental resources with complex planning delivery and increased treatment times. Along with this was the possibility of the exposing previously untreated tissues to a low 'beam path' dose with the now increased number of beams required to meet the stringent planning optimisation parameters. Subsequent volumetric modulated arc therapy (VMAT) has now become commonplace and has been successful in shortening treatment delivery times, through dynamic gantry rotation, dose rate and collimator leaflet positioning during RT delivery [121].

Each organ at risk encountered will have deterministic dose effect; a threshold radiotherapy dose at which damage occurs and causes reversible dysfunction leading to acute side effects, and irreversible damage resulting in long term sequelae. The doses reported were first described by Emami and based upon traditional 2DCRT [123]. As techniques became more sophisticated the QUANTEC papers were released in order to standardise the normal tissue dose constraints used in 3DCRT planning [124,125]. The principles of these dosimetric limitations hold true in the IMRT era however complications arise when considering the radiobiological properties of individual organs and the implications of increased 'beam path' low dose treatment exposures.

1.5.3 Evidence in organ sparing techniques

Within the head and neck, the most frequently experienced long term side effect following RT is xerostomia and as such sparing the parotid glands have been the focus of investigation in order to improve long term quality of life outcomes. In the PARSPORT clinical trial, IMRT was compared to conventional RT in both the radical and post-op setting (60-65Gy in 30#) [126]. Nutting et al reported an absolute reduction in the rate of G2+ xerostomia at 12 months of 35% (95%CI 14-56 p0·003) when the mean dose constraints of 24Gy to the contralateral parotid were used during IMRT delivery. Other retrospective series have reported improved xerostomia rates (without compromising on locoregional recurrence rates), after reducing the parotid mean doses by limiting the superior contralateral field extent in the elective treatment of uninvolved neck [127,128]. As we now have the ability to keep undesired

dose within organ tolerance, for the first time structures which have previously been overlooked are being contoured and dose constraints taken into account to prospectively evaluate if improvement in patient toxicity can be achieved. The DARS study used dysphagia optimised radiotherapy by sparing the swallowing structures outside high dose target volume in patients with T1-4 oropharyngeal and hypopharyngeal cancers [129]. There was an improvement in reported patient swallowing function with this approach and subsequently dysphagia optimised radiotherapy is beginning to move into routine practice. Not all normal tissue sparing trials have shown positive outcomes. The COSTAR trial spared the ipsilateral cochlear from RT mean doses above 35.7Gy (cochlear tolerance 40-45Gy) in patients receiving post-operative RT following resection of parotid tumours [130]. There was no difference in post treatment hearing loss when compared to 3D conformal RT, however in using this technique, there were higher rates of long term xerostomia presumably due to higher contralateral parotid doses delivered and beam path involvement of minor salivary glands. This study speculated that the previously presumed threshold tolerance for the cochlear may be too high, and reinforced the requirement for normal tissue tolerance modelling in the IMRT era.

1.5.4 Mandibular RT tolerance

It has been well documented that the use of IMRT has reduced the incidence of mandibular ORN, however, there are few verified dosimetric parameters setting out mandibular constraints for RT planning [131]. As such, routine practice is to avoid high dose spots (Dmax 60-70Gy) within the mandible outside target volumes which may be compromised on a case by case basis in order to achieve optimal coverage elsewhere.

The MD Anderson group published a retrospective matched plan analysis of 68 cases and 131 controls with oropharyngeal cancers receiving definitive RT [132]. Dose-Volume Histogram (DVH) bins for the volume of the mandible receiving 35Gy to 70Gy were significantly higher in those who developed ORN. 80% of cases had a volume receiving 44Gy≥42% and 58Gy≥25% which led to recommending these parameters as mandibular constraints. Similarly other dosimetric evaluation series have quoted volume receiving 60Gy as the best predictor for future ORN development, others

volume receiving 50Gy [133, 134]. Interestingly Owosho et al dosimetrically analysed the specific ORN site in 44 patients who developed ORN after radical treatment (n=12 OCSCC) and reported that 96% of ORN-affected regions of the jaw received over 60Gy [135]. Following this, lower mean mandibular doses were achieved when patients with oropharyngeal cancer were treated with radical intensity modulated proton therapy (IMPT) as compared to IMRT (25.6Gy vs. 41.2Gy for IMRT, $P < 0.001$). The retrospective data collection and disparity in patient cohorts (IMPT n=50, IMRT n=543) meant the lower incidence of ORN in the IMPT group could only be suggested rather than firmly attributed to the alternate RT technique.

Although dosimetric parameters have a pronounced effect on ORN development, there are still patients who receive high dose RT to the head and neck with large mandibular volumes and do not develop this complication. Clearly dosimetric parameters are only part of the picture (figure 7).

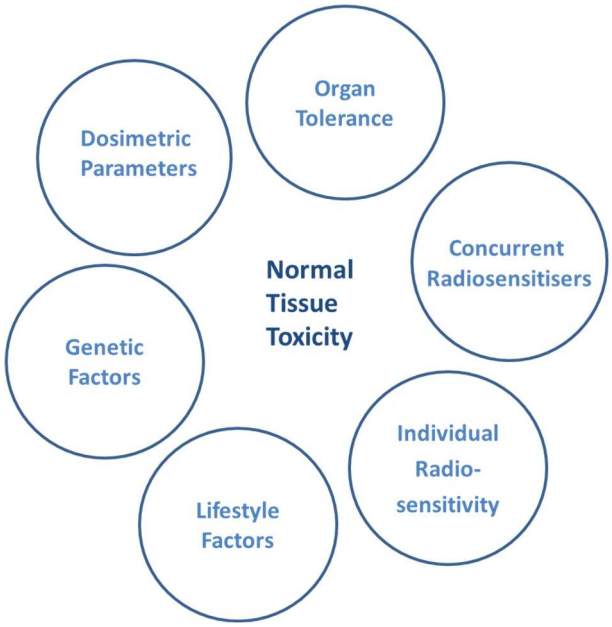

Figure 7: Contributing factors to normal tissue toxicity following RT.

1.6 Radiogenomics

There is an ever growing body of evidence supporting the hypothesis that genetic variation contributes to the development of radiotherapy toxicity [136]. The construction of polygenic risk models will move further towards developing predictive assays and subsequent personalised radiotherapy strategies (figure 8).

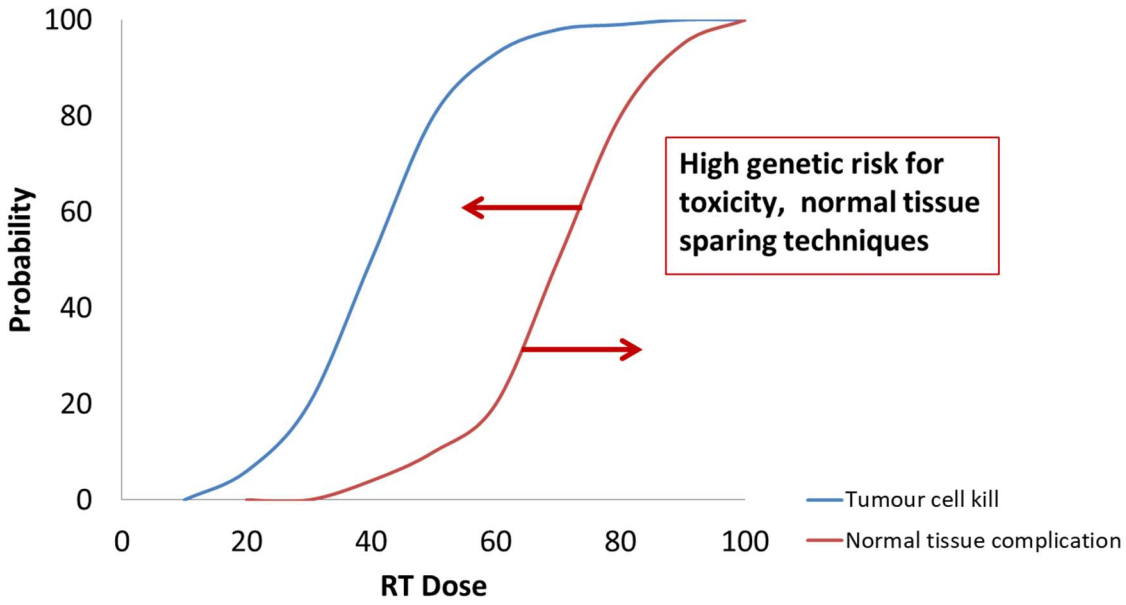

Figure 8: Example of theoretical change in normal tissue RT tolerance depending upon genetic risk. As radiation dose increases so does the likelihood of tumour cell kill (blue line) and normal tissue toxicity (red line), with genetic prediction assay there may be freedom to escalate doses in a proportion of cases.

1.6.1 Evidence from candidate gene studies

A number of studies have investigated the impact of common genetic variation upon the risk of long term toxicities (including ORN) following radiotherapy to the head and neck. Lyons et al [105] reported an association between functional polymorphisms in the TGF-β1 gene with ORN after examining 140 patients of multiple head and neck cancer sites treated with external beam radiotherapy (EBRT), brachytherapy and concurrent chemoradiotherapy (CRT). After comparing 39 patients with ORN and 101 without they concluded that the presence of the T variant allele at SNP rs1800469 increased the risk of developing ORN with odds ratio (OR) of 5.7 (95%CI 1.7-19.2) for homozygote and 3.6 (95%CI 1.3-10.0) for heterozygote. Danielsson et al [137] also investigated SNPs associated with ORN and focussed upon genes that had an impact upon the oxidative stress response. They examined SNPs within OGG1, MTH1, CAT, SOD2A, NOS3, GSTP1, GSTA1 and NFE2L2. Out of 74 patients, 37 had developed ORN within a 24 month time-frame following EBRT treatment. The presence of a G allele at SNP rs1695 (GSTP1 gene) seemed to increase the chance of developing ORN with OR 4.36 (95%CI 1.24-15.33). In addition to this, Borchiellini et al [138] reported ORN and skin fibrosis as end points. The genes examined within this cohort of 122 patients with oropharyngeal, hypopharyngeal or laryngeal cancer were again those involved

in DNA repair; XRCC1, ERCC1, ERCC2, ERCC5 along with TP53 and MDM2. The Pro allele of TP53 (rs1042522) was associated with increased chance of developing ORN and TT genotype of rs1047768 (ERCC5 gene) implicated in the development of late skin fibrosis. Alsbeih et al [139] further characterised the role of XRCC1 (rs25487) and TGF-β1 (rs1982073) in the context of subcutaneous fibrosis in a cohort of 60 patients with nasopharyngeal carcinoma who had received either EBRT or CRT as their treatment. The presence of C allele at rs1982073 was protective against subcutaneous fibrosis with OR 0.41 (95%CI 0.20-0.86) and similarly A allele at rs25487 OR 0.30 (95%CI 0.10-0.89).

A number of other studies have taken a different approach in concentrating on acute rather than long term side effects of RT; with the most heavily investigated SNPs lying on the X-ray Repair Cross Complementing Group 1 (XRCC1) gene. This gene encodes the XRCC1 protein which is known to participate in the base excision repair pathway in response to single strand DNA breaks following exposure to ionising radiation [140]. Pratesi et al [141] were the first group to assess rs25487 (XRCC1) in relation to the development of mucositis, skin erythema and dysphagia in 101 patients with a wide variety of head and neck cancers following RT/CRT. They concluded that the presence of the A allele increased individuals risk of developing oral mucositis 3.01 (95%CI 1.27-7.11). Li et al and Chen et al similarly found that the same genotype was associated with acute side effects in patients with nasopharyngeal carcinoma, they reported an increased risk of grade 2/3 acute dermatitis with an OR 2.65 (95% CI 1.04-6.73) and 2.860 (95% CI 1.354-6.043) respectively [142,143] . Contrary to these reports Venkatesh et al did not find a significant association between SNPs within XRCC1 (including rs25487) and acute toxicities after examining a cohort of 183 patients with a plethora of primary head and neck cancer sites[144]. This group also focussed on a further SNP (rs1805794) within NBN gene (whose coded proteins play an essential part of DNA damage recognition and repair) and showed that the genotype CC increased the risk of developing oral mucositis (OR 3.75 (95% CI 1.201-11.70)). Other XRCC1 SNPs have been studied such as rs1799782 by Nanda et al and found to be linked to oral mucositis, dermatitis and laryngeal toxicity with OR 2.91, 5.076 and 5.0 respectively [145] . SNPs within other DNA damage repair genes and genes triggered

in response to reactive oxygen species have been implicated in the development of acute toxicities following head and neck RT/CRT namely Ku70 (rs132788, rs2267437), XRCC3 (rs861539), GSTP1 (rs1695), GSK3B (rs37557) and APC (rs454886) [137,146,147,148].

1.6.2 Evidence from Genome Wide Association Studies (GWAS)

With the development of genome wide association studies (GWAS) we are now able to examine the causal link between common genetic variants by using SNP arrays without prior hypothesis. This approach can identify new candidate genes however still requires detailed knowledge of the biological pathways involved so as to interpret the significance of identified SNPs and complete subsequent validation studies. These studies are limited when sample sizes are small and with demographic diversity, they are also open to the possibility of false positives due to multiple testing.

Following the formation of the Radiogenomics Consortium, large genome wide association studies and meta-analyses have taken place focussing on the risks of radiotherapy related toxicities in prostate, breast and lung cancer [149]. The first of which was Kerns et al (2010) who successfully identified an association between SNPs within FSHR gene and erectile dysfunction in African-American men who had undergone radiotherapy for prostate cancer [150]. Further, much larger GWAS studies have now reported after utilising the RAPPER, RADIOGEN, gene-PARE, LeND patient cohorts identifying new SNPs that have not been targets in candidate gene approaches (table 5) [151–153]. They have confirmed that a number of loci are likely to be contributing the radiosensitivity of normal tissues and development of long term toxicities and these assays will be prospectively validated in the ongoing REQUITE study [154].

Author	Year	Sample size	Tumour site	SNP (Gene/ loci)	OR (95%CI)	Endpoint
Kerns	2010	27 cases 52 controls	Prostate	rs2268363 (FSHR)	7.03 (3.4-14.7)	Erectile Dysfunction
Kerns	2013	79 cases 241 controls	Prostate	rs7120482 rs17630638 (11q14.3)	6.7 (2.8-16.1) 5.1 (2.2-11.6)	Late Rectal Bleeding
Kerns	2013	346	Prostate	8 x SNP cluster (9p21.2 IFNK / MOB3B)	-	Change in American Urological Association Score
Fachal	2014	741	Prostate	7 x SNP cluster rs7582141 (q21.1/ TANC1)	6.17 (2.25-6.9)	Late toxicity (>2-5years)
Barnett	2013	1850 (RAPPER)	Prostate Breast	Multiple SNPs Multiple loci	Not validated to significant level in replication cohorts	Late toxicity – Standardised Total Average Toxicity (STAT)
Seibold	2015	753	Breast	rs2682585 (XRCC1)	0.77 (0.61-096)	Late skin toxicity, breast fibrosis, STAT
Kerns	2016	1564 (RAPPER, RADIOGEN, gene-PARE, CCI)	Prostate	rs17599026 rs7720298 (KDM3B/ 5q31.2, DNAH5/ 5p15.2)	3.12 (2.08-4.69) 2.71 (1.9-3.86)	Urinary frequency, Decreased urinary stream, STAT
Andreassen	2016	5456 17 cohorts (inc RAPPER, RADIOGEN, GenePARE, Ghent, CCI)	Prostate Breast	rs1801516 (ATM)	1.49 (1.17-1.88) – acute toxicity 1.27 (1.02-1.58) -fibrosis	Acute skin/ rectal toxicity, telangiectasia, fibrosis, late rectal toxicity, STAT
Zhang	2016	2000	Breast, H&N, Prostate	rs1801516 (ATM)	1.78 (1.07-2.94)	Late subcutaneous fibrosis
Kerns	2020	3871 (RAPPER, RADIOGEN, GenePARE, U-Ghent, CCI-BT)	Prostate	rs17055178 rs10969913 rs11122573 rs147121532	Pmeta= 6.2x10-10 2.9x10-10 1.8x10-8 Pconditional=4.7x10-6 (rs147121532)	Urinary frequency, haematuria, rectal bleeding, decreased urinary stream. STAT

Table 5: Summary of reported GWAS and large meta-analysis examining radiotherapy toxicity endpoints.

1.7 Thesis Aims

Patients presenting with locally advanced OCSCC represent a poor prognostic cohort where aggressive multimodality therapies lead to detrimental effect on long term quality of life. Although it is clear patients presenting with these tumours need escalated therapies it is unclear whether this will be a feasible option in a group where long term smoking, alcohol misuse and (often undiagnosed) comorbidities necessitate modifications to the 'ideal' standard of care treatments. Within this group, it is not only important to strive for improved survival outcomes through incorporating novel therapies into radical management plans, but also take steps to moderate the long term side effects of standard of care therapies in order to facilitate such future escalation strategies. The specific aims of this thesis are:

Characterising Locally Advanced Oral Cavity Cancer

1. Evaluate the deliverability of standard of care adjuvant treatment regimes to a 'real world' population of patients with locally advanced OCSCC.
    a. Identifying treatment barriers and reasons for modifications in therapy, thus informing the design of future escalation studies.

Seeking Improved Outcomes in Locally Advanced Oral Cavity Cancer

2. Demonstrate the feasibility and early clinical outcomes of the NICO (Neoadjuvant and Adjuvant Nivolumab as Immune Checkpoint Inhibition in Oral Cavity Cancer) phase II window of opportunity clinical trial

Seeking personalised radiotherapy strategies in Locally Advanced Oral Cavity Cancer

3. Apply novel radio genomic SNP array sequencing to better the likelihood of developing osteoradionecrosis of the jaw (ORN) following H&N radiotherapy.

4. Characterise the role of radiotherapy dosimetric parameters in the development of ORN within a high risk group and creating a normal tissue complication probability model to guide mandibular sparing during adjuvant RT for resected LA OCSCC.

Chapter 2

Addressing the real world challenges of adjuvant therapy in locally advanced oral cavity cancer.

2.1 Introduction

As previously outlined within Chapter 1, current treatment strategies for locally advanced oral cavity squamous cell carcinoma (LA OCSCC) typically employ multimodality therapy (surgery and adjuvant (chemo)radiotherapy (CRT/RT)) to eradicate primary disease and mitigate the risk of future recurrence. Due to the intensity of treatment, clinicians tread a narrow therapeutic index; aiming for reduced risk of cancer recurrence whilst avoiding intolerable side effects which can affect long term quality of life. Although the realities of delivering these toxic treatments to a patient group who have multiple comorbidities, long term smoking/alcohol excess and undergone life-changing reconstructive maxillofacial surgery are referenced in national guidelines, adaptations to 'gold standard' therapies are not endorsed [155].

Reliable pre-operative staging is extremely valuable when embarking upon complex therapeutic pathways. In order to adequately stage patients before surgical resection imaging, with MRI, CT, USS is correlated with physical examination and palpation [156]. This unavoidably introduces subjective interpretation of findings and also inter-observer variability. Ultimately accurate staging will not only be beneficial to patients in improving their journey and providing realistic expectations of their treatment path but also to ensure a streamlined service with early recruitment to clinical trials if available.

Delays to initiating adjuvant RT following radical surgery have a negative impact upon survival [157,158]. A large observational cohort study conducted by Harris et al confirmed the survival advantage of shorter intervals between surgery and adjuvant RT. They reported an improvement in median OS of 4.1 years (95%CI 3.4-4.7) for 25,216 SCCHN patients within their cohort who had an interval of under 42 days compared to those over 50 days [70]. Given these findings, the British Association of Head and Neck Oncology (BAHNO) Standards and the National Comprehensive Cancer Network

(NCCN) advocate initiating adjuvant treatment within 42 days in all sub-sites to minimise the impact of treatment delays upon outcomes and clearly this relies upon a coordinated service [159, 160].

Through auditing current practice in two large tertiary referral Head & Neck units against the recommended adjuvant treatment path (outlined within the United Kingdom National Multidisciplinary Guidelines and BAHNO standards [155, 161]), this work will highlight the difficulties in delivering the currently recommended adjuvant treatments to our patient population, and challenges in improving outcomes for this particular group.

2.2 Hypotheses

- **There is discordance between initial clinical and/or radiological staging and final definitive pathological staging.**

The accuracy of pre-operative staging will be determined.

- **Patients are failing to initiate adjuvant RT within six weeks of surgery (as per BAHNO standards [159, 161]).**

Assessing the deliverability of this target will inform whether the particular complexities of head and neck surgery and subsequent recovery periods need to be taken into account in expected treatment times.

- **Temporal changes in performance status following surgical ablation/reconstruction impacts negatively upon provision of anticipated "gold standard" adjuvant treatment.**

Assessment of the frequency with which patients are currently able to complete the course of standard adjuvant therapy will take place focussing upon proportions of patients suitable for adjuvant CRT compared to those who received CRT and reasons for changing treatment path.

2.3 Methods

2.3.1 Ethics

Approval for retrospective data collection and audit was obtained from Aintree University Hospital/The Clatterbridge Cancer Centre and North Manchester General Hospital audit departments.

2.3.2 Patient population

Patients with LA OCSCC based on the seventh edition of the American Joint Committee on Cancer Staging (i.e. T1-4 N1-3 or any T3-T4 N0) treated between October 2014 – October 2016 with radical surgery were identified via Somerset Cancer Register [45, 162].

2.3.3 Patient treatment and outcomes

All cases undergoing radical surgery were planned for adjuvant RT/CRT depending on established pathological risk factors (presence of extracapsular extension and involved surgical margins ≤1mm). Patient outcomes were obtained through retrospective case note review; of note performance status (PS) was documented at two different time points with evaluations made by different assessors (initially by operating surgeon and latterly by treating oncologist). Detailed tumour resection pathology reports, imaging reports and initial clinical examination documentation were obtained and surgical length of stay with staging information recorded. Surgical complications were graded using the Clavien-Dindo classification system (see appendix 6) [163]. RT was delivered using Volumetric Modulated Arc Therapy (VMAT) with 66gy in 33 fractions prescribed with concurrent cisplatin either 100 mg/m^2 every 21 days for 3 cycles or 40mg/m^2 weekly. If cisplatin was contraindicated substitution with carboplatin could be considered. The adjuvant RT regimes were 60-66Gy in 30-33 fractions depending on individual treating clinical oncologist preference and pathological risk factors. 3 patient received 50Gy/20# as an abbreviated course of RT due to coexisting comorbidities and assessed level of fitness.

2.3.3 Statistical Analysis

Data were analysed using IBM SPSS v24.0 (IBM Corp). Kaplan-Meier survival curves were used to analyse overall survival (OS) and progression free survival (PFS) within the population as a whole, and again in patients with pathological indications for

adjuvant CRT. The Cohen's Kappa statistic (cK) was used to assess inter-rater agreement [164].

2.4 Results

2.4.1 Patient characteristics

A total of 158 patients were initially identified; however 29 patients were subsequently excluded from analysis (primary site other than the oral cavity and/or histological type other than SCC). Of these remaining 129 patients with LA OCSCC there were 55 females and 74 males with an average age of 64 years (39-86 years). 53% were current cigarette smokers and 73% current consumers of alcohol (Table 6).

Patient Characteristics		Frequency (%)	Mean	Min/Max
Age	**<50**	13 (10.1)	64 yrs	39-86 yrs
	51-60	32 (24.8)		
	61-70	42 (32.6)		
	71-80	32 (24.8)		
	>81	10 (7.8)		
Sex	**Male**	74 (57.4)		
	Female	55 (42.6)		
Smoking status	**Non**	34 (26.4)		
	Ex	25 (19.4)		
	Current	69 (53.5)		
Alcohol	**Nil**	32 (24.8)		
	Current	95 (73.6)		
	Unknown	2 (1.6)		
PS at initial assessment	**PS 0**	72 (55.8)		
	PS 1	34 (26.4)		
	PS 2	14 (10.9)		
	PS 3	7 (5.4)		
	PS 4	1 (0.8)		
	Unknown	1 (0.8)		
PS at adjuvant assessment	**PS 0**	12 (9.3)		
	PS 1	46 (35.6)		
	PS 2	43 (33.3)		
	PS 3	16 (12.4)		
	PS 4	1 (0.8)		
	PS 5	1 (0.8)		
	Unknown	10 (7.8)		
Time to RT/CRT	**20-35 days**	16 (17.2)	47.4 days	25-116 days
	36-42 days	21 (22.6)		
	43-49 days	26 (28.0)		
	50-56 days	16 (17.2)		
	≥57 days	12 (12.9)		
	Unknown	2 (2.2)		
Adjuvant treatment	**CRT**	20 (15.5)		
	RT	73 (55.8)		
	None	36 (28.7)		

Table 6: Patient and treatment characteristics.

A total of 93 (72.1%) patients received post-operative adjuvant treatment. PS was assessed prior to surgical resection and again prior to adjuvant treatment planning; initially by operating surgeon, latterly by treating oncologist, and confirmed following MDT discussion. This information was obtained through case note review and MDT documentation reports. At presentation the majority of patients (72/129, 55.8%) were PS 0 (Table 6). At post-operative assessment only 12 patients were assessed as PS 0 with 89 patients now PS 1 or 2; the most frequent PS drop was 1 point (46%). 8 (6.2%) patients had an improvement in PS following surgical resection; the majority (8) having a rise of 1 point (Figure 9).

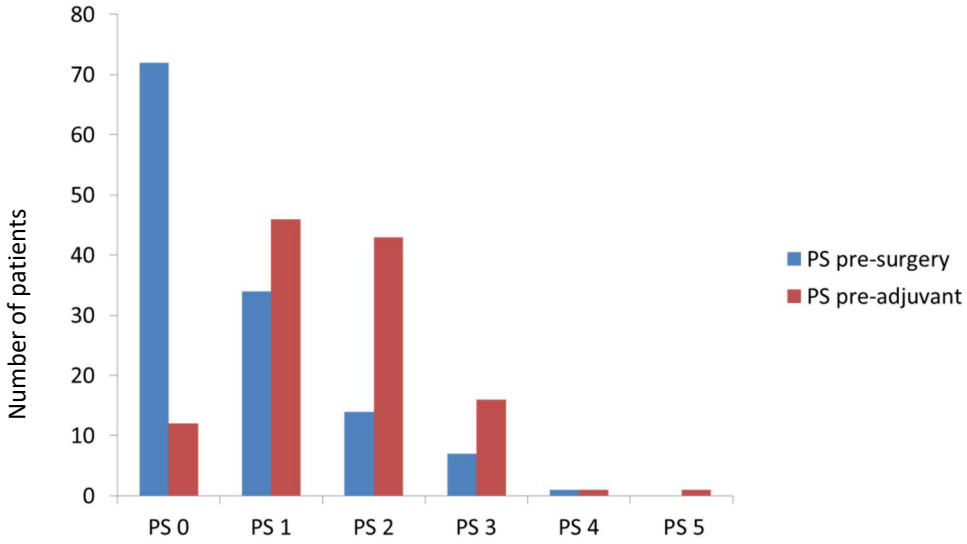

Figure 9: PS before and after surgery

2.4.2 Deviation from 'gold standard' adjuvant treatment

Following standard protocols for adjuvant treatment, 93 patients would have been recommended for CRT, (involved margin <1mm and ECS, see table 7). Of this group, only 20 received CRT; due to deterioration in PS post-surgery (43%), poor PS at first assessment (20%), post-operative complications (8%), early recurrence (7%), comorbidities (3%), previous head and neck RT (3%), patient declined (4%) and no reason documented (13%). Of note there were 30 (33%) aged over 70 years with high risk pathological factors, none of whom received chemotherapy in addition to their adjuvant RT. It was not specified within clinic notes if age was taken into account when deciding whether to offer CRT however it was evident that the majority of these patients had PS≥2 (83%). As noted in Chapter 1 there is a lack of proven

survival benefit in the addition of chemotherapy to adjuvant radiotherapy in this group. However as our treated population changes, there remains discord between clinicians over whether individual patients who are physically very fit would benefit.

Of the 20 patients who underwent CRT, all received cisplatin chemotherapy; five were planned to have weekly 40mg/m2 infusions and fifteen 100mg/m2 every 21 days. Six completed the planned course of three cycles of cisplatin chemotherapy. The remaining 14 patients had at least one cycle of treatment omitted due to chemotherapy toxicities.

73 patients underwent adjuvant RT alone. Despite the recommendation for post-operative RT based on pathological features 36 patients received no adjuvant treatment. Reasons for omitting adjuvant RT were post-operative deterioration in PS (36%), prior head and neck RT (14%), recurrence prior to commencement of RT (8%), patient choice (14%), death prior to treatment (3%), and unknown (25%). Six individuals received palliative RT.

2.4.3 Patient survival outcomes

Median OS and DFS for the whole population were 38 months (95%CI 18.8-57.2) and 34 months (95%CI 21.9-46.1) respectively (Figure 10). The three-year OS rate was 44.8% which is in keeping with the three-year OS rate of 45-47% quoted by the National Cancer Registration and Analysis Service (NCRAS) [165].

Median OS for patients with high risk pathological features was 54 months in those receiving CRT (16.6-91.4), 23 months in those receiving adjuvant RT (95%CI 14.6-31.4) and 9 months in those receiving no adjuvant treatment (95%CI 5.1-12.9) (Figure 11).

Tumour characteristics		Frequency (%)
Margin	**Involved (<1mm)**	56 (43.4)
	1-5mm	49 (38.0)
	>5mm	24 (18.6)
Nodal ECS	**ECS +**	58 (45.0)
	ECS -	68 (52.7)
	Not assessed	3 (2.3)
Clinical Tumour Stage	**T1**	6 (6.7)
	T2	41 (31.5)
	T3	8 (6.7)
	T4	74 (55)
Clinical Nodal Stage	**N0**	81(62.7)
	N1	22 (17.1)
	N2a	3 (2.3)
	N2b	12 (9.3)
	N2c	6 (4.7)
	Nx	5 (3.8)
Radiological Tumour Stage	**T1**	8 (6.2)
	T2	22 (17.1)
	T3	11 (8.5)
	T4	75 (58.1)
	Not assessed	3 (2.3)
Radiological Nodal Stage	**N0**	63 (48.8)
	N1	22 (17.1)
	N2a	1 (0.8)
	N2b	27 (20.9)
	N2c	11 (8.5)
	Nx	5 (3.9)
Pathological Tumour Staging	**T1**	6 (4.7)
	T2	38 (29.5)
	T3	24 (18.6)
	T4	61 (47.3)
Pathological Nodal Staging	**N0**	39 (30.2)
	N1	38 (29.5)
	N2a	1 (0.8)
	N2b	35 (27.1)
	N2c	11 (8.5)
	Nx	5 (3.9)

Table 7: Summary of tumour characteristics (AJCC Cancer TNM Staging 7th edition)

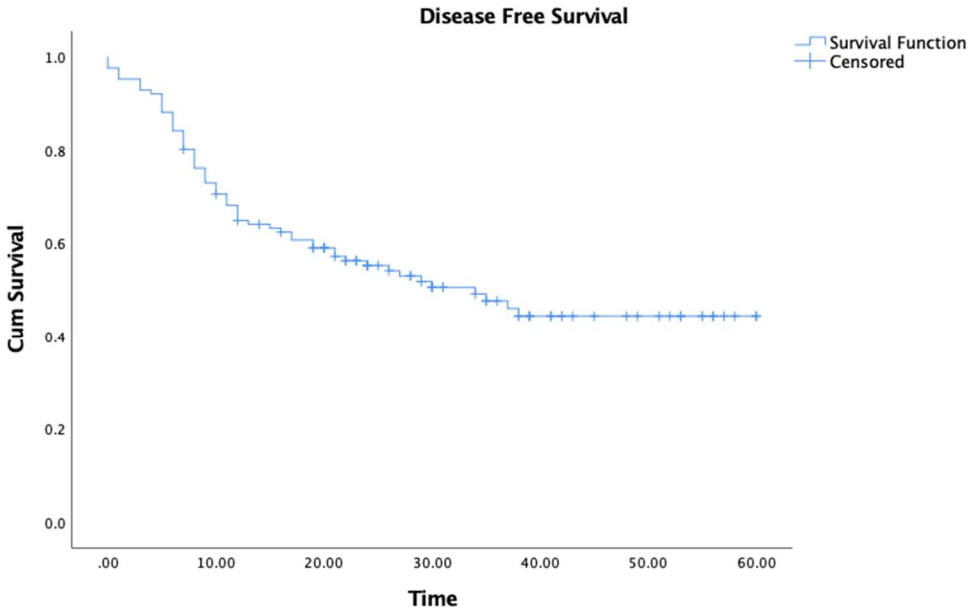

Figure 10: Whole population Disease Free Survival Kaplan-Meier

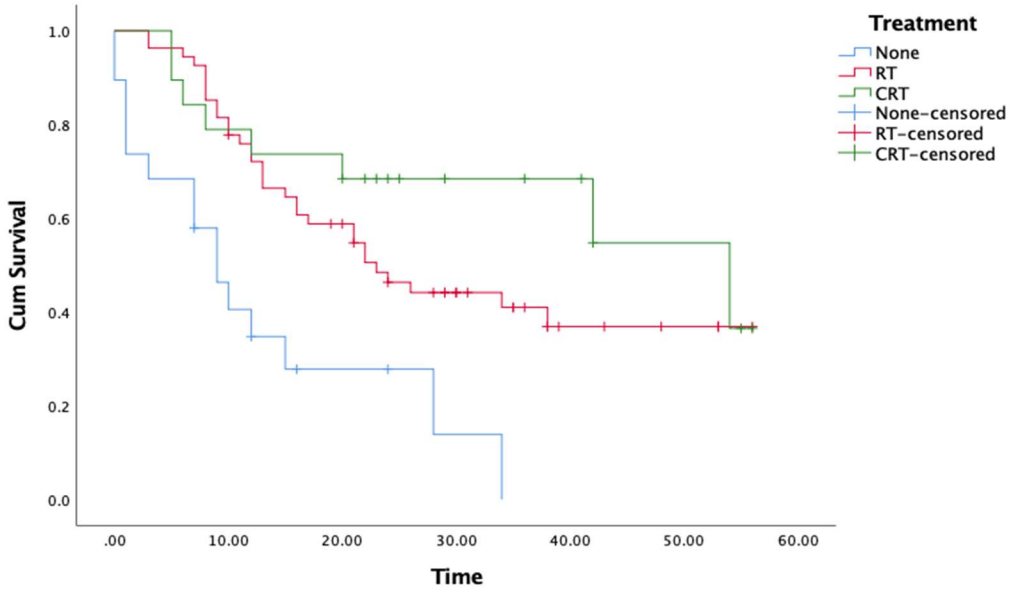

Figure 11: Whole population overall survival Kaplan-Meier for patients with high risk features stratified to adjuvant treatment. CRT (green line), RT (red line), no adjuvant treatment (blue line).

2.4.4 Meeting the 42 day standard

The modal time to commence adjuvant treatment was 42 days (max 116, min 28); 37 patients (40%) began adjuvant CRT/RT within 42 days and 85% (79) began within 56 days. There were 12 patients who took ≥56 days to begin adjuvant treatment and the reasons for this were recovery from post-operative complications (46%), administration error / did not attend when requested (8%), patient moved to different area (8%) and unknown (38%). A delay in initiating adjuvant therapy was associated with longer recovery times and higher complication rate. For those who did not initiate adjuvant therapy within 42 days the median length of hospital stay post-surgery was 16 days along with grade IIIa-V Clavien-Dindo complication rate (appendix 6) of 30% (16); compared to 11 days and complication rate of 8% (3) in the group of patients who did meet the 42 day standard (Figure 12).

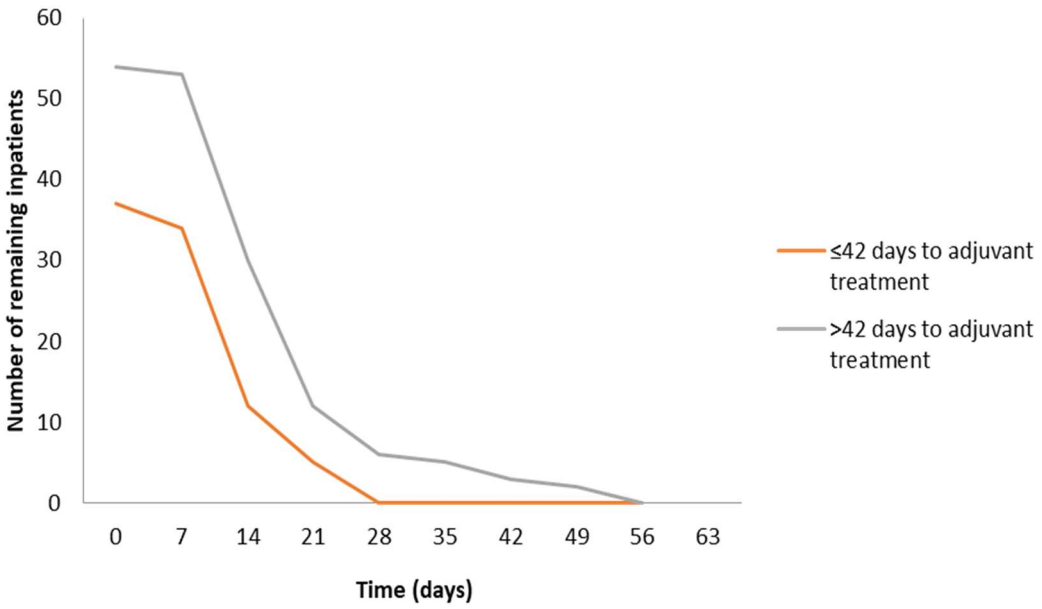

Figure 12: Reducing number of inpatients per week post radical surgery and time to adjuvant CRT/RT.

2.4.5 *Accuracy of pre-surgical staging*

There was concordance between clinical and pathological tumour staging in 72% of cases (cK 0.551), assessment of nodal staging was less reliable with 49% concordance (cK 0.282). When evaluating radiological tumour staging there was 65% agreement with pathological tumour staging (cK 0.462). Radiological nodal staging showed a 44% concordance with 35% of cases upstaged and 20% down-staged following pathology reporting (cK 0.223). 5 individuals could not be compared as their neck was not included on MRI imaging or they did not undergo neck dissection after imaging. (See tables 8 ai-diii).

Clinical T stage (Tc)	**Pathological T stage (Tp)**				**Total**
	1	**2**	**3**	**4**	
1	**2**	3	0	1	6
2	4	**29**	5	3	41
3	0	1	**6**	1	8
4	0	5	13	**56**	74
Total	**6**	**38**	**24**	**61**	**129**

(ai)

Tc vs Tp	**N**	**%**
Pathologically downstaged	25	19%
Same	93	72%
Pathologically upstaged	13	10%
Total	**129**	**100.0%**

(aii)

Tc vs Tp	**Value**	**Asympt. Stand. Error**	**Approx. T**	**Approx. Significance**
Measure of Agreement: Kappa	0.551	0.057	4.270	.000

(aiii)

Radiological T stage (Tr)	**Pathological T stage (Tp)**				**Total**
	1	**2**	**3**	**4**	
1	**1**	4	2	2	9
2	5	**21**	4	2	32
3	0	5	**6**	0	11
4	0	8	11	**57**	76
X	0	0	1	0	1
Total	**6**	**38**	**24**	**61**	**129**

(bi)

Tr vs Tp	N	%
Pathologically downstaged	30	23%
Same	85	65%
Pathologically upstaged	14	11%
Total	**129**	**100.0%**

(bii)

Tr vs Tp	Value	Asympt. Stand. Error	Approx. T	Approx. Significance
Measure of Agreement: Kappa	0.462	0.057	9.226	.000

(biii)

Clinical N stage (Nc)	Pathological N stage (Np)					Total
	0	**1**	**2a**	**2b**	**2c**	
0	**36**	25	0	16	4	81
1	1	**11**	1	7	2	22
2a	1	0	**0**	2	0	3
2b	0	3	0	**9**	0	12
2c	1	0	0	0	**5**	6
Total	**39**	**38**	**1**	**35**	**11**	**124**

(ci)

Nc vs Np	N	%
Pathologically downstaged	6	5%
Same	61	49%
Pathologically upstaged	57	46%
Total	**124**	**100.0%**

(cii)

Tr vs Tp	Value	Asympt. Stand. Error	Approx. T	Approx. Significance
Measure of Agreement: Kappa	0.282	0.055	5.921	.000

(ciii)

Radiological N stage (Nr)	Pathological N stage (Np)					Total
	0	**1**	**2a**	**2b**	**2c**	
0	**29**	14	1	14	5	63
1	3	**10**	0	7	2	22
2a	0	0	**0**	1	0	1
2b	5	10	0	**12**	0	27
2c	2	4	0	1	**4**	11
Total	**39**	**38**	**1**	**35**	**11**	**124**

(di)

Nr vs Np	N	%
Pathologically downstaged	25	20%
Same	55	44%
Pathologically upstaged	44	35%
Total	**124**	**100.0%**

NB Unable to compare results in 5 patients (dii)

Nr vs Np	Value	Asympt. Stand. Error	Approx. T	Approx. Significance
Measure of Agreement: Kappa	0.223	0.058	4.270	.000

Table 8: Concordance between ai-iii clinical tumour stage (Tc) and pathological tumour stage (Tp), bi-iii radiological tumour stage (Tr) and pathological tumour stage (Tp), ci-iii clinical nodal stage and pathological nodal stage (Np), di-iii radiological nodal stage (Nr) and pathological nodal stage (Np).

2.5 Discussion

This research highlights the significant challenges evident in the delivery of "ideal" therapeutic regimes to patients with LA OCSCC. In particular, these results provide evidence of a significant deterioration in patients' PS following surgical treatment for this disease, with 88 individuals (68%) experiencing a demonstrable a fall in PS. The drop in physical fitness is a product of their intensely complex surgical resection and reconstruction and patient co-morbidities. The intimate association and disruption to patients' normal upper aerodigestive tract leads to prolonged recovery times, increased length of hospital stay and the subsequent, increased risk of post-operative complications [166]. Ultimately once patients have recovered from their surgical procedure, any delays within perioperative management bring the patient close to (or even outside) the recommended window for initiating adjuvant treatment. Altered PS and the sequelae of treatment frequently render patients too unwell to consider concurrent cisplatin chemotherapy or RT alone even if they have pathological risk factors which would suggest treatment is indicated. This is echoed in a large series by Chin et al [167] who noted that frailty and older age were both associated with lower odds of receiving adjuvant RT /CRT (0.66 and 0.56 respectively).

Only 37 (40%) patients receiving adjuvant treatment did so within the national standard of 42 days. For those treated outside the national standard, 56% (30 patients) were still inpatients at 14 days following their operation (compared to 32%, (12 patients) in those treated within 42 days), and there was a higher rate of grade

IIIa-V Clavien-Dindo complications (30% compared to 8%); reinforcing the above conclusions (figure 12). It is evident that this timeline to commencement of adjuvant therapy is not achievable for all patients undergoing surgical procedures for HNSCC and does not take into account the varying surgical complexities across each sub-specialty nor the reality of treating patients with multiple (often undiagnosed) pathologies following a history of long term nicotine and alcohol dependence.

Tri-modality therapy (surgery, chemotherapy and radiotherapy) is an intensive regime which has a dramatic effect upon quality of life [168]. This is reflected in the low proportion of patients completing a full course of adjuvant CRT without modification. Our three year OS rate of 44% reinforces the need for intensification of adjuvant treatments, however the low proportion of patients receiving the current 'gold standard' management shows how difficult this will be to achieve in our population. Similarly the TITAN study highlighted patients with LA OCSCC as a population difficult to escalate treatment due to advancing age and poor performance status. This study had planned to provide induction cisplatin, 5-fluorouracil and docetaxel chemotherapy prior to ablative surgery for patients with resectable HPV negative HNSCC but could not progress from feasibility to phase III due to difficulties recruiting [169]. Clearly patients with LA OCSCC require a nuanced approach to adjuvant treatment with appropriate intensification for those individuals who are fit but also less toxic adjuvant options (namely alternatives to cisplatin chemotherapy) for the majority of patients who have poorer PS and comorbidities. Future clinical trials will consider the integration of new systemic anti-cancer therapies (i.e. immunotherapies) into the neo-adjuvant setting in order to maximise upon the window of opportunity to treat individuals before their physical fitness deteriorates following complex surgical procedures. Careful patient selection and accurate pre-treatment staging is essential to recruit effectively to any study that attempts to enrol at presentation. Joint surgical/oncology review prior to the initiation of such an intensive treatment path would be paramount in order to highlight those suitable to receive the full package of care whilst identifying those earlier who may need a more palliative approach to their treatment.

It is evident that there are significant challenges in accurately assessing tumour stage in the preoperative setting by clinical and radiological means alone. Kreppel et al reported 40% concordance between clinical and pathological staging in 392 OCSCC cases while Koch et al similarly demonstrated 50% concordance between these two staging methods in 501 cases of HNSCC [170, 171]. Hao et al compared detection of cervical lymph node metastases between MRI and histopathological staging in 60 patients with HNSCC; reporting occult cervical metastases rate of 26.8% [172]. Within our study concordance between radiological nodal status and pathology was poor (cK 0.223). The main disparities in nodal staging were for the N0 neck; 34 patients out of 63 initially staged as N0 (54%) were upstaged following pathological review. Nodal staging in HNSCC is a topic of much debate and the N0 neck is notoriously difficult to correctly assess on imaging, supporting the recommendation of neck dissection in patients with ≥15-20% risk of occult metastases regardless of imaging findings [173]. MRI has frequently been compared to CT, USS and PETCT to compare the accuracy of detecting occult metastases and seems to have a similar sensitivity to CT scanning [174,175]. MRI imaging becomes less sensitive in detecting affected lymph nodes if they are borderline in terms of enlargement (i.e. approx. 10mm) or morphological change (shape, presence of necrosis etc.) [175]. More recently diffusion weighted MRI has been shown to improve delineation of nodal disease measuring less than 10mm and therefore may prove useful to integrate into future staging investigations [176, 177]. Poor concordance between radiological and definitive pathology stage and the constraints this places on adjuvant treatment planning emphasises the requirement for recruitment strategies capable of overcoming, or at worst accommodating, the paradox between inaccurate clinical staging and delayed (post-operative) definitive staging.

We recognise some limitations inherent in this survey. The retrospective nature of the data collection meant that there was reliance upon case note documentation; however records were cross-referenced across two NHS trusts to verify data. Review of notes at both surgical and oncology NHS trust sites allowed inter-observer variability in scoring PS and noting treatment toxicities. Despite this, all patients were discussed at multidisciplinary team meetings where PS is reviewed routinely thus

minimising this variability. Inclusion of consecutive cases, managed in the respective units, was made in an attempt to mitigate potential selection bias. There was a high rate of discordance between radiological and pathological staging. The length of time between radiological staging and surgery was not collected and so there is potential for tumour progression in this time accounting for this discordance; however similar rates of 'down staging' of disease were reported thus validating our conclusions. Assessment of tumour Human papillomavirus (HPV) status was not deemed relevant given the low prevalence in oral cavity cancer and, in addition, routine HPV testing is not currently recommended in non-oropharyngeal sites [17,18].

2.6 Conclusion

This study has brought to the forefront the reality of treating patients in the true population with multimodality therapies. Discordance in radiological and pathological staging along with deterioration in performance status as a consequence of treatment intensity necessitates management plans and procedures capable of adaptation to ensure individuals receive the appropriate adjuvant regimes. Future clinical trials should be designed to focus upon the neo-adjuvant treatment window and upon developing alternative, less toxic adjuvant regimes for patients with high risk LA OCSCC in order to allow intensification of therapy thus improved outcomes.

Chapter 3
Altering treatment to improve quality of life; Genetic variants associated with mandibular osteoradionecrosis following radiotherapy for head and neck malignancy

3.1 Introduction

By targeting the window of opportunity between diagnosis and surgery and integrating novel therapeutics for patients with LA OCSCC, we may be able to offer much needed improved survival outcomes. However, in doing so, we will see greater numbers of patients living with the long term side effects of standard of care therapies. Efforts to improve patient quality of life and reduce long term toxicities must coincide with the adoption of escalated adjuvant treatments.

There are many factors which are likely to impact upon individual normal tissue radiation sensitivity (e.g. pre-existing comorbidities and smoking history) however despite individual risk factors it is still unknown why patients with similar demographics receiving identical treatments experience diverse grades of toxicity. Genetic variation has a role to play in the sensitivity of normal tissues to radiation. Through characterising which genetic alterations increase the chance of developing long term consequences of radiotherapy it may be possible to build a predictive model which can be used to aid development of personalised radiotherapy protocols.

Previous GWAS experiments assessing late radiation toxicity have concentrated on toxicity endpoints which are subjective, difficult to quantify and poorly recorded/reported; namely urinary stream, urinary frequency, rectal bleeding and soft tissue/skin fibrosis (see section 1.6.2) [178, 179]. The standardised average toxicity score (STAT) was developed in order to facilitate data pooling across studies and enable the inclusion of large numbers of patients in radiogenomic investigations[180]. This scoring system has contributed to eliminate some of the bias seen across patient groups however, it cannot account for the pathogenesis of differing toxicity endpoints within individually treated normal tissues, nor collection of subjective outcomes with different scoring systems and grading in heterogeneous cohorts[153].

ORN (discussed in section 1.5.1) offers an ideal focus for the development of a predictive genetic biomarker panel as it is a dichotomous outcome which is easily diagnosed and quantified, and eliminates subjective interpretation of side effects (e.g. skin fibrosis following breast irradiation). Multiple candidate gene studies have taken place investigating the association between ORN and single nucleotide polymorphisms within genes that encode proteins targeting fibrosis pathways, oxidative stress response and DNA repair [137,138,181] however it is yet to be a focus of GWAS investigations.

The aim of this study was to discover new common genetic variants predictive of ORN. In doing so we may generate new hypotheses on pathogenesis and contribute to developing a more personalised approach to radiotherapy treatment planning for patients with head and neck cancer.

3.2 Chapter Hypotheses:

- **Performing SNP array sequencing within a cohort of patients who have received head and neck radiotherapy will generate new hypotheses regarding the pathogenesis of ORN.**

Novel mechanisms for the ORN disease process may be identified for future exploration.

- **A panel of common genetic variants will be predictive for developing osteoradionecrosis of the jaw.**

Following the discovery of SNPs that may impact upon risk of developing ORN, findings will be validated using internal single targets, thus producing multi-loci model which may be utilised to facilitate stratifying patients to future personalised radiotherapy strategies.

- **Previously identified SNPs within candidate gene studies may prove significantly associated with ORN and will be explored within this cohort.**

Previous knowledge of causal SNPs that increase susceptibility to developing ORN will be externally validated.

3.2 Materials and Methods

3.2.1 Ethics and Funding

All patients consented to their DNA being used for research studies prior to blood samples being taken with ethical approval from North West – Liverpool Central REC (Ref. No. 10/H1002/53) and Greater Manchester Central REC (Ref. No.08/H1008/32 (CRUK HOPON clinical trial)). Study funding was provided by the Liverpool Head and Neck Centre Patient Research Forum.

3.2.2 Participants and treatment

A case-control study of 152 patients was undertaken. 97 patients took part in the CRUK HOPON clinical trial which was a randomised controlled phase III trial examining whether the delivery of hyperbaric oxygen reduced the likelihood of developing ORN of the jaw following dental procedures in patients who have received over 50Gy of radiotherapy to the head and neck [182]. Of the 97 patient samples arising from this prospective HOPON collection, 93 did not develop ORN despite being deemed high risk by virtue of post treatment dentoalveolar surgery and blinded clinical/radiological assessment for ORN as its primary outcome measure (control cohort). In addition to 4 cases of ORN from the HOPON trial, an independent group of 55 patients recruited at University Hospital Aintree NHS Foundation Trust Head and Neck Cancer Unit who similarly received over 50Gy radiotherapy to head and neck were recruited after developing ORN. Thus the case cohort constituted a total of 59 patients and the control cohort of 93 patients. Within the case cohort a diagnosis of ORN was confirmed from clinical notes and following review of X-rays, clinical photographs and physical examination with Notani grade noted where specified [106]. Radiotherapy treatment information was obtained via study data collection forms or clinical patient records. Treatment was delivered using either 3D conformal or IMRT depending upon individual treating clinician and centre, with doses ranging 50-70Gy delivered over 20-35 fractions. Information on smoking status, alcohol consumption, post radiotherapy dental procedures, and use of bisphosphonates was also obtained during review of clinical notes and trial documentation. All patients had at least 2 years of follow up data available at time of analysis.

3.2.3 DNA extraction

Cell pellets from whole blood collected in ethylenediaminetetraacetic acid (EDTA) containing collection tubes were aliquoted and stored at -80°C. Genomic DNA was extracted from these cell pellets using QIAGEN QIAamp DNA Blood Midi Kit according to manufacturer handbook instructions (1090244 02/2015, QIAGEN Ltd., Manchester, M15 6SH). After adding 100µl proteinase K, 0.3-1ml anticoagulated blood (adjusting volume to 1ml with phosphate buffered saline where necessary), and 1.2ml lysis buffer into tube, samples were mixed by inverting 15 times followed by vigorous shaking for at least 1 minute and incubated at 70°C for 10 minutes. Once removed from incubation 1ml 100% ethanol was added and again samples mixed by inverting 10 times followed by vigorous shaking. The lysed samples were transferred to QIA amp spin columns and placed in 15ml centrifuge tubes. Samples were centrifuged for 3 minutes at 1850g and filtrate discarded. 2ml of the first wash buffer (AW1) was added to columns and samples centrifuged at 4500g for 1 minute and following this 2ml of the second wash buffer (AW2) added and centrifuged again at 4500g for 15 minutes. The collection tube and filtrate was then discarded and columns transferred to clean collection tubes. Columns were eluted in 100µl buffer AE (10 mM Tris-Cl; 0.5 mM EDTA; pH 9.0) twice to create two DNA samples per specimen; one for submission for genotyping and one for future validation. Samples were assessed for DNA quality and quantity using NanoDrop™ One/OneC Microvolume UV-Vis Spectrophotometer and subsequently run on 1% agarose gel.

3.2.4 Genomic sequencing

One set of 100µl DNA samples were sent for SNP array sequencing at Edinburgh Genomics (Ashworth Laboratories, The University of Edinburgh, EH9 3FL). Following quality control (gel electrophoresis and ratio of absorbance at 260:280nm) all samples were prepared and processed by hybridisation, washing, staining and sequenced using the Infinium 24 Global Screening Array V2.0 (Illumina, Inc., Little Chesterford, CB10 1XJ). Results of quality control are shown in appendix 7.

3.2.5 Bioinformatic analysis

Bioinformatics analysis was performed by Dr Phil Antczak (Associate-Director Liverpool Computational Biology facility) and is described below.

3.2.5.1 Associating SNPs to ORN outcome

PLINK (v 1.90b6) was utilised to generate genome wide associations after providing raw data as well as the following options "–allow-extra-chr –assoc –covar file keep-pheno-on-missing-cov –covar-name Alcohol, Smoker, Age –model perm –pfilter 1 –real-ref-alleles –snps-only just-acgt". The dataset was quality controlled using the R package argyle [183] and outlier samples removed. SNPs were extracted for which PLINK returned an empirical p-value based on permutations < 0.01. SNPs were annotated using SNP nexus [184].

3.2.5.2 Identification of a SNP panel predictive of ORN outcome

To identify a potential panel predictive of ORN outcome, the frequencies of all SNPs within the dataset were inputted into a genetic algorithm based predictive modelling approach (GALGO) [185]. This approach aims to identify the smallest possible model predictive of a certain outcome by generating many thousands of models and then using a forward selection approach to identify a representative model. Feature sets were trained within GALGO by applying a Random Forest (RF) classifier [186]. RFs have been shown to deal well with numerous different data types leading to highly accurate models, ideal for this dataset. RFs also have a built-in approach to minimise overtraining based on the out-of-bag strategy which is complemented by GALGOs own data splitting and cross validation strategy. Specifically, GALGO splits the initial dataset into a training (⅔ data) and test (⅓ data) set. The training set is then split once more using the same ratios. The second split is then used for model optimisation while the first split is used for final validation of the model. GALGO ran with the following parameters: feature set size = 15 and goal fitness = 0.95. To ensure that the smaller ORN class was appropriately weighted in the prediction the RF within GALGO were set to the following parameters: mtry = 5, ntree = 300, and class weights = (1.5, 3). GALGO then generated 5000 models using these settings. Once collected a forward selection model was applied to identify a potential representative model. Here features from the 5000 models were ranked by their frequency of inclusion and

sequentially added to a new model testing ability to predict ORN. In addition to this approach a backward selection strategy was employed in order to optimise the smallest possible model predictive of ORN. This was performed using the robust GeneBackwardElimination approach within GALGO.

3.2.6 Validation: PCR and pyrosequencing

The ten top highlighted SNPs of interest were internally validated on the remaining set of 100µl DNA samples using polymerase chain reaction (PCR) and pyrosequencing. Cognizant of the significant findings in previous publications, SNPs rs1695, rs1042522, rs1047768, rs25487 and rs1800469 were checked for significance within the larger model [137,138,187]. We also sought to validate the additional SNP rs1800469 (TGFβ1) given this target approached significance (p 0.07) [181].

Primer design for amplification and sequencing was performed with using Pyromark Assay Design 2.0 software (QIAGEN Ltd.) and was based upon information obtained via dbSNP NCBI (National Centre for Biotechnology Information) [188]. Primers were supplied by Eurofins genomics. PCR was performed using a 25µl reaction comprising 7.5 µl water, 4 µl DNA template, 1 µl primer stock (400nM concentration - 8µl biotinylated primer, 12µl un-biotinylated primer and 180 µl water) and 12.5 µl iQTM Supermix (Bio-Rad Laboratories, Inc.). Annealing temperatures for each primer were optimised using temperature gradient PCR reactions using four temperature settings at one degree intervals. Final annealing temperatures were confirmed following examination of PCR products on 2% agarose gel electrophoresis. Following optimisation, DNA samples were genotyped for SNPs outlined in Table 9.

Primer	Primer sequence 5' -> 3'			PCR cycles	T_a (°C)	Predicted amplicon size (bp)
	Forward	Reverse	Pyrosequencing			
rs11542332	TCAGAAGCTGC CTCTCTTC	CACGGTCTTGTC AATCTCC (5' biotin)	AACTCTCTGTTCCT GTCAC	42	57	102
rs7477958	CCTCTGCTTTA CCACTTAATCA	GGATGGGAATG GTTTAACTAA (5' biotin)	TTACCACTTAATCA GTTATG	42	56	89
rs2348569	TCCATGGAAAT TACTAGGCT (5' biotin)	GTACAGCCCTGT GTCTTTTTC	AGACGCAGGGAC CTGGCAC	42	55	124
rs1415848	GAGACTTTTCT GATTTGAACTA CTC (5' biotin)	GTGCATGGAAT CCAGCAA	GCATGGAATCCAG CAAT	42	57	91
rs7022936	TGCAACAATTT CTTCAGTAA	CTAATTAGAAA ATCGGAGCA (5' biotin)	ACAATTTCTTCAG TAACTAT	42	52	84
rs2105042	CTGCCCACAGA CGTGGAAT (5' biotin)	CTCCGGGAAAG TTCGAACC	AACAAGGCCATCT GCCTTT	42	62	80
rs11605273	AATCCAGAGG AGGAGCCA (5' biotin)	GGTGTTAACTTC AAAATGTTTTTA G	GTTAACTTCAAAA TGTTTTTAG	42	56	91
rs34798038	TGGTGGTAGTT AAGTTCTGAAT	TATCACGGTCCC TTCTTTA (5' biotin)	AGATATTACATGA TCCTTTG	42	53	77
rs530752	TACTGTGGTCC TCTCTTCTG (5' biotin)	CAAAGTGGTTCT AAGTAAGCA	TCTAAGCATTGCC TCA	42	51	106
rs6011731	AGATTTGGGA CAATTCCT (5' biotin)	GCAGCTTATATC ACAGTTCA	GCAGCTTATATCA CAGTTCA	42	51	92
rs1800469	CGGAGGGTGT CAGTGGGA	AGCAATTCTTAC AGGTGTCTGCC (5' biotin)	GCAACAGGACACC TGA	42	62	82

Table 9: List of primers with sequences and optimised annealing temperatures.

PCR products were sequenced with the corresponding primer as outlined in Table 9 using PyroMark Q96 ID pyrosequencer (QIAGEN Ltd.) along and PyroMark Gold Q96 reagents (QIAGEN Ltd.). Briefly, stock sequencing primers were prepared at 10µmol dilution and 1.5 µl of this primer stock added to 43µl annealing buffer to ensure 45 µl within each well of 96 well pyrosequencing plate. A binding mix was prepared with sepharose streptavidin beads and double distilled water; this was combined with pyrosequencing products and after agitating using vortex plate at 350rpm for 10 minutes. Substrates were dissolved in 620µl water and, along with nucleotides,

added to pyrosequencing cartridge. Bound templates were transferred to successive washes in 90% ethanol for 10 seconds, 0.2M sodium hydroxide for 20 seconds and then tris acetate buffer for 10 seconds using vacuum tool. Templates were then transferred to annealing buffer/primer mix within corresponding pyrosequencing plate and heated for 2 minutes at 80°C to denature DNA. The plate was then brought back to room temperature for 2 minutes for annealing and subsequently transferred to PyroMark Q96 ID pyrosequencer for sequencing. Pyrogram analysis was performed using PyroMark Q96 ID Software 2.5 (QIAGEN Ltd.). An extract of example pyrogram is shown in appendix 9.

3.2.7 Validation Statistical Analysis

Statistical analysis was completed using IBM SPSS statistics v27. Univariate logistic regression analysis was performed to validate the association between SNPs within the optimised model and ORN. SNPs correlated with ORN with P values ≤0.2 were included in backward stepwise multivariate logistic regression modelling; variables were entered to determine the model with the lowest akaike information criteria (AIC). Subsequent goodness of fit was assessed using Hosmer-Lemeshow statistic. The area under the receiver operating characteristic curve (AUC ROC) demonstrated model performance.

3.3 Results

3.3.1 Quality assurance of patient samples

Two patients were excluded from final modelling and validation analysis due to insufficient DNA samples to allow PCR and pyrosequencing. Of the remaining 150, nine were highlighted as outliers based on the PCA of SNP data generated using the Illumina Infinium Global Array (Figure 13). Of the analysis set of 141 patients, the median age was 56 (range 16-78) and the majority (107/141, 76%) were males. 63 (45%) patients were diagnosed with a primary oropharyngeal tumour and 54 (38%) primary oral cavity tumour; 57% (80/141) having stage 3 or 4 disease. Patients either received surgery with adjuvant radiotherapy (83/141, 59%), surgery with adjuvant chemoradiotherapy (15/141, 11%), radical radiotherapy (16/141, 11%) or radical chemoradiotherapy (27/141, 19%). A total of 52 patients (including 2 patients from

HOPON cohort) out of 141 (37%) developed ORN with no significant association on univariate analysis with sex, smoking, site of tumour, stage or treatment received (Table 10). The HOPON clinical trial excluded any patients taking bisphosphonates and none of the additional patients recruited had a history of taking bisphosphonates.

		ORN	No ORN	P value
Total		**52**	**89**	
ORN Grade	Grade 1	10 (19.2)		
	Grade 2	7 (13.5)		
	Grade 3	17 (32.7)		
	Unstaged ORN	18 (34.6)		
Sex	Male	43 (82.7)	64 (71.9)	**0.160**
	Female	9 (17.3)	25 (28.0)	
Smoking	Current	24 (46.1)	29 (32.5)	**0.209**
	Ex	13 (25.0)	32 (34.0)	
	Never	15 (28.8)	28 (31.5)	
Alcohol	Current	43 (82.1)	57 (64.0)	**0.125**
	Ex	1 (1.8)	6 (6.7)	
	None	8 (16.1)	14 (15.7)	
	Unknown	0 (0)	12 (13.5)	
Tumour Site	Oropharynx	25 (48.1)	38 (42.7)	**0.277**
	Hypopharynx	0 (0)	3 (3.4)	
	Nasopharynx	0 (0)	5 (5.6)	
	Larynx	1 (1.9)	4 (4.5)	
	Oral Cavity	21 (40.4)	33 (37.1)	
	Other *	4 (6.8)	6 (6.7)	
	Unknown	1 (1.9)	0 (0)	
Stage	1	2 (3.6)	4 (4.5)	**0.555**
	2	6 (10.7)	6 (6.7)	
	3	10 (21.4)	4 (4.5)	
	4a	30 (53.6)	32 (35.9)	
	4b	2 (3.6)	2 (2.2)	
	Unknown	2 (7.1)	41 (46.1)	
Treatment	Surgery + RT	34 (67.9)	49 (55.0)	**0.248**
	Surgery + CRT	5 (8.9)	10 (11.2)	
	Radical RT	9 (16.1)	7 (7.9)	
	Radical CRT	4 (7.1)	23 (25.8)	
Radiotherapy Volumes	Unilateral Neck	17 (32.7)	21 (23.6)	**0.575**
	Bilateral Neck	28 (53.8)	34 (38.2)	
	Unknown	7 (13.5)	34 (38.2)	
Post treatment dental procedures	Yes	14 (26.9)	89 (100)	
	No	19 (36.5)	0 (0)	
	Unknown	19 (36.9)	0 (0)	

Table 10: Patient metadata and association with ORN (Other included salivary gland, sinonasal, skin, cervical oesophagus tumour sites)*

3.3.2 Array sequencing analysis results

Bioinformatics analysis results were recorded and described below by Dr Phil Antczak (Associate-Director Liverpool Computational Biology facility).

3.3.2.1Identifying SNPs that define ORN

A PCA analysis of the dataset showed no specific separation between ORN positive and negative patients (Figure 13). As shown in Figure 13A, gender defines the two groups within our dataset based on the amount of missing data representing the Y chromosome specific SNPs on the array. For the identification of significantly different SNPs between ORN positive and negative we included four additional covariates; gender, age, alcohol consumption, and smoking status. This was to ensure that identified associations are to ORN only. This identified a total of 4053 SNPs.

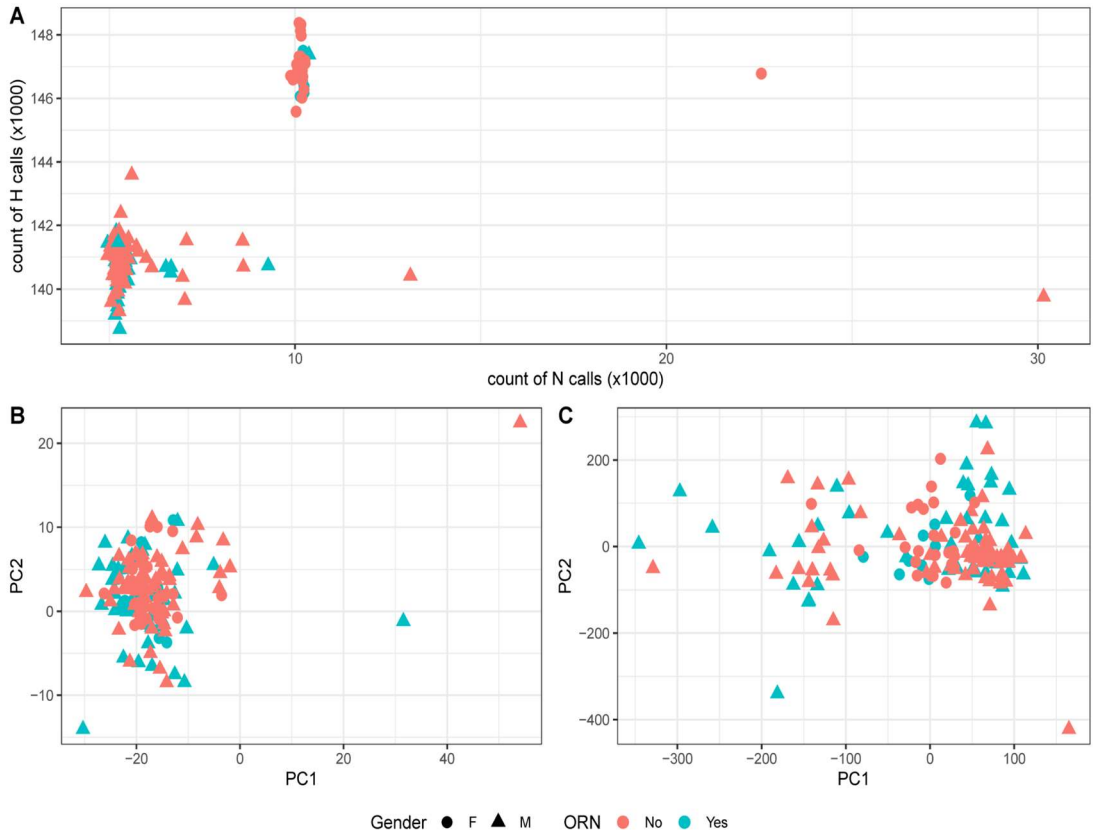

Figure 13: A) Quality control of SNP arrays identifies several samples with high heterozygous (H) and missing data (N). Difference in missing data is explained by gender differences. In addition, three outliers were identified. B) A principal component analysis based on the full dataset shows that several additional outliers were present in the data. C) After removal of potential outliers the PCA shows a well distributed sample space for ORN state.

The significant SNP list were further compared with the data within the 1000 Genomes Project and HapMap [189,190], as expected, controls clustered closely together with the European population within the 1000 Genome Project (Figure 14).

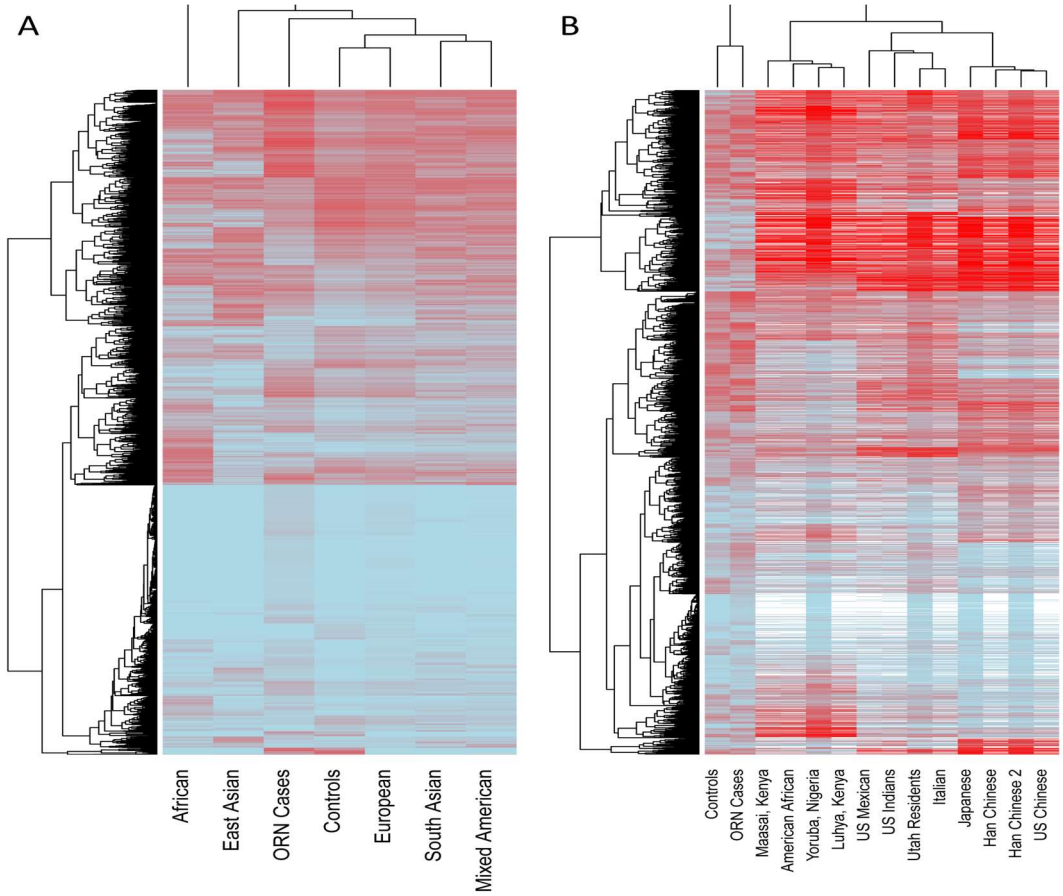

Figure 14: Mapping of the significantly associated 4053 SNPs to the data from the 1000 Genome Project (A) and HapMap (B). Controls closely associate with populations of European descent and most differ with African and East Asian populations.

3.3.2.2 Enrichment Analysis

Annotation of the SNPs identified 1764 overlapped genes and 483 genes within 10000 bases of their position. To better understand the genes the SNPs might have affected, separate functional enrichment analyses of the directly overlapped and nearest genes took place (see appendix 8).

Functional enrichment of the directly overlapping gene set (based on the 1764 genes) highlighted cell junction organization, parasympathetic nervous system development, synapse organisation and neuron differentiation (Figure 15).

Genes within 10000bp to SNPs without direct gene overlap enriched again in nervous system development, bone remodelling, and immune system relevant functions such as CD4+/CD25+ T cell differentiation.

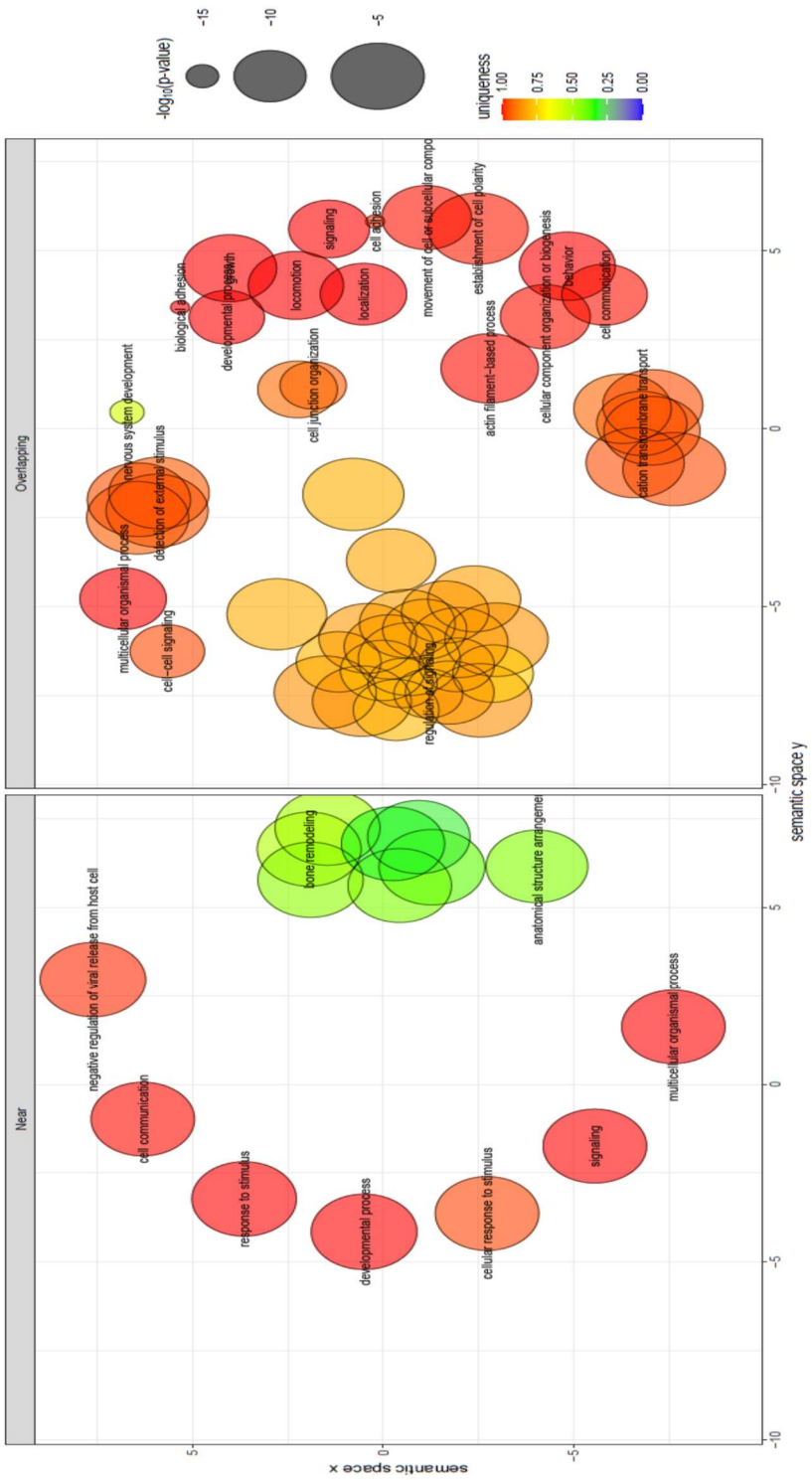

Figure 15: Functional enrichment map for the Gene Ontology Biological process terms of genes within 10000 bps (left) and overlapping genes (right). Functional terms are coloured by their uniqueness defining the similarity of terms within an enrichment. Size of the circle is representative of the p-value returned from the mapping. Axis x and y represent the semantic space based on overlaps of genes between the different GO terms.

3.3.2.3 Utilisation of an 18 SNP panel to predict ORN incidence

To test whether the allele frequencies could predict ORN, feature selection methodology was applied to the data. First the coded allele usage for each sample was extracted and used in a genetic algorithm based feature selection methodology (GALGO). In conjunction with a random Forest classifier, small sets of SNPs able to predict ORN within the patient cohort were identified. GALGO uses a dual training and test strategy linked with a cross-validation methodology to overcome overtraining of the models. The first training split is further split into a second level training/test split which is then used to generate a set of models. To ensure adequate coverage, 5000 models were developed, all of which achieving an accuracy of least 92% within the second level split. To discover a more representative and robust model a forward selection modelling approach on the initial training and test split was applied (Figure 13). The resulting model highlighted that while the control samples were well predicted, ORN cases could be predicted with approximately 70% accuracy (Figure 16). Here the best model reached an overall accuracy of 82%. To test whether this model could be reduced in size, backward selection was applied within GALGO. This resulted in a list of 18 SNPs that within the initial training and test split achieved 92% accuracy (Table 11). Running the model against numerous first splits within GALGO demonstrated the majority of control samples prediction was made (Figure 16B), however misclassification of some ORN cases was apparent

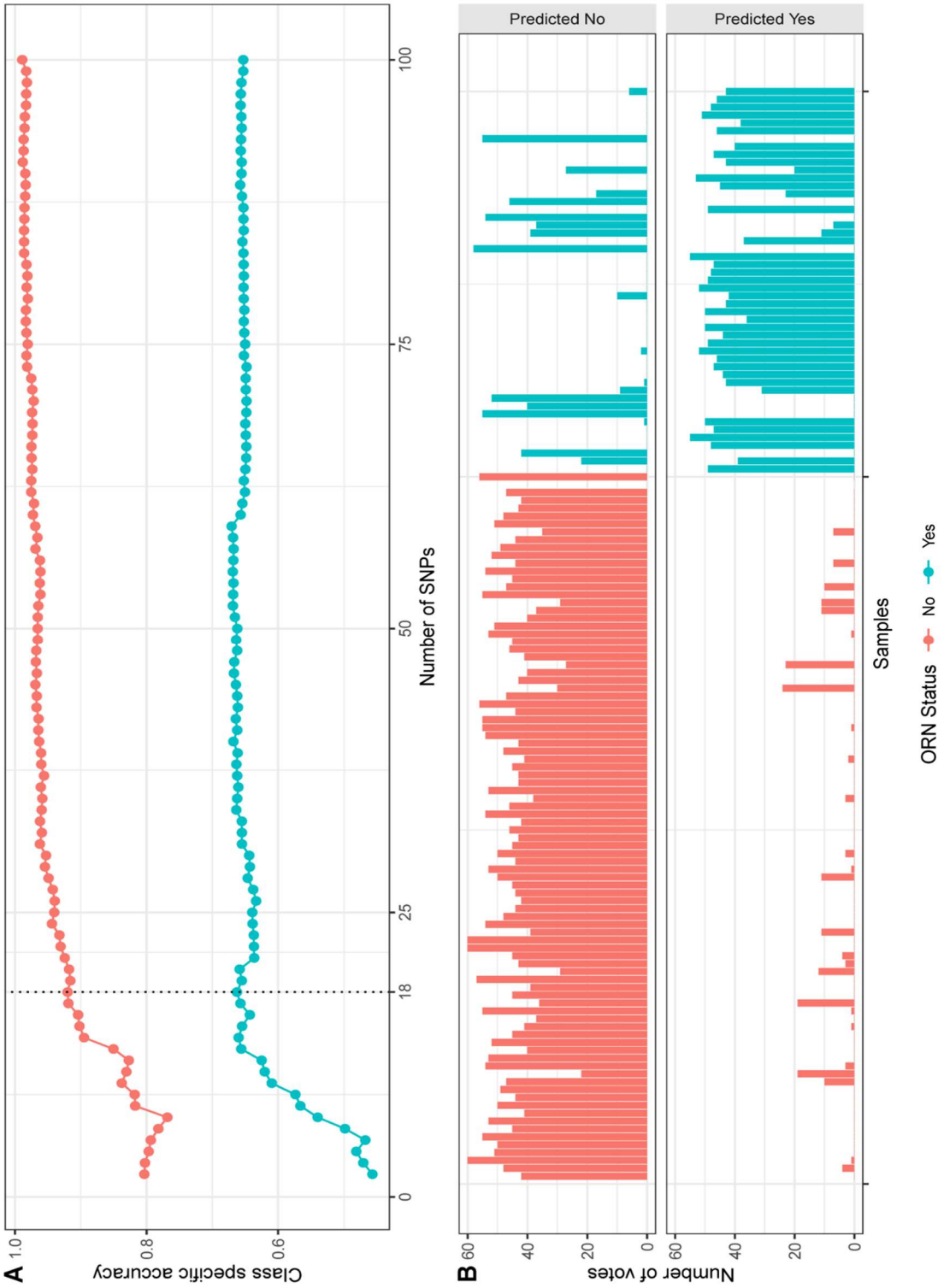

Figure 16: A) Forward selection trajectories indicate that individuals without ORN are easier to predict than ORN cases. B) Optimised 18 SNP model predicting ORN. While all controls are well predicted some ORN cases are still misclassified.

Variation.ID	Chromosome	Position	Gene	Distance	Alternative	Alt.Distance
rs2348569*	chr15	87764938	AC020687.1	61086	NTRK3	NTRK3
rs7477958*	chr10	65877716	CTNNA3	34802	LINC01515	LINC01515
rs11542332*	chr17	82062936	DUS1L	0		
rs1415848*	chr10	111744422	RPS6P15	245481	GPAM	GPAM
rs7022936*	chr9	90094948	IL6RP1	12379	AL161629.2	AL161629.2
rs2105042*	chr6	4229454	AL136309.1	39648	AL162718.1	AL162718.1
rs11605273*	chr11	65479355	AP000769.3	7886	AP000769.1	AP000769.1
rs34798038*	chr9	79589403	TLE4	0		
rs530752*	chr11	62903542	CHRM1	5137	SLC3A2	SLC3A2
rs6011731*	chr20	63317137	COL20A1	0		
rs62109235	chr19	37329328	HKR1	0		
rs72799439	chr2	39017526	SOS1	0		
rs1907158	chr3	26609736	AC099754.1	9594	VENTXP4	VENTXP4
rs117050257	chr11	28209650	METTL15	0		
rs10935916	chr3	153131702	AC117394.1	2062	AC117394.2	AC117394.2
rs114155093	chr1	86803641	AL355981.1	17917	AL049597.1	AL049597.1
rs6443282	chr3	175102206	NAALADL2	0		
rs61875969	chr10	58766077	BICC1	0		

*Table 11: List of 18 SNPs retained within optimised model, achieving 92% accuracy. *Representative selection of 10 SNPs taken through to internal technical validation.*

3.3.3 Validation results: Testing robustness of the optimised 18 SNP panel

In order to internally validate the optimised 18 SNP model, both univariate (UVA) and multivariate (MVA) regression analysis was used on a representative selection of ten targets using pyrosequencing data from our set of 141 patients (Table 11, appendix 10). When significant variables on UVA were incorporated into MVA, the model yielding the lowest AIC (117.5) excluded rs2105042 and rs11605273 whilst retaining rs34798038, rs6011731, rs2348569, rs530752, rs7477958, rs1415848. Significant genotypes were heterozygote rs34798038 (A/G) (p 0.006), rs6011731 (C/T) (p 0.018) and rs530752 (A/G) (p 0.046) along with the rarer variant homozygote genotype for rs2348569 (G/G) (p 0.005) (Table 12). This model produced ROC with AUC 0.859 (Figure 17) and was a good fit to the data assessed by Hosmer and Lemeshow (H-L) test (p>0.05). To further test how well our generated model performs we repeated the modelling with the inclusion of the nine patients removed during the SNP array analysis. This resulted in a marginally smaller AUC of 0.853.

Variable	UVA				MVA		
	Level	Odd's Ratio	95% CI	P-value	Odd's Ratio	95% CI	P-value
rs34798038	(ref A/A)						
	A/G	0.076	(0.01, 0.59)	0.076*	0.048	(0.01, 0.42)	0.006**
	G/G	0	0	1	0	0	1
rs2105042	(ref T/T)						
	C/T	0.742	(0.35, 1.56)	0.432			
	C/C	0.197	(0.05, 0.76)	0.018*			
rs11605273	(Ref G/G)						
	A/G	0.353	(0.10, 1.30)	0.118*			
	A/A	0	0	1			
rs11542332	(ref G/G)						
	A/G	0	0	0.999			
	A/A	0	0	1.0			
rs6011731	(ref T/T)						
	C/T	0.235	(0.07, 0.84)	0.026*	0.172	(0.40, 0.74)	0.018**
	C/C	0	0	1.0	0	0	1.0
rs2348569	(ref A/A)						
	A/G	1.095	(0.52, 2.32)	0.814	1.059	(0.42, 2.71	0.904
	G/G	0.113	(0.02, 0.53)	0.006*	0.086	(0.02, 0.48)	0.005**
rs530752	(ref A/A)						
	A/G	0.235	(0.05, 1.08)	0.064*	0.163	(0.03, 0.97)	0.046**
	G/G	0	0	1	0	0	1
rs1415848	(ref G/G)						
	A/G	1.568	(0.76, 3.24)	0.225	1.553	(0.64, 3.74)	0.327
	A/A	0	0	0.999	0	0	0.998
rs7022936	(ref G/G)						
	A/G	0.692	(0.25, 1.95)	0.487			
	A/A	0	0	0.999			
rs7477958	(ref T/T)						
	C/T	1.110	(0.54, 2.28)	0.778	2.275	(0.87, 5.95)	0.094
	C/C	0.206	(0.04, 0.99)	0.049*	0.251	(0.05, 1.42)	0.117
rs1800469	(Ref C/C)						
	T/C	0.698	(0.334, 1.459)	0.339			
	T/T	0		0.999			
AIC					117.498		
H-L test					Chi 6.273, p=0.617		
Nagelkerke R^2					0.451		
AUC (95% CI)					0.859 (0.795, 0.923)		

*Table 12: Summary statistics for variables included within Univariate (UVA) and retained variables on backward stepwise multivariate regression modelling (MVA) after including SNPs rs34798038, rs2105042, rs11605273, rs6011731, rs2348569, rs530752, rs7477958, rs1415848. *Variables taken through to MVA. **Significant SNPs following MVA.*

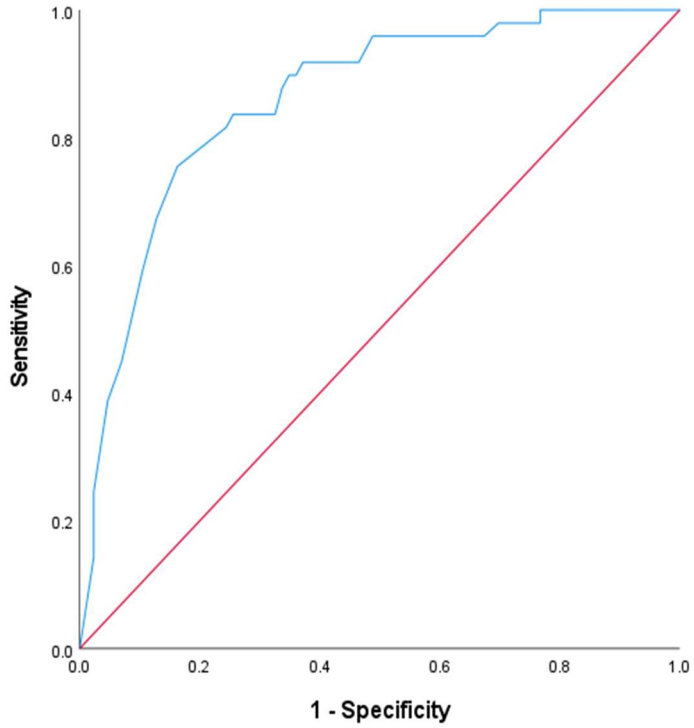

Figure 17: ROC curve demonstrating MVA using validation model (SNPs retained in model - rs34798038, rs6011731, rs2348569, rs530752, rs7477958, rs1415848.)

3.3.4 Validation of literature-based candidate genes

We sought to validate the SNP rs1800469 (TGF-β1) due to this target approaching significance (p 0.07) within the wider model [181]. The presence of the rarer C/T or T/T allele were not found to be significant on UVA when internally validated (Table 12). Other SNPs previously reported within candidate gene studies to be associated with ORN [137,138,187] did not retain significance; rs1695 within GSTP1 (p 0.258), rs1042522 pro allele of TP53 (p 0.557), rs1047768 within ERCC5 (p 0.146), and rs25487 within XRCC1 (p 0.307).

3.4 Discussion

The aim of this work was to assess whether specific genetic profiles could be applied to predict probability of developing ORN following head and neck radiotherapy. The optimised predictive model encapsulates a set of 18 SNPs which are able to distinguish control and ORN cases. This model was more effective in predicting controls rather than ORN cases, and this was echoed in subsequent validation. When validated, six SNPs were retained within the model and four genotypes significantly

reduced the likelihood of developing ORN; rs2348569 (G/G), rs34798038 (A/G), rs6011731 (C/T) and rs530752 (A/G) (Table 12).

This is the first GWAS experiment investigating ORN as a long term toxicity outcome following head and neck radiotherapy. The bioresource obtained from patients recruited to the CRUK HOPON study provided a uniquely well characterised and relevant control cohort (patients received radiotherapy doses >50Gy and underwent dentoalveolar surgery post treatment) and the means to investigate a unique binary outcome with very few confounding factors. In maintaining such unrivalled clean cohorts with blinded assessment of ORN, the 'noise' of data pooling/multiple outcomes seen in other radiogenomic GWAS experiments has been avoided.

The pathophysiology of ORN is poorly understood and theories have evolved from infection following trauma to treatment induced cellular and vascular damage leading to hypoxia and tissue breakdown [112]. More recently, reactive oxygen species (induced through the acute inflammatory response) are thought to play a key role in dysregulating collagen and fibrotic pathways [114]. The resultant promotion of fibrosis and prevention of effective vascularisation has been confirmed through the examination of dento-alveolar bone cores following irradiation; a reduction in microcapillaries correlating to increasing doses [115]. The heterozygote variant (C/T) SNP rs6011731 (p 0.018, OR 0.172) included within the internal validation selection represents an interesting target in being located within COL20A1 (collagen type XX alpha 1 chain). This gene encodes pro-alpha 1 chain of type 1 collagen which plays a key role in the assembly of collagen fibrils, organisation of extracellular matrix and tissue repair [188]. It is also a participant in the integrin pathway which ultimately results in inhibition of angiogenesis via thrombospondin 1 (TSP1) [191]. Similarly the heterozygote (A/G) rs34798038 was seen to reduce the odds of developing ORN (p 0.006, OR 0.048). This SNP lies within transducin like enhancer of split 4 (TLE 4) which is a member of TLE family of transcription repressor genes involved in regulating a number of pathways, including expression of WNT signalling and Runx2/Cbfa1 (that codes for a protein essential for osteoblast differentiation) [192,193]. The knock out of this gene in murine models has led to defective bone mineralisation and cortical bone thinning [194]. The SNP rs2348569 (p 0.005, OR 0.086) lies within an uncharacterised

genomic region, close to non-coding transcripts. Long non-coding RNAs are known to be differentially expressed following tumour irradiation in murine models, however it is currently unclear as to whether SNPs near to these non-coding transcripts may play a role in modulating normal tissue radiosensitivity [195]. A number of the validated genetic variants seem to relate to the described pathogenesis of ORN and may contribute to altered tolerance of the mandible to radiation through defective collagen assembly, angiogenesis and bone mineralisation. However external validation using larger patient cohorts will be required to confirm these findings.

Within the described wider model, 4053 SNPs were highlighted as significant in distinguishing ORN cases from controls and subsequent functional enrichment of overlapping genes highlighted pathways that have not previously been associated with the ORN disease process e.g. parasympathetic nervous system development, synapse organisation, and neuron differentiation. Bone remodelling and the balance between osteoblast and osteoclast activity was previously thought to be regulated by hormones (i.e. parathyroid hormone and insulin like growth factor 1) however more recent evidence supports a more complex interplay between endocrine and neural control. Central control of bone mass is thought to be modulated by a variety of neurotransmitters which can exert an inhibitory or excitatory effect through both beta 2 receptors possessed by osteoblasts and osteoclast nicotinic receptors [196]. Murine models demonstrate osteoclast apoptosis in response to cholinergic signalling promoting increased bone mass, whereas sympathetic signalling has the opposite effect [197]. Irradiating osteoblasts in culture led to elevated levels of acetylcholinesterase and this was confirmed in murine models whereby mouse limb bud irradiation promoted bone formation, osteoblast differentiation and a cholinergic phenotype presumably encouraging repair and remodelling [198]. Interestingly, the validated SNP rs530752 (p 0.046, OR 0.163) lies approximately 8000 base pairs from cholinergic receptor muscarinic 1 (CHRM1) which codes for the muscarinic acetylcholine receptor M1. This receptor is known to centrally regulate haematopoietic stem cell differentiation within the bone marrow via G-CSF [199]. Variants close to this gene may influence the expression of CHRM1, parasympathetic

innervation of mandibular bone and augmentation of osteoblast function [200,201] thus altering repair and remodelling in response to radiotherapy.

Previously identified variants from candidate gene studies examining long term radiation toxicity in head and neck cancer did not prove to be significantly associated with ORN in this study [137,138,187]. Similarly the top 18 SNPs highlighted as significant in our series have not been reported in other studies to be associated with late radiation toxicity, presumably due to the SNP array sequencing eliminating gene selection bias. RS1800469 (TGF-β1) was of particular interest given the evidence reported across a variety of solid tumours linking this target to long term radiation toxicity [181]. TGF-β proteins have a wide range of reported functions; with abnormal bone remodelling, increased fibroblast proliferation and abnormal accumulation of extracellular matrix originally thought to be responsible for poor healing following radiotherapy [202]. TGF-β is also known to modulate inflammation and promotes Th17 cell differentiation from CD4+/CD25+ T cells [203]. Enrichment analysis highlighted SNPs without direct overlap within these immune functions, and although rs1800469 was not significantly associated with ORN during validation analysis, it remains likely that it will have an additive effect within this multi-loci model.

This work has limitations, specifically the small sample size, which potentially increases the possibility of false positive associations, however conclusions have been successfully confirmed through internally validating single targets. In addition, as with all GWAS experiments, there is the potential of missing low frequency loci with small effect sizes and as a result it will be necessary to further confirm findings with larger external validation cohorts. A further limitation is the absence of irradiated mandibular volume and mean/maximum dose data due to historic changes in planning software; future investigations would be strengthened by the inclusion of radiotherapy dosimetric parameters and this will now be achievable with routine mandible contouring and intensity modulated radiotherapy plan evaluation. During QC of the array data, nine patients were excluded based on their positioning within a PCA. One could argue that these individuals may represent a phenotype influenced by an alternative mechanism of interest; however, the study sample size limited further exploration. Interestingly, the validation of the SNPs via pyrosequencing

showed that inclusion of the nine outlier patients did not significantly decrease the AUC of the model, suggesting that technical differences in the array likely significantly influenced their placement in the PCA. The unique control group did include a proportion of patients who received hyperbaric oxygen and it is unknown whether these individuals would have derived benefit from this therapy. As reported the effect is likely to be negligible given the matched patients in the control group having a similar rate of radionecrosis.

3.5 Conclusion

The development of the described model has facilitated the discovery of novel biological mechanisms which may play a role in the development of ORN, namely neurogenesis and neural differentiation. Future investigating the parasympathetic and sympathetic regulation of bone remodelling in response to radiation (and how neural bone homeostasis interacts with inflammatory responses) would take a further step towards understanding this complex phenotype, and could generate new avenues for therapeutic manipulation. Validated loci strengthened previous theories regarding the involvement of collagen deposition (COL20A1) and bone mineralisation (TLE 4) along with strengthening the hypothesis that neural regulation (CHRM1) of bone remodelling has a role to play in the pathogenesis of ORN. With the incidence of head and neck cancer steadily increasing over the last three decades and survival outcomes improving through the use of new anticancer agents, more patients are living with devastating consequences of ORN [8]. It is vitally important that we expand our understanding of this condition and strive to develop biomarkers to prevent its occurrence and improve therapeutic options. If these findings are confirmed in larger, external validation cohorts, this polygenic risk model may contribute to a pre-treatment risk prediction tool and facilitate much needed tailored radiotherapy treatment strategies.

Chapter 4
Altering treatment to improve quality of life; Impact of dosimetric parameters on ORN risk.

4.1 Introduction

Chapter 3 worked towards developing genetic profile which may (when externally validated) be protective for the development of ORN. One criticism for this genetic model is the absence of in-depth dosimetric parameters which can impact upon the individual likelihood of developing ORN.

Although a number of previous series have published dosimetric parameters which increase patient ORN risk [132, 204], there is a lack of normal tissue complication probability models (NTCP) to aid clinicians utilising highlighted parameters for mandibular RT constraints. Along with this, published series evaluating ORN dosimetric risk factors have, in the main, included patients receiving radical CRT/RT for predominantly oropharyngeal primary tumour [134, 132]. Evidence regarding mandibular RT tolerance in the post-operative setting, particularly in locally advanced OCSCC where free bone/tissue flaps are readily placed, is scant. Two longitudinal observational studies have included matched proportions of OCSCC cases with other HNSCC sites, both of which noting the increased risk within this group. Kuhnt et al, who evaluated 776 patients with HNSCC (259 OCSCC) and described a greater ORN risk in those with tumours in the oral cavity (HR = 4.69; 95 % CI: 1.33-16.52), and Moon et al who similarly described higher ORN risk in this subsite (n=68) but only on univariate analysis (HR = 3.02; 95%CI: 1.06-8.61) [131, 205]. These reports seemed to contradict other works which describe increased risk within the oropharyngeal subsite [204]. It seems plausible that the former reports are true as in this setting high dose target volumes often including substantial areas of the mandible. This is mainly a function of the extensive reconstructive procedures undertaken in order to provide optimal functional outcomes following tumour resection, coupled with treating oncologist uncertainty over involved margin location [206]. Although local current practice minimises mandibular 'hot spot' doses of >60Gy during RT planning, these constraints are often compromised for adequate tumour bed coverage. This is especially relevant in the oral cavity subsite where target volumes are in close

proximity to the mandible. In addition, it remains difficult to assess and act promptly upon anatomical variation during treatment (i.e. weight loss) which is likely to alter dose delivered to the mandible during RT courses.

Previous incorporated dosimetric variables into ORN multivariate predictive models in prior works are arbitrary (e.g. selecting 10Gy bin intervals) and traditional regression modelling can result in over-fitting. Least absolute shrinkage and selection operator (LASSO) method for dosimetric toxicity modelling was first recommended by Xu et al [207] and has been used in the evaluation of post head and neck RT saliva function, oral mucositis and acute rectal toxicity following RT for gynaecological cancers [208,209]. This method of regression analysis reduces the dimensionality of large datasets and provides reliable variable selection and prediction [207]. Despite these advantages, in shrinking some coefficients to zero, LASSO can still exclude some variables which may be important. This is a particular problem when collinearity exists, and when cohort numbers are small with large numbers of observations (as is the case with dosimetric data) [210]. The elastic net method solves the limitations associated with LASSO through combining the properties of LASSO with ridge regression (penalising model coefficients and reducing complexity) [211]. In so doing, this regularises model coefficients as well as retaining correlated variables thus maintaining robust variable selection when faced with collinear data and creating a model of greater predictive ability. This method is yet to be utilised in mandibular ORN probability modelling nor in the majority of solid tumour normal tissue complication probability modelling (NTCP).

The future incorporation of checkpoint inhibitors in the radical management of locally advanced OCSCC (see Chapter 5) may lead to an improvement in outcomes for this group and therefore reducing the impact of side effects such as ORN remains a priority to improve long term quality of life for patients. The effective prediction of mandibular ORN in this group will enable improved informed consent procedures, and the potential for more personalised RT dose prescription.

4.1.1 Chapter hypotheses

- **The incidence of ORN in patients with locally advanced OCSCC undergoing radical reconstructive surgery and subsequent post-operative radiotherapy is higher than reported in published literature, which mainly include patients having non-surgical radical treatment.**

The incidence and location of ORN within this population will be determined.

- **The presence of free bone flaps may reduce mandibular RT tolerance.**

Within this patient cohort the integrity of the mandible is disrupted during ablative surgery by mandibulotomy, rim resections and mandibulectomy. Reconstruction often involves placement of free bone flaps. The impact of non-native bone within the mandible upon ORN risk will be assessed.

- **Using LASSO/Elastic net for variable selection and modelling will produce an ORN NTCP model of improved performance than traditional multivariate regression analysis.**

Using the outlined methods of variable selection will be explored and provide an opportunity to incorporate additional dosimetric parameters into NTCP modelling which have previously been overlooked in traditional multivariate regression analyses.

- **ORN models combining dosimetric parameters with genetic parameters may perform better than each in isolation.**

Previous reports have advocated combining dosimetric with non-dosimetric parameters in order to improve NTCP model performance [212]. Attempts to compare this dosimetric model with the optimised genetic risk model obtained in Chapter 3 may demonstrate improved ability to predict ORN cases.

- **Altering contours i.e. by reducing target volume margining may reduce NTCP values in patients with ORN.**

With the development of novel personalised RT strategies, for example anatomy-adaptive adapted radiotherapy (A-ART) using MRI linac, it may be possible to reduce doses to normal tissues through smaller expansion margining and re-planning during RT courses as structural/spatial changes occur. As proof of principle re-planning

patients who developed ORN with reduced target volume margining will demonstrate if a reduction in NTCP is achievable.

4.2 Methods

4.2.1 Ethics

Approval for retrospective data collection and audit was obtained from Aintree University Hospital and The Clatterbridge Cancer Centre NHS Foundation Trust. Patients included in small external validation cohort consented to their collected blood samples to be utilised in head and neck research studies with approval from North West – Liverpool Central REC (Ref. No. 10/H1002/53).

4.2.2 Population

97 patients with locally advanced oral cancers (T1-4 N1-3/T3-4 N0) were identified as being treated with post-operative radiotherapy (60-66Gy in 2Gy per #) following surgical resection from November 2014 to January 2018 with evaluable intensity modulated radiotherapy plans. All patients had either free flap reconstructions and/or intervention disrupting the integrity of the mandible during their surgical procedure. A minimum of two years follow up data was ensured and the start date selected as the time from which Clatterbridge Cancer Centre reliably used intensity modulated radiotherapy (IMRT) planning. One patient was excluded from analysis due to their plan being no longer available within the planning archival data storage. In addition to dosimetric data, information on patient smoking status, alcohol consumption and use of concurrent chemotherapy was collected. Of these 96 patients, 26 had stored blood samples available for single target genotyping (methods outlined in Chapter 3, section 3.2.6).

4.2.3 Scoring of ORN

Patients were categorised as having osteoradionecrosis of the mandible or no osteoradionecrosis after case note review and review of imaging records. Blinded radiological scoring of ORN was performed by Consultant in Oral & Maxillofacial Surgery using the Notani grading system (Figure 6).

4.2.4 Radiotherapy treatment

The high-risk clinical target volume (CTV) covered the surgical tumour bed, inclusive of reconstructed free flap (with margin 5-10mm depending on pathological risk factors) and ipsilateral or bilateral involved lymph node areas within the neck. The low-risk CTV included ipsilateral or contralateral prophylactic lymph node areas within the neck. A margin of 5mm was added in all planes to form the planning target volume (PTV). The prescribed RT dose to high-risk PTV was 60-66 Gy and the dose to low-risk PTV was 54Gy. In those with pathological indications for concurrent chemotherapy, cisplatin was administered at 21 day intervals at a dose of 100mg/m^2.

4.2.5 Dosimetric data

Mandible contours were checked for coverage (entire mandible bone visualised using bone windows excluding teeth), and adjusted if required or added for those patients missing mandible structure set (figure 18). A single plan sum was created for those with separate upper and lower neck plans and those with prescribed doses over/under 2Gy per fraction adjusted using the equivalent dose in 2-Gy fraction calculation and α/β of 3 ($EQD_2 = D\ \frac{d+\left(\frac{\alpha}{\beta}\right)}{2+\left(\frac{\alpha}{\beta}\right)}$). Plans that had been calculated on the standard Analytical Anisotropic Algorithm (AAA) were re-calculated using Acuros XB (Eclipse version 15606, Varian Medical Systems) in order to create plans based on dose-to-medium rather than dose-to-water thus evaluating mandibular doses more accurately. Both cumulative and differential dose volume histograms in 1Gy dose bins were exported for each evaluable patient. Mean, maximum, and minimum doses were also exported.

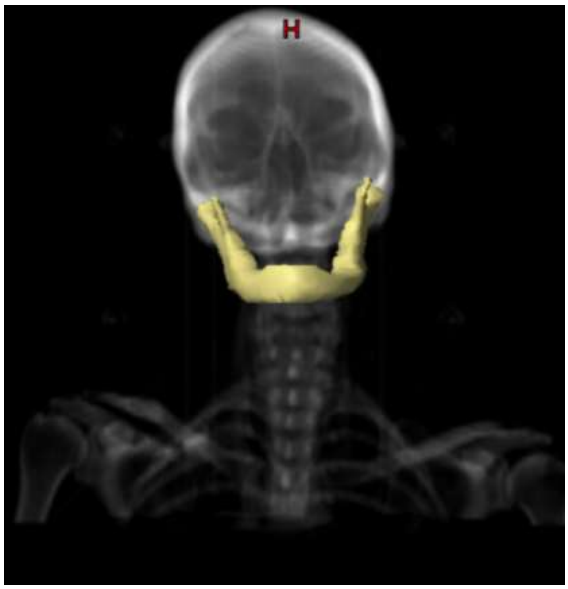

Figure 18: 3D reconstruction of mandible contouring

4.2.6 Statistical Analysis

4.2.6.1 Unpenalised multivariate regression modelling

Data analysis was completed using SPSS Statistics (IBM version 27) and Stata (IC v16, StataCorp). Mean 'dose to percentage structure volume' at 10 Gy intervals, mean, maximum, minimum, total doses with and without ORN were compared using non-parametric Mann Whitney U Test. Chi squared or Fishers Exact Test (when counts were low) were used for clinical categorical variables (e.g. smoking, concurrent chemotherapy etc.). Univariate logistic regression was also completed to assess association between ORN and dosimetric / clinical parameters. Those variables significant on Mann Whitney U/ chi squared test and/or having a p-value of ≤0.2 on univariate analysis were taken on to multivariate modelling. Backward stepwise parameter elimination was performed with entry of clinically relevant variables in separate models. The best performing model was selected taking into consideration akaike information criterion (AIC), deviance and likelihood ratios. Model performance was assessed using the Area Under the Receiver Operating Curve (AUC ROC) and Nagelkerke R^2. Goodness-of-fit was assessed using Hosmer–Lemeshow (H-L) test and calibration plots.

4.2.6.2 NTCP modelling using Elastic net (LASSO)

Following standardisation using the formulae $x = \frac{X-\mu}{\sigma}$, data was split into training and testing cohorts (50% / 50%); models were built on the training set and internally validated on testing set. Variable selection using Elastic Net with 10 fold cross validation was completed. Optimal lambda and Elastic Net alpha were selected in order minimise effect of collinearity and model diagnostics examined using coefficient plots, brier score, calibration plots and AUCROC. Selected dosimetric parameters from elastic net (% volume receiving 47Gy to 60Gy) were averaged to create new variable (mean % volume 47-60Gy) and incorporated into penalised regression with 10 fold cross validation. Model performance was assessed using brier score, AUC ROC, and calibration plot and compared with elastic net performance. Coefficients from the optimal selected model were incorporated into NTCP model using the equation:

$$NTCP = (1+e^{-s})^{-1},$$

Where $s = \beta_0 + \beta_1 x_1 \dots \beta_n x_n$

4.2.7 Assessing impact of altered PTV margin on mandible volumes

Archival contours in those with a diagnosis of ORN were adjusted to create additional target volume structure set with reduced CTV to PTV margin (Pm) (figure 19). Change in volume was noted for each and for one, example patient the VMAT plan was recalculated and optimised as per new contours. Dosimetric parameters were extracted as per section 4.2.5 and plotted on NTCP model curve to assess potential improvement in toxicity risk following altered contouring / planning techniques.

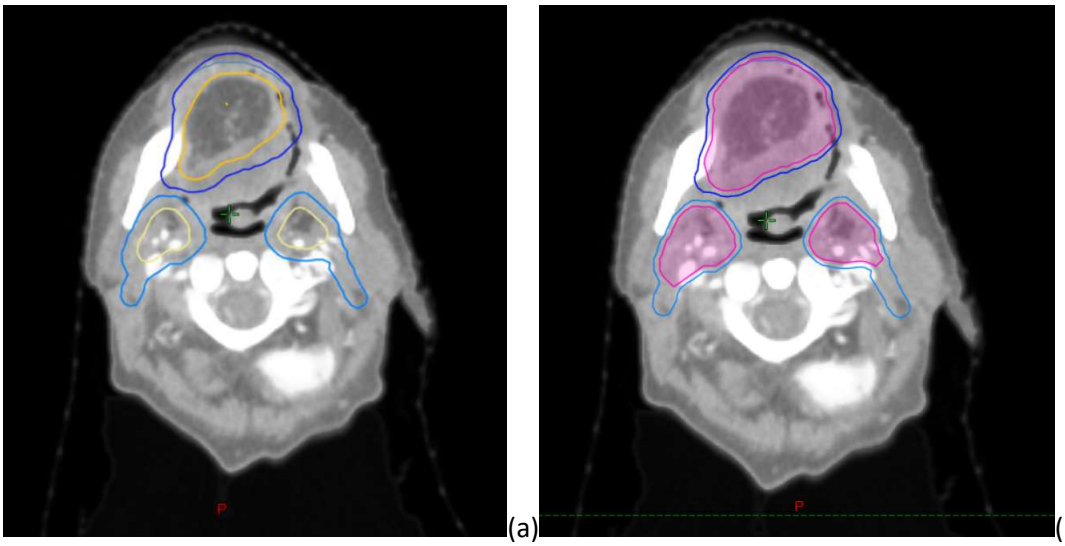

Figure 19: a) Archival contour for example case with tumour bed (inclusive of reconstructed free flap) included in high risk CTV (orange) with 5mm margin from CTV to PTV (dark blue). Prophylactic nodal areas within low dose CTV (yellow) with 5mm margin from CTV to PTV (light blue). (b) Reduction of CTV-PTV margin to 3mm (pink).

4.2.8 Genotyping with single targets

DNA extraction in a selection of 26 patients from within this cohort who had both dosimetric data and stored blood samples available took place. Following DNA extraction, previously demonstrated SNPs of interest within validated model in Chapter 3 were sequenced as previously described. (See section 3.2 for DNA extraction and pyrosequencing methods).

4.2.9 Comparing model performance

Both the validated SNP profile model (Chapter 3 section 3.3.3) and dosimetric model were run on this small external validation cohort. ROC curve, Brier statistic and H-L test were used to assess which model was the better predictor of ORN.

4.3 Results

4.3.1 Patient characteristics

Summary of patient characteristics are outlined in Table 13. Of the 96 patients included in the analysis the majority 93.7% underwent free flap reconstructive procedures (plus mandibulotomy, mandibulectomy or dental clearance). Of the patients without free flap reconstruction (n=6) three had mandibular rim resections, one had mandibulotomy and one dental clearance procedures. 68 (70.8%) had stage 4 disease and the remainder (29.2%) had stage 3. 17 patients out of 96 (17.7%) developed ORN with an average time from RT to ORN of 17.9 months and majority

having Notani grade 3 disease (64.7%). There were close to half of patient received unilateral and bilateral radiotherapy (51% and 49% respectively). All cases developed ORN within the treated high dose PTV (Figure 20). The average DVH for those with ORN is compared with those without ORN in Figure 21 and displays the relationship between volume of mandible receiving dose and toxicity.

Factor		**ORN**	**No ORN**	**Total**	**P value**
ORN		17 (17.7)	79 (82.3)	96	
Grade	Notani 1	3			
	Notani 2	3			
	Notani 3	11			
Sex	Male	9 (52.9)	46 (58.2)	57 (59.4)	**0.789**
	Female	8 (47.1)	36 (45.6)	41 (42.7)	
Smoking	Current	9 (52.9)	25 (31.6)	34 (35.4)	**0.277**
	Ex	5 (29.4)	35 (44.3)	40 (41.7)	
	Never	3 (17.6)	19 (24.1)	22 (22..9)	
Tumour Site	Mandible	4 (23.5)	20 (25.3)	24 (25)	**0.363**
	Maxillary alveolus	0 (0)	10 (2.7)	10 (10.4)	
	Tongue	7 (41.2)	29 (36.7)	36 (37.5)	
	Floor of mouth	6 (35.3)	13 (16.5)	19 (19.8)	
	Buccal	0 (0)	5 (6.3)	5 (5.2)	
	Hard palate	0 (0)	2 (2.5)	2 (2.1)	
Stage	3	6 (35.3)	22 (27.8)	28 (29.2)	**0.564**
	4a	11 (64.7)	57 (72.2)	68 (70.8)	
Flap type	Scapular	0 (0)	7 (8.8)	7 (7.3)	**0.337**
	Radial forearm	9 (52.9)	33 (41.7)	42 (43.8)	
	DCIA	3 (17.6)	4 (5.1)	7 (7.3)	
	Fibular	1 (5.9)	15 (18.9)	16 (16.7)	
	Anterolateral thigh	4 (23.5)	12 (15.2)	16 (16.7)	
	MSAP	0 (0)	2 (2.5)	2 (2.1)	
	Rectus abdominus	0 (0)	1 (1.3)	1 (1)	
	None	0 (0)	5 (6.3)	5 (5.2)	
	Rim resection	3 (14.2)	17 (26.5)	20 (23.5)	**0.615**

Mandibular intervention	Mandibulotomy	4 (19.0)	6 (8.1)	10 (11.7)	**(free bone flap)**
	Mandibulectomy	6 (28.6)	23 (31.1)	29 (34.1)	
	Dental Clearance	8 (38.1)	18 (24.3)	26 (30.6)	
Non-surgical Treatment	Adjuvant RT	16 (94.1)	66 (83.5)	82 (84.4)	**0.452**
	Adjuvant CRT	1 (5.8)	13 (16.5)	14 (17.7)	
RT Fields	Unilateral	7 (41.2)	42 (53.2)	49 (51.0)	**0.370**
	Bilateral	10 (58.8)	37 (46.8)	47 (49.0)	
Recurrence	Locoregional (HD PTV)	0 (0)	16 (20.3)	16 (16.7)	
	Locoregional (outside HD PTV)	1 (5.8)	8 (10.1)	9 (9.4)	
	Locoregional (clinical)	0 (0)	3 (3.8)	3 (3.1)	
	Distant Metastasis	2 (11.8)	7 (8.9)	10 (10.4)	
Postop wound infection	Yes	1 (5.8)	12 (15.2)	14 (14.6)	**0.453**
	No	16 (94.1)	67 (84.8)	83 (86.5)	

Table 13: Summary of patient characteristics with chi-square/fishers exact p-value.

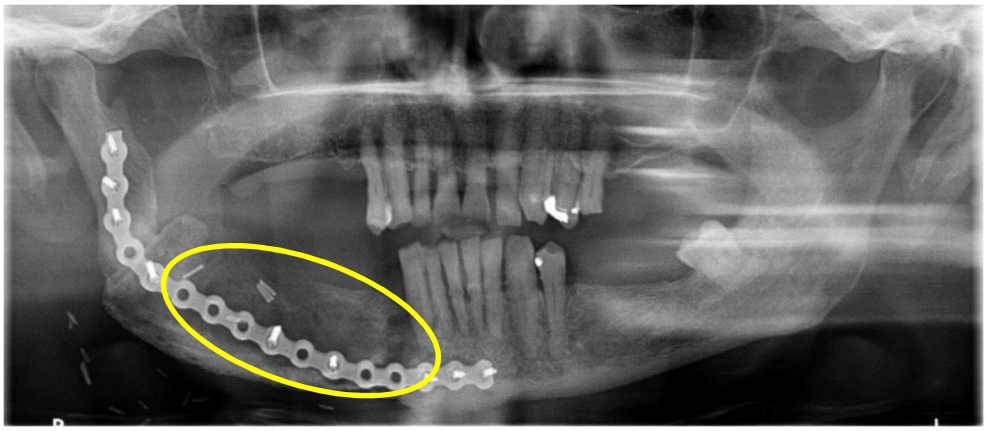

(a)

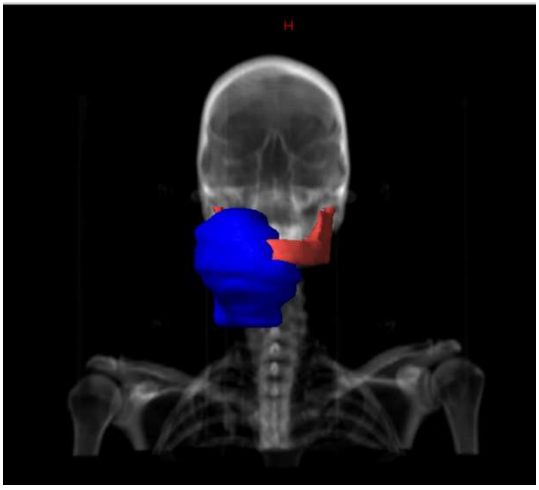

(b)

Figure 20: (a) Blinded review of each case took place with site of ORN outlined on OPG (yellow). (b) RT plans were checked for location of high dose PTV (blue) and correlated with outlined site of mandibular disease. As indicated by shown example, all cases of ORN were within high dose PTV.

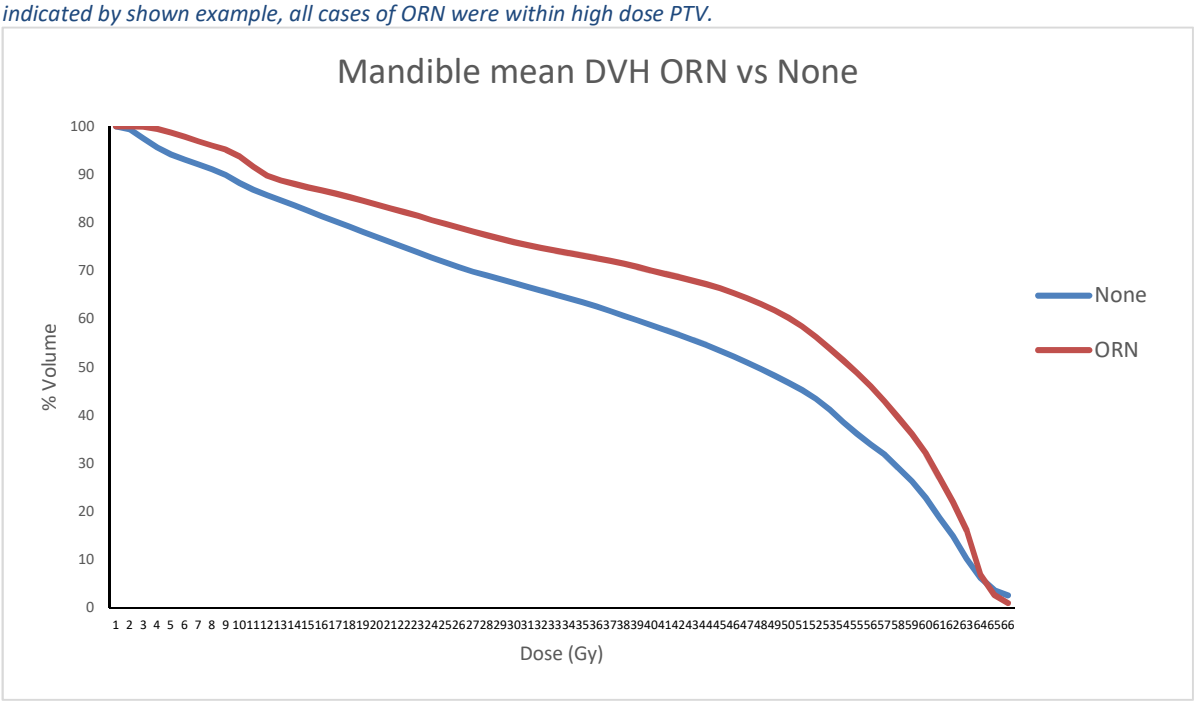

Figure 21: Comparison of mean cumulative DVH for those with ORN (red line) and those without (blue line).

4.3.2 Exploratory data analysis and correlations

None of the collected clinical parameters were significantly associated with ORN however the % volume receiving 40 and 50 Gy along with mean dose were shown to be significant on Mann Whitney U test (p 0.03, 0.01 and 0.01 respectively) (Table 14). Mapping correlations revealed the mean dose was closely correlated (Spearman Rho >0.7) with the majority of dosimetric variables as well as each dosimetric parameter with its neighbouring bin (Table 15).

Variable	ORN (n=17)	No ORN (n=79)	Difference (95% CI)	p-value
% Volume (Gy)				
10	91.6 (6.0)	85.6 (16.6)	6 (3.65, 8.35)	0.72
20	83.1 (11.2)	74.5 (19.8)	8.6 (1.81, 15.39)	0.14*
30	75.4 (15.5)	65.4 (21.7)	10 (1.37, 18.63)	0.08*
40	69.1 (17.8)	56.3 (21.7)	12.8 (2.77, 22.33)	**0.03****
50	58.1 (17.6)	43.8 (19.0)	14.3 (5.14, 23.46)	**0.01****
60	25.6 (20.5)	17.0 (15.1)	8.6 (-1.45, 18.65)	0.13*
Mean	45.1 (7.0)	39.1 (9.9)	6 (1.51, 10.49)	**0.01****
Total	63.1 (2.5)	63.7 (2.0)	-0.6 (-1.84, 0.64)	0.47
Min	3.9 (2.7)	3.9 (3.0)	0 (-1.42, 1.42)	0.62
Max	64.8 (2.3)	64.7 (2.3)	0.1 (-1.07, 1.27)	0.66

Table 14: Summary Statistics for dosimetric data. Showing means (std dev), difference is difference in means.

Correlations

Variable	vol10	vol20	vol30	vol40	vol50	vol60	average	max	min	total
vol10	1.00	.71**	.48**	.38**	.27**	.03	.43**	-.10	.75**	-.11
vol20	.71**	1.00	.92**	.83**	.66**	.12	.76**	-.03	.49**	.00
vol30	.48**	.92**	1.00	.96**	.80**	.18	.83**	.02	.30**	.00
vol40	.38**	.83**	.96**	1.00	.91**	.27**	.84**	.04	.20*	-.02
vol50	.27**	.66**	.80**	.91**	1.00	.50**	.78**	.22*	.14	.03
vol60	.03	.12	.18	.27**	.50**	1.00	.28**	.79**	-.01	.40**
average	.43**	.76**	.83**	.84**	.78**	.28**	1.00	.07	.41**	.21*
max	-.10	-.03	.02	.04	.22*	.79**	.07	1.00	-.11	.60**
min	.75**	.49**	.30**	.20*	.14	-.01	.41**	-.11	1.00	.08
total	-.11	.00	.00	-.02	.03	.40**	.21*	.60**	.08	1.00

**. Correlation is significant at the 0.01 level (2-tailed).

*. Correlation is significant at the 0.05 level (2-tailed).

Table 15: Table mapping correlations between dosimetric variables. Yellow indicates positively correlated variables spearman ρ ≥0.7. Strong positive correlations (≥0.8) indicated in red.

4.3.3 Univariate and multivariate analysis

Univariate regression revealed the volume receiving 20-60Gy (in 10Gy bins) and mean dose as having p value <0.2 and so were taken through to multivariate regression analysis. Current smoking and concurrent chemotherapy were selected as important clinical factors to assess given previous evidence suggesting an impact upon ORN risk [134]. In addition, the presence of a free bone flap was included due to the significant disruption to the mandible this brings and speculated impact upon ORN risk. No clinical variables were significantly associated on univariate analysis (although being a current smoker was approaching, p=0.26) (table 16). Due to collinearity demonstrated between mean dose and other dosimetric variables two separate multivariate models were created:

- Model 1 incorporating %volume receiving 20, 30, 40, 50, 60Gy plus the clinical factors smoking, concurrent chemotherapy, and presence of bone flap.
- Model 2 incorporating mean dose, smoking, concurrent chemotherapy, and presence of bone flap.

The % volume receiving 50Gy was retained as significant on backward selection with p 0.017 and OR of 1.04. Similarly in model 2 the mean dose retained significance (p 0.02, OR 1.11). Upon review of model fit and performance it was evident that Model 1 was superior with a lower AIC of 90.06 and H-L chi^2 5.76. There was only a marginal difference in AUC between the two models (0.69 and 0.70) (Table 17). Comparator plotted ROC curves are shown in Figure 22. Significant variables had marginally increased odds ratios which was thought to reflect the collinear data across dosimetric variables and further supported moving to attempt penalised regression in order to eliminate this bias.

Variable	Level	Odd's Ratio	95% Confidence Interval	P-value
Vol10		1.03	(0.97, 1.09)	0.31
Vol20*		1.03	(0.99, 1.08)	0.16
Vol30*		1.02	(0.99, 1.06)	0.13
Vol40*		1.03	(1.00, 1.06)	**0.04**
Vol50*		1.04	(1.01, 1.07)	**0.01**
Vol60*		1.03	(0.99, 1.06)	**0.08**
Average*		1.12	(1.02, 1.21)	**0.01**
Max		1.10	(0.89, 1.36)	0.38
Min		0.82	(0.86, 1.21)	0.82
Total		0.56	(0.92, 1.18)	0.56
Smoking*	**(Baseline=None)**			
	Current	2.28	(0.54, 9.58)	0.26
	Ex	0.91	(0.19, 4.21)	0.89
Chemo*	**(Baseline=No)**			
	Yes	1.47	(0.30, 7.25)	0.63
Bone flap*	**(Baseline=No)**			
	Yes	0.79	(0.24, 2.27)	0.62

*Table 16: Univariate regression results. % volume receiving 40Gy, 50Gy, 60Gy and average dose were significantly associated with ORN at the 5% level (bold). * indicates variable taken through to multivariate analysis.*

	Model 1				Model 2			
Variable	**Entered variables**	**Odd's Ratio**	**95% CI**	**P-value**	**Entered variables**	**Odd's Ratio**	**95% CI**	**P-value**
Vol20	X							
Vol30	X							
Vol40	X							
Vol50	X	1.039	(1.007, 1.072)	0.017				
Vol60	X							
Average					X	1.115	(1.023, 1.215)	0.013
Smoking	X				X			
Chemo	X				X			
Bone flap	X				X			
AIC	90.057				91.653			
H-L test	Chi^2 5.755 p=0.675				Chi^2 8.650 p=0.373			
Nagelkerke R^2	0.108				0.133			
AUC ROC	0.692				0.704			
Deviance	88.057				89.653			

Table 17: Multivariate modelling and summary performance statistics. % volume receiving 50Gy was retained as significant at the 5% level in Model 1 and the average dose in Model 2. None of the clinical variables were retained on backward selection.

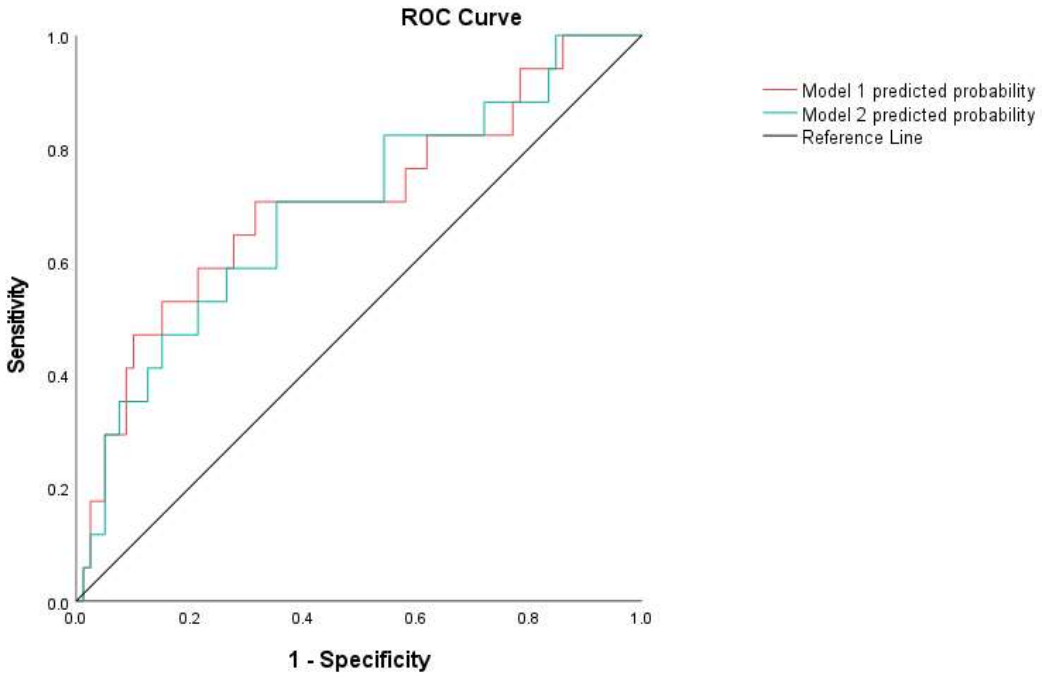

Figure 22: Comparison ROC curves for both Model 1 (0.692) and Model 2 (0.704).

4.3.4 Influential Observations

Upon plotting cooks distance and examining residual plots it was evident that one observation had a significant influence upon the modelling results (patient number 95) (Figure 23). When these individual dosimetric observations and RT plan was examined, both were representative of the patient group as a whole. When these observations were excluded there was only a marginal change in model performance with AUC ROC 0.689. Model fit statistics were unchanged (H-L test 5.755, AIC 90.057) and so this outlier was retained within the analysis.

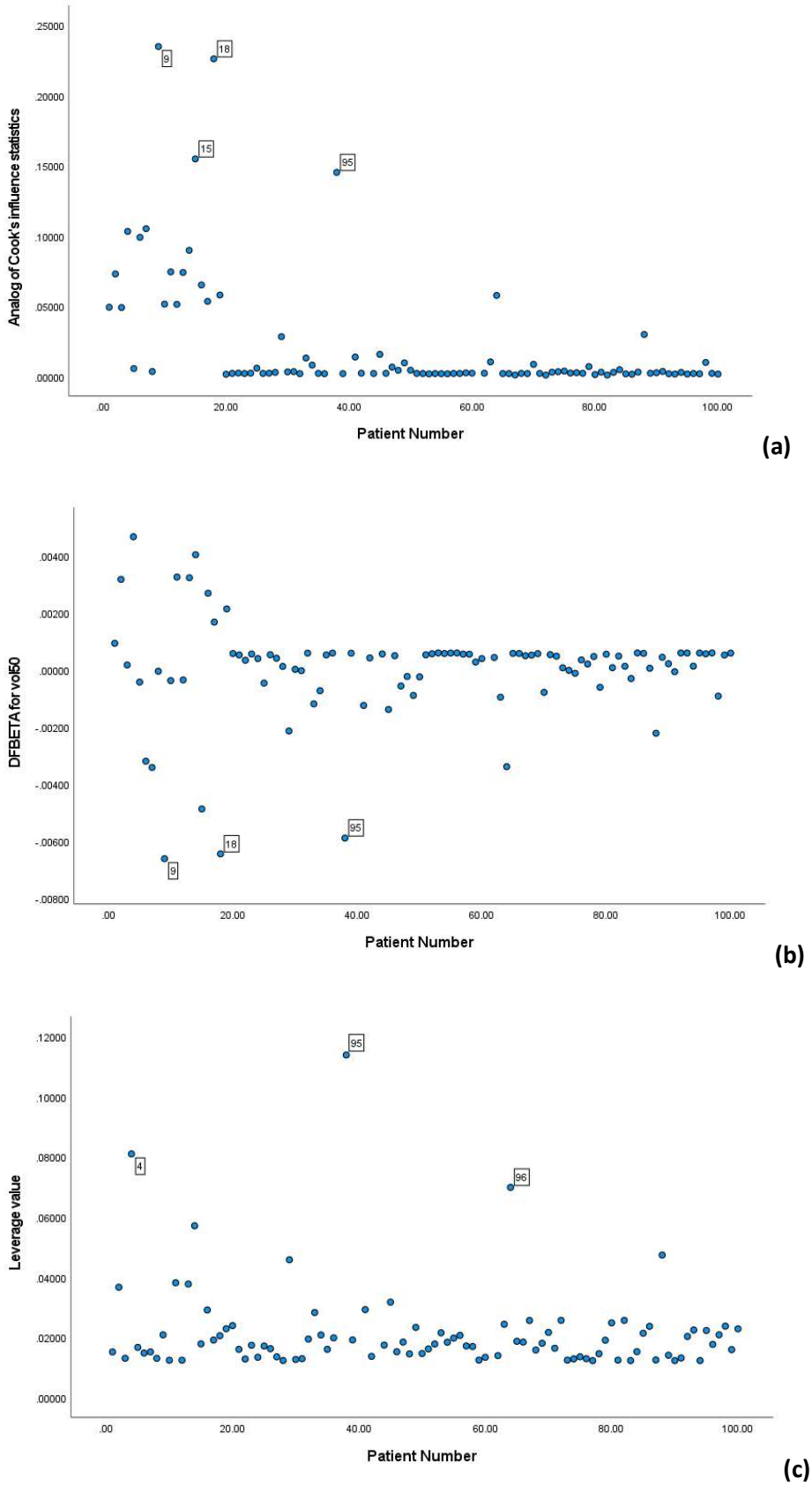

Figure 23: Plotting (a) Cook's Distance, (b) DFBETA values and (c) leverage values against patient number highlight influential observations. Patient number 95 is consistently highlighted in each as an outlier.

4.3.5 Elastic net for variable selection

In order to minimise the impact of collinearity demonstrated during multivariate regression, elastic net was used for feature selection and penalised regression analysis. Following 10 fold cross validation an optimal lambda at 0.32, and alpha of 0.25 were selected (Figure 24). The optimal model highlighted the % volume receiving 47-60Gy and current smoking as features of importance. Coefficient paths and cross validation were plotted and displayed in figure 25.

4.3.6 Penalised logistic regression

In an attempt to improve fit and create a more parsimonious model, the successive variables from % volume receiving 47 to 60Gy were averaged to create one variable (Vol4760). This was incorporated into penalised regression with 10 fold cross validation whilst controlling for smoking given that this clinical variable was selected by elastic net (Table 18, 19 and 20). Model diagnostic plots revealed an improved brier score (0.13), AUC ROC (0.73) and calibration slope (1.36) (Figures 26 and 27).

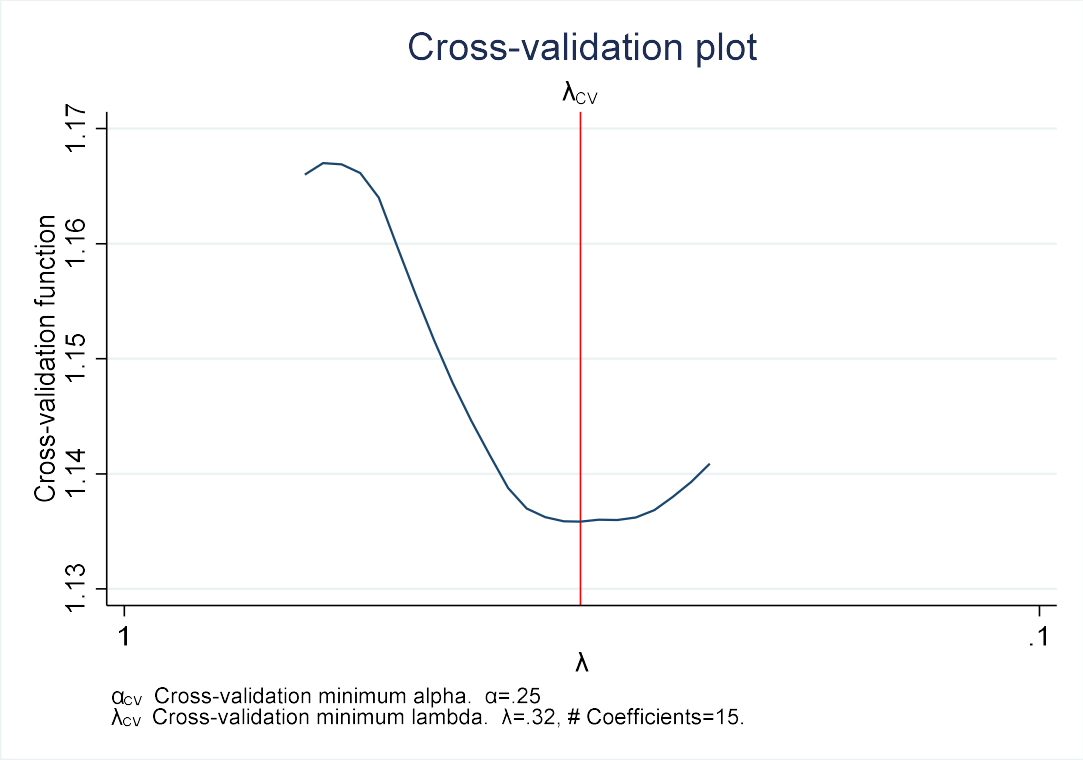

Figure 24: Cross validation plot for elastic net analysis. 10 fold cross validation selected optimal lambda of 0.32 and alpha of 0.25.

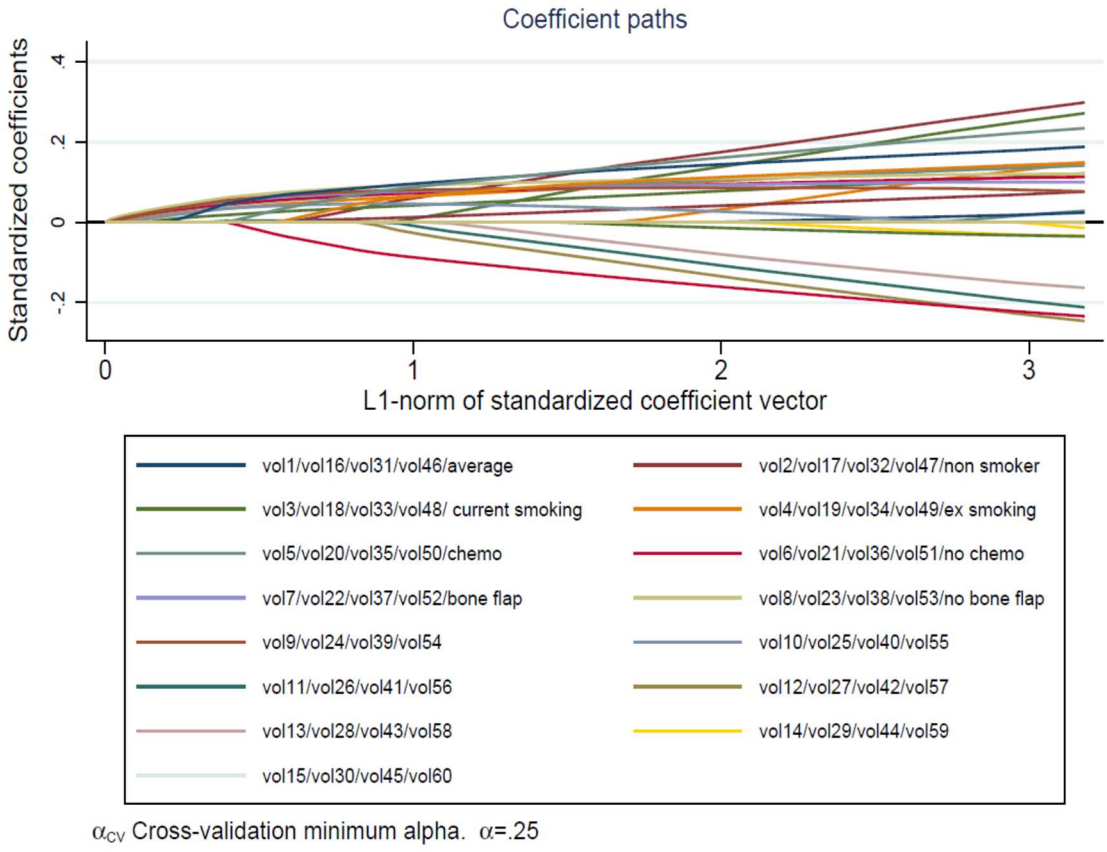

Figure 25: Plotted elastic net shrinkage coefficient paths as a function of standardised sum of coefficients.

Alpha	Patient No	Lambda	CV mean deviance	BIC	Variables added			
0.75	**25**	**0.211**	**1.17**	**57.855**	-			
0.5	**42**	**0.302**	**1.17**	**69.11**	**Vol56**	**Vol57**	**Vol58**	
0.25	**44**	**0.606**	**1.17**	**73.08**	**Vol56**	**Vol57**	**Vol58**	**Vol59**
	45	**0.578**	**1.17**	**76.59**	**Vol55**			
	46	**0.552**	**1.16**	**80.11**	**Vol54**			
	47	**0.527**	**1.16**	**87.47**	**Vol53**	**Vol60**		
	50	**0.458**	**1.15**	**98.03**	**Vol49**	**Vol50**	**Vol52**	
	51	**0.437**	**1.15**	**101.56**	**Vol48**			
	52	**0.418**	**1.14**	**105.11**	**Vol51**			
	54	**0.381**	**1.14**	**108.38**	**Vol47**			
	55	**0.363**	**1.14**	**111.94**	**Current smoking**			
	58**	**0.317**	**1.14**	**111.04**	**Unchanged**			
	59	**0.303**	**1.14**	**114.63**	**Average**			
	62	**0.263**	**1.14**	**117.73**	**Vol46**			
	65	**0.229**	**1.14**	**117.06**	**Unchanged**			

Table 18: Elastic net selected variables and entry points into model at incremental alpha values. Highlighted Variables included in optimal model.

Performance measure		Elastic net	Penalised regression
Brier score		0.14	0.13
AUC ROC		0.68 (p=0.009)	0.73 (p=0.0017)
Calibration slope		1.85	1.36
Penalised Coefficients Training	Deviance	1.02	0.95
Penalised Coefficients Testing	Deviance	0.79	0.76

Table 19: Model performance measures when comparing elastic net (% volume receiving 47Gy-60Gy plus current smoking) along with penalised logistic regression (mean %volume 47-60 plus current smoking).

Variable	Model				
	Entered Variable	β	Odd's Ratio	95% CI	P-value
Mean 47-60	X	0.68	2.24	1.15, 4.35	0.018*
Current smoking	X	0.25	2.85	0.91, 8.97	0.073
Constant		-1.23	0.10	-	0

Table 20: Final penalised regression model.

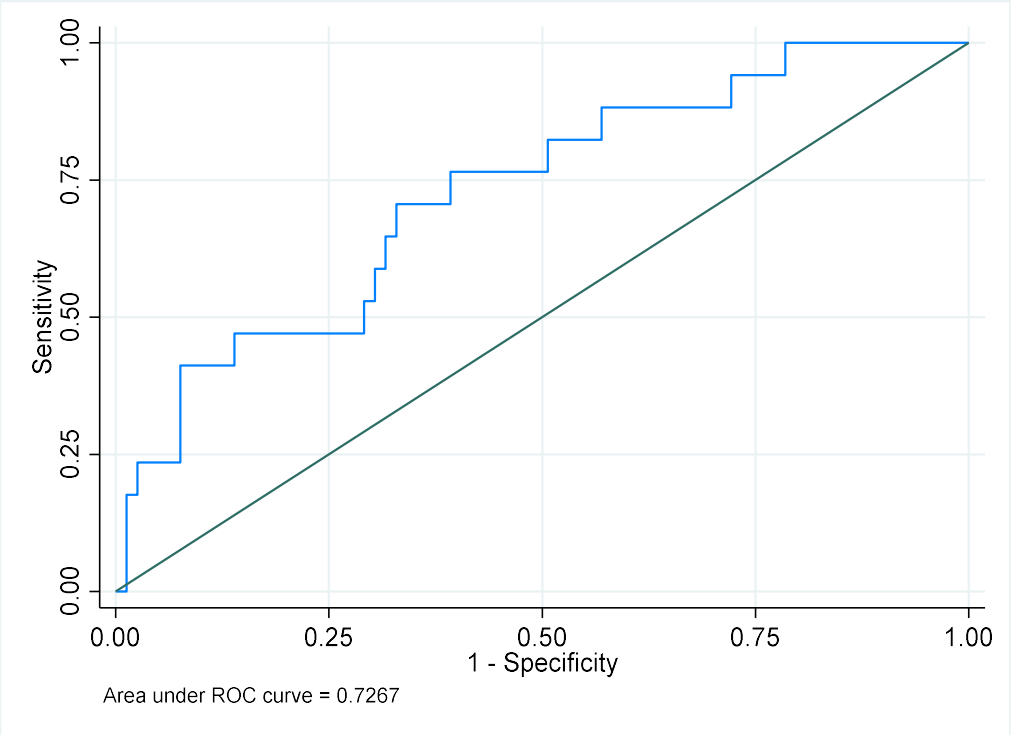

Figure 26: ROC curve for final penalised regression model.

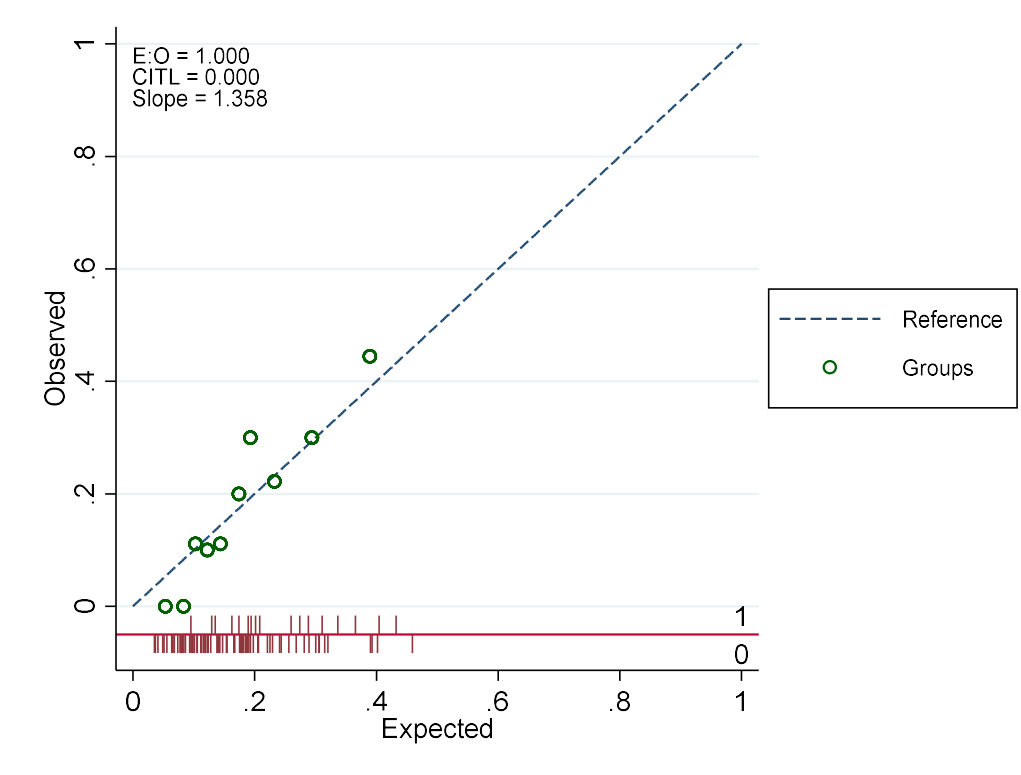

Figure 27: Calibration plot demonstrating good correlation between predicted and observed values.

4.3.7 NTCP Modelling

The final penalised model coefficients (with variable transformation into standardised values) were incorporated into the NTCP model as per the equation:

$$NTCP = (1+e^{-s})^{-1},$$

Where $s = -1.23 + 0.68\left(\frac{vol4760-38.84}{18.31}\right) + 0.25\left(\frac{current\ smoking-2.19}{0.79}\right)$

The results from this were plotted as per figure 28.

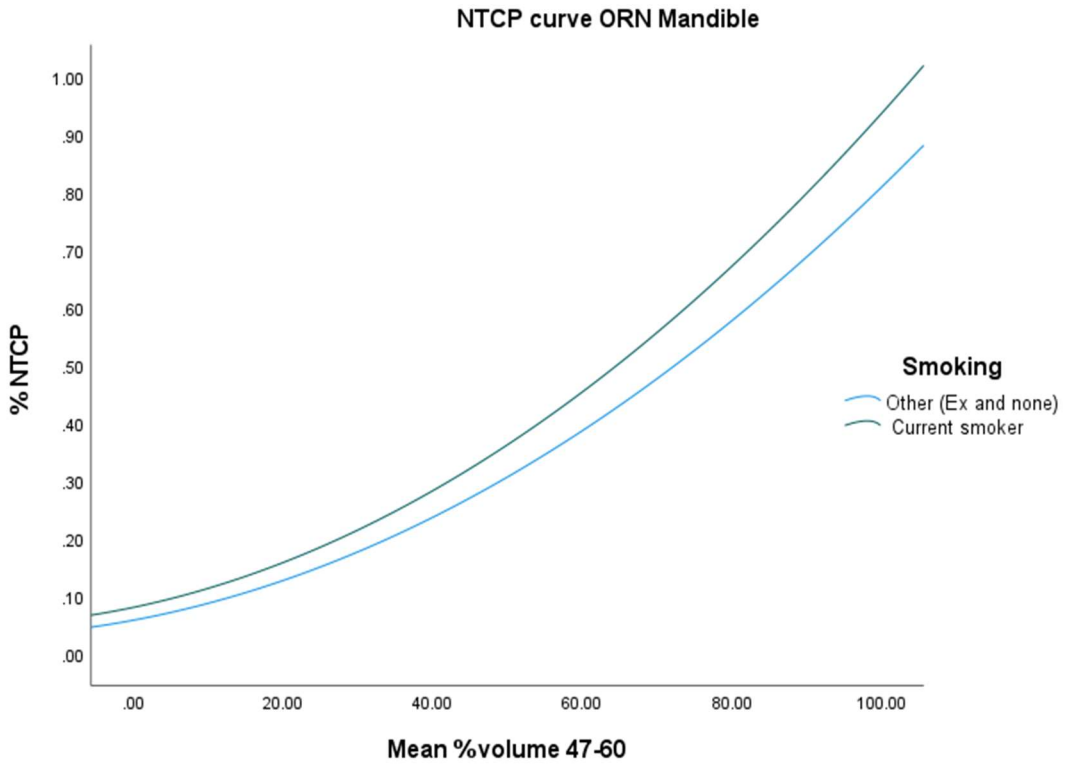

Figure 28: Plotted NTCP curve for mandibular ORN in locally advanced OCSCC (receiving post-operative RT. Stratified for smoking status (current smoker = green curve)

4.3.8 Effect of reduced CTV-PTV margins

Reducing CTV-PTV margins to 3mm for ORN patients resulted in reduced volumes of mandible within high dose PTV, this was understandably more marked for some individuals. The mean reduction in mandibular volume within the PTV was 6.27cm^3. (Table 21)

As proof of principle, one case was re-optimised and planned with comparator mandibular DVH extracted (Figure 29). In this individual there was an 8% reduction in NTCP values by using CTV-PTV margin of 3mm; from 43.4% (5mm margin) to 35.4% (3mm margin).

Patient	Mandible volume	Mandible Overlap (cm^3)		Difference (cm^3)
		PTV 5mm	PTV 3mm	
1	43.7cc	23.5	21.9	1.6
2	66.9cc	31	28.5	2.5
3	44.0cc	5.8	0.6	5.2
4	45.9cc	31.2	29.2	2
5	23.6cc	4	0.3	3.7
6	47.7cc	28.3	22.1	6.2
7	71.7cc	21.6	11.6	10
8	77.7cc	32.4	18.1	14.3
9	49.4cc	8.3	6.3	2
10	63.2cc	13.9	7.3	6.6
11	60.3cc	16.6	3.5	13.1
12	47.3cc	11.2	2.7	8.5
13	55.4cc	5.4	0.6	4.8
14	42.9cc	4.3	1.7	2.6
15	60.8cc	17.3	7.5	9.8
16	91.6cc	17.2	7.1	10.1
17	67.3cc	5.3	1.7	3.6

Table 21: Difference in mandibular volumes following CTV-PTV margin reduction.

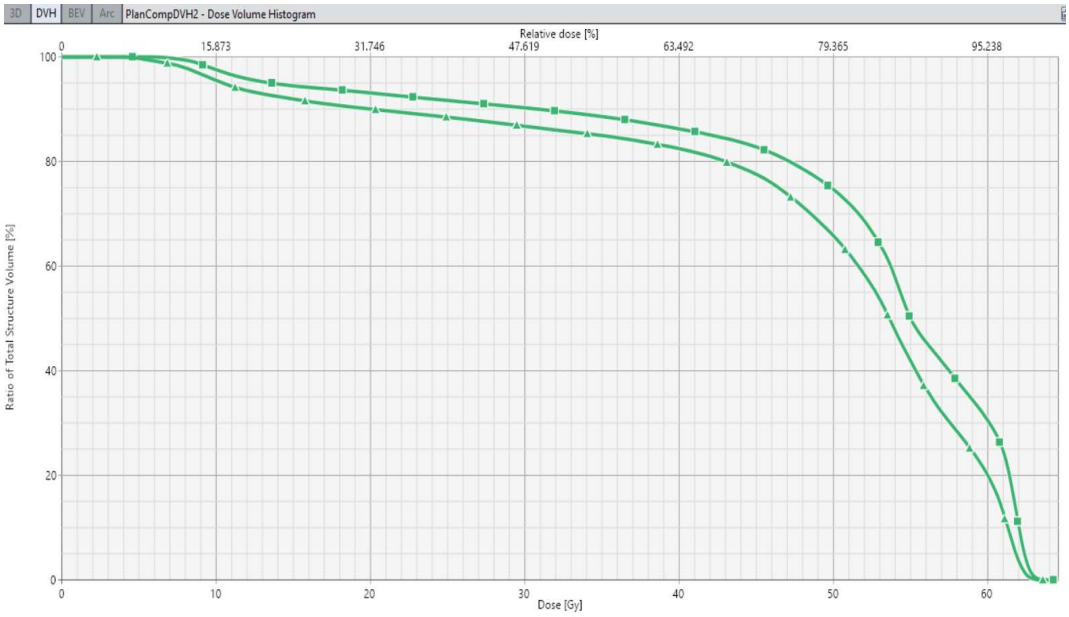

Figure 29: Comparison mandibular DVH graphs; 5mm margin (square marker), 3mm margin (triangle marker).

4.3.9 Comparison dosimetric model with SNP model

26 patients from within this dosimetry cohort had available blood tests for genotyping (4 patients with ORN and 22 without). Summary of patient characteristics and SNP frequencies are within Table 22. In order to demonstrate performance comparison of the previously developed SNP model from Chapter 3 and optimised dosimetric model, both were run using coefficients outlined within Table 12 and Table 20. The SNP model obtained a calibration slope of 0.69 and AUC ROC of 0.67 and so had greater discriminative ability than the dosimetric model (Table 23, Figure 30), however larger sample sizes must be obtained in the future to confirm these conclusions. In addition it was not possible to calculate a new model combining dosimetric and SNP data, again due to the small sample size.

Variable	Level	ORN	No ORN	Total
Smoking	Current	3 (75)	7 (32.8)	10 (38.5)
	Ex	0	9 (40.9)	9 (34.6)
	None	1 (25)	6 (27.3)	7 (26.9)
Non-surgical treatment	CRT	0	1	
	RT	4	25	
Site	Mandible	2	6	
	Tongue	2	8	
	Maxillary Alveolus	0	3	
	Floor of mouth	0	4	
	Buccal	0	2	
rs7477958	T/T	2 (50)	13 (59.1)	15 (57.7)
	T/C	1 (25)	7 (31.8)	8 (30.8)
	C/C	1 (25)	2 (9.1)	3 (11.5)
rs34798038	A/A	4 (100)	17 (77.3)	21 (80.8)
	A/G	0	5 (22.7)	5 (19.2)
	G/G	0	0	0
rs2348569	A/A	2 (50)	11 (50)	13 (50)
	A/G	2 (50)	10 (45.5)	12 (46.2)
	G/G	0	1 (4.5)	1 (3.8)
rs6011731	T/T	4 (100)	19 (86.4)	23 (88.4)
	C/T	0	3 (13.6)	3 (11.5)
	C/C	0	0	0
rs530752	A/A	4 (100)	19 (86.4)	23 (50)
	A/G	0	2 (9.1)	2 (7.6)
	G/G	0	1 (4.5)	1 (3.8)
rs1415848	G/G	2 (50)	9 (40.9)	11 (42.3)
	A/G	1 (25)	10 (45.5)	11 (42.3)
	A/A	1 (25)	3 (13.6)	4 (15.4)

Table 22: Summary of dosimetry cohort with available blood tests for genotyping, including SNP allele frequencies.

	Dosimetric model	SNP model
AUC ROC (95% CI)	0.55 (0.28, 0.81)	0.67 (0.45, 0.87)
H-L test	Chi^2 0.60 (p=1.00)	Chi^2 0.62 (p=1.00)
Calibration slope	0.132	0.699
Brier score	0.152	0.154

Table 23: Comparison of performance statistics for dosimetric and SNP model run on small external cohort.

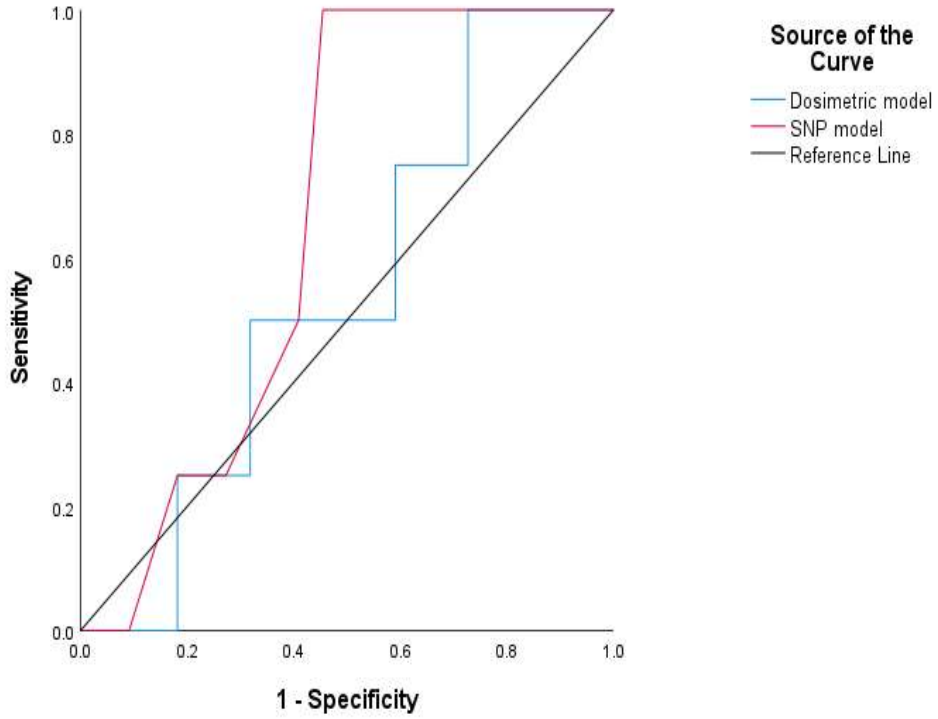

Figure 30: Comparator ROC curves for dosimetric and SNP model.

4.4 Discussion

4.4.1 ORN rates within a high risk cohort

This work has demonstrated an incidence of 18% for ORN following adjuvant (C)RT in patients undergoing LA OCSS resection and reconstructive procedures. This is similar to rates described by more recent series such as recently presented by Moring et al [213] quoting incidence of 19.8% and is reminiscent of rates described in the pre-IMRT era; notably higher than the 4-10% previously reported in published series where patients were having non-surgical radical treatment (IMRT) [109]. It is likely that the large volumes of the mandible included in high dose RT treatment volumes due to

the close proximity of the mandible to the tumour bed are a major contributor to the increased ORN risk in this cohort. In addition, generous contouring which results from clinician unsurity over involved margin location following anatomical changes after the placement of free flaps.

Although clear guidance exists for the delineation of both primary and nodal target volumes in the adjuvant setting for HNSCC, there remains lack of consensus over RT contouring practices for OCSCC following reconstruction [214]. Delineation of tumour bed and location of involved resection margins on planning imaging following extensive reconstructive procedures is notoriously difficult, and the principles of reconstructing pre-operative tumour with geometric expansions are difficult to follow in this setting. As such, local convention dictates that whole reconstructed flaps are included within target volumes with margins between 5 and 10mm for microscopic spread (depending upon involved margin status) and an additional 5mm added for set up error, movement and geometric variation. There is now a flap delineation atlas provided by Le Guevelou et al to aid this process however there is still ambiguity over optimal margining [206]. There is naturally resistance in contouring in this manner as it dramatically increases the irradiated volume relative to modestly sized tumours at initial staging, and with this, leads to high volumes of mandible included within target volumes along with increasing outlining time per patient. The recent publication of the GORTEC internationally reviewed consensus guidelines reflects the variation in global practices and, through the lack of agreement reached within their voted topics (e.g. whether the flap should be considered part of the clinical target volume) highlights the need for improved prospective data [215]. The topics that did reach consensus included 'the flap-tissue junction should be considered at higher risk of tumour spread'. Both marginal and in-field recurrences are known to be high in patients having adjuvant (C)RT in this setting with Cho et al quantifying the risk of local and regional relapse as 23% and 28% respectively in a cohort of 114 patients following reconstruction for oropharyngeal/oral cavity cancer (95/114 oral cavity)[216].

Within the described cohort, 16.7% (16 out of 96) experienced locoregional recurrence within high dose target volumes and 9.4% (9 out of 96) out of high dose

target volume detected on interval MRI/CT scanning. There were 3 patients with recurrence evident between the flap-tissue interface, an example of which is shown in figure 31a. Other locoregional failures were too advanced at imaging to accurately review whether recurrence began at junction or elsewhere (figure 31b). Clearly any changes to current voluming practices in attempts to spare normal tissues must be balanced with the high risk of local recurrence. Close collaboration between maxillofacial surgeon, clinical oncologist, pathologist and radiologist would move towards improving localisation of high risk resection margins on RT planning scans, thus facilitating improved target delineation along with sparing low risk reconstructed flap tissue.

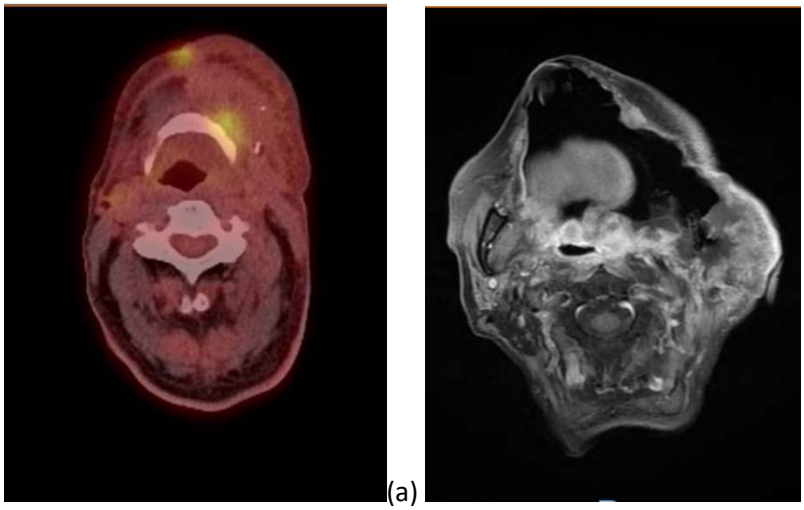
(a) (b)

Figure 31: (a) Example early marginal recurrence detected on PET CT imaging with FDG avid disease evident at flap-normal tissue interface. (b) Example of advanced local recurrence demonstrated on MRI imaging where, due to the extent of disease, it is difficult to locate the original of recurrence.

4.4.2 NTCP modelling

Elastic net and penalised regression analysis is yet to be utilised in parameter selection or NTCP modelling for ORN following head and neck RT. This technique has identified additional significant dosimetric parameters to take into consideration when calculating individual patient NTCP values, which (due to collinearity often seen when examining dosimetric data) would not have been included in traditional multivariate logistic regression analysis. The dosimetric parameters selected are in keeping with previous reports (as discussed in Chapter 1, section 1.5.4) where mean dose and mandibular volumes receiving higher doses i.e. 50Gy and 60Gy increase ORN risk. This analysis takes a logical step forward in noting the spectrum of DVH

bins which are correlated to ORN and provides a practical NTCP model for plan optimisation and organ sparing.

Smoking during head and neck RT is known to increase the chance of acute and long term side effects and ORN is no exception to this [108]. This risk was quantified by Tsai et al who reported a 32% increase in ORN if patients continued to smoke during treatment [134]. It is unclear whether the increased risk is due to coexisting periodontal disease or poor healing post treatment which is so often a result of cigarette smoking. Being a current smoker was selected by elastic net as an important factor to take in consideration during modelling and increased the risk of ORN by 2.8 times. Although only approaching significance (p=0.07), incorporating this factor with mean % volume receiving 47-60Gy provided a model of good discriminative ability (AUCROC 0.73). The use of concurrent chemotherapy was not significantly associated with ORN within our cohort and as such was not retained within modelling estimations (p=0.63, univariate analysis). There are conflicting reports in the literature regarding the association of concurrent chemotherapy with ORN [131,204,217]. The lack of association could be a reflection of the low proportion of patients who received CRT in this cohort (n=14) and so this could prove to be an important factor if numbers were increased in future external validation work.

It has been documented that pre-treatment dental procedures and poor dentition prior to RT can lead to increased incidence of ORN [204]. Both Kuhnt et al and Studer et al identified that having mandibular surgery as part of cancer resection represented a high risk cohort (HR 5.87 95%CI 3.09–11.19)[107,205]. Following this, the inclusion of patients who have undergone mandibular resection, mandibulectomy or dental clearance procedures as part of tumour resection provides a unique, high risk cohort. After including the presence of bone free flap in both traditional and penalised regression analysis it was evident that this did not increase ORN risk relative to other mandibular interventions (p=0.62 on univariate analysis). It is therefore evident that the mandible, whether native or reconstructed, is equally at risk of developing ORN due to the high volumes receiving doses of 47-60Gy.

4.4.3 Combining SNP and dosimetric models

Combining both dosimetric and non-dosimetric parameters has been supported in the past by El Naga et al in order to create models of greater predictive ability [218]. Although numbers included within this external validation cohort were too small to show effective combination of both genomic and dosimetric models, the roc curves in figure 27 provide proof of principle. Interestingly the genomic model seemed to outperform dosimetric models within this cohort however neither model were a good fit to the data and larger patient numbers will be required to effectively validate this hypothesis. The ongoing requite study and radiogenomics consortium projects are now collecting comprehensive dosimetric data and so combined modelling may be achievable in larger patient cohorts [149,154].

4.4.4 Reduction in CTV-PTV margining

Chen et al [219] have demonstrated equivalent locoregional control in patients receiving head and neck radiotherapy after reducing PTV margins from 5mm to 3mm with daily image guidance. Through demonstrating a mean reduction in mandibular volume included within high dose target volumes of 6.27cm^3 after reducing CTV-PTV margins to 3mm across patients with ORN, one can appreciate how small changes in current contouring practices may translate to improvements in normal tissue sparing. The reduction in margining may prove beneficial for selected patients where on treatment image guidance is available, as in the case described, where complete re-planning and optimisation following reduced margining equated to an 8% reduction in NTCP. Local practice has recently changed to employ these reduced margins and has been achievable with current IGRT facilities. Future local audit is planned to assess locoregional failure rates in matched cohorts to demonstrate safety of this this newly adopted protocol.

4.4.5 Study limitations

The retrospective nature of data collection led to difficulties obtaining certain metadata such as use of bisphosphonates and comprehensive alcohol history, the inclusion of these factors may have added information to modelling estimations. The use of DVH bins for modelling does not account for spatial changes during therapy (e.g. weight loss) therefore there may be a disparity between planned dose and

actual dose received. Future moves to adaptive radiotherapy with inter and intrafraction image guidance will aid the improved accuracy of RT delivery and along with this, mandible sparing.

ORN is a long term toxicity which can occur after several years following RT [109], this, coupled with high rates of recurrence which is well documented in LA OCSCC may have led to an underestimation of ORN incidence. It may be that more patients within this cohort will go on to develop this complication and therefore updating data collection after a longer time interval would provide a more comprehensive estimation of ORN risk.

4.5 Conclusion

This work has demonstrated ORN incidence in the post-operative setting for patients with LA OCSCC. This has not been quantified in the past, and will be valuable in terms of consent discussions and adequately preparing patients prior to undergoing adjuvant (C)RT following ablative surgery with reconstruction. Through providing a NTCP model within this unique, high risk cohort, it may be possible (following external validation) to use these parameters in plan optimisation, thus facilitating future organ sparing efforts. It is evident that large volumes of reconstructed flap and mandible are being included within target volumes which may be reduced by altered margining (if adequate on treatment imaging is available), or possibly through a dramatic change in outlining practices i.e. in targeting the flap-tissue interface, however the high incidence of locoregional recurrence leads to natural hesitance in suggesting reduced target definition.

We are potentially embarking on long awaited improved outcomes for these patients, with the addition of new anticancer agents in the neo-adjuvant setting (discussed in chapter 5). Reducing the likelihood of developing ORN must be a priority for future works, in order to provide patients with improved long term quality of life.

Chapter 5

Intensifying treatment to improve survival: Integrating ICI into the radical management of locally advanced oral cancers.

5.1 Introduction

5.1.1 Emerging evidence for (neo)adjuvant ICI HNSCC

Over the last few years, studies in melanoma and non-small cell lung cancer have established that use of adjuvant ICI can improve recurrence free survival for patients with high risk locally advanced disease, and have led to change in practice [101, 102] . This provides proof of concept and supports investigation of these drugs in the curative setting in head and neck cancer, including OSCC, with a growing number of studies in this setting. How and where ICI fits into the multimodality treatment of HNSCC remains uncertain, with multiple different approaches under investigation.

Inclusion of neoadjuvant treatment in particular has several advantages, namely potentiating T cell activation thus priming and exposing the immune system to tumour specific antigens; targeting micrometastatic disease and reducing locoregional/distant relapse[220]. In addition, this approach permits treatment escalation early in an already arduous pathway whereby patients are at their optimal physical condition. Finally, utilising the window of opportunity prior to surgical resection (along with the relative simplicity of tissue sampling in the head and neck) provides an unparalleled resource for translational research, facilitating investigation of the tumour microenvironment without prior exposure to other anticancer therapies.

Table 24 outlines preliminary findings from studies examining the use of ICI in the neoadjuvant setting in those who have resectable SCCHN. Examples of reported studies include the phase I/II CheckMate 358 study which utilised neoadjuvant nivolumab in previously untreated primarily viral associated cancers, within which there was a cohort of 57 patients with resectable HNSCC [221]. Results from this study showed that neoadjuvant nivolumab was well tolerated and did not delay standard of care surgery. Of the 17/34 HPV positive evaluable patients, one (5.9%) achieved a

major pathological response (mPR: ≤10% residual viable tumour) and three (17.6%) achieved a partial pathological response (pPR:>10%-50% residual viable tumour), whereas of the 17/34 HPV negative tumours, one (5.9%) achieved a pPR. Uppaluri et al conducted a phase II trial similarly examining neoadjuvant ICI in locally advanced HNSCC [222]. This treated cohort of 36 HPV negative patients were offered one dose of neoadjuvant pembrolizumab prior to resection/post-operative (C)RT and further adjuvant doses depending on the presence of high risk features. 1 year relapse rates were 16.7% (95%CI 3.6-41.4%) among the 18 patients with high risk pathological features. No patients achieved a completed pathological response however eight (22%) had pTR1, defined as 10-49% (area pathologic response/area pathologic response plus viable tumour), and eight (22%) had pTR2 (>50%).

The available evidence has confirmed the feasibility of integrating ICI into current radical treatment strategies without disrupting standard of care surgical pathways, with only the CIAO study [223] reporting surgical delays (and these in patients who were given additional chemotherapy due to locally progressive disease following neoadjuvant ICI). A significant proportion of patients show primary tumour response at surgery, which may then confer to improved local control and survival; however this remains unproven with limited longer term outcome data. In addition, these studies clearly demonstrate heterogeneity in response, suggesting primary resistance in a proportion of cases.

5.1.2 Identifying markers of response/resistance to ICI

As mentioned above, a key advantage of treatment in the neoadjuvant setting is the ability to collect matched samples before and after ICI; and a number of the above reported (neo)adjuvant studies have explored immunological and tumour intrinsic parameters which may correlate with response using immunohistochemistry, multiplex immunofluorescence, whole genome sequencing, and gene expression profiling via RNA sequencing (RNAseq). Within Checkmate 358 the low numbers of responders meant correlations between pathological appearances and endpoints such as tumour mutational burden (TMB) were not made. Despite this, it was evident that patients with HPV positive tumours generally had lower TMB and displayed a highly inflammatory microenvironment, with heightened expression of immune

Trial	N	Stage	Treatment	Response reporting	Outcome
Ferris et al Checkmate 358 J Immunother Cancer 2021	57	Resectable SCCHN (HPV+/-)	Nivolumab x 2 Resection	Major pathologic response (mPR) = ≤10%RVT (residual viable tumour) Partial pathologic response (pPR) =>10-50%RVT	17/34 HPV+: 23.5% any pathological response 17/34 HPV-: 5.9% any pathological response
Uppaluri et al Clin Cancer Res 2020	36	Resectable Stage III/IV HPV- SCCHN	Pembrolizumab x1, resection, (C)RT, adjuvant pembrolizumab	Proportion of tumour response (TR): pTR-0 (<10%), pTR-1 (10-49%), pTR-2 (>50%)	44% any path response (pTR1+) Nil complete TR (48% clinical to path downstaging)
Wise-Draper et al JCO Abstract 6006 NCT02641093 ASCO 2021	92	T3-4 and/or 2 + LNs HPV + excluded	Pembrolizumab x1, resection, (C)RT + concurrent pembrolizumab	Pathological response (PR) = >10% tumour necrosis or 10% decrease in viable tumour mPR = >70% tumour effect	26/80 PR (6/80 mPR)
Knochelmann et al Cell Rep Med 2021 NCT03021993	12	Stg II-Iva oral cavity	Nivolumab x4 (2 weekly) Resection	Pathological complete response (pCR) or pPR = 30% reduction in tumour size	4/12 pPR
Ferrarotto et al CIAO Clin Cancer Res 2020 NCT03144778	28	Stage II-Iva oropharynx SCC (local recurrence allowed)	Durvalumab x2 or Durvalumab + tremelimumab x2 Resection, RT/CRT	mPR= ≤10% viable tumour cells in primary or nodes	2/25 pCR
Zuur et al IMCISION Nat Commun 2021 NCT03003637	32	T3-4 N0-3 HPV+/- SCCHN (local recurrence allowed)	A: Nivolumab x2 B: Ipilimumab x1, nivolumab x2 Resection (C)RT	Near pCR >90% Any pathological response (PR) >50%	A: 1/6 mPR B: 8/23 mPR
Schoenfeld et al JAMA Oncol 2020	30	T2-4 and/or N+ Oral cavity	Nivolumab x2 vs Nivolumab / Ipilimumab x2, Resection	Pathological effect (PE)>50% Or >90%	15% Nivolumab arm and 33% dual had PE >50%

Table 24: Summary of preliminary reported outcomes from trials incorporating neoadjuvant ICI into radical treatment strategies.

checkpoints [221]. After treating twelve patients with locally advanced OCSCC with neoadjuvant nivolumab Knochelmann et al reported that tumour infiltrating lymphocytes (TILs) from responders expressed CD26 ($p = 0.007$) and Tim3 ($p = 0.045$) while PD-1, Lag3, and Ox40 were not differentially expressed based on pathological response [224]. Uppaluri et al reported a correlation between pTR after neoadjuvant pembrolizumab and baseline tumour PD-L1 expression, immune infiltrate, and IFN-γ pathway activity, but not with TMB [225]. They noted that patients without pTR following neoadjuvant pembrolizumab displayed minimal immune activity in the

baseline tumour specimens. Interestingly, some patients without pTR showed upregulation of immune pathways in their resection sample with increased expression of T cell checkpoint molecules, leading to the hypothesis that additional doses of neoadjuvant ICI, or addition of therapy targeting different immune pathways could increase the proportion of patients with pTR.

As evidenced above, using ICI in the (neo)adjuvant setting is providing pathological responses; albeit less frequently in HPV negative disease than witnessed in other solid tumours [102]. Early reports of improved one year relapse rates from Uppaluri et al [222] in those with high risk pathology (16.7%, 95% CI 3.6-41.4%) along with improved recurrence free survival in those with pathological response are encouraging, however the low numbers included within this study (and similar investigations) lead to caution when interpreting results. The opportunities in biomarker discovery and translational research afforded by targeting the window of opportunity are especially marked in oral cavity cancer where tumours are easily accessible for tissue collection and the low prevalence of HPV driven disease lends to generalising findings to HPV negative HNSCC as a whole. Although ICI integration appears to be safe in terms of surgical scheduling, the suggestion of longer treatment windows from Uppaluri et al prior to resection may lead to concern of tumour progression in the cohort of non-responders. Further information on changes in the immune microenvironment following (neo)adjuvant ICI is warranted in order to develop predictive biomarkers for response to facilitate appropriate and safe neoadjuvant treatment escalation. In addition, as more aggressive neoadjuvant/adjuvant immunotherapy regimens are suggested, their additive toxicities may become difficult to tolerate for a patient population already burdened by significant toxicities of standard of care therapy and comorbidity.

The NICO study was initiated at a similar time to the previously mentioned studies, with specific focus on oral cavity patient cohort, and with the incorporation of both neoadjuvant and adjuvant strategies [226]. This non-randomised phase II study explored the hypothesis that (neo)adjuvant immunotherapy works synergistically with (chemo)radiotherapy, priming and consolidating immune responses; potentially

maximising benefit when patients are at their peak physical state, between surgery and commencement of prescribed adjuvant therapies.

Within this study, patients with locally advanced oral cavity cancer received a single cycle of the PD-1 inhibitor nivolumab prior to ablative reconstructive surgery (figure 32). A further cycle of nivolumab was administered prior to adjuvant (standard of care) (c)RT and again, upon completion of their standard of care adjuvant treatment, a further six cycles of ICI. Tumour tissue was obtained at diagnosis and upon definitive surgical resection in order to provide a means to assess for pathological markers of response to treatment and for future translational research. A total recruitment of 120 patients was planned, however the study was discontinued early (after recruitment of 23 patients) due to withdrawal of funding by pharmaceutical company (Bristol Myers Squibb (BMS)) in light of slow recruitment and strategic realignment by the company. The NICO study was delivered during my PhD, from set up through to recruitment and closure. Here I report preliminary results on the clinical endpoints and pathological assessments; further translational research is ongoing.

5.2 Hypotheses

This main hypotheses investigated in this study are as follows:

- **Integration of ICI into the radical treatment of LA OCSCC is feasible**
- **Utilising this treatment strategy will offer patients improved outcomes without adding significantly to treatment toxicities.**
- **Baseline, or changes in, biomarkers can be utilised to identify patients likely to benefit from ICI in this setting; providing potential means of stratifying treatment.**
- **Similarly, that markers of resistance can be identified and provide potential targets for combinatorial treatment.**

5.3 Methods

5.3.1 Ethics and Funding

The NICO study was sponsored by The Clatterbridge Cancer Centre NHS Foundation Trust, supported by the Liverpool Clinical Trials Centre, and funded by BMS. Ethical

approval was obtained from the Central Bristol Research Ethics Committee (REC Ref. No. 18/LO/0368) and Clinical Trials Authorisation issued by the Medicines and Healthcare Products Regulatory Agency (MHRA).

5.3.2 Study Design

The NICO trial was a non-randomised, multicentre, phase II trial. The full protocol is included in appendix 11, with abbreviated methodology below. Figure 32 summarises trial treatment.

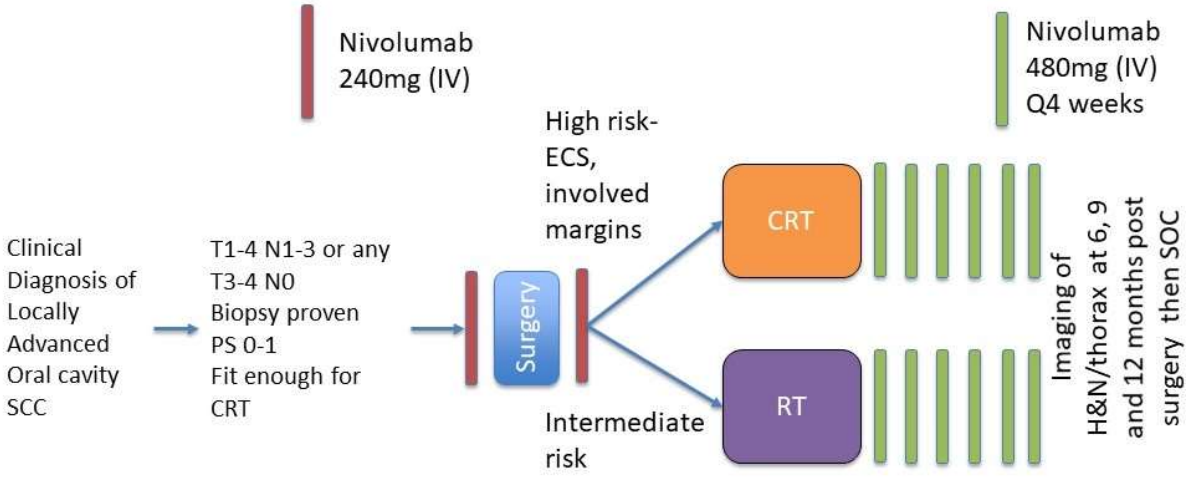

Figure 32: Schematic diagram of NICO trial treatment schedule. Brooker RC, Schache AG, Sacco JJ. NICO Phase II clinical trial - focus on an emerging immunotherapy strategy for the adjuvant treatment of locally-advanced oral cancers. Br J Oral Maxillofac Surg. 2021 Oct;59(8):959-962. doi: 10.1016/j.bjoms.2020.08.059[227]

5.3.3 Trial treatment

5.3.3.1 Nivolumab

The ICI nivolumab was administered to patients 1-2 weeks prior to radical surgery at a flat dose of 240mg. A further single dose of 240mg was given 1-2 weeks before adjuvant (C)RT. Patients received a further 6 doses of nivolumab, given at 4 weekly intervals at a dose of 480mg, within 4 weeks of completing their adjuvant (C)RT (this time interval could be extended by 6 weeks to allow for resolution of grade 2+ toxicities).

5.3.3.2 Standard of care therapy: Surgery

Surgical resection of the primary tumour was performed in order to achieve complete microscopic resection, with (where possible) a clinical margin of 10mm. Primary reconstruction following surgical resection was completed at the discretion of the operating surgeon. Selective neck dissection/modified radical neck dissection was undertaken either ipsilaterally or bilaterally depending upon the presence of tumour encroachment towards midline, and suspicion of contralateral nodal metastases.

5.3.3.3 Standard of care therapy: Adjuvant (C)RT

After surgery, patients were stratified to either RT or CRT depending on pathological features. CRT was indicated in the setting of a positive (≤1 mm) surgical resection margin and/or nodal extra-capsular spread (ECS). Patients with intermediate risk features (T3-4, perineural invasion, vascular invasion and/or >1 positive nodes), but without positive margins (as defined above) and no evidence of extracapsular spread received radiotherapy alone. (C)RT was initiated within 8 weeks (56 days) of surgical resection, equating to a maximum cumulative treatment time of 14 weeks.

RT was delivered once daily (Monday to Friday) across 6 consecutive weeks at a dose of 65Gy to high risk PTV (or 60Gy if intermediate risk factors alone) and 54Gy in 30 fractions to low risk PTV. In order to ensure minimal variation in RT outlining and delivery a Radiotherapy Outlining, Planning and Quality Assurance (RTTQA) protocol and process was developed in collaboration with RTTQA group (www.rttrialsqa.org.uk) and clinical oncology consultants at The Clatterbridge Cancer Centre and The Beatson West Scotland Cancer Centre (included in appendix 12). Cisplatin was administered at a dose of 100mg/m2 on day 1 and day 22 of RT schedule for those patients undergoing concurrent CRT.

5.3.4 Statistical Considerations

5.3.4.1 Outcome measures

There were two primary outcome measures within this study; 1-year disease free survival (DFS: defined as disease recurrence or death at 12 months following surgery) and feasibility of recruitment. Planned secondary endpoints were overall survival (OS: measured at time from recruitment to death from any cause), toxicity (based on

Common Terminology Criteria for Adverse Events, CTCAE V4.), and surgical complications using Clavien Dindo classification (appendix 6).

5.3.4.2Sample size

Original sample size calculations estimated recruitment of approximately 120 patients over a period of 18 months. This was based on a third of all patients with study eligibility criteria having high risk disease (ECS, involved margins) thus requiring adjuvant CRT. A study population of 120 (recruited over 18 months) would therefore recruit 40 patients into the high risk cohort. 12 month PFS for this patient group was estimated at ~65% following standard adjuvant regimes with confidence intervals of 53.9% - 74.2% (assuming n=40). It was concluded that an observed PFS of ≥ 75% (corresponding to a hazard ratio of 0.67), would represent a clinically relevant positive result. All patients were included in feasibility cohort owing to possibility of differing proportions being recruited to either receiving concurrent CRT or radiotherapy within adjuvant treatment portion of study.

This calculation was revised following early trial closure to estimated total recruitment of 30 patients. With 1 year follow-up, estimation of the 12 month DFS would likely have a confidence interval of approximately 20%, meaning that if a DFS of 65% is observed this would have a precision of (45-85%).

5.3.4.3Protocol deviations and amendments

There were three minor protocol deviations reported:

- One in relation to translational samples taken at incorrect time point.
- Two in relation to kit type used for sample collection – wrong kits dispatched from central labs.

There were six substantial protocol amendments. Three related to the alteration of principle investigators and addition of new participating sites. Two related to the re-opening and subsequent early closure of the study following the COVID-19 pandemic. Finally one outlined a number of protocol, patient information sheet and informed consent form changes which included:

1. Time from adjuvant (C)RT to adjuvant nivolumab extended from 6 weeks to 10 weeks

2. Change to follow up scan times from 4 months intervals post-surgery to 6, 9, 12 months post-surgery in order to ensure scans were outside of treatment window
3. (C)RT treatment schedule updated to clarify that any patient experiencing an 8 week or greater interval between surgery and commencement of (C)RT would be withdrawn from the trial
4. Translational research sub-studies were included: a) faecal and oral microbiome sample collection and b) additional diffusion weighted MRI scans
5. Translational protocol was adjusted to increase quantity of blood collected
6. Patient information sheet and consent form updated to satisfy GDPR requirements

5.3.4.4Feasibility measures

Feasibility to recruit sufficient patients was measured by recruitment rate (total number of patients randomised each month), site opening (time taken to open target sites), and patient adherence to the protocol.

5.3.4.5Data analysis

The 1 year disease recurrence rate was defined as a binary variable and estimated alongside a 95% confidence interval assuming a binomial distribution. DFS and OS was calculated using the Kaplan Meier method and compared across subgroups using log rank test. Adverse events (AE) and serious adverse events (SAE) were defined using CTCAE V4.

5.3.5 Translational research

All patients participating in the NICO trial consented to the collection of tumour tissue and blood samples longitudinally across the course of their treatment (Table 25). This allowed several investigations aimed at identifying biomarkers of response, as well as the collection of samples for future research into the biology of OCSCC.

Investigations assessed the predictive value of PDL-1 and tumour infiltrating lymphocyte (TIL) density and type/distribution on tumour response to immunotherapy, along with examining changes in these parameters post neo-adjuvant nivolumab.

Study Procedure	Baseline 28 Days	Treatment 1: Pre Surgery	Surgery	Treatment 2: Post-surgery, pre RT	Treatment 3-8: Post CRT or RT						End of Study treatment visit
Day	≤28 days	7-14 days prior to planned surgery		7-14 days prior to RT	4 weeks after completing (C)RT, then every 28 days (25-31 days)						100 days from date of nivolumab dose 8
					1	2	3	4	5	6	
Blood collection	X		X	X	X		X			X	X
Diagnostic Biopsy (FFPE, All protect +/- fresh frozen)	X										
Tissue sample from surgical specimen (FFPE, All protect +/- fresh frozen)			X								
Tissue sample from progressive disease (FFPE, All protect +/- fresh frozen)											X (recurrence)

Table 25: Schedule for tissue and blood sample collection as part of trial translational protocol.

5.3.5.1PDL1 Expression testing

Archival formalin fixed paraffin embedded (FFPE) biopsy block samples were collected from recruited patients. Samples were cut into 5 x 4-5 µm sections, mounted (unstained) onto Fisherbrand Superfrost Plus charges slides and heated to 58°C for 1 hour. Slides were stored at room temperature and sent to University Hospitals Birmingham NHS Foundation Trust Molecular Pathology Diagnostic Service. Upon receipt, samples were stained for PDL1 using UKAS accredited assay; Dako PD-L1 IHC 28-8 pharmDx kit (Dako/Agilent technologies) and expression reported in the form of combined positive score (CPS) within this reference centre by Dr Philippe Taniere (Consultant Histopathologist and Clinical Service Lead). CPS was defined as the number of positive tumour cells, lymphocytes and macrophages divided by total number of viable tumour cells (multiplied by 100).

5.3.5.2 Tumour Infiltrating Lymphocytes (TILs)

Blinded, pre and post neoadjuvant nivolumab TIL proportion scores were reported by two independent pathologists following review of digital images of mounted, haematoxylin and eosin (H&E) stained FFPE sections. TIL scores were estimated on biopsy specimens and a representative section from post treatment resected tumour selected by scoring pathologist. Scores were calculated as per proportions suggested by Ward et al[228] (Table 26) and compared using Wilcoxon signed rank test.

TIL score	Proportion
1	<20%
2	20-80%
3	>80%

Table 26: TIL proportion scores

5.3.5.3 Pathological Tumour Response

Blinded review of pathological tumour response was again completed by independent pathologist after reviewing the largest cross sectional area of digital images of mounted, H&E stained FFPE sections. Scoring was planned as per equation defined by Stein et al[229]:

$$\%\ Residual\ Viable\ Tumour\ (RVT) = \left(\frac{Total\ Tumour\ Area}{Total\ Tumour\ Bed\ Area}\right) x\ 100$$

Particular note was made of the presence of necrosis, lymphoid infiltrates, plasma cells, cholesterol clefts, proliferative fibrosis, neovascularisation and giant cells. Specimens were scored as 0% RVT, >0 and <10% RVT; 10% RVT and then increasing 10% RVT increments. Complete pathological response (pCR) would be considered as 0% RVT. Major pathological response (MPR) correlated to ≤10% RVT.

5.3.5.4 Gene Expression Profiling

Areas measuring 25-50 mm^2 of squamous cell carcinoma were identified by independent pathologist (Dr Max Robinson, Consultant Cellular Pathologist, Royal Victoria Infirmary, Newcastle upon Tyne) and marked on scanned FFPE slides of biopsy and resection paired specimens. These marked areas were then transferred to freshly cut sections from the same marked block and then scraped, lysed, incubated and transferred into 96 well plate. The library was prepared and amplified with subsequent PCR product clean-up and pooling to create the final library for

sequencing. Sample quality assurance was assessed by ensuring the number of sample 'reads' above six million, percentage reads allocated to positive control of < 40% and relative standard deviation >0.1. Subsequent gene expression profiling and immunophenotyping were analysed using the HTG EdgeSeq Reveal software V4.0.0 2022 (HTG Molecular Diagnostics Inc).

5.4 Results

5.4.1 Recruitment

Initial projected recruitment was estimated at 0.8 patients per month per site, with a target of 10 recruiting centres accumulating 120 patients over a period of 18 months. The NICO study closed early due to delays opening additional recruiting sites along with the coronavirus (COVID-19) pandemic. Following early closure, the recruitment between May 2019 and December 2020 across two participating centres totalled 23 patients (Figure 33). Average recruitment rate was 0.72 (participants per centre per month, allowing for 3 month recruitment pause during COVID-19 pandemic). The time taken to open the study at Greater Glasgow and Clyd site was 90 days and at University College London was 490 days (Table 27). Screening failures are outlined in table 28.

Site name	Days from green-light to site opening	Since start trial			
		Total Screen	Total Randomised	Expected	Target (year)
University Hospital Aintree	0	41	19	16.5	12.0
Greater Glasgow & Clyde	90	16	4	6.5	3.2
University College Hospital (London)	490	0	0	0.0	18.0

Table 27: Table demonstrating site opening times in days from study greenlight along with actual and projected patient recruitment targets for each individual site.

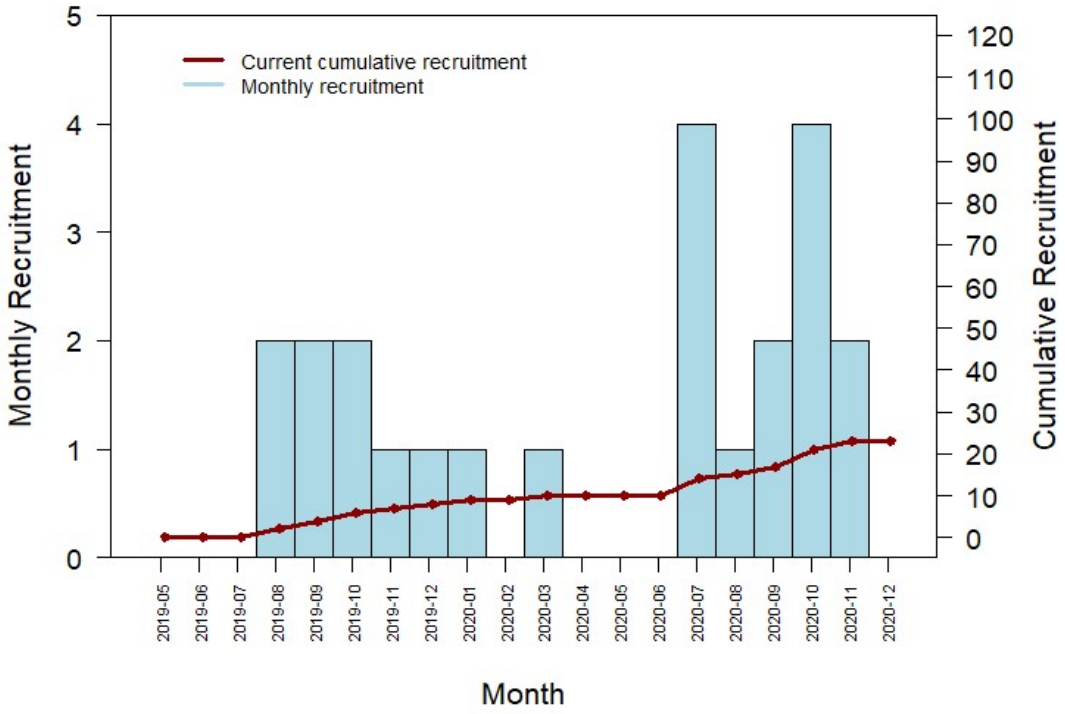

(a)

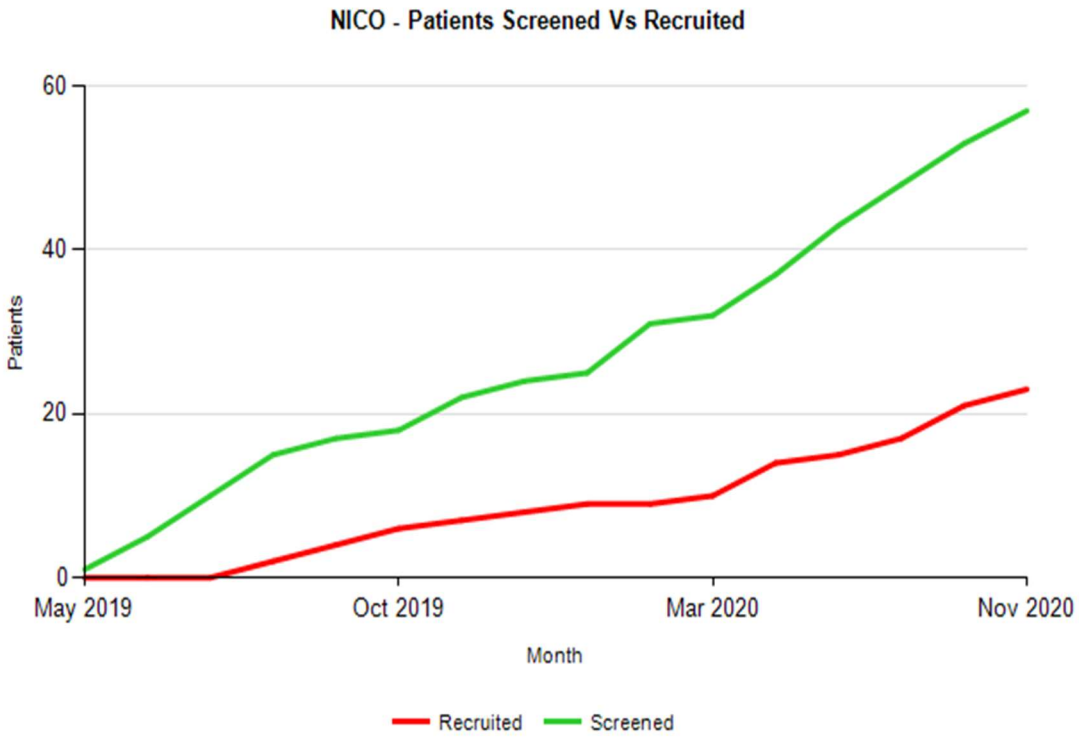

(b)

Figure 33: a) Actual recruitment per month (blue bars) and cumulative recruitment (purple). (b) Cumulative recruitment (red) over time compared with screened patients (green).

Total Screened		57
Total Recruited		23
Screening failures		34
Reason for screening failures	Altered staging after investigation review	6
	Unfit for chemotherapy (severe comorbidities)	8
	Radiotherapy in last 3 years to H&N	1
	No reason given	15

Table 28: Table demonstrating patients screened for trial inclusion and reasons for screening failures.

5.4.2 Patient population

The mean age at recruitment was 57 years (range 24-72) with 14 male and 9 female participants. The majority of patients had either a mandibular (39%, 9/23) or tongue primary tumour (30%, 7/23). 74% (17/23) were current alcohol drinkers; four participants drinking >35 units of alcohol per week. In addition 13 patients (57%) were previous or current smokers. All patients were staged as having locally advanced disease; see table 29.

5.4.3 Compliance with study treatment

Of the 23 patients recruited, only seven received the full planned course of 8 cycles of nivolumab. Six patients received only one cycle of neoadjuvant nivolumab prior to surgical resection and then withdrew from further participation, the reasons for which are; one patient was downstaged following surgery, one had inoperable disease at surgery, one patient died of post-operative complications, one experienced diverticular perforation prior to surgery, and one had poor wound healing and declined radiotherapy (table 29). The remaining nine participants received either one or two neoadjuvant cycles of treatment however stopped the adjuvant portion of nivolumab early, either due to drop in performance status (1), protracted G2+ toxicity (4), patient choice (3) and early local recurrence (1). One patient did not receive any of the planned study treatment due to acute deterioration and gastroenteritis infection prior to receiving cycle one of nivolumab (figure 34).

Patient	Age	Site	Stage (r)	Stage (p)	Margin	ECS	Surgical delay	Adjuvant treatment	Nivolumab cycles			Reason for stopping
									Pre surgery	Pre (C)RT	Adjuvant	
2-011	50	Tongue	T2N1	T3N2b	Involved	1	Nil	CRT	1	1	6	NA
2-012	73	Mandible	T4aN1	T4aN0	2.0	0	Nil	RT	1	1	2	Local recurrence
2-013	67	RMT	T4aN1	T4aN0	4.0	0	Nil	RT	1	1	6	NA
2-016	72	Mandible	T4aN1	Unwell prior to initiation – no trial treatment								
2-017	41	Tongue	T3N0	T3N1	1.4	0	Nil	RT	1	0	0	Patient choice, relocated
2-018	55	Buccal mucosa	T4aN1	T3N0	5.0	0	Nil	RT	1	1	6	NA
2-020	58	Tongue	T3N0	T1N0	2.5	0	Nil	Nil	1	0	0	Pathological downstaging
2-022	47	Mandible	T4bN0	T4aN0	1.1	0	Nil	RT	1	1	6	NA
2-026	55	FOM	T4aN2c	T4aN2c	2.0	0	Nil	RT	1	1	1	Diarrhoea/colitis
2-029	69	FOM	T4aN2b	T4aN3b	Involved	1	Nil	Nil	1	0	0	Died in post operative period – heart failure
2-031	34	FOM	T4aN2b	NA	NA	NA	Inoperable	Nil	1	0	0	Inoperable
2-028	62	Mandible	T4aN2b	T4aN0	6.0	0	Nil	Nil	1	0	0	Poor wound healing/ flap necrosis, declined RT
2-032	64	Mandible	T4aN1	T4aN2b	2.3	0	Nil	RT	1	1	6	NA
2-033	65	Mandible	T4aN2b	T4aN0	2.0	0	Nil	RT	1	1	6	NA
2-034	72	Mandible	T4aN2b	T4aN1	0.9	0	Nil	CRT	1	1	6	NA
2-036	63	Tongue	T4N2b	T4aN3b	Involved	1	Nil	CRT	1	1	0	PS drop after CRT
2-039	46	Maxillary alveolus	T4bN1	T4aN1	1.0	0	Nil	CRT	1	1	2	Diarrhoea/colitis
2-040	40	Mandible	T4aN2b	T2N2b	0.9	1	Nil	CRT	1	1	3	Patient choice
2-041	64	Mandible	T3N2b	T3N1	0.6	0	Nil	CRT	1	1	5	Patient choice
20-002	63	FOM	T2N2c	T2N3b	2.0	1	Nil	CRT	1	1	1	Diarrhoea/colitis Died – Lung cancer 14.02.21
20-006	67	Tongue	T4aN2c	T3N2c	1.0	0	7 days	CRT	1	0	4	Diarrhoea/colitis
20-010	24	Tongue	T3N2c	T3N3b	<1.0	1	Nil	CRT	1	1	0	Non-compliant with protocol
20-011	67	Tongue	T3N0	NA	NA	NA	Debulking operation	Nil	1	0	0	Diverticulitis and GI perforation Toxic epidermal necrolysis. Died 05/04/21

Table 29: Summary table of individual patients recruited to NICO trial. Including pathological staging, treatment received and reasons for discontinuing study treatment.

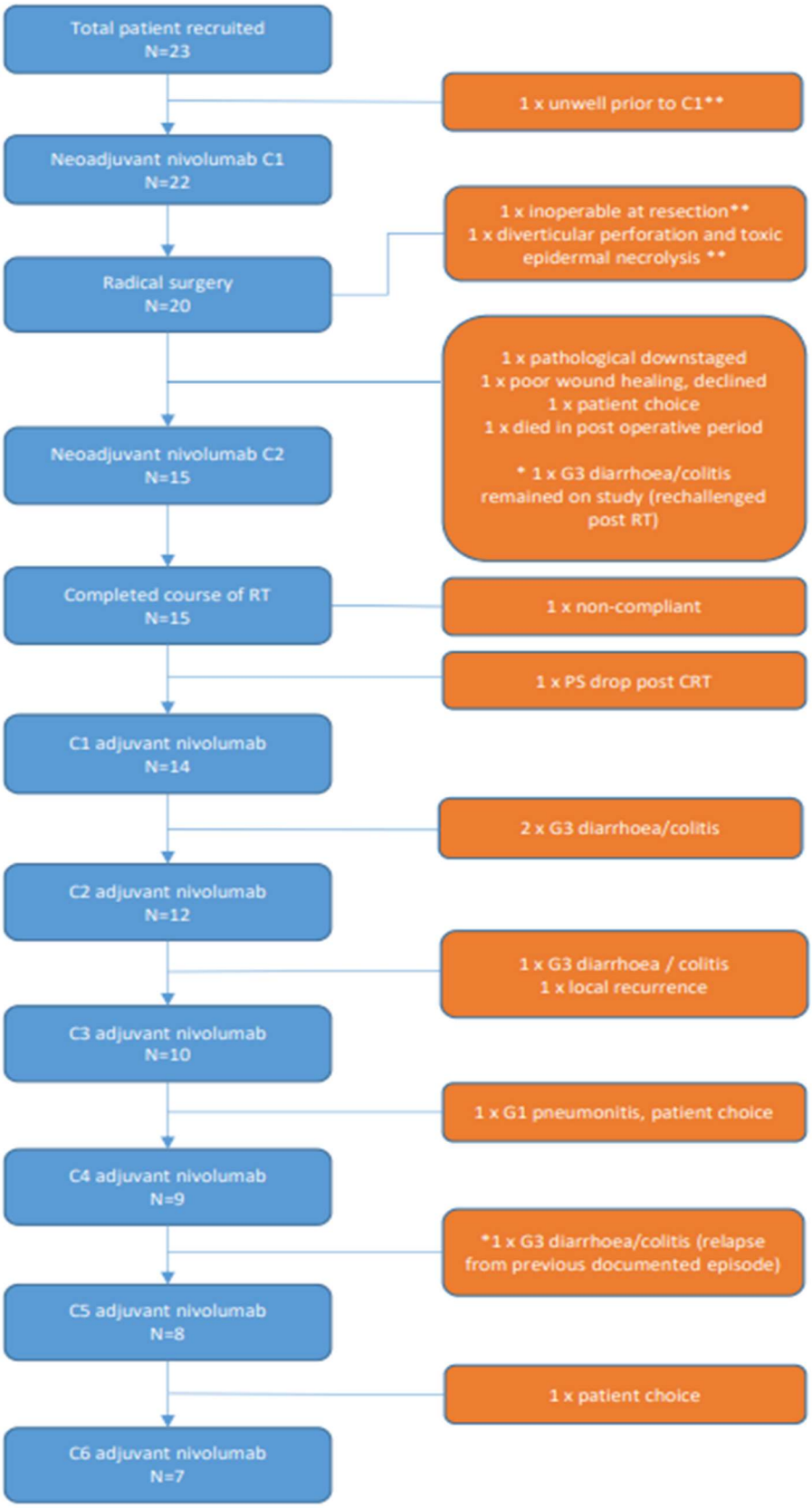

Figure 34: Schema demonstrating patients' progression through trial treatment (blue), toxicity events and reasons for withdrawal (orange). (indicates patient with two separate episodes of toxicity after being re-challenged with nivolumab) (** indicates patients not included in survival analysis or translational research experiments)*

Patient number	Radiological T	Radiological N	Pathological T	Pathological N
2-011	2	1	3	2b
2-012	4	1	4	0
2-013	4	1	4	0
2-016	4	1	No neoadjuvant treatment	
2-017	3	0	3	1
2-018	4	1	3	0
2-020	3	0	1	0
2-022	4	0	4	0
2-026	4	2c	4	2c
2-028	4	2b	4	0
2-029	4	2b	4	3b
2-031	4	2b	Inoperable	
2-032	4	1	4	2b
2-033	4	2b	4	0
2-034	4	2b	4	1
2-036	4	2b	4	3b
2-039	4	1	4	1
2-040	4	2b	2	2b
2-041	3	2b	3	1
20-002	2	2c	2	3b
20-006	4	2c	3	2c
20-010	3	2c	3	3b
20-011	3	0	Inoperable	

Figure 35: Table outlining individual patient radiological staging (prior to neoadjuvant nivolumab) and pathological staging (post neoadjuvant nivolumab). Those patients pathologically upstaged following treatment are highlighted in blue and those downstaged in orange.

5.4.4 Surgical treatment and toxicity

Of the patients who underwent radical surgery, 20% (4/20) experienced Clavien dindo toxicity scores of grade 3 or above which was in-keeping with 16% rate of grade 3 toxicity seen in data presented in our previous study from a series of patients undergoing ablative reconstructive surgery for locally advanced OCSCC in chapter 2 [230]. One patient died in the post-operative period due to progressive (previously undiagnosed) heart failure, pulmonary oedema and lower respiratory tract infection unrelated to neoadjuvant nivolumab. There was one patient who experienced a delay to surgery of 7 days following an episode of diarrhoea/colitis secondary to

neoadjuvant nivolumab. Two patients did not proceed with their planned resection; one had advanced disease which was deemed to be inoperable (determined intraoperatively) and one underwent a palliative debulking procedure after an episode of diverticulitis and bowel perforation rendering them too unwell to go ahead as scheduled. This episode was also presumed to be unrelated to this individual's preoperative nivolumab.

5.4.5 Standard adjuvant ((C)RT) treatment and toxicity

Of the 20 patients who underwent radical resection, ten had pathological indications for concurrent CRT (surgical resection margin ≤1mm and/or presence of ECS), and nine had indications for RT alone (although one patient decided against having adjuvant RT due to healing problems after radical surgery). One patient disease was downstaged from radiologically T3N0 on pathological review to T1N0 and so did not have adjuvant treatment (figure 35). There was no note of pathological evidence of response upon independent pathological review in this case.

As expected, the commonest side effect experienced during RT/CRT was mucositis with 50% (9/18) of patients suffering with grade 3+ toxicity. This is in keeping with high rates of (C)RT related acute toxicity seen in EORTC 22931 and RTOG 9501[63,64] and to be expected given the proximity of high dose treatment regions to the oral cavity (Table 30). Pain, weight loss, radiation dermatitis, fatigue and nausea were also widely reported.

Toxicity	Any grade	Grade 3+
Mucositis	15 (94%)	9 (56%)
Pain/sore throat	13 (81%)	8 (50%)
Weight loss	8 (50%)	4 (25%)
Radiation dermatitis	11 (69%)	4 (25%)
Nausea and vomiting	9 (56%)	5 (31%)
fatigue	5 (31%)	1 (6%)
Acute kidney injury	3 (19%)	1 (6%)
Dry mouth	8 (50%)	0

Table 30 : CTCAE V4 reported toxicity across adjuvant (C)RT phase of treatment.

5.4.6 Nivolumab toxicity

There were a total of 12 SAEs reported across the course of the NICO study. Two patients had recurrent admissions with the same complaint leading to multiple SAEs. There was one SUSAR relating to a reported episode of toxic epidermal necrolysis. The most frequently occurring toxicity was immunotherapy induced hypothyroidism and colitis (Table 31). All episodes of hypothyroidism were of grade 1 and were detected on routine blood tests taken during the adjuvant phase of the study, two patients had mild symptoms of cold intolerance and constipation which resolved upon thyroid hormone replacement. Colitis occurred in four individuals and was the reason for early discontinuation of adjuvant treatment in three patients. In the main, colitis symptoms resolved after patients were provided with oral steroids, albeit a protracted course in two individuals. One patient experienced severe diarrhoea of grade 4 and colitis of grade 3, this required multiple admissions and therapies outlined below in case report 2 (section 5.4.6.2).

ICI related toxicity	Any grade	Grade 3+
Hypothyroid	5 (23%)	0
Adrenal insufficiency	2 (9%)	0
Rash	1 (4%)	0
Pneumonitis	1 (4%)	0
Colitis	4 (18%)	3 (14%)
Diarrhoea	5 (23%)	4 (18%)
Hepatitis	1 (4%)	0
Toxic epidermal necrolysis	1 (4%)	1 (4%)

Table 31: CTCAE V4 ICI related toxicity.

5.4.7 Example patient case reports

The clinical course of patients recruited to the NICO study varied widely, three examples of which are outlined below:

5.4.7.1 Patient 1

Patient 1 was a fit and well 72 year old gentleman with a lifelong smoking history who drank alcohol to excess. Although over 70 years he had no medical problems and no limitation to his physical fitness and therefore was deemed suitable for concurrent

chemoradiotherapy treatment. He first presented complaining of a lump in his cheek which was biopsied in Sept 2020 and confirmed the presence of moderately differentiated SCC. His tumour seemed to be originating from the left mandible, invading the cortex/marrow and extending into the retromolar trigone; MRI neck and CT chest staged his cancer as T4N2b and he was confirmed to be eligible for inclusion on NICO study. He underwent his neoadjuvant nivolumab and then left hemimandibulectomy and left level I-IV neck dissection without delay. The final pathological tumour staging was T4aN1 and confirmed an involved margin at 0.88mm. His post-operative course was uncomplicated and he began his adjuvant chemoradiotherapy at day 48 post-surgery with his pre CRT dose of nivolumab administered on schedule. He suffered the expected side effects of mucositis and radiation dermatitis during CRT however these were mild and he tolerated treatment extremely well,; maintaining his oral intake throughout. He began the adjuvant portion of nivolumab within four weeks of completing his CRT and finished all six cycles of nivolumab without omission or delay. He experienced grade 1 hypothyroidism following cycle two of adjuvant nivolumab which resolved with thyroid hormone replacement therapy. His post treatment scans have shown no recurrent disease and he remains on standard of care follow up (at 12 months post-surgery).

5.4.7.2 Patient 2

Patient 2 was a 46 year old gentleman, again fit and well with no past medical history. He presented with loose teeth and an enlarging nodule coming through skin overlying his right maxilla which was initially treated as a dental abscess (figure 36). His staging investigations confirmed him to have a T4aN1 SCC of the maxillary alveolus and he consented for inclusion on NICO study. His initial treatment with neoadjuvant nivolumab and surgical resection/reconstruction went ahead as planned without complication. His pathology confirmed T4N1 tumour with involved margins and invasion into inferior orbital nerve. Unfortunately his adjuvant treatment presented many challenges. Following his first cycle of cisplatin he was admitted with grade three nausea and poor oral intake. He continued to struggle through CRT treatment

with ongoing nausea, mucositis and pain leading to the omission of his second cycle of chemotherapy. By the end of CRT he was reliant on his gastrostomy tube and had lost a significant amount of weight. Patient 2 required six weeks for his acute CRT side effects to subside whereby he began his adjuvant nivolumab treatment. After two cycles of treatment he started to notice a disturbance in his bowel habit with frequent diarrhoea, and blood/mucous in his stools. Despite intravenous methylprednisolone his symptoms did not improve and flexible sigmoidoscopy revealed florid immunotherapy related colitis. He had a short lived improvement in his symptoms after two doses of infliximab however his diarrhoea returned as he tapered his steroids and he was admitted again for escalation of his steroids and vedulizumab. Unfortunately, once again, his colitis did not improve after this medication switch and he was soon initiated on tofacitinib. He continues to receive tofacitinib and oral steroids on a regular basis and is under close supervision of the local gastroenterologist and immunotherapy toxicity team. His follow up MRI and CT scans have to date been stable with no evidence of recurrent disease (at 14 months post-surgery).

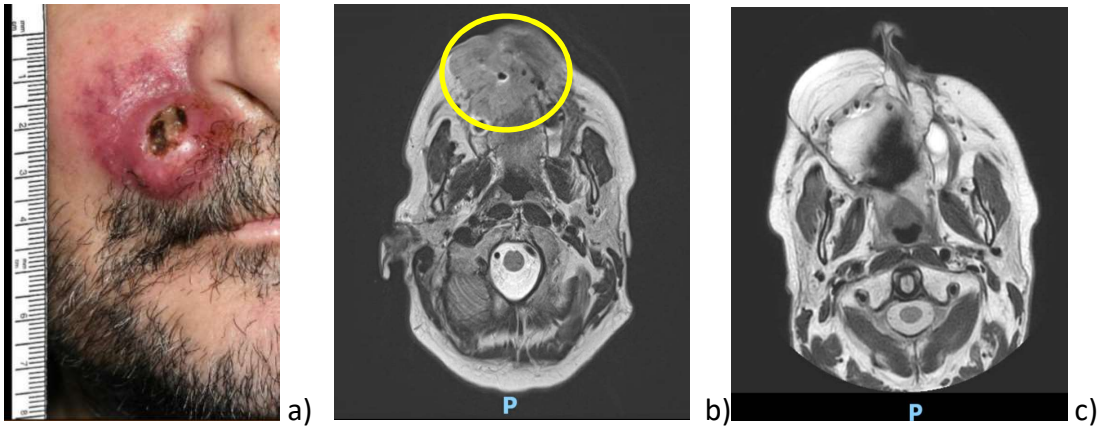

Figure 36: Patient 2 a) clinical photograph of maxillary alveolus SCC fistulating through skin prior to surgical resection. b) pre-treatment axial slice of MRI neck (T2 weighted) T4 right maxillary alveolus lesion shown (yellow circle). c) axial slice of MRI neck (T2 weighted) taken 12 months post surgical resection with reconstructed osseous free flap shown and no evidence of recurrent disease.

5.4.7.3Patient 3

Patient 3 was a 34 year old lady who had a past history of T2N0 SCC tongue (left hemiglossectomy), rheumatoid arthritis with Raynaud's, hypothyroidism, and coeliac disease. She presented approximately four months after her initial left

hemiglossectomy with an enlarging left neck lump and progressively worsening earache. Imaging and fine needle aspirate confirmed the presence of T4N2b SCC left oral tongue. Whole body PET CT scanning reported that this was localised disease and it was planned to resect her tumour following MDT discussions. As she had not undergone previous head and neck radiotherapy and was keen for all available curative treatment options she consented for inclusion on NICO study. Her rheumatoid arthritis was not active and she had not taken steroids or disease modifying anti-rheumatic drugs for 5 years. She received her first cycle of nivolumab without complication however her operation and examination under anaesthesia did not go as planned. It was noted that her disease was more advanced than imaging suggested with direct tumour involvement of the epiglottis, and in order to adequately resect she would require total glossolaryngectomy; the procedure was therefore abandoned. Re-discussion at MDT brought concerns regarding the significant quality of life implications of such extensive surgery and the patient wished to retain the ability to speak. Her treatment plan was adjusted whereby she discontinued participation on NICO and initiated induction chemotherapy and following this, CRT. Despite having an initial good response to treatment her disease quickly relapsed locally; she sadly died three months after completing primary CRT (figure 37).

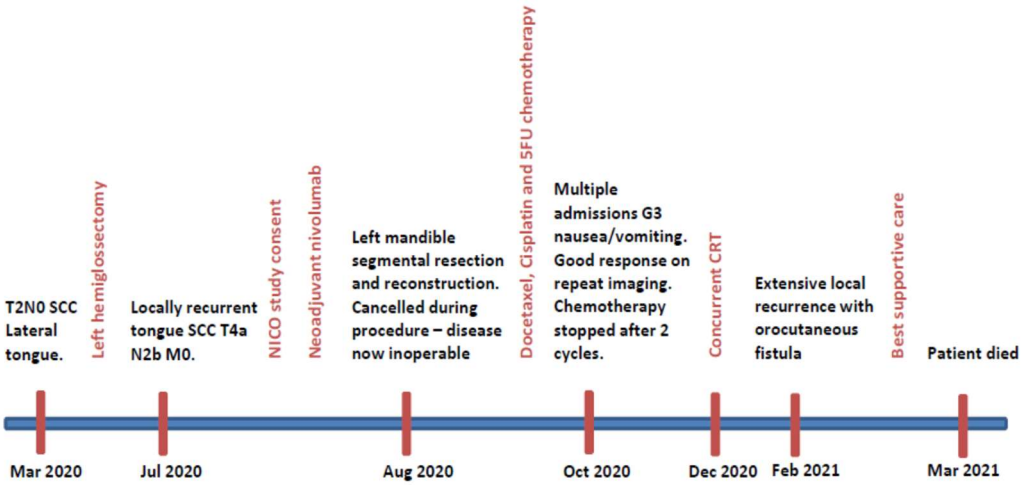

Figure 37: Schematic outlining patient 3 clinical course.

5.4.8 Patient outcomes

To date there have been two patients who have been diagnosed with recurrent head and neck SCC. Both occurred during the adjuvant phase of treatment; one with local recurrence and another with distant metastases. Both patients were too unwell at recurrence to receive any additional palliative anticancer treatments. Another individual was diagnosed with a second primary lung cancer in the follow up period. Of the 20 patients who underwent radical resection, 17 patients had no evidence of recurrence on follow up imaging or clinical examination after receiving their trial treatment and remain on observation as per standard of care. 12 month overall was 77% (after excluding patient 2-016 as they did not receive nivolumab treatment) and 12 month disease free survival was 85%. This excluded patients 2-031 and 20-011 due to inoperability and patient 2-016 as they did not receive nivolumab treatment (Figures 38 and 39).

5.4.9 Tumour infiltrating lymphocyte scores and PDL1 CPS scores

19 patients were included in this analysis owing to the availability of paired samples (two patients having no post treatment specimen due to inoperability, one patient having no pre-treatment sample as it was obtained abroad and one patient did not receive nivolumab). The majority of patients were noted to have static TIL scores across their pre and post resection specimens 12/19 (63%). Five (26%) patient scores increased (by one point) and two (11%) decreased (by one point) (Table 32). There was no statistically significant difference between the two measurement points on Wilcoxon sum rank test p=0.26. Most patients 12/19 (63%) had PD-L1 CPS scores of <1%. Due to low patient numbers it is difficult to draw comparisons with expression in other reported cohorts, however this seems to be higher than the 46% with PDL1 CPS scores <1% reported in a recent study examining (neo)adjuvant anti-PD1 inhibitor in predominantly OCSCC [231]. There was no significant disease free survival difference between patients with low, intermediate or high PD-L1 scores nor change in TIL scores (resulting log rank p=0.54 and p=0.60 respectively) (Figure 40).

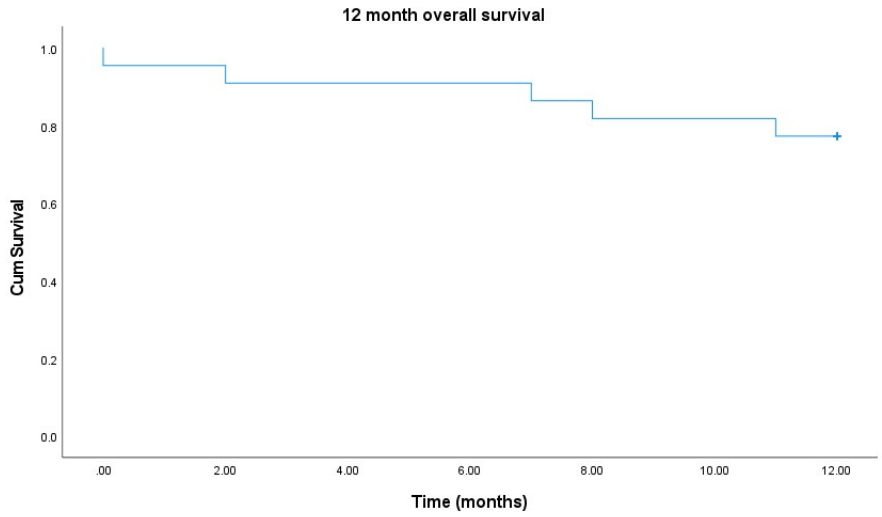

Means and Medians for Survival Time

Mean[a]				Median			
		95% Confidence Interval				95% Confidence Interval	
Estimate	Std. Error	Lower Bound	Upper Bound	Estimate	Std. Error	Lower Bound	Upper Bound
10.545	.703	9.167	11.924	.	.	.	.

a. Estimation is limited to the largest survival time if it is censored.

Figure 38: Overall survival Kaplan-Meier graph. Patient 2-016 excluded from analysis as they did not receive nivolumab treatment.

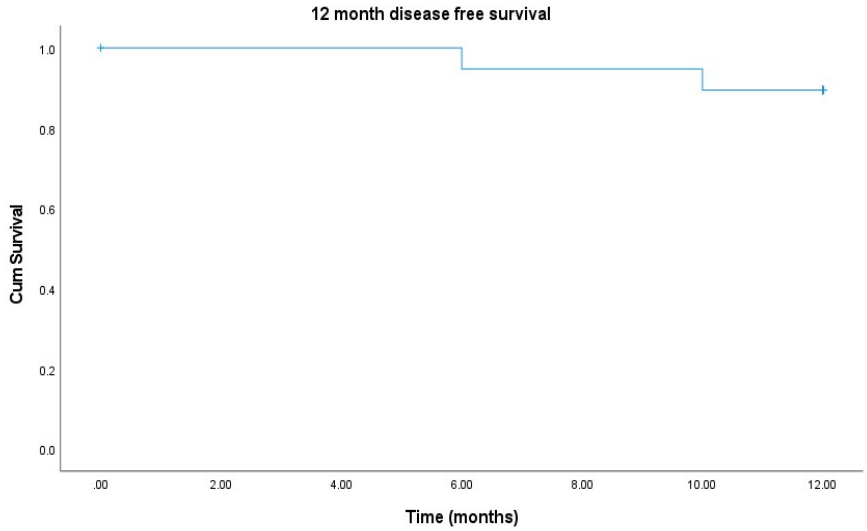

Means and Medians for Survival Time

Mean[a]				Median			
		95% Confidence Interval				95% Confidence Interval	
Estimate	Std. Error	Lower Bound	Upper Bound	Estimate	Std. Error	Lower Bound	Upper Bound
11.579	.319	10.955	12.203	.	.	.	.

a. Estimation is limited to the largest survival time if it is censored.

Figure 39:12 month disease free survival Kaplan-Meier graph. Patient 2-016 excluded from analysis as they did not receive nivolumab treatment. Patients 2-031 and 20-011 excluded due to inoperability and therefore did not complete treatment course. Death without progression demonstrated as censored event.

Pt number	Pathology notes	TILS pre	TILs post	Biopsy PDL1 CPS score
2-011	-	2	2	<1%
2-012	-	2	2	<1%
2-013	Necrosis	2	3	<1%
2-017	-	2	2	<1%
2-018	-	3	3	<1%
2-020	-	2	2	5-10%
2-022	-	2	3	<1%
2-026	-	2	2	<1%
2-028	Necrosis, giant cells	2	3	60-70%
2-029	-	1	1	<1%
2-031	-	2	X	10-20%
2-032	-	2	2	2-3%
2-033	-	2	2	<1%
2-034	-	2	2	20-30%
2-036	-	2	3	<1%
2-039	-	1	1	<1%
2-040	-	3	2	10-20%
2-041	-	1	1	5-10%
20-006	Giant cells, foamy macrophages	X	3	<1%
20-010	-	3	2	60-70%
20-011	-	3	X	55-60%
20-002	-	2	3	60-70%

Table 32: Tumour Infiltrating Lymphocyte scores for individual patients pre neo-adjuvant nivolumab and post neo-adjuvant nivolumab with corresponding PDL1 score.

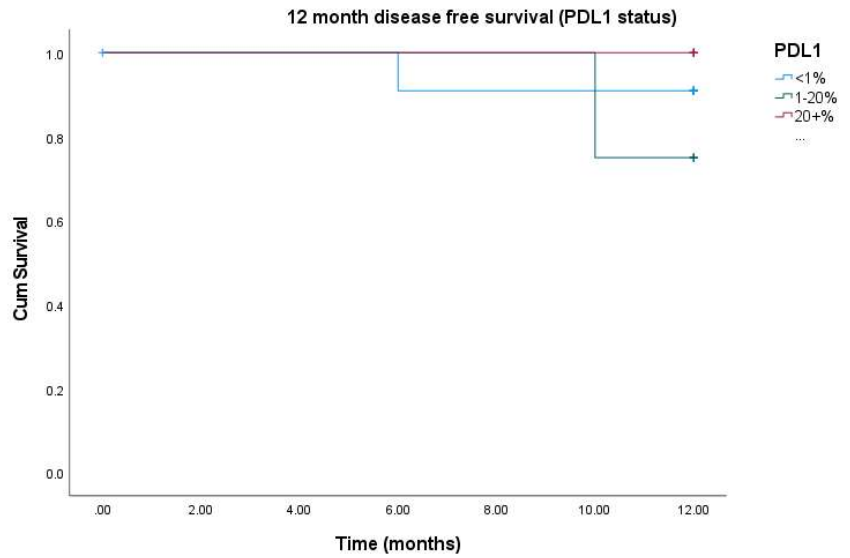

a)

Overall Comparisons

	Chi-Square	df	Sig.
Log Rank (Mantel-Cox)	1.241	2	.538

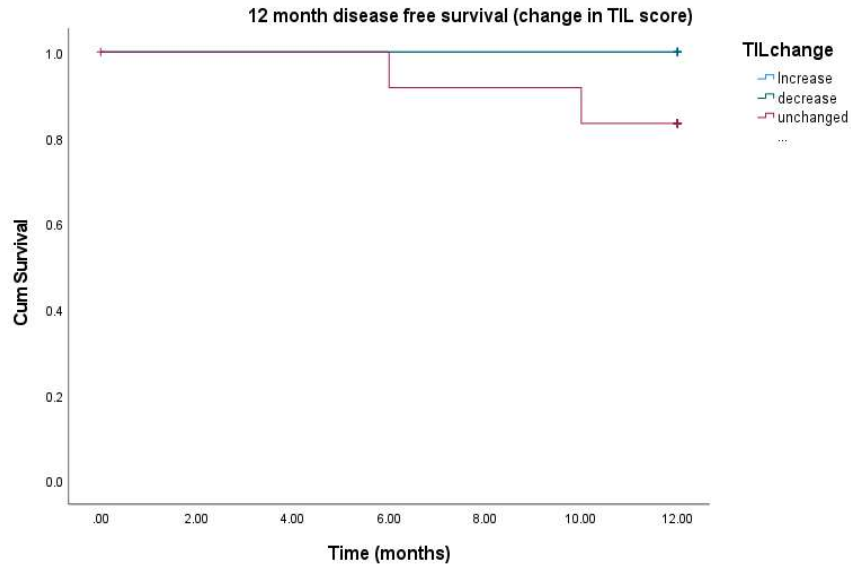

b)

Overall Comparisons

	Chi-Square	df	Sig.
Log Rank (Mantel-Cox)	1.009	2	.604

Figure 400: 12 month disease free survival split into comparator groups for PDL1 expression (a) and TIL score change (b).

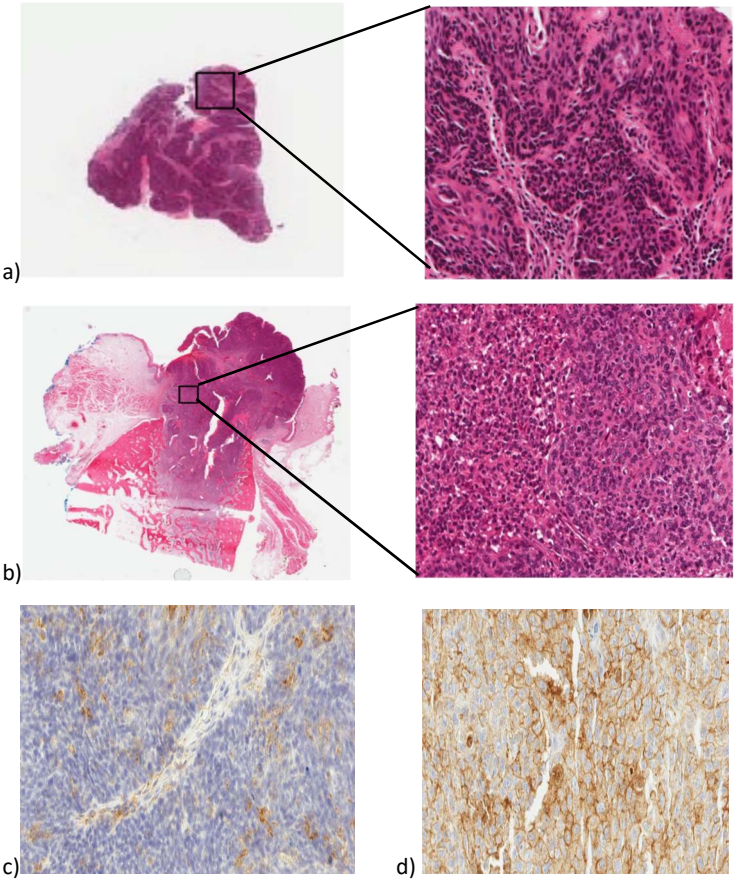

Figure 411: Example scanned images of H&E stained FFPE tissue from patient 2-013. a) shows H&E stained FFPE pre-treatment biopsy specimen with TIL score of 2 (x20 magnification) and b) the post cycle 1 nivolumab sample with increase in TIL score of 3. c) PDL-1 staining CPS score of <1 from pre-treatment biopsy sample (patient 2-013). d) PDL-1 staining CPS score of 60-70% from pre-treatment biopsy sample (patient 20-010).

5.4.10 Preliminary gene expression analysis results

Again, 19 paired biopsy and resection FFPE tissue samples were available for analysis (example slides figure 41). All samples bar one biopsy specimen passed quality control (QC) (appendix 13). Biopsy sample 2-013 demonstrated relative standard deviation below 0.1 and this sample was continually seen as an outlier during PCA analysis; the presumed reason for this is likely to be a reduction in biopsy sample quality. This sample was excluded from further analysis at the time of writing however future specimen examination is planned to ensure the reasons for failing QC is investigated thoroughly.

Preliminary results demonstrate separation between biopsy and resection specimen differential gene expression on principle component analysis. Along with a significant fold change in 14 probes following treatment with neoadjuvant nivolumab (Table 33). The greatest change being in FOS (fold change 3.34) and IL6 (fold change 3.11).

Immunophenotyping signatures (Figure 42) showed increase in regulatory and CD8+ T cells post treatment. Analysis and exploration of significant targets are ongoing.

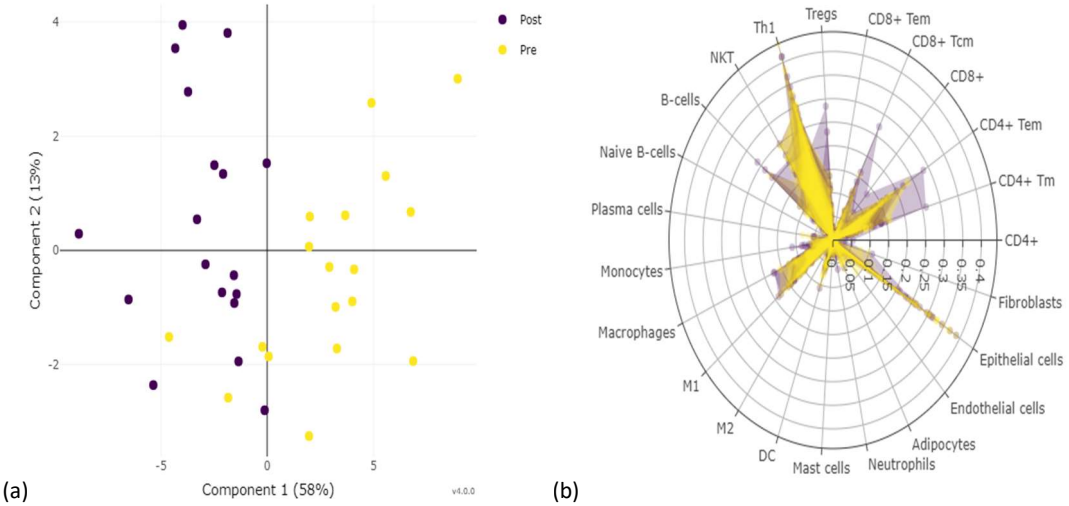

Figure 422: (a) PCA demonstrating differential probe expression from biopsy specimen (yellow) compared to resection specimen (purple). (b) Radar plot demonstrating change in immunophenotype signatures at biopsy (yellow) compared with resection sample (purple)

Probe	Mean normalized Post	Mean normalized Pre	AveExpr	Fold Change	rawP Post.vs.Pre	adjP Post.vs.Pre
ATF3_activating	683	229	8.83	2.98	3.66E-11	5.10E-08
EGR1	4349	1477	11.51	2.94	2.84E-09	1.98E-06
IL6	878	282	9.18	3.11	1.10E-08	5.13E-06
FOS	10162	3038	12.69	3.34	3.55E-07	1.17E-04
EGR3	579	255	8.70	2.27	4.20E-07	1.17E-04
ATF3_repressing	2005	731	10.42	2.74	9.92E-06	2.30E-03
IFNL2	201	113	7.29	1.77	1.53E-05	2.50E-03
CSF3	1112	334	8.51	2.76	1.60E-05	2.50E-03
LIF	565	227	8.63	2.48	1.62E-05	2.50E-03
CSK	1431	2048	10.76	-1.43	3.86E-05	4.90E-03
OSM	503	212	8.48	2.37	3.87E-05	4.90E-03
CD72	368	212	8.18	1.73	4.82E-05	5.60E-03
CD69	662	376	9.02	1.76	8.48E-05	9.10E-03
HMX2	78	36	5.83	2.09	1.07E-04	1.07E-02

Table 33 : Differentially expressed probes with an adjusted significance level of <0.01.

5.5 Discussion

The NICO clinical trial was developed in order to investigate the feasibility of recruitment to a course of (neo)adjuvant nivolumab in patients with locally advanced OCSCC. Unfortunately due to difficulties in site opening and the ongoing COVID-19 pandemic recruitment rates did not meet our projected targets of 10 patients per month. Approximately one third of patients screened were recruited to the study and only three centres out of the projected ten were opened. The prolonged period between study 'greenlight' and third site opening was approximately 16 months; owing in part to the complex nature of trial set up, where treatments are delivered across multiple specialties working in different treating centres within the same cancer network. Screening failures were attributable to severe comorbidities in 8 out of 34 patients (24%), reinforcing conclusions drawn in Chapter 2 whereby many of our population of patients have coexisting medical problems which necessitate adaptations to 'gold standard' adjuvant regimes following surgical resection of their locally advanced OCSCC. The known disparities between initial clinical staging and radiological staging in clinical practice is also highlighted in Chapter 2 and leads to challenges when planning adjuvant treatment in advance of definitive surgery; ultimately resulting in 18% (4 out of 34) of NICO screening failures. Only seven patients received the full course of treatment with the majority discontinuing early due to toxicity and patient choice as discussed below.

5.5.1 Toxicity and deviations from treatment path

The addition of a neoadjuvant dose of nivolumab was, in the main, well tolerated. Two patients had delays to radical surgery; one due to immunotherapy induced colitis (delaying surgery by one week) and the other due to diverticular perforation and toxic epidermal necrolysis (TEN). The latter patients delay led to her becoming too unwell to undergo radical surgery. In other studies examining short courses of neoadjuvant ICI prior to resection, surgical delays were rare and <4 weeks in all cases [221,225]. Ferris et al reported two patients with G3+ toxicity (colitis and skin rash) after neoadjuvant nivolumab; the timing of the emergence of these toxicities is unclear however they did not lead to the discontinuation of therapy [221]. It is a possibility that the single

patient who did not proceed with surgery on the NICO study may have experienced the same clinical course without neoadjuvant ICI therapy, however, these complications were significant and highlight the need to better understand the mechanism of ICI induced toxicity along with identifying those at higher risk for such toxicities prior to embarking a course of treatment.

Despite the generally well tolerated neoadjuvant portion of treatment only 50% (7/14) of those who embarked on the adjuvant course completed as planned. The reason for this was ICI related toxicity (28% 4/14), local recurrence (7% 1/14) and patient choice (14% 2/14). 2 patients out of the 9 (22%) who had high risk features and were planned for chemoradiotherapy completed a full course of adjuvant treatment compared to 5 of 8 (63%) planned for radiotherapy alone. This reflects once again the intensity of current adjuvant regimes, and (as evidenced in Chapter 2) the lack of physical reserve in this patient group who have undergone reconstructive surgery.

The rate of G3+ ICI related toxicity was 22% (5/23) and was attributed to colitis/diarrhoea and TEN. This is higher than was reported by Uppaluri et al seeing just 1 patient (8%) similarly treated with six cycles of adjuvant ICI experiencing grade 3+ hypothyroidism [225]. In addition the numbers of patients with G3+ ICI induced colitis are higher than have been seen when using ICI in other solid tumours; closer to 2-3% in melanoma series [232]. It may be that the balance between the oral and faecal microbiome has a role to play in the differing toxicity rates and is certainly an area for future exploration, particularly in this cohort of patients who are likely to have a disturbance in the oral microbial populations [233].

5.5.2 Response measurement

There was a lack of measurable pathological response seen within our group of patients, although it is noted that there was evidence of necrosis, foamy macrophages and giant cells in three post resection samples (two of these individuals having a PDL1 CPS score of <1% and the other PDL1 CPS score of 60-70%). On the NICO trial, patients underwent surgery between one and two weeks after neoadjuvant nivolumab. Ferris et al also reported low pathological response rates;

1/17 (5.9%) partial pathological response, within their HPV negative group despite a longer neoadjuvant treatment period (treating patients with resectable HNSCC with two cycles of neoadjuvant nivolumab and surgery on day 29). Converse to this Uppaluri et al reported pathological treatment response in 16/36 (44%) of HPV negative patients with resectable HNSCC. These patients were treated to a similar schedule as NICO with one cycle of neoadjuvant ICI and surgery between two and three weeks. This ongoing variation in response seen between the neoadjuvant studies, including NICO, highlights tumour heterogeneity and the need for further investigation into the complex interplay between tumour and immune system. Whether measurable pathological responses confers to statistically significant reduced rates of local or distant relapse in this patient group remains to be seen; it may be that the benefit of neoadjuvant ICI is seen through priming the immune system and subsequent impact on micrometastatic disease negating the importance of neoadjuvant ICI scheduling and direct primary tumour response.

5.5.3 TILs and PDL1 CPS scores

The majority of patients had a static TIL score with only 5 patients showing a gain in infiltrating lymphocytes following neoadjuvant ICI, there was no correlation between TIL score and PDL1 expression. Change in patient TIL scores did not seem to predict survival outcomes however it is speculated that a longer period of ICI treatment may have provided more time for primary tumour response in individuals with increased TIL scores.

The majority of patients were found to have PDL1 CPS scores of <1% (56%, 13/23) with equal numbers showing a PDL1 expression of >20% (22%, 5/23) and 1-20%, (5/23, 22%). This is converse to the proportions of patients in Keynote 048 whereby the predominant expression within the oral cavity cohort was within the >20% group (63% 193/305) with 1-20% group being 37% (112/305) [94]. A later abstract describing subgroup analysis examining the previously unreported <1% group specified low numbers of patients had PDL1 CPS scores of <1% (171 of 1160 included patients) and this included all tumour subsites and did not specify the number of oral cavity patients within this [234]. Similarly expression of PDL1 was reported to be >1% in 64% of patients included in a purely HPV negative cohort (88% of which oral cavity SCC)

treated with (neo)adjuvant anti PD1 inhibitor following resection [231]. The high proportions of patients with PDL1 scores of <1% could explain the low rates of pathological response and static TIL scores within this cohort. In addition longer follow up periods and inclusion of larger patient numbers in future investigations may demonstrate a significant survival difference in this patient population. The future planned analysis of changing proportions of intratumoural (and circulating) immune cell subpopulations in response to neoadjuvant ICI may prove to be significant in biomarker identification.

5.5.4 Gene expression profiling

In order to characterise the changing intratumoural immune landscape following neoadjuvant ICI and characterise biomarkers for response we undertook paired immune gene expression profiling using the HTG precision Immuno-oncology panel, the preliminary results of which are available at the time of writing. There was a significant upregulation in FOS and IL6. The FOS protein family are integral members of the AP-1 transcription factor complex, which (in conjunction with JUN proteins) are known to regulate cell proliferation, activate T cells and facilitate PDL1 expression. IL-6 codes for pro-inflammatory cytokine and overexpression is known to be associated with higher risk pathological features and poorer outcomes in head and neck cancer[235,236]. These results indicate significant alterations in gene expression following ICI and warrant further exploration, as do the differing immunophenotype signatures (Figure 43) which show increase in regulatory and CD8+ T cells. Analysis and exploration of significant targets are ongoing; longer follow up period will help to assess whether these changes relate to a favourable response to ICI.

5.5.5 Patient outcomes

To date, one patient out of the 19 (5%) who received radical surgery experienced a local recurrence within the one year follow up period. One patient has died as a result of distant metastases and one from a second primary lung cancer. The individual who recurred locally had a pT4a tumour of the mandibular alveolus resected with intermediate risk pathological features; moderately differentiated SCC with no perineural or vascular invasion, closest margin of 2.0mm (with negative marginal biopsies) and no involved lymph nodes. Their recurrence was noted approximately

five months after surgery having had adjuvant radiotherapy and two cycles of adjuvant nivolumab. TIL scores were static (score of 2) in both the pre and post resection specimens and baseline PDL1 score was <1%. Interrogation of their radiotherapy plan and scans at relapse revealed the recurrence to be centred within the high dose PTV (Figure 43). There is evidently a cohort of patients within this intermediate group whereby local recurrence risk remains high. There is still much debate over the effect of radiotherapy upon the tumour microenvironment and whether its use can enhance or suppress the immune response. With some preclinical data suggesting certain dose and fractionations promoting immune mediated tumour cell death and converse to this other groups reporting radiation induced hypoxia and sterilisation of tumours resulting in an immunosuppressive environment and the promotion of tumour cell migration [237]. Clearly there is still much to learn regarding the pro or anti-immunogenic response within the tumour microenvironment and how certain factors i.e. timing of ICI, dose and fractionation of radiotherapy can have an effect.

The 1 year DFS of 85% in this patient group is higher than that previously reported in the literature (≈ 50%), see section 1.3.2. Whether this improvement is durable will be demonstrated with longer follow up periods.

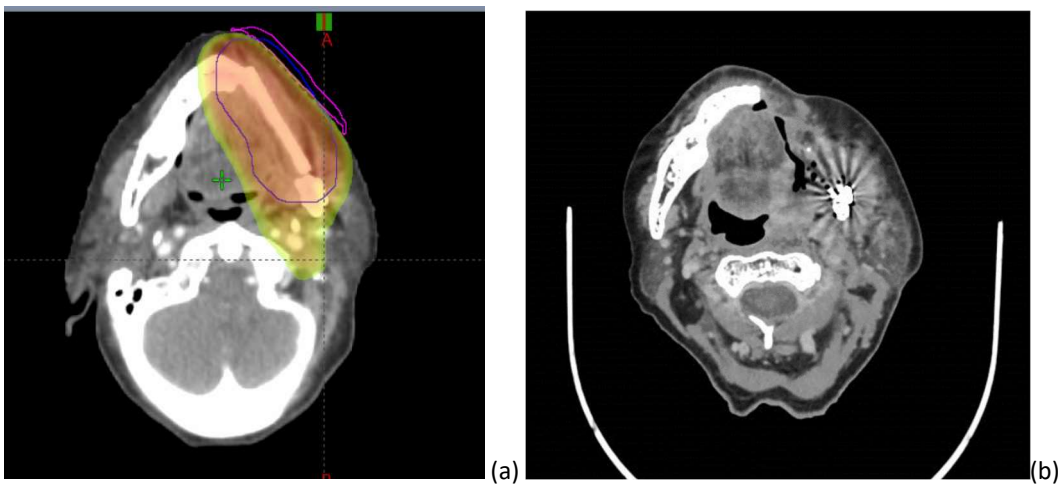

Figure 433: Axial CT images from patient diagnosed with local recurrence after receiving treatment on NICO study. a) radiotherapy planning scan with area in orange demonstrating high dose PTV and b) diagnostic scan at local recurrence..

5.5.6 Limitations

One of the main limitations of this study were the low patient numbers which led to difficulty in coming to firm conclusions over the impact of introducing ICI into the patient pathway. The assessment of pathological response as percentage of viable tumour was limited by the availability of complete resected tumour specimens at blinded pathological review, as a result only the presence of histological features of response (i.e. necrosis etc.) could be assessed. In addition, one biopsy specimen was not examined as this sample was obtained abroad and could not be located.

5.6 Conclusion

The introduction of neoadjuvant and adjuvant ICI into the radical management of locally advanced oral cancer is feasible and has demonstrated lower relapse rates than reported for those receiving standard of care therapy. In the main, neoadjuvant ICI did not impact on the delivery of standard of care therapies however, the rates of G3 ICI related colitis were higher than previously reported. The reason for this remains unclear but highlights the need to further understand the mechanisms of ICI toxicity within this particular cohort. Future planned pairwise gene expression profiling may provide further insight into the tumour microenvironment following ICI therapy.

Chapter 6
Summary and Future Directions

The work outlined within this thesis has an overarching aim to improve survival outcomes for patients with locally advanced head and neck cancers undergoing multimodality therapies, and work towards individuals living with fewer long term consequences of cancer treatment.

The scale of the challenges present within this population was outlined within Chapter 2 whereby a high proportion of patients (88%) were unable to commence planned standard of care adjuvant regimes due to the impact of aggressive ablative reconstructive surgeries and coexisting comorbidities on their performance status. Only 40% of patients initiated adjuvant treatment within the recommended time frame of 42 days secondary to protracted inpatient stay and complications arising in the post-operative period, and 28% of patients had no adjuvant treatment despite pathological indications with consequential switch to palliative treatment intent.

It is thus clear, that institution of any additional therapy would be very challenging, and indeed that first and foremost improving patient access and tolerability of existing treatment would allow for better outcomes.

Focussing on holistic approach to care must be a priority for those embarking on such difficult treatment paths in order to aid the tolerability of treatments. Empowering patients to initiate behavioural change through alcohol and smoking cessation advice, nutritional support and exercise promotion may mitigate severe side effects and prevent future cancer recurrences. This may be achieved through integrated prehabilitation programmes and close collaborations with clinicians with specialist interest in frailty in oncology. While this was not a subject of my thesis, this is an ongoing interest with active collaborations within the Liverpool Head and Neck Centre and participation in the soon to open feasibility study investigating a patient centred approach to exercise for patients with head and neck cancer (ACTIOHN study).

In addition to improving tolerability through optimising fitness and chronic coexisting medical conditions, survival outcomes may be improved and side effects reduced, by patient stratification for therapy.

6.1 Reducing side effects

With the possibility of patients living longer following their cancer treatment there is an ever increasing clinical need to identify which patients would be at risk of the more severe side effects of adjuvant therapies. This was explored by using osteoradionecrosis as an endpoint.

In Chapter 3 a panel of common genetic variants were identified which were protective against this much dreaded consequence of head and neck radiotherapy along with suggesting novel physiological mechanisms for the development of ORN. The regulation of bone remodelling following radiotherapy was highlighted as an area for future investigation which could ultimately lead to the development of new therapeutic options. The identified SNP panel may be used in the future to guide a more personalised approach to adjuvant radiotherapy planning. One limitation of this work was the lack of dosimetric data within this investigated cohort and so this was further explored within Chapter 4.

Through the evaluation of modern IMRT plans for those receiving treatment to the oral cavity following surgical resection and reconstruction, novel dosimetric parameters which increased the risk of ORN were identified. The incidence of ORN was noted to be higher within this group when compared with historical literature including patients with predominantly oropharyngeal primary sites.

Both genomic and dosimetric models take a step towards identifying those at risk of ORN prior to undergoing treatment, and upon validation, will provide guidance for clinicians and the means to better select patients for treatment in the future. Combining the two models in a small cohort were unable to effectively predict ORN, however this is an area which remains of interest and with greater patients numbers may provide a clinically useful tool to guide patient selection for dose escalation studies and conversely treatment de-escalation studies for those in intermediate recurrence risk categories.

6.2 Improving outcomes

Immunotherapy, and in particular immune checkpoint blockade, provides exciting potential for treatment escalation; holding out the promise of durable benefit with non-synergistic toxicity. In an attempt to explore the feasibility and tolerability of such an addition to standard adjuvant regimes the NICO trial was set up; adding (neo)adjuvant ICI to patients standard of care adjuvant (chemo)radiotherapy following ablative surgery. The study had been powered to allow assessment of disease free survival in the high risk group in particular in an otherwise homogenous patient group (oral cavity alone, HPV negative). Unfortunately we were unable to complete the study as planned, due to challenges in recruitment (particularly on the background of COVID) and ultimately a change in priorities by the funder. The slow recruitment was mainly due to the lack of opened sites rather than patient or clinician reluctance. This in turn reflects the complexity of the study and involvement of multiple teams of clinicians; however our experience suggests that these barriers can be overcome and that this is a therapy that could be delivered in standard of care setting. Initial results suggest a survival benefit in this approach, with higher numerical PFS and OS than in our patients with similar disease stage treated previously with standard of care adjuvant therapies. While this could at least partially reflect selection bias, other studies provide support for this. For example early reports within a cohort of 76 patients with resectable high risk head and neck cancer receiving (neo)adjuvant pembrolizumab show reported 1-year disease free survival of 67% (95%CI 0.52-0.85) in those with high-risk features and 93% (95%CI 0.84-1) in those with intermediate-risk features[231].

However, this treatment regimen was not without additive toxicity in a group already receiving highly toxic and intensive treatments. In particular, the rate of ICI induced colitis was higher than previously seen in the literature. With such limited patient numbers it is difficult to interpret whether this is a true representation of the population; nevertheless highlights the need to further understand the mechanisms of ICI toxicity. Recent evidence has suggested that the gut microbiome and the abundance of certain microbes is a significant factor for the development of ICI toxicity (particularly immunotherapy related colitis)[238]. Dysbiosis within OCSCC subsite has been well documented [239] and it is therefore reasonable to speculate that

the higher rates of ICI toxicity may be a result of colonization of certain species either within microbial communities of the oral mucosa, tumour or gut. Examining the oral and faecal microbiome before and after first line ICI within this patient population may prove to take a step forward in answering this question. With this in mind, further work is underway with the now locally recruiting 'Immunotherapy in the treatment of recurrent/metastatic head and neck squamous cell carcinoma (HNSCC)- Assessing early indicators of treatment response with diffusion weighted MRI and the microbiome' (REC 21/SC/0074). This will hope to take a further step towards characterising the microbiome within this patient group and how different populations alter following ICI therapy; providing an additional insight into the complex relationship between the immune system and response to treatment in those with HNSCC.

Larger studies with longer follow up periods must be completed in order to draw firm conclusions on whether (neo)adjuvant ICI will be beneficial to those with locally advanced OCSCC. Translational experiments investigating alterations in gene expression following ICI are ongoing with the anticipation of improving current understanding of the tumour – immune microenvironment and response biomarkers. If ICI were to be integrated into current standard of care therapy, optimal timing and scheduling must be clarified. Certainly the majority of ICI related toxicity occurred in the adjuvant portion of treatment. Whether the benefit of ICI exists in the neoadjuvant priming of the immune response and negates the requirement for prolonged adjuvant courses (and the added toxicity this brings) remains to be answered.

6.4 Conclusions

In summary, this thesis has brought to the forefront the difficulties in treating patients with locally advanced OCSCC, and the magnitude of issues faced in providing patients with optimal therapeutic pathways. Delivering ICI (neo)adjuvantly following curative surgery in this patient group continues to have the potential to improve survival outcomes; future analysis of gene expression and immunophenotype signatures will provide further insight into the tumour microenvironment and

changes following ICI administration. The additive toxicities noted following ICI therapy require further investigation, and may impact negatively upon the deliverability of treatment if integrated into standard of care regimes.

The new understanding of ORN pathogenesis and dosimetric mandibular constraints have provided a basis for future personalised radiotherapy strategies and therapeutic options. This will offer improved long term quality of life for patients treated with head and neck radiotherapy and facilitate the move to escalate treatment in poorer prognosis groups.

References:

1. Sabatini ME, Chiocca S. Human papillomavirus as a driver of head and neck cancers. *Br J Cancer*. 2020;(August 2019). doi:10.1038/s41416-019-0602-7

2. Chaturvedi AK, Anderson WF, Lortet-Tieulent J, et al. Worldwide trends in incidence rates for oral cavity and oropharyngeal cancers. *J Clin Oncol*. 2013;31(36):4550-4559. doi:10.1200/JCO.2013.50.3870

3. Jemal A, Bray F, Ferlay J. Global Cancer Statistics: 2011. *CA Cancer J Clin*. 1999;49(2):1,33-64. doi:10.3322/caac.20107.Available

4. Mummudi N, Agarwal JP, Chatterjee S, Mallick I, Ghosh-Laskar S. Oral Cavity Cancer in the Indian Subcontinent – Challenges and Opportunities. *Clin Oncol*. 2019;31(8):520-528. doi:10.1016/j.clon.2019.05.013

5. UK CR. Head and neck cancer incidence. https://www.cancerresearchuk.org/health-professional/cancer-statistics/statistics-by-cancer-type/head-and-neck-cancers/incidence#ref-. Accessed March 23, 2021.

6. Taib BG, Oakley J, Dailey Y, et al. Socioeconomic deprivation and the burden of head and neck cancer—Regional variations of incidence and mortality in Merseyside and Cheshire, North West, England. *Clin Otolaryngol*. 2018;43(3):846-853. doi:10.1111/coa.13067

7. Bellis MA, Hughes K, Nicholls J, Sheron N, Gilmore I, Jones L. The alcohol harm paradox: Using a national survey to explore how alcohol may disproportionately impact health in deprived individuals. *BMC Public Health*. 2016;16(1):1-10. doi:10.1186/s12889-016-2766-x

8. Schache AG, Powell NG, Cuschieri KS, et al. HPV-related oropharynx cancer in the United Kingdom: An evolution in the understanding of disease etiology. *Cancer Res*. 2016;76(22):6598-6606. doi:10.1158/0008-5472.CAN-16-0633

9. Brown KF, Rumgay H, Dunlop C, et al. The fraction of cancer attributable to modifiable risk factors in England, Wales, Scotland, Northern Ireland, and the United Kingdom in 2015. *Br J Cancer*. 2018;118(8):1130-1141. doi:10.1038/s41416-018-0029-6

10. Caliri AW, Tommasi S, Besaratinia A. Relationships among smoking, oxidative stress, inflammation, macromolecular damage, and cancer. *Mutat Res - Rev Mutat Res*. 2021;787:108365. doi:10.1016/j.mrrev.2021.108365

11. Chen A, Chen L, Vaughan A, et al. Head and Neck tobacco smoking during radiation for head and neck cancer is associated with unfavourable outcome. *Int J Radiat Oncol Biol Phys*. 2011;79(2):414-419. doi:10.1016/j.ijrobp.2009.10.050

12. Giraldi L, Leoncini E, Pastorino R, Wu V. Alcohol and cigarette consumption predict mortality in patients with head and neck cancer : a pooled analysis within the International Head and Neck Cancer Epidemiology (INHANCE) Consortium Original article. 2017;(August):2843-2851. doi:10.1093/annonc/mdx486

13. Hakenewerth AM, Millikan RC, Rusyn I, et al. Effects of polymorphisms in alcohol metabolism and oxidative stress genes on survival from head and neck cancer. *Cancer Epidemiol*. 2013;37(4):479-491. doi:10.1016/j.canep.2013.03.010

14. Di Credico G, Polesel J, Dal Maso L. Alcohol drinking and head and neck cancer risk : the joint effect of intensity and duration. *Br J Cancer*. 2020;123(9):1456-1463. doi:10.1038/s41416-020-01031-z

15. Ren Z, Liu W, Qin H, Xu Y, Yu D. Effect of family history of cancers and environmental factors on risk of nasopharyngeal carcinoma in Guangdong , China. *Cancer Epidemiol*. 2010;34(4):419-424. doi:10.1016/j.canep.2010.04.011

16. Bedi R. Betel-quid and tobacco chewing among the United Kingdom's Bangladeshi community. *Br J Cancer*. 1996;74(SUPPL. 29):73-77.

17. Abogunrin S, Di Tanna GL, Keeping S, Carroll S, Iheanacho I. Prevalence of human papillomavirus in head and neck cancers in European populations: a meta-analysis. *BMC Cancer*. 2014;14(1):968. doi:10.1186/1471-2407-14-968

18. Upile NS, Shaw RJ, Jones TM, et al. Squamous Cell Carcinoma of the Head and Neck Outside the Oropharynx Is Rarely Human Papillomavirus Related. *Laryngoscope*. 2014;124(12):2739-2744. doi:10.1002/lary.24828

19. Chaturvedi AK. Epidemiology and Clinical Aspects of HPV in Head and Neck Cancers. *Head Neck Pathol*. 2012;6(SUPPL. 1):16-24. doi:10.1007/s12105-012-0377-0

20. Goldenberg D, Shahnaz B, Westra WH, et al. Cystic lymph node metastasis in

patients with head and neck cancer: An HPV associated phenomenon. *Head Neck*. 2008;30(7):898–903. doi:10.1002/HED

21. O'Sullivan B, Huang SH, Siu LL, et al. Deintensification candidate subgroups in human papillomavirus-related oropharyngeal cancer according to minimal risk of distant metastasis. *J Clin Oncol*. 2013;31(5):543-550. doi:10.1200/JCO.2012.44.0164

22. Ang KK, Harris J, Wheeler R, et al. Human papillomavirus and survival of patients with oropharyngeal cancer. *NEnglJMed*. 2010;363(1533-4406 (Electronic)):24-35.

23. J.D. Brierley, M.K. Cospodarowicz CW. *TNM Classification of Malignant Tumours. Union for International Cancer Control (8th Edition)*. Wiley Blackwell; 2017.

24. Key TJ, Bradbury KE, Perez-Cornago A, Sinha R, Tsilidis KK, Tsugane S. Diet, nutrition, and cancer risk: What do we know and what is the way forward? *BMJ*. 2020;368(March):1-9. doi:10.1136/bmj.m511

25. Escapa IF, Chen T, Huang Y, Gajare P, Dewhirst FE, Lemon KP. New insights into human nostril microbiome from the expanded Human Oral Microbiome Database (eHOMD): A resource for the microbiome of the human aerodigestive tract. *bioRxiv*. 2018;3(6):1-20. doi:10.1101/347013

26. Lim Y, Fukuma N, Totsika M, Kenny L, Morrison M, Punyadeera C. The performance of an oral microbiome biomarker panel in predicting oral cavity and oropharyngeal cancers. *Front Cell Infect Microbiol*. 2018;8(AUG):1-9. doi:10.3389/fcimb.2018.00267

27. Komiya Y, Shimomura Y, Higurashi T, et al. Patients with colorectal cancer have identical strains of Fusobacterium nucleatum in their colorectal cancer and oral cavity. *Gut*. 2019;68(7):1335-1337. doi:10.1136/gutjnl-2018-316661

28. Lawrence MS, Sougnez C, Lichtenstein L, et al. Comprehensive genomic characterization of head and neck squamous cell carcinomas. *Nature*. 2015;517(7536):576-582. doi:10.1038/nature14129

29. Canning M, Guo G, Yu M, et al. Heterogeneity of the head and neck squamous cell carcinoma immune landscape and its impact on immunotherapy. *Front Cell Dev Biol*. 2019;7(APR):1-19. doi:10.3389/fcell.2019.00052

30. Keck MK, Zuo Z, Khattri A, et al. Integrative analysis of head and neck cancer identifies two biologically distinct HPV and three non-HPV subtypes. *Clin Cancer Res*.

2015;21(4):870-881. doi:10.1158/1078-0432.CCR-14-2481

31. Ferris RL. Immunology and immunotherapy of head and neck cancer. *J Clin Oncol*. 2015;33(29):3293-3304. doi:10.1200/JCO.2015.61.1509

32. Badoual C, Hans S, Rodriguez J, et al. Prognostic value of tumor-infiltrating CD4+ T-cell subpopulations in head and neck cancers. *Clin Cancer Res*. 2006;12(2):465-472. doi:10.1158/1078-0432.CCR-05-1886

33. Balermpas P, Michel Y, Wagenblast J, et al. Tumour-infiltrating lymphocytes predict response to definitive chemoradiotherapy in head and neck cancer. *Br J Cancer*. 2014;110(2):501-509. doi:10.1038/bjc.2013.640

34. Kim HS, Lee JY, Lim SH, et al. Association between PD-L1 and HPV status and the prognostic value of PD-L1 in oropharyngeal squamous cell carcinoma. *Cancer Res Treat*. 2016;48(2):527-536. doi:10.4143/crt.2015.249

35. Satgunaseelan L, Gupta R, Madore J, et al. Programmed cell death-ligand 1 expression in oral squamous cell carcinoma is associated with an inflammatory phenotype. *Pathology*. 2016;48(6):574-580. doi:10.1016/j.pathol.2016.07.003

36. He J, Zhang Y, Kang S, et al. Prognostic significance of programmed cell death 1 (PD-1) or PD-1 ligand 1 (PD-L1) expression in epithelial-originated cancer: A meta-analysis. *Med (United States)*. 2015;94(6):e515. doi:10.1097/MD.0000000000000515

37. Yamamoto T, Kimura T, Ueta E, Tatemoto Y, Osaki T. Characteristic cytokine generation patterns in cancer cells and infiltrating lymphocytes in oral squamous cell carcinomas and the influence of chemoradiation combined with immunotherapy on these patterns. *Oncology*. 2003;64(4):407-415. doi:10.1159/000070300

38. Kim HR, Ha S-J, Hong MH, et al. PD-L1 expression on immune cells, but not on tumor cells, is a favorable prognostic factor for head and neck cancer patients. *Sci Rep*. 2016;6(1):36956. doi:10.1038/srep36956

39. Memorial Sloan Kettering Cancer Centre Early-Stage Oral Cavity Cancer Patient and Caregivers Education. https://www.mskcc.org/cancer-care/patient-education/early-stage-oral-cavity. Accessed June 14, 2021.

40. Lwin CT, Hanlon R, Lowe D, et al. Accuracy of MRI in prediction of tumour thickness

and nodal stage in oral squamous cell carcinoma. *Oral Oncol*. 2012;48(2):149-154. doi:10.1016/j.oraloncology.2011.11.002

41. Johnson DE, Burtness B, Leemans CR, Lui VWY, Bauman JE, Grandis JR. Head and neck squamous cell carcinoma. *Nat Rev Dis Prim*. 2020;6(1). doi:10.1038/s41572-020-00224-3

42. Kim MM, Califano JA. Molecular pathology of head-and-neck cancer. *Int J Cancer*. 2004;112(4):545-553. doi:10.1002/ijc.20379

43. Paver EC, Currie AM, Gupta R, Dahlstrom JE. Human papilloma virus related squamous cell carcinomas of the head and neck: diagnosis, clinical implications and detection of HPV. *Pathology*. 2020;52(2):179-191. doi:10.1016/j.pathol.2019.10.008

44. Jardim JF, Francisco ALN, Gondak R, Damascena A, Kowalski LP. Prognostic impact of perineural invasion and lymphovascular invasion in advanced stage oral squamous cell carcinoma. *Int J Oral Maxillofac Surg*. 2015;44(1):23-28. doi:10.1016/j.ijom.2014.10.006

45. Amin M, Edge S, Greene F, Eds. et al. *American Joint Committee on Cancer (AJCC) Cancer Staging Manual, 8th Edn.* 8th ed. New York: Springer US; 2017.

46. Ganly I, Goldstein D, Carlson DL, et al. Long-term regional control and survival in patients with "low-risk," early stage oral tongue cancer managed by partial glossectomy and neck dissection without postoperative radiation: The importance of tumor thickness. *Cancer*. 2013;119(6):1168-1176. doi:10.1002/cncr.27872

47. Lydiatt W, O'Sullivan B, Patel S. Major Changes in Head and Neck Staging for 2018. *Am Soc Clin Oncol Educ B*. 2018;(38):505-514. doi:10.1200/edbk_199697

48. Nunez D, Kenyon G, Paleri V. *United Kingdom National Multidisciplinary Guidelines for Head and Neck Cancer*. Vol 124.; 2010. doi:10.1017/S0022215110001969

49. D'Cruz AK, Vaish R, Kapre N, et al. Elective versus Therapeutic Neck Dissection in Node-Negative Oral Cancer. *N Engl J Med*. 2015;373(6):521-529. doi:10.1056/nejmoa1506007

50. National Institute for Health and Clinical Excellence. Cancer of the upper aerodigestive tract: assessment and management in people aged 16 and over | Guidance and guidelines | NICE. 2019;(February 2016).

https://www.nice.org.uk/guidance/ng36.

51. Pignon JP, Maître A le, Maillard E, Bourhis J. Meta-analysis of chemotherapy in head and neck cancer (MACH-NC): An update on 93 randomised trials and 17,346 patients. *Radiother Oncol*. 2009;92(1):4-14. doi:10.1016/j.radonc.2009.04.014

52. Iyer NG, Tan DSW, Tan VKM, et al. Randomized trial comparing surgery and adjuvant radiotherapy versus concurrent chemoradiotherapy in patients with advanced, nonmetastatic squamous cell carcinoma of the head and neck: 10-year update and subset analysis. *Cancer*. 2015;121(10):1599-1607. doi:10.1002/cncr.29251

53. Spiotto MT, Jefferson G, Wenig B, Markiewicz M, Weichselbaum RR, Koshy M. Differences in Survival With Surgery and Postoperative Radiotherapy Compared With Definitive Chemoradiotherapy for Oral Cavity Cancer. *JAMA Otolaryngol Neck Surg*. 2017;60637(7):691-699. doi:10.1001/jamaoto.2017.0012

54. Sutton DN, Brown JS, Rogers SN, Vaughan ED, Woolgar JA. The prognostic implications of the surgical margin in oral squamous cell carcinoma. *Int J Oral Maxillofac Surg*. 2003;32(1):30-34. doi:10.1054/ijom.2002.0313

55. Brinkman D, Callanan D, O'Shea R, Jawad H, Feeley L, Sheahan P. Impact of 3 mm margin on risk of recurrence and survival in oral cancer. *Oral Oncol*. 2020;110(June):104883. doi:10.1016/j.oraloncology.2020.104883

56. Mitchell DA, Kanatas A, Murphy C, Chengot P, Smith AB, Ong TK. Margins and survival in oral cancer. *Br J Oral Maxillofac Surg*. 2018;56(9):820-829. doi:10.1016/j.bjoms.2018.06.021

57. Zanoni DK, Migliacci JC, Xu B, et al. A proposal to redefine close surgical margins in squamous cell carcinoma of the oral tongue. *JAMA Otolaryngol - Head Neck Surg*. 2017;143(6):555-560. doi:10.1001/jamaoto.2016.4238

58. Bajwa MS, Houghton D, Java K, et al. The relevance of surgical margins in clinically early oral squamous cell carcinoma. *Oral Oncol*. 2020;110:104913. doi:https://doi.org/10.1016/j.oraloncology.2020.104913

59. Fletcher GH, Evers WT. Radiotherapeutic management of surgical recurrences and postoperative residuals in tumors of the head and neck. *Radiology*. 1970;95(1):185-188. doi:10.1148/95.1.185

60. Tupchong L, Phil D, Scott CB, et al. Randomized study of preoperative versus postoperative radiation therapy in advanced head and neck carcinoma: Long-term follow-up of RTOG study 73-03. *Int J Radiat Oncol Biol Phys*. 1991;20(1):21-28. doi:10.1016/0360-3016(91)90133-O

61. Mishra RC, Singh DN, Mishra TK. Post-operative radiotherapy in carcinoma of buccal mucosa, a prospective randomized trial. *Eur J Surg Oncol*. 1996;22(5):502-504. doi:10.1016/S0748-7983(96)92969-8

62. Adelstein DJ, Lavertu P, Saxton JP, et al. Mature results of a phase III randomized trial comparing concurrent chemoradiotherapy with radiation therapy alone in patients with stage III and IV squamous cell carcinoma of the head and neck. *Cancer*. 2000;88(4):876-883. doi:10.1002/(SICI)1097-0142(20000215)88:4<876::AID-CNCR19>3.0.CO;2-Y

63. Bernier J, Domenge C, Jacques Bernier, M.D., Ph.D., Christian Domenge MD, et al. Postoperative irradiation with or without concomitant chemotherapy for locally advanced head and neck cancer. *N Engl J Med*. 2004;350(19):1945-1952. doi:10.1056/NEJMoa032641

64. Cooper, Giobbie-hurder A, Jonasson O, et al. Postoperative Concurrent Radiotherapy and Chemotherapy for High-Risk Squamous-Cell Carcinoma of the Head and Neck. *N Engl J Med*. 2004;350(19):1819-1827.

65. National Cancer Institute. https://ctep.cancer.gov/protocoldevelopment/electronic_applications/docs/CTCAE_v5_Quick_Reference_5x7.pdf. Accessed May 2021.

66. Fletcher GH, Friedman M. *Clinical Dose Response Curve of Subclinical Aggregates of Epithelial Cells and Its Practical Application in the Management of Human Cancers.* (Friedman M, ed.). Charles C Thomas; 1974.

67. Peters L, Goepfert H, Ang K. Evaluation of the dose for postoperative radiation therapy of head and neck cancer: first report of a prospective randomized trial. *Int J Radiat Oncol Biol Phys*. 1993;26:3-11.

68. Withers HR, Taylor JMG, Maciejewski B. The hazard of accelerated tumor clonogen repopulation during radiotherapy. *Acta Oncol (Madr)*. 1988;27(2):131-146. doi:10.3109/02841868809090333

69. Rosenthal DI, Mohamed ASR, Garden AS, et al. Final Report of a Prospective Randomized Trial to Evaluate the Dose-Response Relationship for Postoperative Radiation Therapy and Pathologic Risk Groups in Patients With Head and Neck Cancer. *Int J Radiat Oncol Biol Phys*. 2017;98(5):1002-1011. doi:10.1016/j.ijrobp.2017.02.218

70. Harris JP, Chen M, Orosco RK, Sirjani D, Divi V, Hara W. Association of survival with shorter time to radiation therapy after surgery for US patients with head and neck cancer. *JAMA Otolaryngol - Head Neck Surg*. 2018;144(4):349-359. doi:10.1001/jamaoto.2017.3406

71. Ghanem AI, Schymick M, Bachiri S, et al. The effect of treatment package time in head and neck cancer patients treated with adjuvant radiotherapy and concurrent systemic therapy. *World J Otorhinolaryngol - Head Neck Surg*. 2019;5(3):160-167. doi:10.1016/j.wjorl.2018.09.005

72. Shaikh T, Handorf EA, Murphy CT, Mehra R, Ridge JA, Galloway TJ. The Impact of Radiation Treatment Time on Survival in Patients With Head and Neck Cancer. *Int J Radiat Oncol Biol Phys*. 2016;96(5):967-975. doi:10.1016/j.ijrobp.2016.08.046

73. Bourhis J, Overgaard J, Audry H, et al. Hyperfractionated or accelerated radiotherapy in head and neck cancer: a meta-analysis. *Lancet*. 2006;368(9538):843-854. doi:10.1016/S0140-6736(06)69121-6

74. Boeckman HJ, Trego KS, Turchi JJ. Cisplatin sensitizes cancer cells to ionizing radiation via inhibition of nonhomologous end joining. *Mol Cancer Res*. 2005;3(5):277-285. doi:10.1158/1541-7786.MCR-04-0032

75. Strojan P, Vermorken J, Beitler J, et al. Cumulative cisplatin dose in concurrent chemotherapy for head and neck cancer: A systematic review. *Head Neck*. 2014;36(10):1391. doi:10.1002/HED

76. Colevas AD. Commentary on "Weekly Low-Dose Versus Three-Weekly High-Dose Cisplatin for Concurrent Chemoradiation in Locoregionally Advanced Non-Nasopharyngeal Head and Neck Cancer: A Systematic Review and Meta-Analysis of Aggregate Data." *Oncologist*. 2017;22(9):1022-1023. doi:10.1634/theoncologist.2017-0232

77. Leoncini E, Ricciardi W, Cadoni G, et al. Adult height and head and neck cancer: A

pooled analysis within the INHANCE Consortium. *Head Neck*. 2014;36(10):1391. doi:10.1002/HED

78. Noronha V, Joshi A, Patil VM, et al. Once-a-week versus once-every-3-weeks cisplatin chemoradiation for locally advanced head and neck cancer: a phase III randomized noninferiority trial. *J Clin Oncol*. 2018;36(11):1064-1072. doi:10.1200/JCO.2017.74.9457

79. Jacobs C, Meyers F, Hendrickson C, Kohler M, Carter S. A randomized phase III study of cisplatin with or without methotrexate for recurrent squamous cell carcinoma of the head and neck. A Northern California oncology group study. *Cancer*. 1983;52(9):1563-1569. doi:10.1002/1097-0142(19831101)52:9<1563::AID-CNCR2820520904>3.0.CO;2-R

80. Forastiere AA, Metch B, Schuller DE, Ensley JF, Hutchins LF, Triozzi P et al. Randomised comparision of cisplatin plus fluorouracil and carboplatin plus fluorouracil versus methotrexate in advanced squamous cell carcinoma of head and neck ,A Southwest oncology Group study. *J Clin Oncol off J AM Soc Clin oncol*. 1992;10(1245-51):1245-1251. doi:10.1200/JCO.1992.10.8.1245

81. Vermorken JB, Remenar E, Van Herpen C, et al. Cisplatin, fluorouracil, and docetaxel in unresectable head and neck cancer. *N Engl J Med*. 2007;357(17):1695-1704. doi:10.1056/NEJMoa071028

82. National Institute for Health and Care Excellence. Cetuximab for treating recurrent or metastatic squamous cell cancer of the head and neck. 2017;(August 2017):22.

83. Rapidis A, Sarlis N, Lefebvre JL, Kies M. Docetaxel in the treatment of squamous cell carcinoma of the head and neck. *Ther Clin Risk Manag*. 2008;4(5):865-886. doi:10.2147/tcrm.s3133

84. Vermorken JB, Stöhlmacher-Williams J, Davidenko I, et al. Cisplatin and fluorouracil with or without panitumumab in patients with recurrent or metastatic squamous-cell carcinoma of the head and neck (SPECTRUM): An open-label phase 3 randomised trial. *Lancet Oncol*. 2013;14(8):697-710. doi:10.1016/S1470-2045(13)70181-5

85. Argiris A, Li S, Savvides P, et al. Phase III Randomized Trial of Chemotherapy With or Without Bevacizumab in Patients With Recurrent or Metastatic Head and Neck

Cancer. *J Clin Oncol*. 2019;37(34):3266-3274. doi:10.1200/JCO.19.00555

86. Pardoll DM. The blockade of immune checkpoints in cancer immunotherapy. *Nat Rev Cancer*. 2012;12(4):252-264. doi:10.1038/nrc3239

87. Seiwert TY, Burtness B, Mehra R, et al. Safety and clinical activity of pembrolizumab for treatment of recurrent or metastatic squamous cell carcinoma of the head and neck (KEYNOTE-012): an open-label, multicentre, phase 1b trial. *Lancet Oncol*. 2017;17(7):956-965. doi:10.1016/S1470-2045(16)30066-3

88. Bauml J, Seiwert TY, Pfister DG, et al. Pembrolizumab for platinum- and cetuximab-refractory head and neck cancer: Results from a single-arm, phase II study. *J Clin Oncol*. 2017;35(14):1542-1549. doi:10.1200/JCO.2016.70.1524

89. Segal NH, Ou S-HI, Balmanoukian A, et al. Safety and efficacy of durvalumab in patients with head and neck squamous cell carcinoma: results from a phase I/II expansion cohort. *Eur J Cancer*. 2019;109:154-161. doi:10.1016/j.ejca.2018.12.029

90. Ferris RL, Blumenschein G, Fayette J, et al. Nivolumab for Recurrent Squamous-Cell Carcinoma of the Head and Neck. *N Engl J Med*. 2016;375(19):1856-1867. doi:10.1056/NEJMoa1602252

91. Ferris RL, Blumenschein G, Fayette J, et al. Nivolumab vs investigator's choice in recurrent or metastatic squamous cell carcinoma of the head and neck: 2-year long-term survival update of CheckMate 141 with analyses by tumor PD-L1 expression. *Oral Oncol*. 2018;81(April):45-51. doi:10.1016/j.oraloncology.2018.04.008

92. Ferris RL, Blumenschein G, Fayette J, et al. Nivolumab vs investigator's choice in recurrent or metastatic squamous cell carcinoma of the head and neck: 2-year long-term survival update of CheckMate 141 with analyses by tumor PD-L1 expression. *Oral Oncol*. 2018;81(April):45-51. doi:10.1016/j.oraloncology.2018.04.008

93. Cohen EEW, Soulières D, Le Tourneau C, et al. Pembrolizumab versus methotrexate, docetaxel, or cetuximab for recurrent or metastatic head-and-neck squamous cell carcinoma (KEYNOTE-040): a randomised, open-label, phase 3 study. *Lancet*. 2019;393(10167):156-167. doi:10.1016/S0140-6736(18)31999-8

94. Burtness B, Harrington KJ, Greil R, et al. Pembrolizumab alone or with chemotherapy versus cetuximab with chemotherapy for recurrent or metastatic squamous cell

carcinoma of the head and neck (KEYNOTE-048): a randomised, open-label, phase 3 study. *Lancet*. 2019;394(10212):1915-1928. doi:10.1016/S0140-6736(19)32591-7

95. National Institute for Heath and Care Excellence. Pembrolizumab for untreated metastatic or unresectable recurrent head and neck squamous cell carcinoma. 2020;(November 2020):1-23. www.nice.org.uk/guidance/ta661.

96. Marta GN, Riera R, Bossi P, et al. Induction chemotherapy prior to surgery with or without postoperative radiotherapy for oral cavity cancer patients: Systematic review and meta-analysis. *Eur J Cancer*. 2015;51(17):2596-2603. doi:10.1016/j.ejca.2015.08.007

97. Bossi P, Lo Vullo S, Guzzo M, et al. Preoperative chemotherapy in advanced resectable OCSCC: Long-term results of a randomized phase III trial. *Ann Oncol*. 2014;25(2):462-466. doi:10.1093/annonc/mdt555

98. Zhong LP, Zhang CP, Ren GX, et al. Long-term results of a randomized phase III trial of TPF induction chemotherapy followed by surgery and radiation in locally advanced oral squamous cell carcinoma. *Oncotarget*. 2015;6(21):18707-18714. doi:10.18632/oncotarget.4531

99. Tao Y, Auperin A, Sire C, et al. Improved outcome by adding concurrent chemotherapy to cetuximab and radiotherapy for locally advanced head and neck carcinomas: Results of the GORTEC 2007-01 Phase III Randomized Trial. *J Clin Oncol*. 2018;36(31):3084-3090. doi:10.1200/JCO.2017.76.2518

100. Harrington KJ, Soulières D, Le Tourneau C, et al. Quality of Life With Pembrolizumab for Recurrent and/or Metastatic Head and Neck Squamous Cell Carcinoma: KEYNOTE-040. *JNCI J Natl Cancer Inst*. 2020;113:1-11. doi:10.1093/jnci/djaa063

101. Antonia SJ, Villegas A, Daniel D, et al. Durvalumab after Chemoradiotherapy in Stage III Non–Small-Cell Lung Cancer. *N Engl J Med*. 2017;377(20):1919-1929. doi:10.1056/NEJMoa1709937

102. Amaria RN, Menzies AM, Burton EM, et al. Neoadjuvant systemic therapy in melanoma: recommendations of the International Neoadjuvant Melanoma Consortium. *Lancet Oncol*. 2019;20(7):e378-e389. doi:10.1016/S1470-2045(19)30332-8

103. Moore ZR, Pham NL, Shah JL, et al. Risk of Unplanned Hospital Encounters in Patients Treated With Radiotherapy for Head and Neck Squamous Cell Carcinoma. *J Pain Symptom Manage*. 2019;57(4):738-745.e3. doi:10.1016/j.jpainsymman.2018.12.337

104. Harris M. The conservative management of osteoradionecrosis of the mandible with ultrasound therapy. *Br J Oral Maxillofac Surg*. 1992;30(5):313-318. doi:10.1016/0266-4356(92)90181-H

105. Lyons A, Ghazali N. Osteoradionecrosis of the jaws: current understanding of its pathophysiology and treatment. *Br J Oral Maxillofac Surg*. 2008;46(8):653-660. doi:10.1016/j.bjoms.2008.04.006

106. Notani K ichi, Yamazaki Y, Kitada H, et al. Management of mandibular osteoradionecrosis corresponding to the severity of osteoradionecrosis and the method of radiotherapy. *Head Neck*. 2003;25(3):181-186. doi:10.1002/hed.10171

107. Studer G, Bredell M, Studer S, Huber G, Glanzmann C. Risk Profile for Osteoradionecrosis of the Mandible in the IMRT Era. *Strahlentherapie und Onkol*. 2016;192(1):32-39. doi:10.1007/s00066-015-0875-6

108. Aarup-Kristensen S, Hansen CR, Forner L, Brink C, Eriksen JG, Johansen J. Osteoradionecrosis of the mandible after radiotherapy for head and neck cancer: risk factors and dose-volume correlations. *Acta Oncol (Madr)*. 2019;58(10):1373-1377. doi:10.1080/0284186X.2019.1643037

109. Frankart AJ, Frankart MJ, Cervenka B, Tang AL, Krishnan DG, Takiar V. Osteoradionecrosis: Exposing the Evidence Not the Bone. *Int J Radiat Oncol Biol Phys*. 2021;109(5):1206-1218. doi:10.1016/j.ijrobp.2020.12.043

110. Royal College Radiologists. https://www.rcr.ac.uk/sites/default/files/radiotherapy-consent-form-for-lower-head-and-neck-cancer.pdf. 2021.

111. Shaw R, Tesfaye B, Bickerstaff M, Silcocks P, Butterworth C. Refining the definition of mandibular osteoradionecrosis in clinical trials: The cancer research UK HOPON trial (Hyperbaric Oxygen for the Prevention of Osteoradionecrosis). *Oral Oncol*. 2017;64:73-77. doi:10.1016/j.oraloncology.2016.12.002

112. Marx RE. A New Concept of Its Pathophysiology. *Growth (Lakeland)*. 1983.

113. Myers I. Infectious diseases of the jaws. *J Oral Surg*. 1970;28(17e26).

114. Delanian S, Lefaix JL. The radiation-induced fibroatrophic process: Therapeutic perspective via the antioxidant pathway. *Radiother Oncol*. 2004;73(2):119-131. doi:10.1016/j.radonc.2004.08.021

115. Patel V, Di Silvio L, Kwok J, et al. The impact of intensity-modulated radiation treatment on dento-alveolar microvasculature in pharyngeal cancer implant patients. *J Oral Rehabil*. 2020;47(11):1411-1421. doi:10.1111/joor.13084

116. Delanian S, Depondt J, Lefaix JL. Major healing of refractory mandible osteoradionecrosis after treatment combining pentoxifylline and tocopherol: A phase II trial. *Head Neck*. 2005;27(2):114-123. doi:10.1002/hed.20121

117. Rice N, Polyzois I, Ekanayake K, Omer O, Stassen LFA. The management of osteoradionecrosis of the jaws - A review. *Surgeon*. 2015;13(2):101-109. doi:10.1016/j.surge.2014.07.003

118. Shaw RJ, Butterworth CJ, Silcocks P, et al. HOPON (Hyperbaric Oxygen for the Prevention of Osteoradionecrosis): A Randomized Controlled Trial of Hyperbaric Oxygen to Prevent Osteoradionecrosis of the Irradiated Mandible After Dentoalveolar Surgery. *Int J Radiat Oncol Biol Phys*. 2019;104(3):530-539. doi:10.1016/j.ijrobp.2019.02.044

119. D'Souza J, Lowe D, Rogers SN. Changing trends and the role of medical management on the outcome of patients treated for osteoradionecrosis of the mandible: Experience from a regional head and neck unit. *Br J Oral Maxillofac Surg*. 2014;52(4):356-362. doi:10.1016/j.bjoms.2014.01.003

120. National Institude for Health and Care Research. https://fundingawards.nihr.ac.uk/award/NIHR131050. Accessed June 2021.

121. Teoh M, Clark CH, Wood K, Whitaker S, Nisbet A. Volumetric modulated arc therapy: A review of current literature and clinical use in practice. *Br J Radiol*. 2011;84(1007):967-996. doi:10.1259/bjr/22373346

122. Cheung KY. Intensity modulated radiotherapy: Advantages, limitations and future developments. *Biomed Imaging Interv J*. 2006;2(1):1-19. doi:10.2349/biij.2.1.e19

123. Burman C, Kutcher GJ, Emami B, Goitein M. Fitting of normal tissue tolerance data to

an analytic function. *Int J Radiat Oncol Biol Phys*. 1991;21(1):123-135. doi:10.1016/0360-3016(91)90172-Z

124. Dénes Á, Boldogkoi Z, Uhereczky G, et al. Central autonomic control of the bone marrow: Multisynaptic tract tracing by recombinant pseudorabies virus. *Neuroscience*. 2005;134(3):947-963. doi:10.1016/j.neuroscience.2005.03.060

125. Kirkpatrick JP, van der Kogel AJ, Schultheiss TE. Radiation Dose-Volume Effects in the Spinal Cord. *Int J Radiat Oncol Biol Phys*. 2010;76(3 SUPPL.):42-49. doi:10.1016/j.ijrobp.2009.04.095

126. Nutting CM, Morden JP, Harrington KJ, et al. Parotid-sparing intensity modulated versus conventional radiotherapy in head and neck cancer (PARSPORT): A phase 3 multicentre randomised controlled trial. *Lancet Oncol*. 2011;12(2):127-136. doi:10.1016/S1470-2045(10)70290-4

127. Spencer CR, Gay HA, Haughey BH, et al. Eliminating radiotherapy to the contralateral retropharyngeal and high level ii lymph nodes in head and neck squamous cell carcinoma is safe and improves quality of life. *Cancer*. 2014;120(24):3994-4002. doi:10.1002/cncr.28938

128. Iyizoba-Ebozue Z, Murray LJ, Ramasamy S, et al. Radiotherapy for Oropharyngeal Carcinoma With an Uninvolved Contralateral Neck: The Safety of Omission of Contralateral High Level II and Retropharyngeal Lymph Nodes From Elective Target Volumes. *Clin Oncol*. 2021;33(5):331-339. doi:10.1016/j.clon.2020.12.007

129. Nutting C, Rooney K, Foran B, et al. Results of a randomized phase III study of dysphagia-optimized intensity modulated radiotherapy (Do-IMRT) versus standard IMRT (S-IMRT) in head and neck cancer. *J Clin Oncol*. 2020;38(15_suppl):6508. doi:10.1200/JCO.2020.38.15_suppl.6508

130. Nutting CM, Morden JP, Beasley M, et al. Results of a multicentre randomised controlled trial of cochlear-sparing intensity-modulated radiotherapy versus conventional radiotherapy in patients with parotid cancer (COSTAR; CRUK/08/004). *Eur J Cancer*. 2018;103(September 2017):249-258. doi:10.1016/j.ejca.2018.08.006

131. Moon DH, Moon SH, Wang K, et al. Incidence of, and risk factors for, mandibular osteoradionecrosis in patients with oral cavity and oropharynx cancers. *Oral Oncol*. 2017;72:98-103. doi:10.1016/j.oraloncology.2017.07.014

132. Mohamed ASR, Hobbs BP, Hutcheson KA, et al. Dose-volume correlates of mandibular osteoradionecrosis in Oropharynx cancer patients receiving intensity-modulated radiotherapy: Results from a case-matched comparison. *Radiother Oncol*. 2017;124(2):232-239. doi:10.1016/j.radonc.2017.06.026

133. Den Haan N, Van den Bosch L, Van den Hoek A, et al. PO-0732 NTCP model for osteoradionecrosis after definitive radiotherapy in head and neck cancer patients. *Radiother Oncol*. 2019;133:S376. doi:10.1016/s0167-8140(19)31152-1

134. Tsai CJ, Hofstede TM, Sturgis EM, et al. Osteoradionecrosis and radiation dose to the mandible in patients with oropharyngeal cancer. *Int J Radiat Oncol Biol Phys*. 2013;85(2):415-420. doi:10.1016/j.ijrobp.2012.05.032

135. Owosho AA, Yom SHK, Han Z, et al. Comparison of mean radiation dose and dosimetric distribution to tooth-bearing regions of the mandible associated with proton beam radiation therapy and intensity-modulated radiation therapy for ipsilateral head and neck tumor. *Oral Surg Oral Med Oral Pathol Oral Radiol*. 2016;122(5):566-571. doi:10.1016/j.oooo.2016.07.003

136. West CM, Barnett GC. Genetics and genomics of radiotherapy toxicity: Towards prediction. *Genome Med*. 2011;3(8). doi:10.1186/gm268

137. Danielsson D, Brehwens K, Halle M. Influence of genetic background and oxidative stress response on risk of mandibular osteoradionectrosis after radiotherapy of head and neck cancer. *Head Neck*. 2014;55:1-28. doi:10.1002/hed

138. Borchiellini D, Etienne-Grimaldi MC, Bensadoun RJ, et al. Candidate apoptotic and DNA repair gene approach confirms involvement of ERCC1, ERCC5, TP53 and MDM2 in radiation-induced toxicity in head and neck cancer. *Oral Oncol*. 2017;67:70-76. doi:10.1016/j.oraloncology.2017.02.003

139. Alsbeih GA, El-Sebaie MM, Al-Rajhi NM, et al. Association between XRCC1 G399A Polymorphism and Late Complications to Radiotherapy in Saudi Head and Neck Cancer Patients. *J Egypt Natl Canc Inst*. 2008;20(3):302-308.

140. Seibold P, Behrens S, Schmezer P, et al. XRCC1 Polymorphism Associated with Late Toxicity after Radiation Therapy in Breast Cancer Patients. *Int J Radiat Oncol Biol Phys*. 2015;92(5):1084-1092. doi:10.1016/j.ijrobp.2015.04.011

141. Pratesi N, Mangoni M, Mancini I, et al. Association between single nucleotide polymorphisms in the XRCC1 and RAD51 genes and clinical radiosensitivity in head and neck cancer. *Radiother Oncol*. 2011;99(3):356-361. doi:10.1016/j.radonc.2011.05.062

142. Li H, You Y, Lin C, et al. XRCC1 codon 399Gln polymorphism is associated with radiotherapy-induced acute dermatitis and mucositis in nasopharyngeal carcinoma patients. *Radiat Oncol*. 2013;8(1):1. doi:10.1186/1748-717X-8-31

143. Chen H, Mendxin W, Guisheng L. Association between XRCC1 single-nucleotide polymorphism and acute radiation reaction in patients with nasopharyngeal carcinoma: A cohort study. *Medicine (Baltimore)*. 2017;96(44):e8202. doi:10.1097/MD.0000000000008202

144. Venkatesh GH, Manjunath VB, Mumbrekar KD, et al. Polymorphisms in radio-responsive genes and its association with acute toxicity among head and neck cancer patients. *PLoS One*. 2014;9(3). doi:10.1371/journal.pone.0089079

145. Nanda SS, Gandhi AK, Rastogi M, et al. Evaluation of XRCC1 Gene Polymorphism as a Biomarker in Head and Neck Cancer Patients Undergoing Chemoradiation Therapy. *Int J Radiat Oncol Biol Phys*. 2018;101(3):593-601. doi:10.1016/j.ijrobp.2018.03.039

146. Yu J, Huang Y, Liu L, et al. Genetic polymorphisms of Wnt/B-catenin pathway genes are associated with the efficacy and toxicities of radiotherapy in patients with nasopharyngeal carcinoma. *Oncotarget*. 2016;7(50):82528-82537. doi:10.18632/oncotarget.12754

147. Ren JH, Dai XF, Yan GL, et al. Acute oral mucositis in nasopharyngeal carcinoma patients treated with radiotherapy: Association with genetic polymorphism in DNA DSB repair genes. *Int J Radiat Biol*. 2014;90(3):256-261. doi:10.3109/09553002.2014.873558

148. Werbrouck J, De Ruyck K, Duprez F, et al. Acute Normal Tissue Reactions in Head-and-Neck Cancer Patients Treated With IMRT: Influence of Dose and Association With Genetic Polymorphisms in DNA DSB Repair Genes. *Int J Radiat Oncol Biol Phys*. 2009;73(4):1187-1195. doi:10.1016/j.ijrobp.2008.08.073

149. West C, Rosenstein BS. Establishment of a radiogenomics consortium. *Radiother Oncol*. 2010;94(1):117-118. doi:10.1016/j.radonc.2009.12.007

150. Kerns SL, Ostrer H, Stock R, et al. Genome-wide association study to identify single nucleotide polymorphisms (SNPs) associated with the development of erectile dysfunction in African-American men after radiotherapy for prostate cancer. *Int J Radiat Oncol Biol Phys*. 2010;78(5):1292-1300. doi:10.1016/j.ijrobp.2010.07.036

151. Barnett GC, Thompson D, Fachal L, et al. A genome wide association study (GWAS) providing evidence of an association between common genetic variants and late radiotherapy toxicity. *Radiother Oncol*. 2014;111(2):178-185. doi:10.1016/j.radonc.2014.02.012

152. Ho AY, Atencio DP, Peters S, et al. Genetic Predictors of Adverse Radiotherapy Effects: The Gene-PARE project. *Int J Radiat Oncol Biol Phys*. 2006;65(3):646-655. doi:10.1016/j.ijrobp.2006.03.006

153. Kerns SL, Dorling L, Fachal L, et al. Meta-analysis of Genome Wide Association Studies Identifies Genetic Markers of Late Toxicity Following Radiotherapy for Prostate Cancer. *EBioMedicine*. 2016;10:150-163. doi:10.1016/j.ebiom.2016.07.022

154. Seibold P, Webb A, Aguado-Barrera ME, et al. REQUITE: A prospective multicentre cohort study of patients undergoing radiotherapy for breast, lung or prostate cancer. *Radiother Oncol*. 2019;138:59-67. doi:10.1016/j.radonc.2019.04.034

155. Paleri V, Roland N. Introduction to the United Kingdom National Multidisciplinary Guidelines for Head and Neck Cancer. *J Laryngol Otol*. 2016;130(S2):S3-S4. doi:10.1017/s0022215116000359

156. Grégoire V, Lefebvre JL, Licitra L, Felip E. Squamous cell carcinoma of the head and neck: EHNS-ESMO-ESTRO clinical practice guidelines for diagnosis, treatment and follow-up. *Ann Oncol*. 2010;21(SUPPL. 5):184-186. doi:10.1093/annonc/mdq185

157. Ghanem AI, Schymick M, Bachiri S, et al. The effect of treatment package time in head and neck cancer patients treated with adjuvant radiotherapy and concurrent systemic therapy. *World J Otorhinolaryngol - Head Neck Surg*. 2019;(xxxx). doi:10.1016/j.wjorl.2018.09.005

158. Huang J, Barbera L, Brouwers M, Browman G, Mackillop WJ. Does delay in starting treatment affect the outcomes of radiotherapy? A systematic review. *J Clin Oncol*. 2003;21(3):555-563. doi:10.1200/JCO.2003.04.171

159. BAHNO Standards Working Group. British Association of Head & Neck Oncologists Standards 2009. BAHNO. https://bahno.org.uk/_userfiles/pages/files/bahnostandardsdoc09.pdf. Published 2009.

160. National Comprehensive Cancer Network. NCCN Clinical Practice Guidelines in Oncology (NCCN Guidelines): Head and Neck Cancers. *Natl Compr Cancer Netw*. 2017;version 2. https://www.nccn.org/professionals/physician_gls/pdf/head-and-neck.pdf.

161. Schache A, Kerawala C, Ahmed O, et al. British Association of Head and Neck Oncologists (BAHNO) standards 2020. *J Oral Pathol Med*. 2021;50(3):262-273. doi:10.1111/jop.13161

162. Somerset Cancer Register. www.somersetscr.nhs.uk/about-the-scr/. Accessed August 1, 2019.

163. Dindo D, Demartines N, Clavien P-A. Classification of Surgical Complications: A New Proposal With Evaluation in a Cohort of 6336 Patients and Results of a Survey. *Ann Surg*. 2004;240(2). https://journals.lww.com/annalsofsurgery/Fulltext/2004/08000/Classification_of_Surgical_Complications__A_New.3.aspx.

164. McHugh ML. Interrater reliability: the kappa statistic. *Biochem medica*. 2012;22(3):276-282.

165. NCIN: national cancer intelligence network. Oral Cavity Cancer : Survival Trends in England. 2010;(November).

166. Hazari A, Walton P. The UK National Flap Registry (UKNFR): A National Database for all pedicled and free flaps in the UK. *J Plast Reconstr Aesthet Surg*. 2015;68(12):1633-1636. doi:10.1016/j.bjps.2015.10.008

167. Chin AL, Pollom EL, Lee NY, Tsai CJ. (P064) Patterns of Care in Adjuvant Therapy for Resected Oral Cavity Squamous Cell Cancer in the Elderly. *Int J Radiat Oncol*. 2017;98(2, Supplement):E32. doi:https://doi.org/10.1016/j.ijrobp.2017.02.160

168. So WKW, Chan RJ, Chan DNS, et al. Quality-of-life among head and neck cancer survivors at one year after treatment - A systematic review. *Eur J Cancer*.

2012;48(15):2391-2408. doi:10.1016/j.ejca.2012.04.005

169. Shaw R, Nanson G, Coffrey T. TITAN – Feasibility Study – Trial of induction TPS therapy in locoregionally advanced head and neck cancer. Randomised controlled unblended multi-centre phase III trial of neo-adjuvant induction chemotherapy for HPV –ve HNSCC. (T=taxane, P=platinum, F=flu. *NCRI Cancer Conf Abstr*. 2013. Abstracts.ncri.org.uk/abstract/titan-feasibility-study-trial-of-induction-tpf-therapy-in-locoregionally-advanced-head-and-neck-cancer-randomised-controlled-unblinded-multi-centre-phase-iii-trial-of-neo-adjuv/.

170. Kreppel M, Nazarli P, Grandoch A, et al. Clinical and histopathological staging in oral squamous cell carcinoma – Comparison of the prognostic significance. *Oral Oncol*. 2016;60:68-73. doi:10.1016/j.oraloncology.2016.07.004

171. Koch WM, Ridge JA, Forastiere A, Manola J. Comparison of clinical and pathological staging in head and neck squamous cell carcinoma: results from Intergroup Study ECOG 4393/RTOG 9614. *Arch Otolaryngol Head Neck Surg*. 2009;135(9):851-858. doi:10.1001/archoto.2009.123

172. Hao S-P, Ng S-H. Magnetic Resonance Imaging versus Clinical Palpation in Evaluating Cervical Metastasis from Head and Neck Cancer. *Otolaryngol Neck Surg*. 2000;123(3):324-327. doi:10.1067/mhn.2000.105252

173. Paleri V, Urbano TG, Mehanna H, et al. Management of neck metastases in head and neck cancer: United Kingdom National Multidisciplinary Guidelines. *J Laryngol Otol*. 2016;130(S2):S161-S169. doi:DOI: 10.1017/S002221511600058X

174. Bolzoni A, Cappiello J, Piazza C, et al. Diagnostic Accuracy of Magnetic Resonance Imaging in the Assessment of Mandibular Involvement in Oral-Oropharyngeal Squamous Cell Carcinoma: A Prospective Study. *Arch Otolaryngol Neck Surg*. 2004;130(7):837-843. doi:10.1001/archotol.130.7.837

175. Sun J, Li B, Li CJ, et al. Computed tomography versus magnetic resonance imaging for diagnosing cervical lymph node metastasis of head and neck cancer: A systematic review and meta-analysis. *Onco Targets Ther*. 2015;8:1291-1313. doi:10.2147/OTT.S73924

176. Vandecaveye V, Keyzer F De. Diffusion-weighted MRI in head and neck cancer : experience to date and future potential. 2013;5:319-331.

177. Chawla S, Kim S, Wang S PH, Chawla S, Kim S, Wang S, Poptani H. Diffusion-weighted imaging in head and neck cancers. *Futur Oncol*. 2009;5(7):959-975. doi:10.2217/fon.09.77.Diffusion-weighted

178. Rattay T, Talbot CJ. Finding the Genetic Determinants of Adverse Reactions toRadiotherapy. *Clin Oncol*. 2014;26(5):301-308. doi:10.1016/j.clon.2014.02.001

179. Kerns SL, Dorling L, Fachal L, et al. Meta-analysis of Genome Wide Association Studies Identifies Genetic Markers of Late Toxicity Following Radiotherapy for Prostate Cancer. *EBioMedicine*. 2016;10:150-163. doi:10.1016/j.ebiom.2016.07.022

180. Barnett GC, West CML, Coles CE, et al. Standardized total average toxicity score: A scale- and grade-independent measure of late radiotherapy toxicity to facilitate pooling of data from different studies. *Int J Radiat Oncol Biol Phys*. 2012;82(3):1065-1074. doi:10.1016/j.ijrobp.2011.03.015

181. Lyons AJ, West CM, Risk JM, et al. Osteoradionecrosis in head-and-neck cancer has a distinct genotype-dependent cause. *Int J Radiat Oncol Biol Phys*. 2012;82(4):1479-1484. doi:10.1016/j.ijrobp.2011.05.016

182. Shaw R, Butterworth C, Tesfaye B, et al. HOPON (Hyperbaric Oxygen for the Prevention of Osteoradionecrosis): A randomised controlled trial of hyperbaric oxygen to prevent osteoradionecrosis of the irradiated mandible: Study protocol for a randomised controlled trial. *Trials*. 2018;19(1):1-10. doi:10.1186/s13063-017-2376-7

183. Chang CC, Chow CC, Tellier LCAM, Vattikuti S, Purcell SM, Lee JJ. Second-generation PLINK: Rising to the challenge of larger and richer datasets. *Gigascience*. 2015;4(1):1-16. doi:10.1186/s13742-015-0047-8

184. Morgan AP. argyle: An R package for analysis of illumina genotyping arrays. *G3 Genes, Genomes, Genet*. 2016;6(2):281-286. doi:10.1534/g3.115.023739

185. Trevino V, Falciani F. GALGO: An R package for multivariate variable selection using genetic algorithms. *Bioinformatics*. 2006;22(9):1154-1156. doi:10.1093/bioinformatics/btl074

186. Breiman L. Random forests. *Mach Learn*. 2001;45:5-32. doi:10.1201/9780429469275-8

187. Alsbeih G, Al-Harbi N, Al-Hadyan K, El-Sebaie M, Al-Rajhi N. Association between normal tissue complications after radiotherapy and polymorphic variations in TGFB1 and XRCC1 genes. *Radiat Res*. 2010;173(4):505-511. doi:10.1667/RR1769.1

188. Sayers EW, Beck J, Bolton EE, et al. Database resources of the National Center for Biotechnology Information. *Nucleic Acids Res*. 2021;49(D1):D10-D17. doi:10.1093/nar/gkaa892

189. No Title. https://www.ncbi.nlm.nih.gov/variation/tools/1000genomes/. Accessed February 2, 2019.

190. No Title. https://ftp.ncbi.nlm.nih.gov/hapmap/. Accessed February 2, 2019.

191. Belinky F, Nativ N, Stelzer G, et al. PathCards: Multi-source consolidation of human biological pathways. *Database*. 2015;2015(2):1-13. doi:10.1093/database/bav006

192. Zaidi SK, Javed A, Choi JY, et al. A specific targeting signal directs Runx2/Cbfa1 to subnuclear domains and contributes to transactivation of the osteocalcin gene. *J Cell Sci*. 2001;114(17):3093-3102.

193. Milili M, Gauthier L, Veran J, Mattei MG, Schiff C. A new Groucho TLE4 protein may regulate the repressive activity of Pax5 in human B lymphocytes. *Immunology*. 2002;106(4):447-455. doi:10.1046/j.1365-2567.2002.01456.x

194. Wheat JC, Krause DS, Shin TH, et al. The corepressor Tle4 is a novel regulator of murine hematopoiesis and bone development. *PLoS One*. 2014;9(8). doi:10.1371/journal.pone.0105557

195. Tang J, Huang Y, Nguyen DH, Costes S V., Snijders AM, Mao JH. Genetic background modulates lncRNA-coordinated tissue response to low dose ionizing radiation. *Int J Genomics*. 2015;2015. doi:10.1155/2015/461038

196. Huang S, Li Z, Liu Y, et al. Neural regulation of bone remodeling: Identifying novel neural molecules and pathways between brain and bone. *J Cell Physiol*. 2019;234(5):5466-5477. doi:10.1002/jcp.26502

197. Spieker J, Frieß JL, Sperling L, Thangaraj G, Vogel-Höpker A, Layer PG. Cholinergic control of bone development and beyond. *Int Immunopharmacol*. 2020;83(January):106405. doi:10.1016/j.intimp.2020.106405

198. Thangaraj G, Manakov V, Cucu A, Fournier C, Layer PG. Inflammatory effects of TNFα are counteracted by X-ray irradiation and AChE inhibition in mouse micromass cultures. *Chem Biol Interact*. 2016;259:313-318. doi:10.1016/j.cbi.2016.03.027

199. Pierce H, Zhang D, Magnon C, et al. Cholinergic Signals from the CNS Regulate G-CSF-Mediated HSC Mobilization from Bone Marrow via a Glucocorticoid Signaling Relay. *Cell Stem Cell*. 2017;20(5):648-658.e4. doi:10.1016/j.stem.2017.01.002

200. Eimar H, Tamimi I, Murshed M, Tamimi F. Cholinergic regulation of bone. *J Musculoskelet Neuronal Interact*. 2013;13(2):124-132.

201. Bataille C, Mauprivez C, Haÿ E, et al. Different sympathetic pathways control the metabolism of distinct bone envelopes. *Bone*. 2012;50(5):1162-1172. doi:10.1016/j.bone.2012.01.023

202. Pohlers D, Brenmoehl J, Löffler I, et al. TGF-β and fibrosis in different organs - molecular pathway imprints. *Biochim Biophys Acta - Mol Basis Dis*. 2009;1792(8):746-756. doi:10.1016/j.bbadis.2009.06.004

203. Zhang S. The role of transforming growth factor β in T helper 17 differentiation. *Immunology*. 2018;155(1):24-35. doi:10.1111/imm.12938

204. Owosho AA, Tsai CJ, Lee RS, et al. The prevalence and risk factors associated with osteoradionecrosis of the jaw in oral and oropharyngeal cancer patients treated with intensity-modulated radiation therapy (IMRT): The Memorial Sloan Kettering Cancer Center experience. *Oral Oncol*. 2017;64:44-51. doi:10.1016/j.oraloncology.2016.11.015

205. Kuhnt T, Stang A, Wienke A, Vordermark D, Schweyen R, Hey J. Potential risk factors for jaw osteoradionecrosis after radiotherapy for head and neck cancer. *Radiat Oncol*. 2016;11(1):1-7. doi:10.1186/s13014-016-0679-6

206. Le Guevelou J, Bastit V, Marcy PY, et al. Flap delineation guidelines in postoperative head and neck radiation therapy for head and neck cancers. *Radiother Oncol*. 2020;151:256-265. doi:10.1016/j.radonc.2020.08.025

207. Xu CJ, Van Der Schaaf A, Schilstra C, Langendijk JA, Van'T Veld AA. Impact of statistical learning methods on the predictive power of multivariate normal tissue complication probability models. *Int J Radiat Oncol Biol Phys*. 2012;82(4):e677-e684.

doi:10.1016/j.ijrobp.2011.09.036

208. Lee TF, Huang EY. The different dose-volume effects of normal tissue complication probability using lasso for acute small-bowel toxicity during radiotherapy in gynecological patients with or without prior abdominal surgery. *Biomed Res Int*. 2014;2014(August). doi:10.1155/2014/143020

209. Teng F, Fan W, Luo Y, et al. A Risk Prediction Model by LASSO for Radiation-Induced Xerostomia in Patients With Nasopharyngeal Carcinoma Treated With Comprehensive Salivary Gland–Sparing Helical Tomotherapy Technique. *Front Oncol*. 2021;11(February):1-9. doi:10.3389/fonc.2021.633556

210. Ali A, Tibshirani RJ. The generalized lasso problem and uniqueness. *Electron J Stat*. 2019;13(2):2307-2347. doi:10.1214/19-EJS1569

211. Zou H, Hastie T. Regularization and variable selection via the elastic net. *J R Stat Soc Ser B Stat Methodol*. 2005;67(2):301-320. doi:10.1111/j.1467-9868.2005.00503.x

212. Beetz I, Schilstra C, Burlage FR, et al. Development of NTCP models for head and neck cancer patients treated with three-dimensional conformal radiotherapy for xerostomia and sticky saliva: The role of dosimetric and clinical factors. *Radiother Oncol*. 2012;105(1):86-93. doi:10.1016/j.radonc.2011.05.010

213. Moring M, Mast H, Wolvius E. Mandibular osteoradionecrosis after postoperative radiotherapy for oral cavity cancer. *ESTRO*. 2022;Presentation (Session 12). https://www.estro.org/Congresses/ESTRO-2022/571/12-headandneck/10195/mandibulareosteoradionecrosisafterpostoperativeradi.

214. Evans M, Beasley M. Target delineation for postoperative treatment of head and neck cancer. *Oral Oncol*. 2018;86(October):288-295. doi:10.1016/j.oraloncology.2018.08.011

215. Carsuzaa F, Lapeyre M, Gregoire V, et al. Recommendations for postoperative radiotherapy in head & neck squamous cell carcinoma in the presence of flaps: A GORTEC internationally-reviewed HNCIG-endorsed consensus. *Radiother Oncol*. 2021;160:140-147. doi:10.1016/j.radonc.2021.04.026

216. Cho Y, Yoon HI, Lee IJ, et al. Patterns of local recurrence after curative resection and reconstruction for oropharyngeal and oral cancers: Implications for postoperative

radiotherapy target volumes. *Head Neck*. 2019;41(11):3916-3923. doi:https://doi.org/10.1002/hed.25928

217. Reuther T, Schuster T, Mende U, Kübler AC. Osteoradionecrosis of the jaws as a side effect of radiotherapy of head and neck tumour patients - A report of a thirty year retrospective review. *Int J Oral Maxillofac Surg*. 2003;32(3):289-295. doi:10.1054/ijom.2002.0332

218. Takiar V, Garden AS, Ma D, et al. Reirradiation of head and neck cancers with intensity modulated radiation therapy: Outcomes and analyses. *Int J Radiat Oncol Biol Phys*. 2016;95(4):1117-1131. doi:10.1016/j.ijrobp.2016.03.015

219. Chen AM, Farwell DG, Luu Q, Donald PJ, Perks J, Purdy JA. Evaluation of the planning target volume in the treatment of head and neck cancer with intensity-modulated radiotherapy: what is the appropriate expansion margin in the setting of daily image guidance? *Int J Radiat Oncol Biol Phys*. 2011;81(4):943-949. doi:10.1016/j.ijrobp.2010.07.017

220. Topalian S, Taube J, Pardoll D. Neoadjuvant checkpoint blockade for cancer immunotherapy. *Science (80-)*. 2020;367(6477):eaax0182. doi:10.1126/science.aax0182

221. Ferris RL, Spanos WC, Leidner R, et al. Neoadjuvant nivolumab for patients with resectable HPV-positive and HPV-negative squamous cell carcinomas of the head and neck in the CheckMate 358 trial. *J Immunother Cancer*. 2021;9(6):e002568. doi:10.1136/jitc-2021-002568

222. Uppaluri R, Campbell KM, Egloff AM, et al. Neoadjuvant and Adjuvant Pembrolizumab in Resectable Locally Advanced, Human Papillomavirus–Unrelated Head and Neck Cancer: A Multicenter, Phase II Trial. *Clin Cancer Res*. 2020;26(19):5140-5152. doi:10.1158/1078-0432.ccr-20-1695

223. Ferrarotto R, Bell D, Rubin ML, et al. Checkpoint inhibitors assessment in oropharynx cancer (CIAO): Safety and interim results. *J Clin Oncol*. 2019;37(15_suppl):6008. doi:10.1200/JCO.2019.37.15_suppl.6008

224. Knochelmann H, Horton JD, Meek M, et al. Immune signatures associated with response to neoadjuvant PD-1 blockade in oral cavity cancer. *J Clin Oncol*. 2019;37(15_suppl):6055. doi:10.1200/JCO.2019.37.15_suppl.6055

225. Uppaluri R, Campbell KM, Egloff AM, et al. Neoadjuvant and adjuvant pembrolizumab in resectable locally advanced human papillomavirus-Unrelated Head and Neck Cancer: a Multicentre, Phase 2 Trial. *Am Assoc Cancer Res*. 2020. doi:10.1158/1078-0432.CCR-20-1695

226. US National Library of Medicine. No Title. Clinical Trials.Gov. https://clinicaltrials.gov/ct2/show/NCT03721757. Accessed June 2, 2022.

227. Brooker RC, Schache AG, Sacco JJ. NICO Phase II clinical trial - focus on an emerging immunotherapy strategy for the adjuvant treatment of locally-advanced oral cancers. *Br J Oral Maxillofac Surg*. 2021;59(8):959-962. doi:10.1016/j.bjoms.2020.08.059

228. Ward MJ, Thirdborough SM, Mellows T, et al. Tumour-infiltrating lymphocytes predict for outcome in HPV-positive oropharyngeal cancer. *Br J Cancer*. 2014;110(2):489-500. doi:10.1038/bjc.2013.639

229. Stein JE, Lipson EJ, Cottrell TR, et al. Pan-tumor pathologic scoring of response to PD-(L)1 blockade. *Clin Cancer Res*. 2020;26(3):545-551. doi:10.1158/1078-0432.CCR-19-2379

230. Brooker RC, Hobkirk A, Cashman H, et al. Adjuvant management of locally advanced oral squamous cell carcinoma – real-world challenges and opportunities. *Br J Oral Maxillofac Surg*. 2020. doi:10.1016/j.bjoms.2020.08.034

231. Wise-Draper TM, Takiar V, Mierzwa ML, et al. Association of pathological response to neoadjuvant pembrolizumab with tumor PD-L1 expression and high disease-free survival (DFS) in patients with resectable, local-regionally advanced, head and neck squamous cell carcinoma (HNSCC). *J Clin Oncol*. 2021;39(15_suppl):6006. doi:10.1200/JCO.2021.39.15_suppl.6006

232. Wolchok JD, Chiarion-Sileni V, Gonzalez R, et al. Overall Survival with Combined Nivolumab and Ipilimumab in Advanced Melanoma. *N Engl J Med*. 2017;377(14):1345-1356. doi:10.1056/NEJMoa1709684

233. Irani S, Barati I, Badiei M. Periodontitis and oral cancer - current concepts of the etiopathogenesis. *Oncol Rev*. 2020;14(1):23-34. doi:10.4081/oncol.2020.465

234. Burtness B, Rischin D, Greil R, Soulières D, Tahara M, de Castro G. Efficacy of first-

line (1L) pembrolizumab by PD-L1 combined positive score <1, 1-19, and ≥20 in recurrent and/or metastatic (R/M) head and neck squamous cell carcinoma (HNSCC): KEYNOTE-048 subgroup analysis. Abstract LB-258 / 2. In: *Proceedings of the 111th Annual Meeting of the American Association for Cancer Research; 2020 June 22-24. Philadelphia (PA): AACR; 2020.* ; 2020.

235. Choudhary MM, France TJ, Teknos TN, Kumar P. Interleukin-6 role in head and neck squamous cell carcinoma progression. *World J Otorhinolaryngol - head neck Surg*. 2016;2(2):90-97. doi:10.1016/j.wjorl.2016.05.002

236. Atsaves V, Leventaki V, Rassidakis GZ, Claret FX. AP-1 Transcription Factors as Regulators of Immune Responses in Cancer. *Cancers (Basel)*. 2019;11(7):1037. doi:10.3390/cancers11071037

237. Colton M, Cheadle EJ, Honeychurch J, Illidge TM. Reprogramming the tumour microenvironment by radiotherapy: implications for radiotherapy and immunotherapy combinations. *Radiat Oncol*. 2020;15(1):1-11. doi:10.1186/s13014-020-01678-1

238. Andrews MC, Duong CPM, Gopalakrishnan V, et al. Gut microbiota signatures are associated with toxicity to combined CTLA-4 and PD-1 blockade. *Nat Med*. 2021;27(8):1432-1441. doi:10.1038/s41591-021-01406-6

239. Irfan M, Delgado RZR, Frias-Lopez J. The Oral Microbiome and Cancer. *Front Immunol*. 2020;11:591088. doi:10.3389/fimmu.2020.591088

Appendices

Appendix 1: Brooker RC, Sacco JJ, Schache AG. Integration of Checkpoint Inhibitors into the Management of Locally Advanced Head and Neck Cancer: Future Perspectives. Clin Oncol. 2019;31(7):424-431. doi:10.1016/j.clon.2019.04.011

Appendix 2: Brooker RC, Hobkirk A, Cashman H, et al. Adjuvant management of locally advanced oral squamous cell carcinoma – real-world challenges and opportunities. Br J Oral Maxillofac Surg. 2020. doi:10.1016/j.bjoms.2020.08.034

Appendix 3: Brooker RC, Antczak P, Liloglou T, et al. Genetic variants associated with mandibular osteoradionecrosis following radiotherapy for head and neck malignancy. Radiother Oncol. 2021;165:87-93. doi:10.1016/j.radonc.2021.10.0204

Appendix 4: Brooker RC, Schache AG, Sacco JJ. NICO Phase II clinical trial - focus on an emerging immunotherapy strategy for the adjuvant treatment of locally-advanced oral cancers. Br J Oral Maxillofac Surg. 2021;59(8):959-962. doi:10.1016/j.bjoms.2020.08.059

Appendix 5: Brooker RC, Hobkirk A, Cashman H, et al. Complications and their consequences for multimodality treatment delivery in locally advanced oral cavity cancer. Poster number 46. British Association of Head & Neck Oncologists Annual Scientific Meeting 2021

Appendix 6: Clavien Dindo classification of surgical. Table extracted from: Dindo D, Demartines N, Clavien PA. Classification of surgical complications: A new proposal with evaluation in a cohort of 6336 patients and results of a survey. Ann Surg. 2004;240(2):205-240(2):205-213. doi:10.1097/01.sla.0000133083.54934.ae [163]

Grade	Definition
Grade I	Any deviation from the normal postoperative course without the need for pharmacological treatment or surgical, endoscopic, and radiological interventions. Allowed therapeutic regimens are: drugs used as antiemetics , antipyretics, analgesics, diuretics, electrolytes, and physiotherapy. This grade also includes wound infections opened at the bedside
Grade II	Requiring pharmacological treatment with drugs other than such allowed for grade I complications. Blood transfusion and total parenteral nutrition are also included.
Grade III • IIIa • IIIb	Requiring surgical , endoscopic or radiological intervention Intervention not under general anaesthesia Intervention under general anaesthesia
Grade IV • IVa • IVb	Life-threatening complication (including CNS complications)* requiring IC/ICU management Single organ dysfunction (including dialysis) Multi-organ dysfunction
V	Death of patient
Suffix ‘d’	If the patient suffers complication at the time of discharge the suffix ‘d’ is added to the respective grade of complication. This label indicates the need for a follow-up to fully evaluate the complication.

- Brain haemorrhage, ischaemic stroke, subarachnoid bleeding, but excluding transient ischaemic attack. CNS: central nervous system, IC: intermediate care, ICU: intensive care unit

Appendix 7: Quality control report from Edinburgh Genomics, assessing extracted DNA prior to Infinium global screening array.

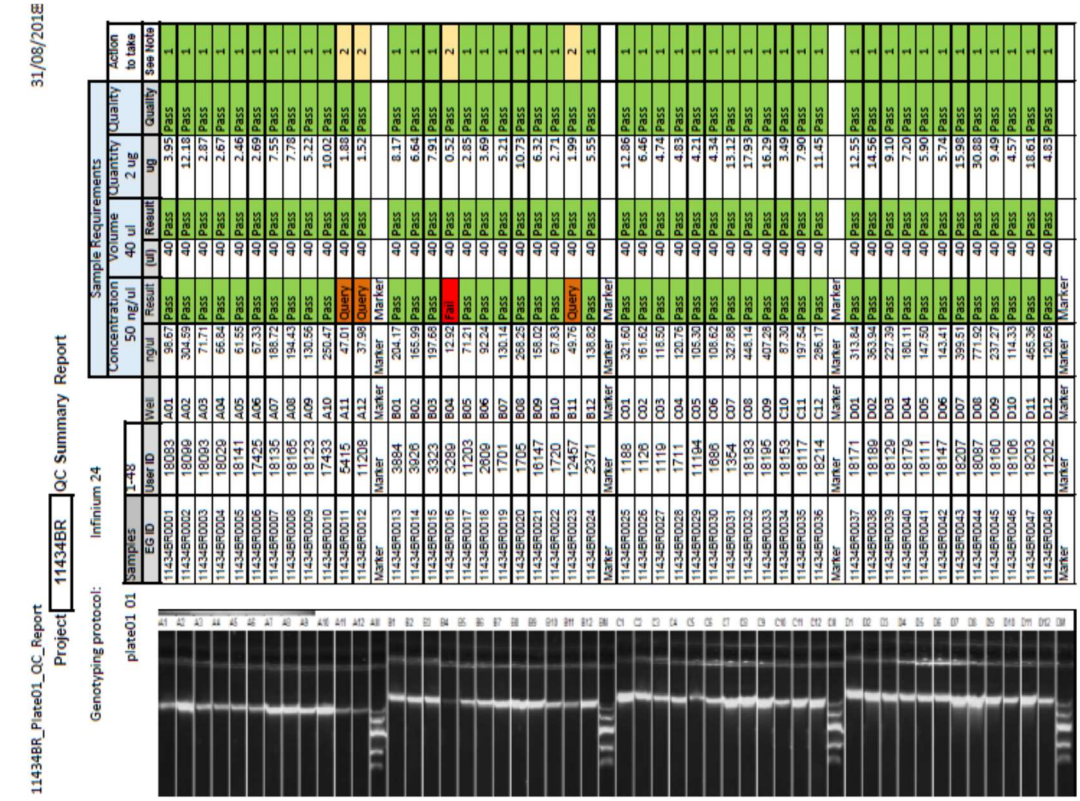

11434BR_Plate01_QC_Report — 31/08/2018

Project: 11434BR — QC Summary Report

Genotyping protocol: Infinium 24

plate01 01

Samples	1-48	Sample Requirements								Action to take
		Concentration 50 ng/ul		Volume 40 ul		Quantity 2 ug		Quality		
EG ID	User ID	Well	ng/ul	Result	(ul)	Result	ug	Result	See Note	
11434BR0001	18083	A01	98.67	Pass	40	Pass	3.95	Pass		1
11434BR0002	18090	A02	304.59	Pass	40	Pass	12.18	Pass		1
11434BR0003	18043	A03	71.71	Pass	40	Pass	2.87	Pass		1
11434BR0004	18029	A04	66.84	Pass	40	Pass	2.67	Pass		1
11434BR0005	18141	A05	61.55	Pass	40	Pass	2.46	Pass		1
11434BR0006	17425	A06	67.33	Pass	40	Pass	2.69	Pass		1
11434BR0007	18135	A07	188.72	Pass	40	Pass	7.55	Pass		1
11434BR0008	18185	A08	194.43	Pass	40	Pass	7.78	Pass		1
11434BR0009	18123	A09	130.56	Pass	40	Pass	5.22	Pass		1
11434BR0010	17433	A10	250.47	Pass	40	Pass	10.02	Pass		1
11434BR0011	5415	A11	47.01	Query	40	Pass	1.88	Pass		2
11434BR0012	11208	A12	37.98	Query	40	Pass	1.52	Pass		2
Marker		Marker		Marker						
11434BR0013	3884	B01	204.17	Pass	40	Pass	8.17	Pass		1
11434BR0014	3926	B02	165.99	Pass	40	Pass	6.64	Pass		1
11434BR0015	3323	B03	197.68	Pass	40	Pass	7.91	Pass		1
11434BR0016	3289	B04	12.92	Fail	40	Pass	0.52	Pass		2
11434BR0017	11203	B05	71.21	Pass	40	Pass	2.85	Pass		1
11434BR0018	2609	B06	92.24	Pass	40	Pass	3.69	Pass		1
11434BR0019	1701	B07	130.14	Pass	40	Pass	5.21	Pass		1
11434BR0020	1705	B08	268.25	Pass	40	Pass	10.73	Pass		1
11434BR0021	16147	B09	158.02	Pass	40	Pass	6.32	Pass		1
11434BR0022	1720	B10	67.83	Pass	40	Pass	2.71	Pass		1
11434BR0023	12457	B11	49.76	Query	40	Pass	1.99	Pass		2
11434BR0024	2371	B12	138.82	Pass	40	Pass	5.55	Pass		1
Marker		Marker		Marker						
11434BR0025	1188	C01	321.60	Pass	40	Pass	12.86	Pass		1
11434BR0026	1126	C02	161.62	Pass	40	Pass	6.46	Pass		1
11434BR0027	1119	C03	118.50	Pass	40	Pass	4.74	Pass		1
11434BR0028	1711	C04	120.76	Pass	40	Pass	4.83	Pass		1
11434BR0029	11104	C05	105.30	Pass	40	Pass	4.21	Pass		1
11434BR0030	1686	C06	108.62	Pass	40	Pass	4.34	Pass		1
11434BR0031	1354	C07	327.88	Pass	40	Pass	13.12	Pass		1
11434BR0032	18183	C08	448.14	Pass	40	Pass	17.93	Pass		1
11434BR0033	18195	C09	407.29	Pass	40	Pass	16.29	Pass		1
11434BR0034	18153	C10	87.30	Pass	40	Pass	3.49	Pass		1
11434BR0035	18117	C11	197.54	Pass	40	Pass	7.90	Pass		1
11434BR0036	18214	C12	286.17	Pass	40	Pass	11.45	Pass		1
Marker		Marker		Marker						
11434BR0037	18171	D01	313.84	Pass	40	Pass	12.55	Pass		1
11434BR0038	18189	D02	363.94	Pass	40	Pass	14.56	Pass		1
11434BR0039	18129	D03	227.39	Pass	40	Pass	9.10	Pass		1
11434BR0040	18179	D04	180.11	Pass	40	Pass	7.20	Pass		1
11434BR0041	18111	D05	147.50	Pass	40	Pass	5.90	Pass		1
11434BR0042	18147	D06	143.41	Pass	40	Pass	5.74	Pass		1
11434BR0043	18207	D07	399.51	Pass	40	Pass	15.98	Pass		1
11434BR0044	18087	D08	771.92	Pass	40	Pass	30.88	Pass		1
11434BR0045	18160	D09	237.27	Pass	40	Pass	9.49	Pass		1
11434BR0046	18106	D10	114.33	Pass	40	Pass	4.57	Pass		1
11434BR0047	18203	D11	465.36	Pass	40	Pass	18.61	Pass		1
11434BR0048	11202	D12	120.68	Pass	40	Pass	4.83	Pass		1
Marker		Marker		Marker						

11434BR_Plate01_QC_Report — 31/08/2018

Project: 11434BR — QC Summary Report

Genotyping protocol: Infinium 24

plate01

Samples	49-96	Sample Requirements								Action to take
		Concentration 50 ng/ul		Volume 40 ul		Quantity 2 ug		Quality		
EG ID	User ID	Well	ng/ul	Result	(ul)	Result	ug	Result	See Note	
11434BR0049	11204	E01	282.72	Pass	40	Pass	11.31	Pass		1
11434BR0050	11209	E02	93.37	Pass	40	Pass	3.73	Pass		1
11434BR0051	11197	E03	166.84	Pass	40	Pass	6.67	Pass		1
11434BR0052	18220	E04	246.73	Pass	40	Pass	9.87	Pass		1
11434BR0053	11187	E05	199.37	Pass	40	Pass	7.97	Pass		1
11434BR0054	12449	E06	136.49	Pass	40	Pass	5.46	Pass		1
11434BR0055	11201	E07	209.75	Pass	40	Pass	8.39	Pass		1
11434BR0056	11196	E08	126.19	Pass	40	Pass	5.05	Pass		1
11434BR0057	11210	E09	97.89	Pass	40	Pass	3.92	Pass		1
11434BR0058	11188	E10	195.84	Pass	40	Pass	7.83	Pass		1
11434BR0059	18237	E11	261.47	Pass	40	Pass	10.46	Pass		1
11434BR0060	18256	E12	33.74	Fail	40	Pass	1.35	Pass		2
Marker		Marker		Marker						
11434BR0061	18243	F01	206.50	Pass	40	Pass	8.26	Pass		1
11434BR0062	18250	F02	457.82	Pass	40	Pass	18.30	Pass		1
11434BR0063	18231	F03	230.28	Pass	40	Pass	9.21	Pass		1
11434BR0064	18225	F04	198.38	Pass	40	Pass	7.94	Pass		1
11434BR0065	30007	F05	93.02	Pass	40	Pass	3.72	Pass		1
11434BR0066	85069	F06	149.62	Pass	40	Pass	5.98	Pass		1
11434BR0067	85070	F07	154.70	Pass	40	Pass	6.19	Pass		1
11434BR0068	110003	F08	105.51	Pass	40	Pass	4.22	Pass		1
11434BR0069	30010	F09	140.59	Pass	40	Pass	5.62	Pass		1
11434BR0070	85060	F10	124.00	Pass	40	Pass	4.96	Pass		1
11434BR0071	85041	F11	135.72	Pass	40	Pass	5.43	Pass		1
11434BR0072	85036	F12	140.09	Pass	40	Pass	5.60	Pass		1
Marker		Marker		Marker						
11434BR0073	85063	G01	125.06	Pass	40	Pass	5.00	Pass		1
11434BR0074	35601	G02	111.30	Pass	40	Pass	4.45	Pass		1
11434BR0075	296008	G03	179.69	Pass	40	Pass	7.19	Pass		1
11434BR0076	85043	G04	79.68	Pass	40	Pass	3.19	Pass		1
11434BR0077	85044	G05	171.43	Pass	40	Pass	6.86	Pass		1
11434BR0078	85039	G06	172.56	Pass	40	Pass	6.90	Pass		1
11434BR0079	296004	G07	182.15	Pass	40	Pass	7.29	Pass		1
11434BR0080	3009	G08	282.22	Pass	40	Pass	11.29	Pass		1
11434BR0081	110002	G09	77.50	Pass	40	Pass	3.10	Pass		1
11434BR0082	23901	G10	104.45	Pass	40	Pass	4.18	Pass		1
11434BR0083	85047	G11	85.61	Pass	40	Pass	3.42	Pass		1
11434BR0084	241001	G12	114.33	Pass	40	Pass	4.57	Pass		1
Marker		Marker		Marker						
11434BR0085	85048	H01	110.10	Pass	40	Pass	4.40	Pass		1
11434BR0086	85054	H02	75.66	Pass	40	Pass	3.03	Pass		1
11434BR0087	85049	H03	67.33	Pass	40	Pass	2.69	Pass		1
11434BR0088	85052	H04	100.71	Pass	40	Pass	4.03	Pass		1
11434BR0089	85051	H05	145.60	Pass	40	Pass	5.82	Pass		1
11434BR0090	30008	H06	153.71	Pass	40	Pass	6.15	Pass		1
11434BR0091	85050	H07	70.30	Pass	40	Pass	2.81	Pass		1
11434BR0092	85024	H08	83.14	Pass	40	Pass	3.33	Pass		1
11434BR0093	85045	H09	168.53	Pass	40	Pass	6.74	Pass		1
11434BR0094	85025	H10	177.42	Pass	40	Pass	7.10	Query		2
11434BR0095	3001	H11	87.73	Pass	40	Pass	3.51	Pass		1
11434BR0096	3002	H12	161.69	Pass	40	Pass	6.47	Pass		1
Marker		Marker		Marker						

11434BR_Plate02_QC_Report 31/08/2018

Project 11434BR QC Summary Report

Genotyping protocol: Infinium 24

plate02

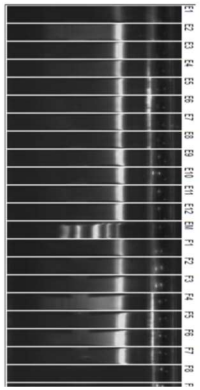

Samples	49-96		Sample Requirements						
			Concentration 50 ng/ul		Volume 40 ul		Quantity 2 ug	Quality	Action to take
EG ID	User ID	Well	ng/ul	Result	(ul)	Result	ug	Quality	See Note
11434BR0145	85011	E01	32.51	Fail	40	Pass	1.30	Pass	2
11434BR0146	306001	E02	184.55	Pass	40	Pass	7.38	Pass	1
11434BR0147	30002	E03	127.00	Pass	40	Pass	5.08	Pass	1
11434BR0148	353001	E04	83.19	Pass	40	Pass	3.33	Pass	1
11434BR0149	118001	E05	75.46	Pass	40	Pass	3.02	Pass	1
11434BR0150	30001	E06	79.18	Pass	40	Pass	3.17	Pass	1
11434BR0151	83071	E07	78.11	Pass	40	Pass	3.12	Pass	1
11434BR0152	29701	E08	59.85	Pass	40	Pass	2.39	Pass	1
11434BR0153	85058	E09	146.83	Pass	40	Pass	5.87	Pass	1
11434BR0154	350006	E10	140.60	Pass	40	Pass	5.62	Pass	1
11434BR0155	HN0186	E11	122.85	Pass	40	Pass	4.91	Pass	1
11434BR0156	789985	E12	196.58	Pass	40	Pass	7.86	Pass	1
Marker	Marker	Marker	Marker	Marker					
11434BR0157	352021	F01	89.92	Pass	40	Pass	3.60	Pass	1
11434BR0158	352023	F02	89.77	Pass	40	Pass	3.59	Pass	1
11434BR0159	850832	F03	127.57	Pass	40	Pass	5.10	Pass	1
11434BR0160	119002	F04	184.77	Pass	40	Pass	7.39	Pass	1
11434BR0161	85034	F05	194.15	Pass	40	Pass	7.77	Pass	1
11434BR0162	HN0151	F06	300.52	Pass	40	Pass	12.02	Pass	1
11434BR0163	85014	F07	150.26	Pass	40	Pass	6.01	Pass	1
Empty	Empty	F08	0.00	N/A	0	N/A	0.00	N/A	N/A

11434BR_Plate02_QC_Report 31/08/2018

Project 11434BR QC Summary Report

Genotyping protocol: Infinium 24

plate02 02

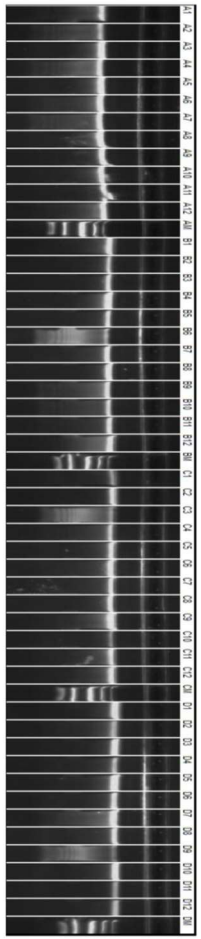

Samples	1-48		Sample Requirements						
			Concentration 50 ng/ul		Volume 40 ul		Quantity 2 ug	Quality	Action to take
EG ID	User ID	Well	ng/ul	Result	(ul)	Result	ug	Quality	See Note
11434BR0097	85027	A01	216.34	Pass	40	Pass	8.65	Pass	1
11434BR0098	85026	A02	200.66	Pass	40	Pass	8.03	Pass	1
11434BR0099	30003	A03	321.00	Pass	40	Pass	12.84	Pass	1
11434BR0100	350004	A04	251.06	Pass	40	Pass	10.04	Pass	1
11434BR0101	80002	A05	230.73	Pass	40	Pass	9.23	Pass	1
11434BR0102	30004	A06	232.30	Pass	40	Pass	9.29	Pass	1
11434BR0103	85029	A07	219.63	Pass	40	Pass	8.79	Pass	1
11434BR0104	30017	A08	262.94	Pass	40	Pass	10.52	Pass	1
11434BR0105	350002	A09	180.33	Pass	40	Pass	7.21	Pass	1
11434BR0106	30006	A10	147.76	Pass	40	Pass	5.91	Pass	1
11434BR0107	306003	A11	168.30	Pass	40	Pass	6.73	Pass	1
11434BR0108	3003	A12	228.44	Pass	40	Pass	9.14	Pass	1
Marker	Marker	Marker	Marker	Marker					
11434BR0109	85064	B01	178.97	Pass	40	Pass	7.16	Pass	1
11434BR0110	30011	B02	75.31	Pass	40	Pass	3.01	Pass	1
11434BR0111	30013	B03	103.52	Pass	40	Pass	4.14	Pass	1
11434BR0112	30012	B04	258.79	Pass	40	Pass	10.35	Pass	1
11434BR0113	85066	B05	90.49	Pass	40	Pass	3.62	Pass	1
11434BR0114	299005	B06	336.17	Pass	40	Pass	13.45	Query	2
11434BR0115	30015	B07	127.71	Pass	40	Pass	5.11	Pass	1
11434BR0116	30014	B08	193.93	Pass	40	Pass	7.76	Pass	1
11434BR0117	85015	B09	173.24	Pass	40	Pass	6.93	Pass	1
11434BR0118	3006	B10	122.56	Pass	40	Pass	4.90	Pass	1
11434BR0119	85016	B11	118.12	Pass	40	Pass	4.72	Pass	1
11434BR0120	306002	B12	268.60	Pass	40	Pass	10.74	Pass	1
Marker	Marker	Marker	Marker	Marker					
11434BR0121	85018	C01	70.66	Pass	40	Pass	2.83	Pass	1
11434BR0122	85020	C02	103.66	Pass	40	Pass	4.15	Pass	1
11434BR0123	299001	C03	346.48	Pass	40	Pass	13.86	Query	2
11434BR0124	850210	C04	97.79	Pass	40	Pass	3.91	Pass	1
11434BR0125	85019	C05	120.77	Pass	40	Pass	4.83	Pass	1
11434BR0126	85023	C06	163.15	Pass	40	Pass	6.53	Pass	1
11434BR0127	85031	C07	104.59	Pass	40	Pass	4.18	Pass	1
11434BR0128	85033	C08	115.62	Pass	40	Pass	4.62	Pass	1
11434BR0129	30005	C09	304.32	Pass	40	Pass	12.17	Pass	1
11434BR0130	299003	C10	42.60	Query	40	Pass	1.70	Pass	2
11434BR0131	85037	C11	150.34	Pass	40	Pass	6.01	Pass	1
11434BR0132	85040	C12	202.52	Pass	40	Pass	8.10	Pass	1
Marker	Marker	Marker	Marker	Marker					
11434BR0133	350005	D01	180.19	Pass	40	Pass	7.21	Pass	1
11434BR0134	85009	D02	83.62	Pass	40	Pass	3.34	Pass	1
11434BR0135	85010	D03	138.81	Pass	40	Pass	5.55	Pass	1
11434BR0136	85001	D04	57.56	Pass	40	Pass	2.30	Pass	1
11434BR0137	85002	D05	331.59	Pass	40	Pass	13.26	Pass	1
11434BR0138	85005	D06	74.45	Pass	40	Pass	2.98	Pass	1
11434BR0139	85007	D07	441.83	Pass	40	Pass	17.67	Pass	1
11434BR0140	85004	D08	91.71	Pass	40	Pass	3.67	Pass	1
11434BR0141	85013	D09	222.06	Pass	40	Pass	8.88	Query	2
11434BR0142	85006	D10	133.94	Pass	40	Pass	5.36	Pass	1
11434BR0143	85008	D11	42.03	Query	40	Pass	1.68	Pass	2
11434BR0144	85012	D12	82.90	Pass	40	Pass	3.32	Pass	1
Marker	Marker	Marker	Marker	Marker					

Appendix 8: Results from functional enrichment analysis of the (a) directly overlapping (b) near genes

Term_id	term_name	p_value	term_ size	source
CORUM:3959	SKI-SMAD3-SMAD4 complex, TGF(beta)-dependent	0.05658807	3	CORUM
CORUM:3205	SMAD3-SKI-NCOR complex	0.05658807	3	CORUM
CORUM:3206	SMAD4-SKI-NCOR complex	0.05658807	3	CORUM
CORUM:3740	SKI-SMAD3-SMAD4 complex	0.05658807	3	CORUM
GO:0007155	cell adhesion	4.4251E-16	1492	GO:BP
GO:0022610	biological adhesion	4.4251E-16	1499	GO:BP
GO:0007399	nervous system development	1.253E-15	2449	GO:BP
GO:0009653	anatomical structure morphogenesis	2.1697E-13	2797	GO:BP
GO:0048731	system development	2.5378E-13	5052	GO:BP
GO:0007275	multicellular organism development	5.5835E-13	5613	GO:BP
GO:0000902	cell morphogenesis	1.3876E-12	1037	GO:BP
GO:0048699	generation of neurons	3.2817E-12	1559	GO:BP
GO:0022008	neurogenesis	4.1726E-12	1675	GO:BP
GO:0030182	neuron differentiation	4.1726E-12	1412	GO:BP
GO:0048856	anatomical structure development	4.2728E-12	6106	GO:BP
GO:0048468	cell development	4.2728E-12	2100	GO:BP
GO:0048666	neuron development	4.2728E-12	1149	GO:BP
GO:0034330	cell junction organization	8.4887E-12	722	GO:BP
GO:0023051	regulation of signalling	2.469E-11	3578	GO:BP
GO:0010646	regulation of cell communication	2.9291E-11	3543	GO:BP
GO:0032990	cell part morphogenesis	3.6335E-11	699	GO:BP
GO:0120039	plasma membrane bounded cell projection morphogenesis	3.6335E-11	678	GO:BP
GO:0048858	cell projection morphogenesis	4.913E-11	682	GO:BP
GO:0031175	neuron projection development	1.3401E-10	1012	GO:BP
GO:0032989	cellular component morphogenesis	1.3596E-10	791	GO:BP
GO:0048812	neuron projection morphogenesis	1.4116E-10	664	GO:BP
GO:0120036	plasma membrane bounded cell projection organization	1.4116E-10	1569	GO:BP
GO:0000904	cell morphogenesis involved in differentiation	3.0523E-10	749	GO:BP
GO:0030030	cell projection organization	3.0523E-10	1609	GO:BP
GO:0007267	cell-cell signalling	3.239E-10	1722	GO:BP
GO:0050793	regulation of developmental process	4.9059E-10	2605	GO:BP
GO:0032502	developmental process	4.9059E-10	6628	GO:BP
GO:0048667	cell morphogenesis involved in neuron differentiation	1.9141E-09	602	GO:BP
GO:0050808	synapse organization	4.6344E-09	428	GO:BP
GO:0098609	cell-cell adhesion	7.0099E-09	894	GO:BP
GO:0051094	positive regulation of developmental process	7.0099E-09	1341	GO:BP

GO:0023052	signalling	8.1443E-09	6810	GO:BP
GO:0007416	synapse assembly	4.0072E-08	180	GO:BP
GO:0065008	regulation of biological quality	5.3698E-08	4131	GO:BP
GO:0048589	developmental growth	7.0706E-08	649	GO:BP
GO:0009887	animal organ morphogenesis	7.0706E-08	1073	GO:BP
GO:0120035	regulation of plasma membrane bounded cell projection organization	7.0706E-08	638	GO:BP
GO:0009966	regulation of signal transduction	7.2751E-08	3165	GO:BP
GO:0034329	cell junction assembly	7.2751E-08	438	GO:BP
GO:0034762	regulation of transmembrane transport	9.0657E-08	588	GO:BP
GO:0031344	regulation of cell projection organization	1.0815E-07	656	GO:BP
GO:0007154	cell communication	1.1152E-07	6829	GO:BP
GO:0034765	regulation of ion transmembrane transport	1.3433E-07	583	GO:BP
GO:0050804	modulation of chemical synaptic transmission	1.9822E-07	430	GO:BP
GO:0051179	localization	1.9822E-07	6901	GO:BP
GO:0032501	multicellular organismal process	1.9822E-07	7946	GO:BP
GO:0010975	regulation of neuron projection development	1.997E-07	451	GO:BP
GO:0099177	regulation of trans-synaptic signalling	2.0718E-07	431	GO:BP
GO:0050807	regulation of synapse organization	2.6804E-07	212	GO:BP
GO:0051239	regulation of multicellular organismal process	3.4118E-07	2861	GO:BP
GO:0016043	cellular component organization	3.6523E-07	6566	GO:BP
GO:0048869	cellular developmental process	5.9296E-07	4428	GO:BP
GO:0032879	regulation of localization	7.3607E-07	2872	GO:BP
GO:2000026	regulation of multicellular organismal development	8.303E-07	1447	GO:BP
GO:0099537	trans-synaptic signalling	9.3676E-07	713	GO:BP
GO:0050803	regulation of synapse structure or activity	1.0405E-06	223	GO:BP
GO:0099536	synaptic signalling	1.0414E-06	738	GO:BP
GO:0048513	animal organ development	1.2288E-06	3672	GO:BP
GO:0051963	regulation of synapse assembly	1.2414E-06	99	GO:BP
GO:0006928	movement of cell or subcellular component	1.4093E-06	2311	GO:BP
GO:0030154	cell differentiation	1.4093E-06	4350	GO:BP
GO:0007409	axon genesis	1.5567E-06	478	GO:BP
GO:0071840	cellular component organization or biogenesis	1.6891E-06	6760	GO:BP
GO:0051128	regulation of cellular component organization	1.6891E-06	2412	GO:BP
GO:0098655	cation transmembrane transport	1.9168E-06	914	GO:BP
GO:0007268	chemical synaptic transmission	2.0481E-06	705	GO:BP
GO:0098916	anterograde trans-synaptic signalling	2.0481E-06	705	GO:BP
GO:0007165	signal transduction	2.3998E-06	6309	GO:BP

GO:0022603	regulation of anatomical structure morphogenesis	2.7143E-06	1042	GO:BP
GO:0051240	positive regulation of multicellular organismal process	2.8603E-06	1455	GO:BP
GO:0048705	skeletal system morphogenesis	3.8324E-06	226	GO:BP
GO:0098742	cell-cell adhesion via plasma-membrane adhesion molecules	5.399E-06	277	GO:BP
GO:0032332	positive regulation of chondrocyte differentiation	6.1143E-06	19	GO:BP
GO:0031290	retinal ganglion cell axon guidance	6.1143E-06	19	GO:BP
GO:0006812	cation transport	6.4672E-06	1197	GO:BP
GO:0007166	cell surface receptor signalling pathway	7.8479E-06	3210	GO:BP
GO:0072001	renal system development	8.4774E-06	302	GO:BP
GO:0016358	dendrite development	8.4774E-06	243	GO:BP
GO:0001822	kidney development	9.1475E-06	293	GO:BP
GO:0043087	regulation of GTPase activity	9.1475E-06	493	GO:BP
GO:0060537	muscle tissue development	1.1616E-05	399	GO:BP
GO:0042391	regulation of membrane potential	1.1616E-05	442	GO:BP
GO:0001655	urogenital system development	1.2208E-05	337	GO:BP
GO:0014706	striated muscle tissue development	1.3493E-05	380	GO:BP
GO:0051130	positive regulation of cellular component organization	1.351E-05	1153	GO:BP
GO:0061564	axon development	1.4954E-05	523	GO:BP
GO:1901888	regulation of cell junction assembly	1.5913E-05	202	GO:BP
GO:0035295	tube development	1.6831E-05	1146	GO:BP
GO:0003007	heart morphogenesis	1.7794E-05	251	GO:BP
GO:0055085	transmembrane transport	1.7805E-05	1635	GO:BP
GO:0071805	potassium ion transmembrane transport	2.1845E-05	224	GO:BP
GO:0048729	tissue morphogenesis	2.2078E-05	667	GO:BP
GO:0040007	growth	2.2305E-05	967	GO:BP
GO:0051960	regulation of nervous system development	2.5323E-05	443	GO:BP
GO:0048593	camera-type eye morphogenesis	2.6071E-05	126	GO:BP
GO:0051962	positive regulation of nervous system development	2.8017E-05	276	GO:BP
GO:0044093	positive regulation of molecular function	3.1555E-05	1771	GO:BP
GO:0098662	inorganic cation transmembrane transport	3.4053E-05	794	GO:BP
GO:0006813	potassium ion transport	3.6467E-05	249	GO:BP
GO:0034220	ion transmembrane transport	3.7746E-05	1397	GO:BP
GO:0048592	eye morphogenesis	3.7746E-05	155	GO:BP
GO:0098660	inorganic ion transmembrane transport	4.0892E-05	883	GO:BP
GO:0007517	muscle organ development	4.3896E-05	333	GO:BP
GO:0040011	locomotion	5.1319E-05	2028	GO:BP
GO:0003013	circulatory system process	5.277E-05	637	GO:BP

GO:0031346	positive regulation of cell projection organization	6.3922E-05	359	GO:BP
GO:0072359	circulatory system development	6.5913E-05	1194	GO:BP
GO:0051056	regulation of small GTPase mediated signal transduction	6.6764E-05	328	GO:BP
GO:0051049	regulation of transport	6.6764E-05	1809	GO:BP
GO:0007417	central nervous system development	7.0606E-05	1032	GO:BP
GO:0048638	regulation of developmental growth	7.3721E-05	340	GO:BP
GO:0065009	regulation of molecular function	7.3721E-05	3221	GO:BP
GO:0007610	behaviour	7.593E-05	586	GO:BP
GO:1905114	cell surface receptor signalling pathway involved in cell-cell signalling	9.1398E-05	636	GO:BP
GO:0007507	heart development	9.301E-05	578	GO:BP
GO:0033036	macromolecule localization	9.514E-05	3218	GO:BP
GO:0009888	tissue development	0.00010089	2107	GO:BP
GO:0007411	axon guidance	0.0001157	283	GO:BP
GO:0043269	regulation of ion transport	0.00011977	1379	GO:BP
GO:0097485	neuron projection guidance	0.0001245	284	GO:BP
GO:0001501	skeletal system development	0.00013406	504	GO:BP
GO:0032330	regulation of chondrocyte differentiation	0.00015091	51	GO:BP
GO:1901890	positive regulation of cell junction assembly	0.0001612	97	GO:BP
GO:0030036	actin cytoskeleton organization	0.00017717	709	GO:BP
GO:0051965	positive regulation of synapse assembly	0.00018588	59	GO:BP
GO:0010647	positive regulation of cell communication	0.0001867	1777	GO:BP
GO:0030029	actin filament-based process	0.00018915	808	GO:BP
GO:0035556	intracellular signal transduction	0.00020912	2772	GO:BP
GO:0016477	cell migration	0.00022172	1649	GO:BP
GO:0002009	morphogenesis of an epithelium	0.00022817	560	GO:BP
GO:0035239	tube morphogenesis	0.000237	950	GO:BP
GO:0045595	regulation of cell differentiation	0.00024188	1679	GO:BP
GO:0007420	brain development	0.00025574	754	GO:BP
GO:0044087	regulation of cellular component biogenesis	0.00025574	990	GO:BP
GO:0048813	dendrite morphogenesis	0.0002736	145	GO:BP
GO:0045597	positive regulation of cell differentiation	0.0002736	879	GO:BP
GO:1904888	cranial skeletal system development	0.00029424	69	GO:BP
GO:0007010	cytoskeleton organization	0.00032232	1423	GO:BP
GO:0060562	epithelial tube morphogenesis	0.00032353	329	GO:BP
GO:0060042	retina morphogenesis in camera-type eye	0.00032353	62	GO:BP
GO:0060322	head development	0.00034406	798	GO:BP
GO:0097120	receptor localization to synapse	0.00034406	55	GO:BP

GO:0048583	regulation of response to stimulus	0.00035072	4278	GO:BP
GO:0001764	neuron migration	0.00035839	157	GO:BP
GO:0070588	calcium ion transmembrane transport	0.00035839	320	GO:BP
GO:0006811	ion transport	0.0004134	3661	GO:BP
GO:0060284	regulation of cell development	0.0004134	502	GO:BP
GO:0050770	regulation of axonogenesis	0.00043858	159	GO:BP
GO:0023056	positive regulation of signalling	0.00043858	1782	GO:BP
GO:0007264	small GTPase mediated signal transduction	0.00043858	515	GO:BP
GO:0099173	post synapse organization	0.0004554	169	GO:BP
GO:0043547	positive regulation of GTPase activity	0.00047417	413	GO:BP
GO:0048706	embryonic skeletal system development	0.00048248	123	GO:BP
GO:0022607	cellular component assembly	0.00048248	3010	GO:BP
GO:0001823	mesonephros development	0.00049919	97	GO:BP
GO:0051336	regulation of hydrolase activity	0.000513	1321	GO:BP
GO:0030155	regulation of cell adhesion	0.00054137	748	GO:BP
GO:0007423	sensory organ development	0.00055253	567	GO:BP
GO:0043085	positive regulation of catalytic activity	0.00059188	1418	GO:BP
GO:0021545	cranial nerve development	0.00064307	51	GO:BP
GO:0003008	system process	0.00066643	2293	GO:BP
GO:0061036	positive regulation of cartilage development	0.00066808	31	GO:BP
GO:0002062	chondrocyte differentiation	0.0006731	108	GO:BP
GO:0060996	dendritic spine development	0.00074573	100	GO:BP
GO:0001657	ureteric bud development	0.00081218	92	GO:BP
GO:0060560	developmental growth involved in morphogenesis	0.00081518	236	GO:BP
GO:0072073	kidney epithelium development	0.0008264	137	GO:BP
GO:0048880	sensory system development	0.00083332	389	GO:BP
GO:0031589	cell-substrate adhesion	0.00085898	367	GO:BP
GO:0010842	retina layer formation	0.00090155	26	GO:BP
GO:0099560	synaptic membrane adhesion	0.00090155	26	GO:BP
GO:0072163	mesonephric epithelium development	0.00090443	93	GO:BP
GO:0072164	mesonephric tubule development	0.00090443	93	GO:BP
GO:0010720	positive regulation of cell development	0.00092102	302	GO:BP
GO:0003206	cardiac chamber morphogenesis	0.00094944	120	GO:BP
GO:0048701	embryonic cranial skeleton morphogenesis	0.00097454	46	GO:BP
GO:0006935	chemotaxis	0.00101472	653	GO:BP
GO:0048704	embryonic skeletal system morphogenesis	0.00102362	94	GO:BP
GO:1904062	regulation of cation transmembrane transport	0.001084	360	GO:BP
GO:0051716	cellular response to stimulus	0.00108433	7781	GO:BP

GO:0007215	glutamate receptor signalling pathway	0.00110733	54	GO:BP
GO:0051234	establishment of localization	0.00112534	5372	GO:BP
GO:0042330	taxis	0.00113797	656	GO:BP
GO:0008104	protein localization	0.00116926	2770	GO:BP
GO:0051489	regulation of filopodium assembly	0.00117381	47	GO:BP
GO:0035108	limb morphogenesis	0.00118963	141	GO:BP
GO:0035107	appendage morphogenesis	0.00118963	141	GO:BP
GO:0060429	epithelium development	0.00122805	1325	GO:BP
GO:0007167	enzyme linked receptor protein signalling pathway	0.00128749	1103	GO:BP
GO:0044057	regulation of system process	0.00130778	623	GO:BP
GO:0030010	establishment of cell polarity	0.00130778	142	GO:BP
GO:0050806	positive regulation of synaptic transmission	0.00133688	152	GO:BP
GO:0048870	cell motility	0.00133688	1828	GO:BP
GO:0061035	regulation of cartilage development	0.00133688	71	GO:BP
GO:0051674	localization of cell	0.00133688	1828	GO:BP
GO:0044089	positive regulation of cellular component biogenesis	0.00137335	540	GO:BP
GO:0003015	heart process	0.00137335	298	GO:BP
GO:0008015	blood circulation	0.0014412	553	GO:BP
GO:0060047	heart contraction	0.00145855	288	GO:BP
GO:0006816	calcium ion transport	0.00154621	436	GO:BP
GO:0035637	multicellular organismal signalling	0.00157496	204	GO:BP
GO:0009581	detection of external stimulus	0.00173652	145	GO:BP
GO:0001763	morphogenesis of a branching structure	0.00175461	195	GO:BP
GO:0060349	bone morphogenesis	0.0018447	99	GO:BP
GO:1902531	regulation of intracellular signal transduction	0.00188372	1842	GO:BP
GO:0061061	muscle structure development	0.00194439	645	GO:BP
GO:0060173	limb development	0.00194439	176	GO:BP
GO:0048736	appendage development	0.00194439	176	GO:BP
GO:0150063	visual system development	0.00199324	383	GO:BP
GO:0030001	metal ion transport	0.00219216	514	GO:BP
GO:0035418	protein localization to synapse	0.00222001	83	GO:BP
GO:0097061	dendritic spine organization	0.00222001	83	GO:BP
GO:0090596	sensory organ morphogenesis	0.00226882	262	GO:BP
GO:0009582	detection of abiotic stimulus	0.00227547	148	GO:BP
GO:0048646	anatomical structure formation involved in morphogenesis	0.00231901	1202	GO:BP
GO:0003407	neural retina development	0.00236324	75	GO:BP
GO:0031032	actomyosin structure organization	0.0023688	199	GO:BP
GO:0099601	regulation of neurotransmitter receptor activity	0.0025119	84	GO:BP
GO:0051491	positive regulation of filopodium assembly	0.00256066	30	GO:BP

GO:0022604	regulation of cell morphogenesis	0.00271083	309	GO:BP
GO:0045794	negative regulation of cell volume	0.00280369	5	GO:BP
GO:0006810	transport	0.00281677	5224	GO:BP
GO:0030334	regulation of cell migration	0.00286612	999	GO:BP
GO:0035249	synaptic transmission, glutamatergic	0.00289988	94	GO:BP
GO:0001654	eye development	0.00295818	379	GO:BP
GO:0021675	nerve development	0.00310166	77	GO:BP
GO:0051345	positive regulation of hydrolase activity	0.00312513	783	GO:BP
GO:0010648	negative regulation of cell communication	0.00312685	1468	GO:BP
GO:0045494	photoreceptor cell maintenance	0.00312685	45	GO:BP
GO:0055010	ventricular cardiac muscle tissue morphogenesis	0.00312685	45	GO:BP
GO:0035265	organ growth	0.00312685	182	GO:BP
GO:0072006	nephron development	0.00315349	142	GO:BP
GO:0007611	learning or memory	0.00325485	257	GO:BP
GO:0044085	cellular component biogenesis	0.00325657	3257	GO:BP
GO:0060997	dendritic spine morphogenesis	0.00332538	61	GO:BP
GO:0007169	transmembrane receptor protein tyrosine kinase signalling pathway	0.00332538	760	GO:BP
GO:0023057	negative regulation of signalling	0.00333402	1471	GO:BP
GO:0099545	trans-synaptic signalling by trans-synaptic complex	0.00353176	9	GO:BP
GO:0048639	positive regulation of developmental growth	0.00360491	184	GO:BP
GO:0050954	sensory perception of mechanical stimulus	0.00368841	174	GO:BP
GO:0060402	calcium ion transport into cytosol	0.00411833	165	GO:BP
GO:0021554	optic nerve development	0.00417724	14	GO:BP
GO:0007613	memory	0.00419736	116	GO:BP
GO:0032880	regulation of protein localization	0.00439174	922	GO:BP
GO:0050769	positive regulation of neurogenesis	0.00441198	229	GO:BP
GO:0050790	regulation of catalytic activity	0.00479251	2545	GO:BP
GO:0007156	homophilic cell adhesion via plasma membrane adhesion molecules	0.00485725	167	GO:BP
GO:0071625	vocalization behaviour	0.00497847	20	GO:BP
GO:0070848	response to growth factor	0.00508813	759	GO:BP
GO:0099175	regulation of post synapse organization	0.00514101	90	GO:BP
GO:0048663	neuron fate commitment	0.00521753	64	GO:BP
GO:0046847	filopodium assembly	0.00521753	64	GO:BP
GO:0007528	neuromuscular junction development	0.00532459	48	GO:BP
GO:0008347	glial cell migration	0.00537818	56	GO:BP
GO:0071495	cellular response to endogenous stimulus	0.00537818	1422	GO:BP
GO:0008016	regulation of heart contraction	0.00537818	254	GO:BP

GO:0010817	regulation of hormone levels	0.00547451	536	GO:BP
GO:0010810	regulation of cell-substrate adhesion	0.00565331	222	GO:BP
GO:0048523	negative regulation of cellular process	0.00568782	5139	GO:BP
GO:0045165	cell fate commitment	0.00601813	267	GO:BP
GO:0021520	spinal cord motor neuron cell fate specification	0.00601813	10	GO:BP
GO:0071313	cellular response to caffeine	0.00601813	10	GO:BP
GO:0060538	skeletal muscle organ development	0.00601813	170	GO:BP
GO:1903522	regulation of blood circulation	0.00601813	301	GO:BP
GO:2001028	positive regulation of endothelial cell chemotaxis	0.00601813	15	GO:BP
GO:0007157	heterophilic cell-cell adhesion via plasma membrane cell adhesion molecules	0.00613729	49	GO:BP
GO:0045778	positive regulation of ossification	0.00613729	49	GO:BP
GO:0106027	neuron projection organization	0.00625071	92	GO:BP
GO:0048738	cardiac muscle tissue development	0.00633571	224	GO:BP
GO:0007160	cell-matrix adhesion	0.00635258	235	GO:BP
GO:0097475	motor neuron migration	0.00646972	6	GO:BP
GO:0051964	negative regulation of synapse assembly	0.00646972	6	GO:BP
GO:0021631	optic nerve morphogenesis	0.00646972	6	GO:BP
GO:0003205	cardiac chamber development	0.00651996	161	GO:BP
GO:0048754	branching morphogenesis of an epithelial tube	0.00663515	151	GO:BP
GO:0009968	negative regulation of signal transduction	0.00665508	1364	GO:BP
GO:0030900	forebrain development	0.00682565	385	GO:BP
GO:0022898	regulation of transmembrane transporter activity	0.00684928	281	GO:BP
GO:0009967	positive regulation of signal transduction	0.00688085	1598	GO:BP
GO:0002790	peptide secretion	0.00688085	421	GO:BP
GO:0050772	positive regulation of axonogenesis	0.00690163	84	GO:BP
GO:0021775	smoothened signalling pathway involved in ventral spinal cord interneuron specification	0.00724775	3	GO:BP
GO:0035846	oviduct epithelium development	0.00724775	3	GO:BP
GO:0021776	smoothened signalling pathway involved in spinal cord motor neuron cell fate specification	0.00724775	3	GO:BP
GO:0050905	neuromuscular process	0.00725135	103	GO:BP
GO:0045216	cell-cell junction organization	0.00743929	216	GO:BP
GO:1902414	protein localization to cell junction	0.00756281	113	GO:BP
GO:0023061	signal release	0.00756281	496	GO:BP
GO:0051270	regulation of cellular component movement	0.00758623	1141	GO:BP
GO:2000145	regulation of cell motility	0.00758623	1061	GO:BP

GO:0007605	sensory perception of sound	0.00758623	153	GO:BP
GO:0009790	embryo development	0.0076887	1035	GO:BP
GO:0055008	cardiac muscle tissue morphogenesis	0.00783978	59	GO:BP
GO:0048167	regulation of synaptic plasticity	0.00798904	185	GO:BP
GO:0003229	ventricular cardiac muscle tissue development	0.00805323	51	GO:BP
GO:0045785	positive regulation of cell adhesion	0.00805323	437	GO:BP
GO:0050767	regulation of neurogenesis	0.00826997	366	GO:BP
GO:0010811	positive regulation of cell-substrate adhesion	0.00829181	124	GO:BP
GO:0043010	camera-type eye development	0.00829181	331	GO:BP
GO:0060411	cardiac septum morphogenesis	0.00829181	68	GO:BP
GO:0051668	localization within membrane	0.00845512	77	GO:BP
GO:0060401	cytosolic calcium ion transport	0.00845512	186	GO:BP
GO:0021602	cranial nerve morphogenesis	0.00893736	29	GO:BP
GO:0001568	blood vessel development	0.00913195	792	GO:BP
GO:0002028	regulation of sodium ion transport	0.00939209	87	GO:BP
GO:0003208	cardiac ventricle morphogenesis	0.00939209	69	GO:BP
GO:0060415	muscle tissue morphogenesis	0.00939209	69	GO:BP
GO:0046578	regulation of Ras protein signal transduction	0.00995856	199	GO:BP
GO:0010769	regulation of cell morphogenesis involved in differentiation	0.0101175	97	GO:BP
GO:0016055	Wnt signalling pathway	0.01042196	529	GO:BP
GO:0050796	regulation of insulin secretion	0.01042922	189	GO:BP
GO:0010469	regulation of signalling receptor activity	0.01042922	189	GO:BP
GO:0060412	ventricular septum morphogenesis	0.01042922	37	GO:BP
GO:0040008	regulation of growth	0.01062601	681	GO:BP
GO:0048871	multicellular organismal homeostasis	0.01073542	530	GO:BP
GO:0021537	telencephalon development	0.01091814	256	GO:BP
GO:0021517	ventral spinal cord development	0.01091814	45	GO:BP
GO:0002791	regulation of peptide secretion	0.01091814	325	GO:BP
GO:0198738	cell-cell signalling by wnt	0.01105874	531	GO:BP
GO:0031000	response to caffeine	0.01105874	17	GO:BP
GO:0060998	regulation of dendritic spine development	0.01150825	62	GO:BP
GO:0040012	regulation of locomotion	0.01150825	1104	GO:BP
GO:0032835	glomerulus development	0.01150825	62	GO:BP
GO:0048588	developmental cell growth	0.01179797	235	GO:BP
GO:0010770	positive regulation of cell morphogenesis involved in differentiation	0.01179797	80	GO:BP
GO:0061138	morphogenesis of a branching epithelium	0.01249525	181	GO:BP
GO:0032412	regulation of ion transmembrane transporter activity	0.01262353	270	GO:BP

GO:0007519	skeletal muscle tissue development	0.01262881	160	GO:BP
GO:0061001	regulation of dendritic spine morphogenesis	0.01262881	46	GO:BP
GO:0009719	response to endogenous stimulus	0.01262881	1683	GO:BP
GO:0001944	vasculature development	0.0129523	830	GO:BP
GO:0061337	cardiac conduction	0.01304586	150	GO:BP
GO:0051966	regulation of synaptic transmission, glutamatergic	0.01329616	72	GO:BP
GO:0051017	actin filament bundle assembly	0.01357565	161	GO:BP
GO:0050708	regulation of protein secretion	0.01394068	295	GO:BP
GO:0014904	myotube cell development	0.01470214	39	GO:BP
GO:0030501	positive regulation of bone mineralization	0.01470214	39	GO:BP
GO:0008038	neuron recognition	0.01478215	47	GO:BP
GO:0090190	positive regulation of branching involved in ureteric bud morphogenesis	0.01480188	18	GO:BP
GO:0045580	regulation of T cell differentiation	0.01517148	152	GO:BP
GO:0071363	cellular response to growth factor stimulus	0.01517148	731	GO:BP
GO:0071692	protein localization to extracellular region	0.01532348	392	GO:BP
GO:0055065	metal ion homeostasis	0.01532348	667	GO:BP
GO:0032409	regulation of transporter activity	0.01532348	297	GO:BP
GO:0007389	pattern specification process	0.01617228	442	GO:BP
GO:0050890	cognition	0.01617228	298	GO:BP
GO:0030073	insulin secretion	0.01617228	218	GO:BP
GO:0061572	actin filament bundle organization	0.01679047	164	GO:BP
GO:0060078	regulation of postsynaptic membrane potential	0.01686232	143	GO:BP
GO:0090066	regulation of anatomical structure size	0.01723653	518	GO:BP
GO:0050773	regulation of dendrite development	0.01763581	103	GO:BP
GO:0010976	positive regulation of neuron projection development	0.01803007	165	GO:BP
GO:0007163	establishment or maintenance of cell polarity	0.01821226	220	GO:BP
GO:0009306	protein secretion	0.01834012	384	GO:BP
GO:0051058	negative regulation of small GTPase mediated signal transduction	0.01834012	57	GO:BP
GO:0003151	outflow tract morphogenesis	0.01861021	75	GO:BP
GO:0090276	regulation of peptide hormone secretion	0.01910175	221	GO:BP
GO:1905155	positive regulation of membrane invagination	0.01910175	13	GO:BP
GO:0010935	regulation of macrophage cytokine production	0.01910175	13	GO:BP
GO:0071415	cellular response to purine-containing compound	0.01910175	13	GO:BP
GO:0060100	positive regulation of phagocytosis, engulfment	0.01910175	13	GO:BP

GO:0003279	cardiac septum development	0.01910175	104	GO:BP
GO:0035592	establishment of protein localization to extracellular region	0.01910175	385	GO:BP
GO:0097553	calcium ion transmembrane import into cytosol	0.01929011	145	GO:BP
GO:0048585	negative regulation of response to stimulus	0.01929011	1733	GO:BP
GO:0060541	respiratory system development	0.01929011	199	GO:BP
GO:0048522	positive regulation of cellular process	0.0199599	5757	GO:BP
GO:0060485	mesenchyme development	0.02008147	291	GO:BP
GO:1905278	positive regulation of epithelial tube formation	0.02010425	8	GO:BP
GO:1905276	regulation of epithelial tube formation	0.02010425	8	GO:BP
GO:0022030	telencephalon glial cell migration	0.02014174	26	GO:BP
GO:0021801	cerebral cortex radial glia guided migration	0.02014174	26	GO:BP
GO:2001259	positive regulation of cation channel activity	0.02015056	76	GO:BP
GO:0048644	muscle organ morphogenesis	0.02015056	76	GO:BP
GO:0031345	negative regulation of cell projection organization	0.02021031	189	GO:BP
GO:0048747	muscle fiber development	0.02021031	58	GO:BP
GO:0030278	regulation of ossification	0.02027153	115	GO:BP
GO:0060079	excitatory postsynaptic potential	0.02027153	105	GO:BP
GO:0048762	mesenchymal cell differentiation	0.02039899	234	GO:BP
GO:0007296	vitellogenesis	0.02065359	4	GO:BP
GO:0046580	negative regulation of Ras protein signal transduction	0.02182191	50	GO:BP
GO:0060688	regulation of morphogenesis of a branching structure	0.02182191	50	GO:BP
GO:0031644	regulation of nervous system process	0.02182428	147	GO:BP
GO:0099174	regulation of presynapse organization	0.02235816	34	GO:BP
GO:1905606	regulation of presynapse assembly	0.02235816	34	GO:BP
GO:0097106	postsynaptic density organization	0.02235816	34	GO:BP
GO:0060341	regulation of cellular localization	0.02262398	851	GO:BP
GO:0070534	protein K63-linked ubiquitination	0.02262833	59	GO:BP
GO:0043009	chordate embryonic development	0.02262833	616	GO:BP
GO:0030072	peptide hormone secretion	0.02399951	260	GO:BP
GO:0060348	bone development	0.02399951	203	GO:BP
GO:1902914	regulation of protein polyubiquitination	0.024405	27	GO:BP
GO:1900044	regulation of protein K63-linked ubiquitination	0.02588012	14	GO:BP
GO:0010934	macrophage cytokine production	0.02588012	14	GO:BP
GO:0008361	regulation of cell size	0.02588012	182	GO:BP
GO:0051481	negative regulation of cytosolic calcium ion concentration	0.02588012	14	GO:BP

GO:0048741	skeletal muscle fiber development	0.02663052	35	GO:BP
GO:0007422	peripheral nervous system development	0.027433	79	GO:BP
GO:0035113	embryonic appendage morphogenesis	0.02816466	119	GO:BP
GO:0030326	embryonic limb morphogenesis	0.02816466	119	GO:BP
GO:0010977	negative regulation of neuron projection development	0.02832953	140	GO:BP
GO:0046883	regulation of hormone secretion	0.02841679	275	GO:BP
GO:0030038	contractile actin filament bundle assembly	0.02841679	109	GO:BP
GO:0043149	stress finer assembly	0.02841679	109	GO:BP
GO:0042592	homeostatic process	0.02841679	1981	GO:BP
GO:0022029	telencephalon cell migration	0.02880401	61	GO:BP
GO:2000463	positive regulation of excitatory postsynaptic potential	0.02961841	28	GO:BP
GO:0050953	sensory perception of light stimulus	0.02961841	218	GO:BP
GO:0090189	regulation of branching involved in ureteric bud morphogenesis	0.03008272	21	GO:BP
GO:0050962	detection of light stimulus involved in sensory perception	0.03008272	21	GO:BP
GO:0060999	positive regulation of dendritic spine development	0.03008272	44	GO:BP
GO:0003231	cardiac ventricle development	0.03008272	120	GO:BP
GO:0050908	detection of light stimulus involved in visual perception	0.03008272	21	GO:BP
GO:2001014	regulation of skeletal muscle cell differentiation	0.03008272	21	GO:BP
GO:0021940	positive regulation of cerebellar granule cell precursor proliferation	0.03029383	9	GO:BP
GO:0060907	positive regulation of macrophage cytokine production	0.03029383	9	GO:BP
GO:0014033	neural crest cell differentiation	0.03029383	90	GO:BP
GO:0072009	nephron epithelium development	0.03029383	110	GO:BP
GO:0061387	regulation of extent of cell growth	0.03029383	110	GO:BP
GO:0038026	reelin-mediated signalling pathway	0.03029383	9	GO:BP
GO:0099084	postsynaptic specialization organization	0.0303722	36	GO:BP
GO:1905332	positive regulation of morphogenesis of an epithelium	0.0303722	36	GO:BP
GO:0001659	temperature homeostasis	0.0303722	174	GO:BP
GO:0051235	maintenance of location	0.03069636	337	GO:BP
GO:0060675	ureteric bud morphogenesis	0.03156701	62	GO:BP
GO:0003002	regionalization	0.0321618	338	GO:BP
GO:0060419	heart growth	0.0326484	111	GO:BP
GO:0099565	chemical synaptic transmission, postsynaptic	0.0326484	111	GO:BP
GO:0060099	regulation of phagocytosis, engulfment	0.03390105	15	GO:BP
GO:0030111	regulation of Wnt signalling pathway	0.03410752	376	GO:BP

GO:0055082	cellular chemical homeostasis	0.03459548	841	GO:BP
GO:0072171	mesonephric tubule morphogenesis	0.03542264	63	GO:BP
GO:0030888	regulation of B cell proliferation	0.03542264	63	GO:BP
GO:2000310	regulation of NMDA receptor activity	0.03561377	37	GO:BP
GO:0010092	specification of animal organ identity	0.03561377	37	GO:BP
GO:0060840	artery development	0.03599846	102	GO:BP
GO:0055080	cation homeostasis	0.03644335	750	GO:BP
GO:0072507	divalent inorganic cation homeostasis	0.03647409	516	GO:BP
GO:0060041	retina development in camera-type eye	0.03647409	155	GO:BP
GO:0006875	cellular metal ion homeostasis	0.03647409	593	GO:BP
GO:0048514	blood vessel morphogenesis	0.03651658	711	GO:BP
GO:0040019	positive regulation of embryonic development	0.03651658	22	GO:BP
GO:1901699	cellular response to nitrogen compound	0.03651658	724	GO:BP
GO:0098698	postsynaptic specialization assembly	0.03651658	22	GO:BP
GO:0051209	release of sequestered calcium ion into cytosol	0.03651658	123	GO:BP
GO:0098815	modulation of excitatory postsynaptic potential	0.0387183	46	GO:BP
GO:1905330	regulation of morphogenesis of an epithelium	0.0390153	64	GO:BP
GO:0021885	forebrain cell migration	0.0390153	64	GO:BP
GO:0019725	cellular homeostasis	0.03902239	981	GO:BP
GO:1905475	regulation of protein localization to membrane	0.03927814	201	GO:BP
GO:0051283	negative regulation of sequestering of calcium ion	0.03927814	124	GO:BP
GO:0001954	positive regulation of cell-matrix adhesion	0.03936508	55	GO:BP
GO:0009792	embryo development ending in birth or egg hatching	0.03936508	635	GO:BP
GO:2001257	regulation of cation channel activity	0.0399169	190	GO:BP
GO:0097114	NMDA glutamate receptor clustering	0.04012615	5	GO:BP
GO:0035136	forelimb morphogenesis	0.04012615	38	GO:BP
GO:0071242	cellular response to ammonium ion	0.04012615	5	GO:BP
GO:0048665	neuron fate specification	0.04012615	30	GO:BP
GO:0007612	learning	0.04012615	146	GO:BP
GO:0098735	positive regulation of the force of heart contraction	0.04012615	5	GO:BP
GO:0048496	maintenance of animal organ identity	0.04012615	5	GO:BP
GO:0099505	regulation of presynaptic membrane potential	0.04012615	5	GO:BP
GO:0021563	glossopharyngeal nerve development	0.04012615	5	GO:BP
GO:0008582	regulation of synaptic growth at neuromuscular junction	0.04012615	5	GO:BP

GO:0002063	chondrocyte development	0.04012615	30	GO:BP
GO:0060066	oviduct development	0.04012615	5	GO:BP
GO:0030217	T cell differentiation	0.04019019	260	GO:BP
GO:0021510	spinal cord development	0.04075619	104	GO:BP
GO:0048864	stem cell development	0.04099907	84	GO:BP
GO:0009791	post-embryonic development	0.04099907	84	GO:BP
GO:0014031	mesenchymal cell development	0.04099907	84	GO:BP
GO:0050877	nervous system process	0.04100806	1426	GO:BP
GO:0045619	regulation of lymphocyte differentiation	0.04173918	180	GO:BP
GO:0010921	regulation of phosphatase activity	0.04173918	180	GO:BP
GO:1905153	regulation of membrane invagination	0.04203591	16	GO:BP
GO:0070169	positive regulation of biomineral tissue development	0.04203591	47	GO:BP
GO:0031279	regulation of cyclase activity	0.04203591	47	GO:BP
GO:0051660	establishment of centrosome localization	0.04203591	10	GO:BP
GO:1905809	negative regulation of synapse organization	0.04203591	10	GO:BP
GO:0051967	negative regulation of synaptic transmission, glutamatergic	0.04203591	10	GO:BP
GO:0001658	branching involved in ureteric bud morphogenesis	0.04253073	56	GO:BP
GO:1900273	positive regulation of long-term synaptic potentiation	0.04298639	23	GO:BP
GO:1903861	positive regulation of dendrite extension	0.04298639	23	GO:BP
GO:0050896	response to stimulus	0.04302641	9407	GO:BP
GO:0061333	renal tubule morphogenesis	0.04320959	75	GO:BP
GO:0051282	regulation of sequestering of calcium ion	0.04320959	126	GO:BP
GO:0071559	response to transforming growth factor beta	0.04320959	262	GO:BP
GO:1990138	neuron projection extension	0.04406172	170	GO:BP
GO:0001508	action potential	0.04406172	137	GO:BP
GO:0001941	postsynaptic membrane organization	0.0450171	39	GO:BP
GO:0090183	regulation of kidney development	0.04609855	31	GO:BP
GO:0099068	postsynapse assembly	0.04609855	31	GO:BP
GO:0098771	inorganic ion homeostasis	0.04610509	761	GO:BP
GO:0001952	regulation of cell-matrix adhesion	0.04634047	127	GO:BP
GO:0120034	positive regulation of plasma membrane bounded cell projection assembly	0.0463443	106	GO:BP
GO:0051093	negative regulation of developmental process	0.0463443	977	GO:BP
GO:0032231	regulation of actin filament bundle assembly	0.0463443	106	GO:BP
GO:0051050	positive regulation of transport	0.04654066	923	GO:BP
GO:0048538	thymus development	0.04673291	48	GO:BP

GO:0001754	eye photoreceptor cell differentiation	0.04673291	48	GO:BP
GO:0050919	negative chemotaxis	0.04673291	48	GO:BP
GO:0110151	positive regulation of biomineralization	0.04673291	48	GO:BP
GO:0009583	detection of light stimulus	0.04684353	76	GO:BP
GO:0006814	sodium ion transport	0.04855031	241	GO:BP
GO:0045596	negative regulation of cell differentiation	0.04869218	697	GO:BP
GO:0051641	cellular localization	0.0498867	3541	GO:BP
GO:0006801	superoxide metabolic process	0.05008684	67	GO:BP
GO:0001558	regulation of cell growth	0.05090486	426	GO:BP
GO:0055001	muscle cell development	0.05107686	184	GO:BP
GO:0060291	long-term synaptic potentiation	0.05194123	87	GO:BP
GO:0006936	muscle contraction	0.05209872	364	GO:BP
GO:0009914	hormone transport	0.05209872	327	GO:BP
GO:0060350	endochondral bone morphogenesis	0.05209872	58	GO:BP
GO:0010224	response to UV-B	0.05212462	17	GO:BP
GO:0070593	dendrite self-avoidance	0.05212462	17	GO:BP
GO:0007158	neuron cell-cell adhesion	0.05212462	17	GO:BP
GO:0007216	G protein-coupled glutamate receptor signalling pathway	0.05212462	17	GO:BP
GO:0099637	neurotransmitter receptor transport	0.05241185	49	GO:BP
GO:0045761	regulation of adenylate cyclase activity	0.05291915	32	GO:BP
GO:0048598	embryonic morphogenesis	0.05295901	595	GO:BP
GO:0048518	positive regulation of biological process	0.05381094	6363	GO:BP
GO:0050801	ion homeostasis	0.05381094	808	GO:BP
GO:0003281	ventricular septum development	0.05467176	68	GO:BP
GO:0014902	myotube differentiation	0.05473838	119	GO:BP
GO:0048562	embryonic organ morphogenesis	0.05520802	292	GO:BP
GO:0051208	sequestering of calcium ion	0.0554314	130	GO:BP
GO:0003018	vascular process in circulatory system	0.0554314	256	GO:BP
GO:0010959	regulation of metal ion transport	0.0554314	268	GO:BP
GO:0050921	positive regulation of chemotaxis	0.05571994	141	GO:BP
GO:0007028	cytoplasm organization	0.05589996	11	GO:BP
GO:0032836	glomerular basement membrane development	0.05589996	11	GO:BP
GO:0003157	endocardium development	0.05589996	11	GO:BP
GO:1902946	protein localization to early endosome	0.05589996	11	GO:BP
GO:0031223	auditory behaviour	0.05589996	11	GO:BP
GO:0060579	ventral spinal cord interneuron fate commitment	0.05589996	11	GO:BP
GO:0060379	cardiac muscle cell myoblast differentiation	0.05589996	11	GO:BP
GO:0060581	cell fate commitment involved in pattern specification	0.05589996	11	GO:BP

GO:0046879	hormone secretion	0.05589996	317	GO:BP
GO:0032414	positive regulation of ion transmembrane transporter activity	0.05606926	109	GO:BP
GO:0035773	insulin secretion involved in cellular response to glucose stimulus	0.05782355	69	GO:BP
GO:0033037	polysaccharide localization	0.05782355	2	GO:BP
GO:0034230	enkephalin processing	0.05782355	2	GO:BP
GO:0043648	dicarboxylic acid metabolic process	0.05782355	99	GO:BP
GO:0051129	negative regulation of cellular component organization	0.05782355	759	GO:BP
GO:1902336	positive regulation of retinal ganglion cell axon guidance	0.05782355	2	GO:BP
GO:2000742	regulation of anterior head development	0.05782355	2	GO:BP
GO:1905223	epicardium morphogenesis	0.05782355	2	GO:BP
GO:0010650	positive regulation of cell communication by electrical coupling	0.05782355	2	GO:BP
GO:2001026	regulation of endothelial cell chemotaxis	0.05782355	25	GO:BP
GO:1905518	regulation of presynaptic active zone assembly	0.05782355	2	GO:BP
GO:1905520	positive regulation of presynaptic active zone assembly	0.05782355	2	GO:BP
GO:0016048	detection of temperature stimulus	0.05782355	25	GO:BP
GO:0016049	cell growth	0.05782355	495	GO:BP
GO:2000744	positive regulation of anterior head development	0.05782355	2	GO:BP
GO:0045944	positive regulation of transcription by RNA polymerase II	0.05782355	1197	GO:BP
GO:0038190	VEGF-activated neuropilin signalling pathway	0.05782355	2	GO:BP
GO:0070887	cellular response to chemical stimulus	0.05782355	3393	GO:BP
GO:0060060	post-embryonic retina morphogenesis in camera-type eye	0.05782355	2	GO:BP
GO:0060083	smooth muscle contraction involved in micturition	0.05782355	2	GO:BP
GO:0097117	guanylate kinase-associated protein clustering	0.05782355	2	GO:BP
GO:0001895	retina homeostasis	0.05782355	79	GO:BP
GO:0003220	left ventricular cardiac muscle tissue morphogenesis	0.05782355	2	GO:BP
GO:0003017	lymph circulation	0.05782355	2	GO:BP
GO:0051899	membrane depolarization	0.05782355	89	GO:BP
GO:0086064	cell communication by electrical coupling involved in cardiac conduction	0.05782355	25	GO:BP
GO:0010644	cell communication by electrical coupling	0.05817139	33	GO:BP
GO:0035767	endothelial cell chemotaxis	0.05817139	33	GO:BP

GO:0021953	central nervous system neuron differentiation	0.05946358	188	GO:BP
GO:1901701	cellular response to oxygen-containing compound	0.06039652	1227	GO:BP
GO:0090303	positive regulation of wound healing	0.06041485	60	GO:BP
GO:0030323	respiratory tube development	0.06100566	177	GO:BP
GO:0002520	immune system development	0.06112563	1020	GO:BP
GO:0051725	protein de-ADP-ribosylation	0.06166687	6	GO:BP
GO:0035729	cellular response to hepatocyte growth factor stimulus	0.06166687	18	GO:BP
GO:0061196	fungiform papilla development	0.06166687	6	GO:BP
GO:0060359	response to ammonium ion	0.06166687	6	GO:BP
GO:0021910	smoothened signalling pathway involved in ventral spinal cord patterning	0.06166687	6	GO:BP
GO:0061419	positive regulation of transcription from RNA polymerase II promoter in response to hypoxia	0.06166687	6	GO:BP
GO:0050885	neuromuscular process controlling balance	0.06198413	51	GO:BP
GO:0055002	striated muscle cell development	0.06200498	111	GO:BP
GO:0014032	neural crest cell development	0.06242046	80	GO:BP
GO:1990845	adaptive thermogenesis	0.06264503	155	GO:BP
GO:0120032	regulation of plasma membrane bounded cell projection assembly	0.06575633	190	GO:BP
GO:0061178	regulation of insulin secretion involved in cellular response to glucose stimulus	0.06660222	61	GO:BP
GO:0051480	regulation of cytosolic calcium ion concentration	0.06669964	360	GO:BP
GO:0021799	cerebral cortex radially oriented cell migration	0.06694619	34	GO:BP
GO:1901889	negative regulation of cell junction assembly	0.06694619	34	GO:BP
GO:0021952	central nervous system projection neuron axonogenesis	0.06737911	26	GO:BP
GO:0045927	positive regulation of growth	0.06737911	274	GO:BP
GO:0072078	nephron tubule morphogenesis	0.06737911	71	GO:BP
GO:0035235	ionotropic glutamate receptor signalling pathway	0.06737911	26	GO:BP
GO:1903859	regulation of dendrite extension	0.06737911	26	GO:BP
GO:0003148	outflow tract septum morphogenesis	0.06737911	26	GO:BP
GO:0050920	regulation of chemotaxis	0.06737911	226	GO:BP
GO:0007601	visual perception	0.06737911	214	GO:BP
GO:0050951	sensory perception of temperature stimulus	0.06737911	26	GO:BP
GO:0050805	negative regulation of synaptic transmission	0.06737911	71	GO:BP
GO:0120031	plasma membrane bounded cell projection assembly	0.06760022	593	GO:BP
GO:0030335	positive regulation of cell migration	0.06822889	567	GO:BP
GO:0030003	cellular cation homeostasis	0.06831177	673	GO:BP

GO:0014047	glutamate secretion	0.06898682	43	GO:BP
GO:0030031	cell projection assembly	0.06898682	607	GO:BP
GO:0009642	response to light intensity	0.07062144	12	GO:BP
GO:0021936	regulation of cerebellar granule cell precursor proliferation	0.07062144	12	GO:BP
GO:0001768	establishment of T cell polarity	0.07062144	12	GO:BP
GO:0038063	collagen-activated tyrosine kinase receptor signalling pathway	0.07062144	12	GO:BP
GO:1902915	negative regulation of protein polyubiquitination	0.07062144	12	GO:BP
GO:0060993	kidney morphogenesis	0.07099527	92	GO:BP
GO:0060491	regulation of cell projection assembly	0.07126009	192	GO:BP
GO:0010562	positive regulation of phosphorus metabolic process	0.07131676	1001	GO:BP
GO:0045937	positive regulation of phosphate metabolic process	0.07131676	1001	GO:BP
GO:0032535	regulation of cellular component size	0.07184097	388	GO:BP
GO:0010876	lipid localization	0.07229713	530	GO:BP
GO:0010634	positive regulation of epithelial cell migration	0.07343328	181	GO:BP
GO:0030098	lymphocyte differentiation	0.07351136	376	GO:BP
GO:0097107	postsynaptic density assembly	0.07370592	19	GO:BP
GO:0003128	heart field specification	0.07370592	19	GO:BP
GO:0008340	determination of adult lifespan	0.07370592	19	GO:BP
GO:0051146	striated muscle cell differentiation	0.07417206	289	GO:BP
GO:0001569	branching involved in blood vessel morphogenesis	0.07437014	35	GO:BP
GO:0035137	hindlimb morphogenesis	0.07437014	35	GO:BP
GO:0042554	superoxide anion generation	0.07437014	35	GO:BP
GO:0061041	regulation of wound healing	0.07437014	136	GO:BP
GO:0042462	eye photoreceptor cell development	0.07437014	35	GO:BP
GO:0097484	dendrite extension	0.07437014	35	GO:BP
GO:0035303	regulation of dephosphorylation	0.07557151	217	GO:BP
GO:0061383	trabecula morphogenesis	0.07617906	44	GO:BP
GO:0032924	activin receptor signalling pathway	0.07617906	44	GO:BP
GO:0006869	lipid transport	0.07617906	480	GO:BP
GO:2000273	positive regulation of signalling receptor activity	0.07617906	44	GO:BP
GO:1904861	excitatory synapse assembly	0.07751118	27	GO:BP
GO:0014829	vascular associated smooth muscle contraction	0.07751118	27	GO:BP
GO:0110020	regulation of actomyosin structure organization	0.07755331	104	GO:BP
GO:0002027	regulation of heart rate	0.07755331	104	GO:BP
GO:1903829	positive regulation of cellular protein localization	0.07810636	303	GO:BP
GO:0048878	chemical homeostasis	0.07810636	1229	GO:BP

GO:0072088	nephron epithelium morphogenesis	0.07810636	73	GO:BP
GO:0030307	positive regulation of cell growth	0.07810636	171	GO:BP
GO:0071417	cellular response to organonitrogen compound	0.07824752	666	GO:BP
GO:0090630	activation of GTPase activity	0.07828539	115	GO:BP
GO:0001503	ossification	0.0790644	417	GO:BP
GO:0051492	regulation of stress fiber assembly	0.0807224	94	GO:BP
GO:0043113	receptor clustering	0.08217889	54	GO:BP
GO:0051496	positive regulation of stress fiber assembly	0.08217889	54	GO:BP
GO:0048519	negative regulation of biological process	0.08296014	5757	GO:BP
GO:0021954	central nervous system neuron development	0.08348764	84	GO:BP
GO:2000027	regulation of animal organ morphogenesis	0.08381223	184	GO:BP
GO:0031623	receptor internalization	0.08381223	116	GO:BP
GO:0062237	protein localization to postsynapse	0.08462969	45	GO:BP
GO:0071560	cellular response to transforming growth factor beta stimulus	0.08462969	256	GO:BP
GO:0051216	cartilage development	0.08462969	196	GO:BP
GO:0021795	cerebral cortex cell migration	0.08462969	45	GO:BP
GO:0072503	cellular divalent inorganic cation homeostasis	0.08462969	497	GO:BP
GO:0003012	muscle system process	0.08471711	471	GO:BP
GO:0033002	muscle cell proliferation	0.08499025	244	GO:BP
GO:0015871	choline transport	0.08603825	7	GO:BP
GO:0032292	peripheral nervous system axon ensheathment	0.08603825	28	GO:BP
GO:0030324	lung development	0.08603825	173	GO:BP
GO:0001767	establishment of lymphocyte polarity	0.08603825	13	GO:BP
GO:0003222	ventricular trabecula myocardium morphogenesis	0.08603825	13	GO:BP
GO:0022011	myelination in peripheral nervous system	0.08603825	28	GO:BP
GO:0007194	negative regulation of adenylate cyclase activity	0.08603825	20	GO:BP
GO:0007196	adenylate cyclase-inhibiting G protein-coupled glutamate receptor signalling pathway	0.08603825	7	GO:BP
GO:0007638	mechanosensory behaviour	0.08603825	13	GO:BP
GO:0021937	cerebellar Purkinje cell-granule cell precursor cell signalling involved in regulation of granule cell precursor cell proliferation	0.08603825	7	GO:BP
GO:0010522	regulation of calcium ion transport into cytosol	0.08603825	106	GO:BP
GO:0021521	ventral spinal cord interneuron specification	0.08603825	7	GO:BP
GO:0021514	ventral spinal cord interneuron differentiation	0.08603825	13	GO:BP

GO:0019065	receptor-mediated endocytosis of virus by host cell	0.08603825	7	GO:BP
GO:0014832	urinary bladder smooth muscle contraction	0.08603825	7	GO:BP
GO:0014812	muscle cell migration	0.08603825	106	GO:BP
GO:0032489	regulation of Cdc42 protein signal transduction	0.08603825	7	GO:BP
GO:0061003	positive regulation of dendritic spine morphogenesis	0.08603825	20	GO:BP
GO:0060573	cell fate specification involved in pattern specification	0.08603825	7	GO:BP
GO:0033564	anterior/posterior axon guidance	0.08603825	7	GO:BP
GO:0050961	detection of temperature stimulus involved in sensory perception	0.08603825	20	GO:BP
GO:0071286	cellular response to magnesium ion	0.08603825	7	GO:BP
GO:0048842	positive regulation of axon extension involved in axon guidance	0.08603825	7	GO:BP
GO:0048041	focal adhesion assembly	0.08603825	85	GO:BP
GO:0055074	calcium ion homeostasis	0.08603825	472	GO:BP
GO:0045598	regulation of fat cell differentiation	0.08603825	139	GO:BP
GO:0045588	positive regulation of gamma-delta T cell differentiation	0.08603825	7	GO:BP
GO:0048015	phosphatidylinositol-mediated signalling	0.08603825	197	GO:BP
GO:0060219	camera-type eye photoreceptor cell differentiation	0.08603825	28	GO:BP
GO:0075509	endocytosis involved in viral entry into host cell	0.08603825	7	GO:BP
GO:0038007	netrin-activated signalling pathway	0.08603825	13	GO:BP
GO:2000147	positive regulation of cell motility	0.08603825	591	GO:BP
GO:0035728	response to hepatocyte growth factor	0.08603825	20	GO:BP
GO:0035507	regulation of myosin-light-chain-phosphatase activity	0.08603825	7	GO:BP
GO:0042118	endothelial cell activation	0.08603825	13	GO:BP
GO:1904396	regulation of neuromuscular junction development	0.08603825	7	GO:BP
GO:0006874	cellular calcium ion homeostasis	0.08616466	460	GO:BP
GO:0001894	tissue homeostasis	0.08698336	270	GO:BP
GO:0072028	nephron morphogenesis	0.0879398	75	GO:BP
GO:0046530	photoreceptor cell differentiation	0.08827124	65	GO:BP
GO:0009584	detection of visible light	0.08827124	65	GO:BP
GO:0035264	multicellular organism growth	0.08864298	140	GO:BP
GO:0040017	positive regulation of locomotion	0.08864298	606	GO:BP
GO:0051259	protein complex oligomerization	0.08894195	234	GO:BP
GO:0061462	protein localization to lysosome	0.08974309	46	GO:BP
GO:1900544	positive regulation of purine nucleotide metabolic process	0.08974309	46	GO:BP
GO:1900271	regulation of long-term synaptic potentiation	0.08974309	46	GO:BP

GO:0006873	cellular ion homeostasis	0.08974309	687	GO:BP
GO:0045981	positive regulation of nucleotide metabolic process	0.08974309	46	GO:BP
GO:0032411	positive regulation of transporter activity	0.08992538	118	GO:BP
GO:1902284	neuron projection extension involved in neuron projection guidance	0.09001629	37	GO:BP
GO:0050775	positive regulation of dendrite morphogenesis	0.09001629	37	GO:BP
GO:0048846	axon extension involved in axon guidance	0.09001629	37	GO:BP
GO:0051924	regulation of calcium ion transport	0.09054125	259	GO:BP
GO:0051651	maintenance of location in cell	0.09272518	223	GO:BP
GO:0048645	animal organ formation	0.09619057	66	GO:BP
GO:0098868	bone growth	0.09894112	29	GO:BP
GO:1903579	negative regulation of ATP metabolic process	0.09894112	29	GO:BP
GO:0071702	organic substance transport	0.09972702	2766	GO:BP
GO:0030054	cell junction	6.9699E-18	2105	GO:CC
GO:0071944	cell periphery	2.3594E-17	6169	GO:CC
GO:0043005	neuron projection	9.8896E-17	1380	GO:CC
GO:0005886	plasma membrane	2.9663E-16	5681	GO:CC
GO:0042995	cell projection	1.7602E-15	2330	GO:CC
GO:0120025	plasma membrane bounded cell projection	1.7602E-15	2229	GO:CC
GO:0045202	synapse	1.9391E-13	1349	GO:CC
GO:0098590	plasma membrane region	1.3707E-11	1240	GO:CC
GO:0016020	membrane	1.6323E-11	9838	GO:CC
GO:0036477	somatodendritic compartment	2.0544E-11	871	GO:CC
GO:0098794	postsynapse	1.9988E-10	639	GO:CC
GO:0045211	postsynaptic membrane	3.851E-10	280	GO:CC
GO:0030424	axon	4.0784E-10	660	GO:CC
GO:0097060	synaptic membrane	3.5296E-09	384	GO:CC
GO:0043025	neuronal cell body	1.02E-08	518	GO:CC
GO:0044297	cell body	2.1614E-08	592	GO:CC
GO:0098984	neuron to neuron synapse	8.0576E-08	366	GO:CC
GO:0032279	asymmetric synapse	1.1466E-07	340	GO:CC
GO:0097447	dendritic tree	2.9098E-07	640	GO:CC
GO:0014069	postsynaptic density	4.3361E-07	334	GO:CC
GO:0030425	dendrite	5.0423E-07	638	GO:CC
GO:0031226	intrinsic component of plasma membrane	8.476E-07	1726	GO:CC
GO:0034703	cation channel complex	1.1398E-06	227	GO:CC
GO:0005887	integral component of plasma membrane	1.1928E-06	1645	GO:CC
GO:0099572	postsynaptic specialization	1.3083E-06	358	GO:CC
GO:0005911	cell-cell junction	2.3018E-06	494	GO:CC
GO:0005856	cytoskeleton	4.9839E-06	2332	GO:CC

GO:0070161	anchoring junction	5.9737E-06	836	GO:CC
GO:0098839	postsynaptic density membrane	8.9744E-06	94	GO:CC
GO:0005912	adherens junction	1.13E-05	173	GO:CC
GO:0034702	ion channel complex	1.2524E-05	302	GO:CC
GO:0099055	integral component of postsynaptic membrane	2.1735E-05	116	GO:CC
GO:0032420	stereocilium	2.6539E-05	55	GO:CC
GO:1902495	transmembrane transporter complex	3.4271E-05	325	GO:CC
GO:0099634	postsynaptic specialization membrane	3.6995E-05	120	GO:CC
GO:0099699	integral component of synaptic membrane	4.3145E-05	148	GO:CC
GO:0150034	distal axon	4.5214E-05	308	GO:CC
GO:0098936	intrinsic component of postsynaptic membrane	4.5943E-05	122	GO:CC
GO:0099061	integral component of postsynaptic density membrane	4.7362E-05	51	GO:CC
GO:0099240	intrinsic component of synaptic membrane	7.0463E-05	162	GO:CC
GO:0034705	potassium channel complex	7.6504E-05	100	GO:CC
GO:1990351	transporter complex	9.2886E-05	340	GO:CC
GO:0032421	stereocilium bundle	0.00010509	62	GO:CC
GO:0015629	actin cytoskeleton	0.00010717	513	GO:CC
GO:0099146	intrinsic component of postsynaptic density membrane	0.00010911	55	GO:CC
GO:0031224	intrinsic component of membrane	0.00015896	5868	GO:CC
GO:0098793	presynapse	0.00016003	521	GO:CC
GO:0098978	glutamatergic synapse	0.00016003	349	GO:CC
GO:0099060	integral component of postsynaptic specialization membrane	0.00021276	74	GO:CC
GO:0044309	neuron spine	0.00024857	185	GO:CC
GO:0005737	cytoplasm	0.00027535	11911	GO:CC
GO:0016021	integral component of membrane	0.00029831	5711	GO:CC
GO:0098948	intrinsic component of postsynaptic specialization membrane	0.00039658	78	GO:CC
GO:0034704	calcium channel complex	0.00048262	71	GO:CC
GO:0043197	dendritic spine	0.00050926	183	GO:CC
GO:0008076	voltage-gated potassium channel complex	0.00064855	90	GO:CC
GO:0016010	dystrophin-associated glycoprotein complex	0.00153429	19	GO:CC
GO:0016529	sarcoplasmic reticulum	0.00153429	70	GO:CC
GO:0090665	glycoprotein complex	0.00153429	19	GO:CC
GO:0098797	plasma membrane protein complex	0.00158154	694	GO:CC
GO:0016528	sarcoplasm	0.00158154	79	GO:CC
GO:0098858	actin-based cell projection	0.00188409	220	GO:CC
GO:0031252	cell leading edge	0.0028479	422	GO:CC

GO:0098862	cluster of actin-based cell projections	0.00296359	162	GO:CC
GO:0001725	stress finer	0.00384437	68	GO:CC
GO:0097517	contractile actin filament bundle	0.00384437	68	GO:CC
GO:0042641	actomyosin	0.00387087	77	GO:CC
GO:0005891	voltage-gated calcium channel complex	0.00437294	44	GO:CC
GO:0030018	Z disc	0.00439548	126	GO:CC
GO:0099568	cytoplasmic region	0.00517409	269	GO:CC
GO:0043204	perikaryon	0.00572805	160	GO:CC
GO:0032838	plasma membrane bounded cell projection cytoplasm	0.00591119	226	GO:CC
GO:0005829	cytosol	0.00601483	5303	GO:CC
GO:0042383	sarcolemma	0.00601483	140	GO:CC
GO:0031253	cell projection membrane	0.00607799	343	GO:CC
GO:0031594	neuromuscular junction	0.00685923	73	GO:CC
GO:0030426	growth cone	0.0081714	187	GO:CC
GO:0044306	neuron projection terminus	0.0081714	144	GO:CC
GO:0044304	main axon	0.00877075	66	GO:CC
GO:0032432	actin filament bundle	0.00968716	76	GO:CC
GO:0032983	kainate selective glutamate receptor complex	0.01074478	4	GO:CC
GO:0030427	site of polarized growth	0.01213548	193	GO:CC
GO:0031674	I band	0.01254526	139	GO:CC
GO:0032589	neuron projection membrane	0.01258168	60	GO:CC
GO:0042734	presynaptic membrane	0.01258168	150	GO:CC
GO:0016324	apical plasma membrane	0.01385508	361	GO:CC
GO:0097730	non-motile cilium	0.01459581	163	GO:CC
GO:0048471	perinuclear region of cytoplasm	0.01461607	735	GO:CC
GO:0043198	dendritic shaft	0.01518154	36	GO:CC
GO:0031256	leading edge membrane	0.01518154	175	GO:CC
GO:0005930	axoneme	0.0156786	132	GO:CC
GO:0097014	ciliary plasm	0.01841014	134	GO:CC
GO:0045177	apical part of cell	0.01843395	431	GO:CC
GO:0099081	supramolecular polymer	0.01843395	1001	GO:CC
GO:0015630	microtubule cytoskeleton	0.01869264	1307	GO:CC
GO:0005667	transcription regulator complex	0.01869264	432	GO:CC
GO:0030314	junctional membrane complex	0.02116122	5	GO:CC
GO:0060171	stereocilium membrane	0.02116122	5	GO:CC
GO:0008328	ionotropic glutamate receptor complex	0.02156432	47	GO:CC
GO:0060170	ciliary membrane	0.02186456	75	GO:CC
GO:0014701	junctional sarcoplasmic reticulum membrane	0.02190668	10	GO:CC
GO:0043226	organelle	0.02199583	14008	GO:CC
GO:0043679	axon terminus	0.02254201	127	GO:CC
GO:0043195	terminal bouton	0.02325338	57	GO:CC
GO:0016459	myosin complex	0.02325338	57	GO:CC

GO:0044295	axonal growth cone	0.02325338	31	GO:CC
GO:0005604	basement membrane	0.02510014	97	GO:CC
GO:0098889	intrinsic component of presynaptic membrane	0.02514874	77	GO:CC
GO:0017053	transcription repressor complex	0.02514874	77	GO:CC
GO:0098878	neurotransmitter receptor complex	0.02591004	49	GO:CC
GO:0060076	excitatory synapse	0.02591004	49	GO:CC
GO:0099056	integral component of presynaptic membrane	0.02673436	68	GO:CC
GO:0099544	perisynaptic space	0.03218959	2	GO:CC
GO:0001750	photoreceptor outer segment	0.03249021	90	GO:CC
GO:0002142	stereocilia ankle link complex	0.03294806	6	GO:CC
GO:0002141	stereocilia ankle link	0.03294806	6	GO:CC
GO:0043083	synaptic cleft	0.03294806	18	GO:CC
GO:0043232	intracellular non-membrane-bounded organelle	0.03294806	5338	GO:CC
GO:0005938	cell cortex	0.03294806	311	GO:CC
GO:1990075	periciliary membrane compartment	0.03294806	6	GO:CC
GO:0016605	PML body	0.03520919	102	GO:CC
GO:0099512	supramolecular fiber	0.03520919	993	GO:CC
GO:0043228	non-membrane-bounded organelle	0.03521907	5346	GO:CC
GO:0009986	cell surface	0.03742008	899	GO:CC
GO:1990454	L-type voltage-gated calcium channel complex	0.03770149	12	GO:CC
GO:0032426	stereocilium tip	0.03934991	19	GO:CC
GO:0098686	hippocampal mossy fiber to CA3 synapse	0.03934991	35	GO:CC
GO:0030017	sarcomere	0.04343198	208	GO:CC
GO:0062023	collagen-containing extracellular matrix	0.04344101	421	GO:CC
GO:0005581	collagen trimer	0.04534434	95	GO:CC
GO:0016323	basolateral plasma membrane	0.04741727	222	GO:CC
GO:0005587	collagen type IV trimer	0.04780306	7	GO:CC
GO:0009925	basal plasma membrane	0.04780306	247	GO:CC
GO:0036157	outer dynein arm	0.04780306	13	GO:CC
GO:0002139	stereocilia coupling link	0.04780306	7	GO:CC
GO:0097731	9+0 non-motile cilium	0.04780306	129	GO:CC
GO:0097733	photoreceptor cell cilium	0.04780306	118	GO:CC
GO:0030673	axolemma	0.04780306	13	GO:CC
GO:0098796	membrane protein complex	0.04830648	1322	GO:CC
GO:0030312	external encapsulating structure	0.05689275	563	GO:CC
GO:0005929	cilium	0.05771519	672	GO:CC
GO:0045178	basal part of cell	0.05973488	265	GO:CC
GO:0009898	cytoplasmic side of plasma membrane	0.06060181	168	GO:CC
GO:0005794	Golgi apparatus	0.06060181	1623	GO:CC
GO:0098645	collagen network	0.06800652	8	GO:CC

GO:0071144	heteromeric SMAD protein complex	0.06800652	8	GO:CC
GO:0098642	network-forming collagen trimer	0.06800652	8	GO:CC
GO:0030016	myofibril	0.06800652	231	GO:CC
GO:0042709	succinate-CoA ligase complex	0.06924256	3	GO:CC
GO:0097513	myosin II filament	0.06924256	3	GO:CC
GO:0098685	Schaffer collateral - CA1 synapse	0.06924256	80	GO:CC
GO:0012505	endomembrane system	0.07192681	4640	GO:CC
GO:0031012	extracellular matrix	0.07700072	562	GO:CC
GO:0033017	sarcoplasmic reticulum membrane	0.07825239	41	GO:CC
GO:0016342	catenin complex	0.08018788	32	GO:CC
GO:0005815	microtubule organizing center	0.08190415	813	GO:CC
GO:0005802	trans-Golgi network	0.086595	250	GO:CC
GO:0098890	extrinsic component of postsynaptic membrane	0.08779906	9	GO:CC
GO:0098651	basement membrane collagen trimer	0.08779906	9	GO:CC
GO:0036057	slit diaphragm	0.08779906	9	GO:CC
GO:0043194	axon initial segment	0.08779906	16	GO:CC
GO:0036056	filtration diaphragm	0.08779906	9	GO:CC
GO:0014731	spectrin-associated cytoskeleton	0.08779906	9	GO:CC
GO:0005925	focal adhesion	0.08779906	420	GO:CC
GO:0043292	contractile fiber	0.09290858	240	GO:CC
GO:0030315	T-tubule	0.09403617	53	GO:CC
GO:0070160	tight junction	0.09741705	131	GO:CC
GO:0005858	axonemal dynein complex	0.09884721	25	GO:CC
GO:0005261	cation channel activity	2.2328E-08	340	GO:MF
GO:0022836	gated channel activity	9.1335E-07	341	GO:MF
GO:0046873	metal ion transmembrane transporter activity	9.1335E-07	435	GO:MF
GO:0005216	ion channel activity	1.3991E-06	435	GO:MF
GO:0008324	cation transmembrane transporter activity	1.3991E-06	639	GO:MF
GO:0022890	inorganic cation transmembrane transporter activity	1.8021E-06	591	GO:MF
GO:0022803	passive transmembrane transporter activity	2.1551E-05	485	GO:MF
GO:0015267	channel activity	2.1551E-05	484	GO:MF
GO:0030695	GTPase regulator activity	4.2752E-05	487	GO:MF
GO:0015079	potassium ion transmembrane transporter activity	4.2752E-05	161	GO:MF
GO:0005267	potassium channel activity	4.2752E-05	125	GO:MF
GO:0005215	transporter activity	4.2752E-05	1185	GO:MF
GO:0005244	voltage-gated ion channel activity	4.9919E-05	200	GO:MF
GO:0022832	voltage-gated channel activity	5.2144E-05	201	GO:MF
GO:0060589	nucleoside-triphosphatase regulator activity	5.6812E-05	530	GO:MF
GO:0022857	transmembrane transporter activity	6.5414E-05	1075	GO:MF

GO:0005096	GTPase activator activity	9.1989E-05	278	GO:MF
GO:0022843	voltage-gated cation channel activity	9.1989E-05	143	GO:MF
GO:0005509	calcium ion binding	0.00011438	721	GO:MF
GO:0008092	cytoskeletal protein binding	0.00013721	996	GO:MF
GO:0015318	inorganic molecular entity transmembrane transporter activity	0.00019888	831	GO:MF
GO:0015085	calcium ion transmembrane transporter activity	0.00029122	135	GO:MF
GO:0015075	ion transmembrane transporter activity	0.00032934	956	GO:MF
GO:0005262	calcium channel activity	0.00034507	119	GO:MF
GO:0043167	ion binding	0.00041677	6057	GO:MF
GO:0043169	cation binding	0.00047327	4351	GO:MF
GO:0046872	metal ion binding	0.00079056	4260	GO:MF
GO:0050839	cell adhesion molecule binding	0.00128505	546	GO:MF
GO:0016595	glutamate binding	0.00128505	11	GO:MF
GO:0008289	lipid binding	0.00193324	776	GO:MF
GO:0005249	voltage-gated potassium channel activity	0.00198973	89	GO:MF
GO:0098632	cell-cell adhesion mediator activity	0.00209193	49	GO:MF
GO:0005001	transmembrane receptor protein tyrosine phosphatase activity	0.00213115	17	GO:MF
GO:0019198	transmembrane receptor protein phosphatase activity	0.00213115	17	GO:MF
GO:0022839	ion gated channel activity	0.00258085	43	GO:MF
GO:0099094	ligand-gated cation channel activity	0.00264244	110	GO:MF
GO:0005515	protein binding	0.00375079	14767	GO:MF
GO:0005543	phospholipid binding	0.00435641	454	GO:MF
GO:0015276	ligand-gated ion channel activity	0.00791391	140	GO:MF
GO:0022834	ligand-gated channel activity	0.00791391	140	GO:MF
GO:0008022	protein C-terminus binding	0.00791391	202	GO:MF
GO:0098631	cell adhesion mediator activity	0.00906034	58	GO:MF
GO:0044877	protein-containing complex binding	0.00906034	1287	GO:MF
GO:0008013	beta-catenin binding	0.01266864	87	GO:MF
GO:0043168	anion binding	0.01266864	2418	GO:MF
GO:0043177	organic acid binding	0.01954254	120	GO:MF
GO:0019199	transmembrane receptor protein kinase activity	0.02069719	82	GO:MF
GO:0008047	enzyme activator activity	0.02102265	540	GO:MF
GO:0035091	phosphatidylinositol binding	0.02711185	255	GO:MF
GO:0005227	calcium activated cation channel activity	0.02901285	26	GO:MF
GO:0001223	transcription coactivator binding	0.02901285	26	GO:MF
GO:0140297	DNA-binding transcription factor binding	0.03422078	391	GO:MF
GO:0046332	SMAD binding	0.03514697	78	GO:MF
GO:0008066	glutamate receptor activity	0.03514697	27	GO:MF

GO:0098772	molecular function regulator	0.0354143	2363	GO:MF
GO:0005085	guanyl-nucleotide exchange factor activity	0.03923775	217	GO:MF
GO:0003779	actin binding	0.04349183	448	GO:MF
GO:0008046	axon guidance receptor activity	0.04349183	9	GO:MF
GO:0042802	identical protein binding	0.0490395	2067	GO:MF
GO:0071813	lipoprotein particle binding	0.04928363	37	GO:MF
GO:0071814	protein-lipid complex binding	0.04928363	37	GO:MF
GO:0004714	transmembrane receptor protein tyrosine kinase activity	0.04928363	63	GO:MF
GO:0015220	choline transmembrane transporter activity	0.05627024	5	GO:MF
GO:0015277	kainate selective glutamate receptor activity	0.05627024	5	GO:MF
GO:0097109	neuroligin family protein binding	0.05627024	5	GO:MF
GO:0086007	voltage-gated calcium channel activity involved in cardiac muscle cell action potential	0.05627024	5	GO:MF
GO:0036094	small molecule binding	0.06344041	2506	GO:MF
GO:0017124	SH3 domain binding	0.07731841	129	GO:MF
GO:0030228	lipoprotein particle receptor activity	0.07731841	17	GO:MF
GO:0000406	double-strand/single-strand DNA junction binding	0.08276114	2	GO:MF
GO:0050659	N-acetylgalactosamine 4-sulfate 6-O-sulfotransferase activity	0.08276114	2	GO:MF
GO:0050509	N-acetylglucosaminyl-proteoglycan 4-beta-glucuronosyltransferase activity	0.08276114	2	GO:MF
GO:0042328	heparan sulfate N-acetylglucosaminyltransferase activity	0.08276114	2	GO:MF
GO:0016404	15-hydroxyprostaglandin dehydrogenase (NAD+) activity	0.08276114	2	GO:MF
GO:0038025	reelin receptor activity	0.08276114	2	GO:MF
GO:0010855	adenylate cyclase inhibitor activity	0.08276114	2	GO:MF
GO:0010854	adenylate cyclase regulator activity	0.08276114	2	GO:MF
GO:0030020	extracellular matrix structural constituent conferring tensile strength	0.08276114	41	GO:MF
GO:0032559	adenyl ribonucleotide binding	0.08289869	1565	GO:MF
GO:0005042	netrin receptor activity	0.08846345	6	GO:MF
GO:0005319	lipid transporter activity	0.09222789	167	GO:MF
GO:0030234	enzyme regulator activity	0.09355916	1248	GO:MF
GO:0003774	motor activity	0.09427974	134	GO:MF
HPA:0090991	cerebellum; molecular layer - neuropil[≥Low]	0.00149806	265	HPA
HPA:0100211	cerebral cortex; neuropil[≥Low]	0.03723675	4942	HPA
HPA:0100212	cerebral cortex; neuropil[≥Medium]	0.05285336	2588	HPA
HPA:0411231	retina; inner nuclear layer[≥Low]	0.07071389	22	HPA
HPA:0091031	cerebellum; processes in molecular layer[≥Low]	0.07398384	204	HPA

HPA:0091032	cerebellum; processes in molecular layer[≥Medium]	0.07398384	192	HPA
HPA:0091061	cerebellum; synaptic glomeruli - core[≥Low]	0.07398384	296	HPA
HPA:0271133	kidney; distal tubules[High]	0.08505455	8	HPA
HPA:0090992	cerebellum; molecular layer - neuropil[≥Medium]	0.08505455	148	HPA
KEGG:04360	Axon guidance	0.00103255	181	KEGG
KEGG:04724	Glutamatergic synapse	0.00980229	114	KEGG
KEGG:04390	Hippo signaling pathway	0.04866278	157	KEGG
KEGG:04921	Oxytocin signalling pathway	0.04866278	154	KEGG
KEGG:04713	Circadian entrainment	0.04866278	97	KEGG
KEGG:04371	Apelin signalling pathway	0.07362966	136	KEGG
KEGG:05412	Arrhythmogenic right ventricular cardiomyopathy	0.07362966	77	KEGG
KEGG:04510	Focal adhesion	0.07362966	200	KEGG
KEGG:05017	Spinocerebellar ataxia	0.08435128	142	KEGG
KEGG:04020	Calcium signalling pathway	0.08435128	239	KEGG
KEGG:04933	AGE-RAGE signalling pathway in diabetic complications	0.08435128	100	KEGG
REAC:R-HSA-112316	Neuronal System	2.117E-05	400	REAC
REAC:R-HSA-1296071	Potassium Channels	0.00381687	103	REAC
REAC:R-HSA-163685	Integration of energy metabolism	0.07883006	107	REAC
REAC:R-HSA-112315	Transmission across Chemical Synapses	0.07883006	259	REAC
REAC:R-HSA-9022537	Loss of MECP2 binding ability to the NCoR/SMRT complex	0.07883006	6	REAC
REAC:R-HSA-5173105	O-linked glycosylation	0.07883006	107	REAC
REAC:R-HSA-373752	Netrin-1 signalling	0.07908711	49	REAC
REAC:R-HSA-1296072	Voltage gated Potassium channels	0.09368766	43	REAC
TF:M10426_1	Factor: ctcf; motif: CCRSCAGGGGGCGCN; match class: 1	2.0277E-05	4369	TF
TF:M00695_1	Factor: ETF; motif: GVGGMGG; match class: 1	2.0277E-05	7032	TF
TF:M10107_1	Factor: DB1; motif: GGRRRRGRRGGAGGGGGNGRRR; match class: 1	4.9653E-05	2657	TF
TF:M08911_1	Factor: CTCF; motif: NCCRSTAGGGGGCGC; match class: 1	0.00013247	3934	TF
TF:M11613	Factor: TCF-3; motif: ASATCAAAG	0.00013667	1372	TF
TF:M09984_1	Factor: MAZ; motif: GGGGGAGGGGGNGRGRRRGNRG; match class: 1	0.00017948	5555	TF
TF:M10086_1	Factor: TAFII250; motif: RARRWGGCGGMGGNGR; match class: 1	0.00024319	4153	TF
TF:M11531_1	Factor: E2F-2; motif: GCGCGCGCGYW; match class: 1	0.00024319	12351	TF

TF:M02036_1	Factor: WT1; motif: CGCCCCCNCN; match class: 1	0.00024319	5290	TF
TF:M10095	Factor: TCF-3; motif: NNNCTTTGAWSTN	0.00027065	1905	TF
TF:M10107	Factor: DB1; motif: GGRRRRGRRGGAGGGGGNGRRR	0.00034813	5822	TF
TF:M10134_1	Factor: FPM315; motif: GGGAGGAGGRRGRGGRGGRR; match class: 1	0.00060697	585	TF
TF:M11588_1	Factor: FOXK1; motif: NWYGTAAAYAR; match class: 1	0.00061899	1064	TF
TF:M00803_1	Factor: E2F; motif: GGCGSG; match class: 1	0.00061899	10230	TF
TF:M10426	Factor: ctcf; motif: CCRSCAGGGGGCGCN	0.00061899	9305	TF
TF:M01199_1	Factor: RNF96; motif: BCCCGCRGCC; match class: 1	0.00070021	4322	TF
TF:M09984	Factor: MAZ; motif: GGGGGAGGGGGNGRGRRRGNRG	0.00070021	9544	TF
TF:M10111	Factor: ZF5; motif: NGAGCGCGC	0.00123655	2647	TF
TF:M00333_1	Factor: ZF5; motif: NRNGNGCGCGCWN; match class: 1	0.00123655	12401	TF
TF:M07136	Factor: TCF-4; motif: NNASATCAAAGNNN	0.00129511	1852	TF
TF:M10134	Factor: FPM315; motif: GGGAGGAGGRRGRGGRGGRR	0.00132704	2472	TF
TF:M07141	Factor: FPM315; motif: GGAGGAGGRRGRGGRGGRRGR	0.00156069	2175	TF
TF:M00189_1	Factor: AP-2; motif: MKCCCSCNGGCG; match class: 1	0.00177548	6093	TF
TF:M01253	Factor: CNOT3; motif: GGCCGCGSSS	0.00177548	3926	TF
TF:M07141_1	Factor: FPM315; motif: GGAGGAGGRRGRGGRGGRRGR; match class: 1	0.00267365	882	TF
TF:M05509	Factor: ZAC; motif: KGGGGAAGAA	0.003436	318	TF
TF:M03893_1	Factor: WT1; motif: GNGGGGGCGGGG; match class: 1	0.003436	3980	TF
TF:M01873_1	Factor: Egr-1; motif: GCGGGGGCGG; match class: 1	0.003436	2672	TF
TF:M01858	Factor: AP-2beta; motif: GCNNNGGSCNGVGGGN	0.00420565	7418	TF
TF:M01104	Factor: MOVO-B; motif: GNGGGGG	0.00465657	10261	TF
TF:M09669	Factor: TCF-4; motif: NNNCTTTGAWSTN	0.00486164	2228	TF
TF:M10108_1	Factor: WT1; motif: RGGNGGGGGAGGRGGNGGRG; match class: 1	0.0050157	2864	TF
TF:M00915_1	Factor: AP-2; motif: SNNNCCNCAGGCN; match class: 1	0.00509679	4551	TF
TF:M12227_1	Factor: ZIC4; motif: NNCCNCCCRYNGYGN; match class: 1	0.00511154	5898	TF
TF:M01240_1	Factor: BEN; motif: CAGCGRNV; match class: 1	0.00515875	13227	TF
TF:M00695	Factor: ETF; motif: GVGGMGG	0.00555994	10430	TF

TF:M04869	Factor: Egr-1; motif: GCGCATGCG	0.00555994	11232	TF
TF:M00800_1	Factor: AP-2; motif: GSCCSCRGGCNRNRNN; match class: 1	0.00555994	4268	TF
TF:M01072	Factor: HIC1; motif: NSNNNNTGCCCSSNN	0.00555994	4166	TF
TF:M01104_1	Factor: MOVO-B; motif: GNGGGGG; match class: 1	0.00561881	5626	TF
TF:M01219	Factor: SP1:SP3; motif: CCSCCCCCYCC	0.00569919	6812	TF
TF:M04351	Factor: HOXC10; motif: GYMATWAAAN	0.0058272	2121	TF
TF:M10108	Factor: WT1; motif: RGGNGGGGGAGGRGGNGGRG	0.00584682	6511	TF
TF:M00189	Factor: AP-2; motif: MKCCCSCNGGCG	0.00697995	10621	TF
TF:M03896_1	Factor: EGR1; motif: NACGCCCACGCANW; match class: 1	0.00697995	2106	TF
TF:M10020	Factor: OSR2; motif: NNNNCWGCTNCTGNNG	0.00697995	2584	TF
TF:M07354_1	Factor: Egr-1; motif: GCGGGGGCGG; match class: 1	0.00697995	3561	TF
TF:M10699_1	Factor: HOXB5; motif: NYMATTAN; match class: 1	0.00697995	126	TF
TF:M10697_1	Factor: HOXB5; motif: NYMATTAN; match class: 1	0.00697995	126	TF
TF:M10026	Factor: PATZ; motif: GGGGNGGGGGMKGGRRNGGNR N	0.00697995	8389	TF
TF:M11531	Factor: E2F-2; motif: GCGCGCGCGYW	0.00933242	13270	TF
TF:M00938	Factor: E2F-1; motif: TTGGCGCGRAANNGNM	0.00950124	7334	TF
TF:M10026_1	Factor: PATZ; motif: GGGGNGGGGGMKGGRRNGGNR N; match class: 1	0.01259291	4894	TF
TF:M10691_1	Factor: HOXB6; motif: NTAATKRC; match class: 1	0.01259291	1497	TF
TF:M07206_1	Factor: E2F-1; motif: NGGGCGGGARV; match class: 1	0.0136672	10849	TF
TF:M09760_1	Factor: DPF2; motif: NYCACYTCCYCNYYCY; match class: 1	0.01416645	2978	TF
TF:M01219_1	Factor: SP1:SP3; motif: CCSCCCCCYCC; match class: 1	0.0144433	2937	TF
TF:M12313	Factor: ZNF460; motif: NNACNCCCCCCNN	0.0144433	5825	TF
TF:M01873	Factor: Egr-1; motif: GCGGGGGCGG	0.0144433	6738	TF
TF:M10693	Factor: HOXB6; motif: NTAATKRC	0.01612736	2401	TF
TF:M08878_1	Factor: EGR; motif: CGCCCCCGCNN; match class: 1	0.01656865	3224	TF
TF:M07377	Factor: cdx-1; motif: NTTTATKNN	0.01656865	873	TF
TF:M10820	Factor: HOXA11; motif: NGYMATAAAAN	0.01656865	860	TF
TF:M07035	Factor: Beta-catenin; motif: GNNNNCTTTGWTGNY	0.01656865	3660	TF
TF:M04355	Factor: HOXC12; motif: GYAATAAAA	0.01656865	873	TF

TF:M00982_1	Factor: KROX; motif: CCCGCCCCCRCCCC; match class: 1	0.01722747	3518	TF
TF:M00800	Factor: AP-2; motif: GSCCSCRGGCNRNRNN	0.01740637	9119	TF
TF:M07436	Factor: WT1; motif: NNGGGNGGGSGN	0.01806455	6182	TF
TF:M07208	Factor: EGR1; motif: NCNCCGCCCCCGCN	0.01808313	6183	TF
TF:M08948	Factor: LEF-1; motif: NNNCTTTGAT	0.0194007	3498	TF
TF:M04361	Factor: HOXD12; motif: GTAATAAAA	0.02124072	882	TF
TF:M07354	Factor: Egr-1; motif: GCGGGGGCGG	0.02313439	7801	TF
TF:M09892_1	Factor: E2F-1; motif: NNNNGGCGGGAARN; match class: 1	0.02355763	9162	TF
TF:M10748	Factor: GSH2; motif: SYMATTAR	0.02377545	1710	TF
TF:M04633	Factor: TCF-4; motif: NNWTCAAAGN	0.0248757	2602	TF
TF:M10112_1	Factor: Miz-1; motif: NNRGGWGGGGGAGGGGMRR; match class: 1	0.0248757	4075	TF
TF:M10754	Factor: hoxd1; motif: NTAATTAS	0.02551299	1980	TF
TF:M10753	Factor: HOXA1; motif: NTAATTAN	0.02551299	1980	TF
TF:M00982	Factor: KROX; motif: CCCGCCCCCRCCCC	0.02577292	7815	TF
TF:M01857_1	Factor: AP-2alpha; motif: NGCCYSNNGSN; match class: 1	0.02607147	4616	TF
TF:M10111_1	Factor: ZF5; motif: NGAGCGCGC; match class: 1	0.02624461	497	TF
TF:M01587	Factor: FPM315; motif: SRGGGAGGAGGN	0.02689951	3246	TF
TF:M10711	Factor: HOXD4; motif: NYMATTAN	0.02810827	1735	TF
TF:M10776	Factor: hoxd9; motif: GYMATAAAAN	0.02810827	921	TF
TF:M10726_1	Factor: HOXB8; motif: NYMATTAN; match class: 1	0.02810827	229	TF
TF:M10996	Factor: LMX1A; motif: YTAATTAN	0.02826217	1460	TF
TF:M12227	Factor: ZIC4; motif: NNCCNCCCRYNGYGN	0.02927209	11063	TF
TF:M09619	Factor: HNF-3beta; motif: TGTTTACWYWG	0.02981397	3168	TF
TF:M08867_1	Factor: AP2; motif: GCCYGSGGSN; match class: 1	0.02981397	5186	TF
TF:M00250	Factor: Gfi-1; motif: NNNNNNNAAATCACWGYNNNNNNN	0.03076794	1032	TF
TF:M11482	Factor: AP-2gamma; motif: NSCCYNNRGSN	0.03076794	6696	TF
TF:M10696	Factor: HOXA6; motif: NGYMATTANN	0.03076794	4935	TF
TF:M03893	Factor: WT1; motif: GNGGGGGCGGGG	0.03076794	8290	TF
TF:M09603_1	Factor: Egr-1; motif: NNNNNGYGKGGGNGGGNN; match class: 1	0.03152272	1317	TF

TF:M07329_1	Factor: Osx; motif: CCNCCCCCNNN; match class: 1	0.03152272	2509	TF
TF:M10725_1	Factor: HOXD8; motif: GYMATTAN; match class: 1	0.03413352	70	TF
TF:M00803	Factor: E2F; motif: GGCGSG	0.03599169	13190	TF
TF:M08772_1	Factor: HOXA6; motif: NYMATTAN; match class: 1	0.04219652	2568	TF
TF:M04351_1	Factor: HOXC10; motif: GYMATWAAAN; match class: 1	0.04353614	193	TF
TF:M00195_1	Factor: Oct-1; motif: NNNNATGCAAATNAN; match class: 1	0.04389785	550	TF
TF:M04255_1	Factor: FOXO1; motif: GTAAACAW; match class: 1	0.04518092	476	TF
TF:M04515_1	Factor: E2F-1; motif: WWTGGCGCCAAA; match class: 1	0.0474689	12173	TF
TF:M10590_1	Factor: BSX; motif: NYRATTAN; match class: 1	0.04758181	285	TF
TF:M04267_1	Factor: FOXP3; motif: RTAAACA; match class: 1	0.047961	479	TF
TF:M07250	Factor: E2F-1; motif: NNNSSCGCSAANN	0.047961	10703	TF
TF:M10147_1	Factor: ZNF394; motif: NRARWRGAANNNAMWGNAAK; match class: 1	0.047961	1854	TF
TF:M04239_1	Factor: FOXD2; motif: GTAAACA; match class: 1	0.047961	479	TF
TF:M04298	Factor: Cdx-2; motif: GYMATAAAA	0.047961	1174	TF
TF:M04244_1	Factor: FOXI1; motif: GTAAACA; match class: 1	0.047961	479	TF
TF:M03876_1	Factor: Kaiso; motif: GCMGGGRGCRGS; match class: 1	0.047961	9106	TF
TF:M04253_1	Factor: FOXL1; motif: RTAAACA; match class: 1	0.047961	479	TF
TF:M04265_1	Factor: FOXO6; motif: GTAAACA; match class: 1	0.047961	479	TF
TF:M09933	Factor: FOXP1; motif: TNTGTTTMY	0.047961	4164	TF
TF:M12345	Factor: Zbtb37; motif: NYACCGCRNTCACCGCR	0.047961	5505	TF
TF:M11579	Factor: foxl2; motif: NNYGTAAACAN	0.04900402	5888	TF
TF:M07040_1	Factor: GKLF; motif: NNRRGRRNGNSNNN; match class: 1	0.05000108	8156	TF
TF:M10691	Factor: HOXB6; motif: NTAATKRC	0.05023898	5329	TF
TF:M12139_1	Factor: Egr-1; motif: NMCRCCCMCNCNN; match class: 1	0.05025353	698	TF
TF:M00938_1	Factor: E2F-1; motif: TTGGCGCGRAANNGNM; match class: 1	0.05119455	2573	TF
TF:M04869_1	Factor: Egr-1; motif: GCGCATGCG; match class: 1	0.05135193	10253	TF
TF:M12354_1	Factor: ZNF37A; motif: CCYYGGCTCCNTSCCMN; match class: 1	0.05259156	5624	TF

TF:M12351_1	Factor: TIEG1; motif: NCCCNSNCCCCGCCCCC; match class: 1	0.05259156	8180	TF
TF:M10724_1	Factor: HOXD8; motif: GYMATTAN; match class: 1	0.05259156	337	TF
TF:M10148_1	Factor: ZNF418; motif: TGCTTYTRGCYTCTKNN; match class: 1	0.05259156	57	TF
TF:M07329	Factor: Osx; motif: CCNCCCCCNNN	0.0527075	6803	TF
TF:M06948_1	Factor: Sp2; motif: TGGGCGCGCCCA; match class: 1	0.0527075	6205	TF
TF:M04333	Factor: HMX1; motif: ANCAATTAANN	0.0576057	1768	TF
TF:M11677_1	Factor: IRF-3; motif: NGGAAACNGAAACCGAAACN; match class: 1	0.05798404	26	TF
TF:M11609	Factor: LEF-1; motif: ASATCAAAG	0.05798404	3078	TF
TF:M01234	Factor: ipf1; motif: AVCTAATGAG	0.05905347	2788	TF
TF:M12140_1	Factor: Egr-1; motif: NNCRCCCMCGCNN; match class: 1	0.06023527	1561	TF
TF:M11589_1	Factor: FOXK1; motif: NNNGTAAACAN; match class: 1	0.06023527	719	TF
TF:M04863_1	Factor: TF3C-beta; motif: CCNGGAGGGCTTCCTGGAGGAG; match class: 1	0.06139494	8573	TF
TF:M05417	Factor: ZNF641; motif: NAGGGGKGGGGN	0.06582717	127	TF
TF:M04516	Factor: E2F-1; motif: TTTGGCGCCAAA	0.06582717	11383	TF
TF:M10770	Factor: HOXB9; motif: GYMATAAAAN	0.06726314	989	TF
TF:M09826_1	Factor: BTEB3; motif: CCNNSCCNSCCCCKCCCCC; match class: 1	0.0673564	7508	TF
TF:M10696_1	Factor: HOXA6; motif: NGYMATTANN; match class: 1	0.07124683	1223	TF
TF:M07249	Factor: ctcf; motif: CCNCNAGRKGGCRSTN	0.0722336	6715	TF
TF:M04335	Factor: HMX3; motif: NNCAMTTAANN	0.0722336	5434	TF
TF:M04253	Factor: FOXL1; motif: RTAAACA	0.0722336	3720	TF
TF:M04300_1	Factor: Dlx-2; motif: NYAATTAN; match class: 1	0.0722336	1212	TF
TF:M08205_1	Factor: E2F-1:Elk-1; motif: SGCGCSNNAMCGGAAGT; match class: 1	0.0722336	10438	TF
TF:M04267	Factor: FOXP3; motif: RTAAACA	0.0722336	3720	TF
TF:M10694	Factor: HOXA6; motif: NGYMATTANN	0.0722336	3321	TF
TF:M11579_1	Factor: foxl2; motif: NNYGTAAACAN; match class: 1	0.0722336	1157	TF
TF:M00407_1	Factor: RSRFC4; motif: ANKCTAWAAATAGMHYN; match class: 1	0.0722336	98	TF
TF:M09897_1	Factor: Egr-1; motif: NNNNGCGKGGGYGGNRN; match class: 1	0.0722336	993	TF

TF:M04244	Factor: FOXI1; motif: GTAAACA	0.0722336	3720	TF
TF:M11909_1	Factor: POU3F2; motif: NTATGCWAATKAG; match class: 1	0.0722336	1184	TF
TF:M04239	Factor: FOXD2; motif: GTAAACA	0.0722336	3720	TF
TF:M04255	Factor: FOXO1; motif: GTAAACAW	0.0722336	3720	TF
TF:M04265	Factor: FOXO6; motif: GTAAACA	0.0722336	3720	TF
TF:M07289_1	Factor: GKLF; motif: NNNRGGNGNGGSN; match class: 1	0.07243462	10555	TF
TF:M04823_1	Factor: E2F-4; motif: NNTTCCCGCCNN; match class: 1	0.0728089	7850	TF
TF:M06125	Factor: ZNF823; motif: NGRGGGAGGAGG	0.07393685	173	TF
TF:M03811	Factor: AP-2gamma; motif: GCCYNCRGSN	0.07393685	8852	TF
TF:M03896	Factor: EGR1; motif: NACGCCCACGCANW	0.07864993	6129	TF
TF:M11588	Factor: FOXK1; motif: NWYGTAAAYAR	0.0788186	5352	TF
TF:M10772	Factor: hoxd9; motif: GYMATAAAAN	0.08384772	1696	TF
TF:M00210	Factor: OCT-x; motif: CTNATTTGCATAY	0.08620411	4138	TF
TF:M00290_1	Factor: Freac-2; motif: NNANNGTAAACAANNN; match class: 1	0.08932091	268	TF
TF:M08867	Factor: AP2; motif: GCCYGSGGSN	0.09012224	10054	TF
TF:M11611	Factor: LEF-1; motif: ASATCAAAG	0.09015836	3517	TF
TF:M04556_1	Factor: SRY; motif: AACAATNNNCATTGTT; match class: 1	0.09015836	6127	TF
TF:M11022	Factor: IRX2a; motif: ACRYGNNNNACRYGT	0.09064146	9487	TF
TF:M09898	Factor: Egr-2; motif: GNGRRNGWGKGGGNGGRG	0.09329086	6484	TF
TF:M04731	Factor: Blimp-1; motif: NACTTTCAC	0.09382047	3997	TF
TF:M01857	Factor: AP-2alpha; motif: NGCCYSNNGSN	0.09558883	9178	TF
TF:M01199	Factor: RNF96; motif: BCCCGCRGCC	0.09601622	8473	TF
TF:M11558	Factor: FKHL14; motif: NWNNGTMAACAN	0.09640784	4151	TF
TF:M04184_1	Factor: NHLH1; motif: CGCAGCTGCK; match class: 1	0.09640784	380	TF
TF:M07297	Factor: MAZ; motif: CCCTCCCYCYN	0.09640784	2964	TF
TF:M09849	Factor: TIF2; motif: ANANAGAWAAGN	0.09640784	3643	TF
TF:M00190	Factor: C/EBP; motif: NNATTGCNNAANNN	0.09640784	5586	TF
TF:M00333	Factor: ZF5; motif: NRNGNGCGCGCWN	0.097562	15072	TF
TF:M02036	Factor: WT1; motif: CGCCCCCNCN	0.097562	9767	TF
WP:WP2858	Ectoderm Differentiation	0.07686535	143	WP

WP:WP4698	Vitamin D-sensitive calcium signalling in depression	0.07686535	40	WP
WP:WP4148	Splicing factor NOVA regulated synaptic proteins	0.07686535	42	WP

(a)

term_id	term_name	p_value	intersection_size	source
CORUM:6566	SPG33-VAPB complex	0.00714514	2	CORUM
CORUM:5732	NRP2-VEGFC complex	0.00714514	2	CORUM
CORUM:5341	ELMO1-DOCK2 complex	0.00714514	2	CORUM
GO:0048532	anatomical structure arrangement	0.00483055	5	GO:BP
GO:0009887	animal organ morphogenesis	0.00707009	31	GO:BP
GO:0021604	cranial nerve structural organization	0.00779118	4	GO:BP
GO:0021783	preganglionic parasympathetic fiber development	0.01484773	4	GO:BP
GO:0021675	nerve development	0.01484773	7	GO:BP
GO:0021602	cranial nerve morphogenesis	0.01484773	5	GO:BP
GO:0048486	parasympathetic nervous system development	0.01484773	4	GO:BP
GO:0021545	cranial nerve development	0.01484773	6	GO:BP
GO:0032501	multicellular organismal process	0.01484773	123	GO:BP
GO:0048513	animal organ development	0.01484773	68	GO:BP
GO:0007275	multicellular organism development	0.01484773	94	GO:BP
GO:0048856	anatomical structure development	0.01484773	101	GO:BP
GO:0007154	cell communication	0.01534018	109	GO:BP
GO:0007165	signal transduction	0.01738059	102	GO:BP
GO:0051716	cellular response to stimulus	0.01738059	120	GO:BP
GO:0009653	anatomical structure morphogenesis	0.01738059	55	GO:BP
GO:0023052	signalling	0.01804406	108	GO:BP
GO:0002361	CD4-positive, CD25-positive, alpha-beta regulatory T cell differentiation	0.01830808	3	GO:BP
GO:0021612	facial nerve structural organization	0.01830808	3	GO:BP
GO:0048731	system development	0.02217399	85	GO:BP
GO:0046849	bone remodelling	0.02217399	7	GO:BP
GO:0048593	camera-type eye morphogenesis	0.02298752	8	GO:BP
GO:0021561	facial nerve development	0.03051967	3	GO:BP
GO:0021610	facial nerve morphogenesis	0.03051967	3	GO:BP
GO:0050896	response to stimulus	0.03412585	137	GO:BP
GO:0048596	embryonic camera-type eye morphogenesis	0.03412585	4	GO:BP

GO:0048483	autonomic nervous system development	0.03412585	5	GO:BP
GO:0060900	embryonic camera-type eye formation	0.03565657	3	GO:BP
GO:0090596	sensory organ morphogenesis	0.0406009	11	GO:BP
GO:0048729	tissue morphogenesis	0.04847403	19	GO:BP
GO:0048771	tissue remodelling	0.04847403	9	GO:BP
GO:0048592	eye morphogenesis	0.06468501	8	GO:BP
GO:0048871	multicellular organismal homeostasis	0.07040542	16	GO:BP
GO:1902187	negative regulation of viral release from host cell	0.07596151	3	GO:BP
GO:0048048	embryonic eye morphogenesis	0.07596151	4	GO:BP
GO:0031076	embryonic camera-type eye development	0.0871141	4	GO:BP
GO:0061551	trigeminal ganglion development	0.0871141	2	GO:BP
GO:0090500	endocardial cushion to mesenchymal transition	0.0871141	2	GO:BP
GO:0032502	developmental process	0.09042476	101	GO:BP
GO:0001946	lymphangiogenesis	0.09451983	3	GO:BP
GO:0001501	skeletal system development	0.09451983	15	GO:BP
GO:0072001	renal system development	0.09451983	11	GO:BP
GO:0005887	integral component of plasma membrane	0.07100569	36	GO:CC
GO:0031226	intrinsic component of plasma membrane	0.07100569	38	GO:CC
GO:0062186	anandamide epoxidase activity	0.08662559	2	GO:MF
GO:0062189	anandamide 14,15 epoxidase activity	0.08662559	2	GO:MF
GO:0016709	oxidoreductase activity, acting on paired donors, with incorporation or reduction of molecular oxygen, NAD(P)H as one donor, and incorporation of one atom of oxygen	0.08662559	5	GO:MF

(b)

Appendix 9: Extract from example pyrogram (SNP 2105042)

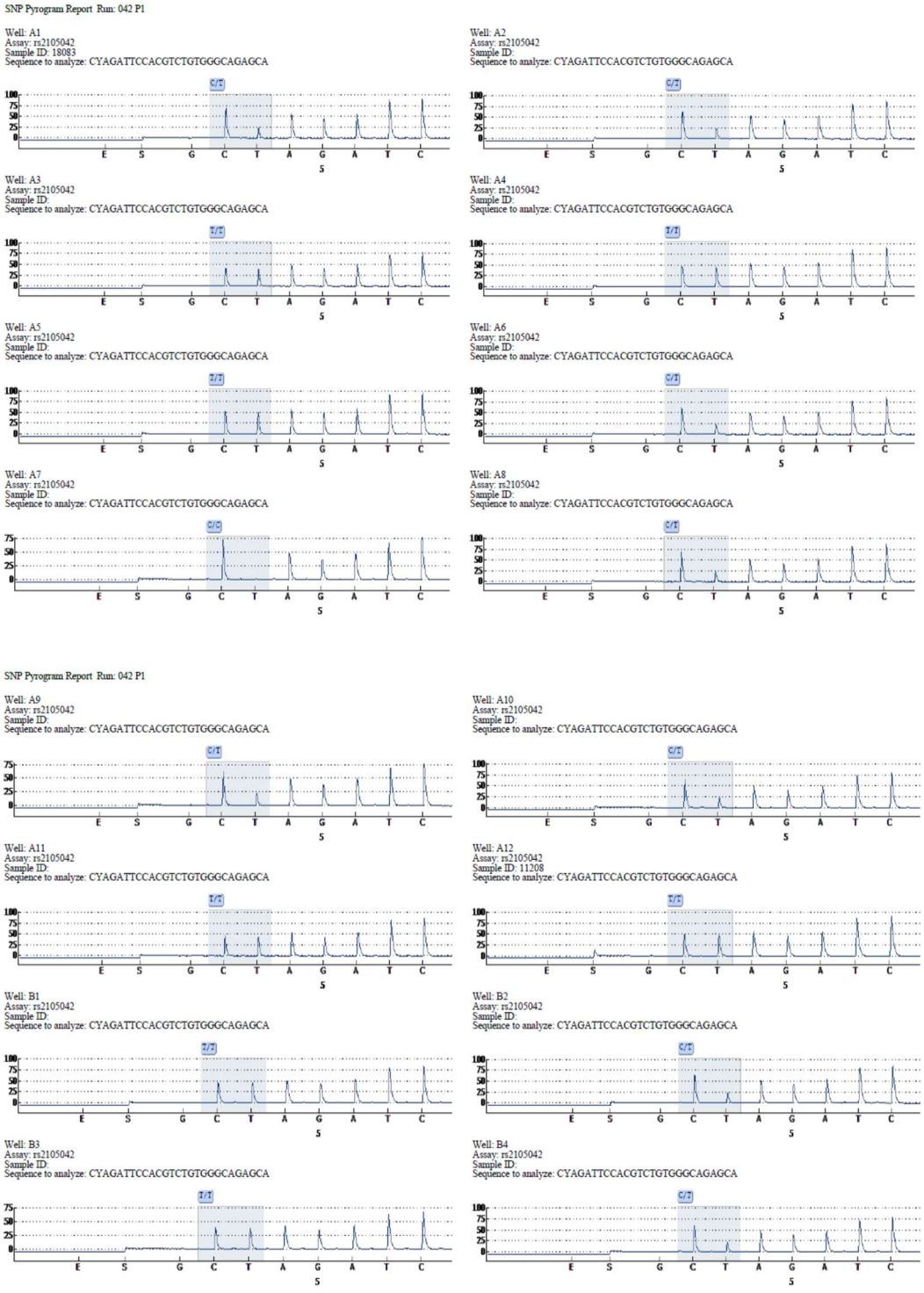

Appendix 10: SNP allele frequencies following pyrosequencing.

dbSNP rs	Location (GRCh38)	Allele	ORN	No ORN
rs7477958	ch10: 65877716	T/T	24	38
		T/C	30	40
		C/C	2	16
rs34798038	ch9:79589403	A/A	54	74
		A/G	2	20
		G/G	0	0
rs2105042	ch6: 4229454	T/T	24	29
		C/T	28	46
		C/C	4	18
rs11605273	ch11: 65479355	C/C	53	81
		C/T	3	13
		T/T	0	0
rs2348569	ch15:87764938	A/A	22	30
		A/G	30	38
		G/G	4	26
rs6011731	ch20: 63317137	A/A	53	74
		A/G	20	19
		G/G	0	1
rs11542332	ch17:82062936	C/C	56	82
		C/T	0	12
		T/T	0	1
rs1415848	ch10:111744422	C/C	25	46
		C/T	27	33
		T/T	0	12
rs530752	ch11:62903542	A/A	52	79
		A/G	3	15
		G/G	0	0
rs7022936	ch9:90094948	G/G	48	72
		G/A	7	15
		A/A	1	7
rs1800469	chr19:41354391	C/C	28	46
		T/C	17	40
		T/T	0	6

Appendix 11: The NICO Clinical Trial Protocol (available digitally)

Appendix 12: The NICO Clinical Trial Radiotherapy Quality Assurance and Outlining Protocol (available digitally)

Appendix 13: HTG analysis QC: a) percentage allocated to positive controls, b) relative standard deviation with one sample (2-013) below 0.1 RSD, c) total reads for each sample.